2012

EPIGENETIC REGULATION OF GENES INVOLVED IN VASCULAR DYSFUNCTION IN PREECLAMPTIC WOMEN

Ahmad Mousa
Virginia Commonwealth University

EPIGENETIC REGULATION OF GENES INVOLVED IN VASCULAR DYSFUNCTION IN PREECLAMPTIC WOMEN

A dissertation submitted in partial fulfillment of the requirements for the degree of Doctor of Philosophy at Virginia Commonwealth University.

by

Ahmad A. Mousa

Bachelor of Dental Surgery, Jordan University of Science and Technology, 2005

Advisor: Scott W. Walsh, Ph.D.

Professor

Department of Obstetrics & Gynecology and Physiology and Biophysics

Virginia Commonwealth University

Richmond, Virginia

January, 2012

ACKNOWLEDGEMENT

I would like to express my sincere gratitude to my Lord (Allah), who gave me the opportunity and the blessings to explore a minute aspect of his amazing creation and to realize how limited we are in front of his greatness and ability. Without his help and mercy I would not be able to do anything good in my life.

I would like next to thank my Mentor Dr. Walsh for providing me with the opportunity to perform research in his lab and be part of his research group. Dr. Walsh largely contributed to my success in my Ph.D. career through his patience, kindness and continuous emotional and intellectual support.

I am very thankful for my Ph.D. committee members for their kindness and support. I thank Dr. Strauss for his continuous help and advice, Dr. Gerk for letting me use his lab equipment, Dr. Pittman for providing me with animal tissue whenever I needed, and Dr. Karnam for the valuable technical support I received from him and his lab members. My thanks to all the staff members of the Department of Physiology and Biophysics and the School of Graduate studies.

My best regards to my labmates and friends whom I always found whenever I needed help. They were like a family for me while being away from my home. I would like to specially thank our lab specialist Sonya Washington and my friends Khalid Abu Zaid, Mehrubon Safaraliev, Alae Yaseen and Nibras Aldolimi for all of what they did for me.

I would like to thank my father, mother, brothers, sisters, father in law, mother in law and brothers and sisters in law for all the support, prayers and blessings they provided to me. Without these people I won't be able to reach at this stage.

I would like to thank Jordan University of Science and Technology for the finical support during my studies. My sincere recognition for Dr. Said khatib who opened my eyes for this opportunity and for all his help and guidance.

Last, but not the least, I would like to express my deep and heartfelt thanks to my beloved wife, Dr. Ikhlas D. Darkhalil, for all the sacrifice she made for me. She has been, always, my pillar, my joy and my guiding light. Her support and encouragement in the end was what made this dissertation possible. I pray that we will stay together for the rest of our life as a happy family.

This has been a great experience, filled with tremendous memories both good and bad. I am convinced that the training and knowledge I have received will help me prosper in my professional life. And again before I finish, I would like to say Thanks God, for helping me finish my Ph.D. and reach this far.

TABLE OF CONTENT

LIST OF TABLES

LIST OF FIGURES

LIST OF ABBRIVIATIONS

5-Aza …….....5-Aza-2-deoxycytidine

ATb1……...angiotensin II receptor b1

BCA…… …….. bicinchoninic acid

BP……... biological process

COL1A1……collagen 1 α 1

COX-2……...……..cyclooxygenase-2

C-section……cesarean section

ddH2O……double deionized water

DIC……..disseminated intravascular coagulopathy

DMSO……..……..dimethyl sulfoxide

DNMT……..DNA methyltransferases

EIA…….……..enzyme immunoassay

ELISA……enzyme-linked immunosorbent assay

FBS…….fetal bovine serum

FDR……...……false discovery rate

GAPDH……..glyceraldehyde 3-phosphate dehydrogenase

HELLP…….….syndrome Hemolysis, elevated liver enzymes, low platelets

HMGB1……...……high mobility group box chromosomal protein 1

ICAM-1……..intercellular adhesion molecule-1

IL-8……..……interleukin-8

IMDM……...……..Iscove's modified Dulbecco's medium

IPA……..Ingenuity Pathways Analysis software

LB……..……..…..lysogeny broth

M-199……..medium-199

MF…… …molecular function

MMP……..... matrix metalloproteinase

MPE……...…….……mild preeclamptic

NF-κB…… nuclear factor-kappa B

NP……...…….….normal pregnant

OD…….….optical density of staining

OxLA……...oxidizing solution enriched with linoleic acid

PBS…….phosphate buffered saline

PMA……..……Phorbol 12-myristate 13-acetate

PPAR……..peroxisome proliferator-activated receptor

PVDF…….Polyvinylidene Fluoride

qRT-PCR……..……quantitative real time PCR

RIPA……....radio immuno precipitation assay buffer

ROS ……...……reactive oxygen species

RXR…….. retinoid X receptor

SDS…….……..sodium dodecyl sulphate

SERPINA3……...….protease inhibitor A3

SPE…….…….…….severe preeclamptic

TAE..……..tris-acetate-EDTA

TBXAS1…….……thromboxane synthase

TEMED……..N, N, N', N'- teramethylethylenediamine

TIMPs……..tissue inhibitors of matrix metalloproteinases

TNFα……..Tumor necrosis factor α

TSS……transcription start site

TXB2……..Thromboxane B2

VSMCs.....……...…….……Vascular smooth muscle cells

ABSTRACT

EPIGENETIC REGULATION OF GENES INVOLVED IN VASCULAR DYSFUNCTION IN PREECLAMPTIC WOMEN

By Ahmad Mousa, BDS

A dissertation submitted in partial fulfillment of the requirements for the degree of Doctor of Philosophy at Virginia Commonwealth University.

Virginia Commonwealth University, 2012
Major Director: Dr. Scott W. Walsh

Professor, Departments of Obstetrics and Gynecology, Physiology and Biophysics

DNA methylation is the most recognizable epigenetic mechanism. In general, DNA hypomethylation is associated with increased gene expression whereas DNA hypermethylation is associated with decreased gene expression. To date, little is known about the role of DNA methylation in the pathophysiology of preeclampsia. In this study, we examined the differences in DNA methylation in omental arteries of normal pregnant and preeclamptic women using the high throughput Illumina HumanMethylation27 BeadChip assay. We found 1,685 genes with a significant difference in DNA methylation at a false discovery rate of < 10% with many inflammatory genes having reduced methylation. The thromboxane synthase gene was the most hypomethylated gene in preeclamptic women as compared to normal pregnant women. When we examined the expression of thromboxane synthase in omental arteries of normal pregnant and preeclamptic women we found it to be significantly increased in preeclamptic women. The increased expression was observed in vascular smooth muscle cells, endothelial cells and infiltrating neutrophils. Experimentally induced DNA hypomethylation increased the expression of thromboxane synthase in the neutrophil-like HL-60 cell line, whereas tumor necrosis factor α (TNFα), a

neutrophil product, increased its expression in cultured human vascular smooth muscle cells (VSMC). These finding suggest that DNA methylation and release of TNFα by infiltrating neutrophils could contribute to the increased expression of thromboxane synthase in systemic blood vessels of preeclamptic women, contributing to the hypertension and coagulation abnormalities. We also explored the possible contribution of DNA methylation to the altered expression of genes involved in collagen metabolism in preeclampsia. Several matrix metalloproteinase (*MMP)* genes, including *MMP1* and *MMP8*, were significantly less methylated in preeclamptic women, whereas *TIMP* and *COL* genes were either significantly more methylated or had no significant change in their DNA methylation status. Experimentally induced DNA hypomethylation increased the expression of MMP-1, but not TIMP-1 or COL1A1, in cultured VSMCs and increased the expression of MMP-1 and MMP-8 in HL-60 cells. These findings suggest that DNA methylation contributes to the imbalance in genes involved in collagen metabolism in blood vessels of preeclamptic women.

CHAPTER 1: GENERAL INTRODUCTION

A. Definition of preeclampsia, its clinical symptoms and complications

Preeclampsia is the clinical definition of a multisystemic syndrome that is diagnosed by new onset of hypertension (systolic blood pressure of equal to or more than 140 mmHg, and/or diastolic blood pressure of equal to or more than 90 mmHg) and proteinuria (300 mg or more of protein in the urine for at least twenty four hours), which occur after twenty weeks of gestation in pregnant women who are otherwise normal[1].

Preeclampsia involves almost every system in the maternal body, with special involvement of the cardiovascular, hepatic, renal, cerebral, and coagulation systems[2]. Preeclampsia is associated with a widespread vasoconstriction, which results in increased total peripheral resistance and mean arterial blood pressure and decreased cardiac output, causing hypertension to occur[3]. Preeclamptic women also have exaggerated sensitivity to vasopressors such as angiotensin II[4] and impaired endothelium-dependent vasorelaxation[5]. Hepatic edema occurs in most of preeclamptic women[2]. Other liver complications in preeclampsia can range from reversible supcapsular and intrahepatic hemorrhage to rupture of the liver capsule and acute intraabdominal bleeding[6]. Hepatic complications are responsible for approximately 20% of maternal mortality in preeclampsia.

Glomerular endotheliosis, glomerular hypertrophy due to swelling of the glomerular endothelium, is the classical lesion of the kidneys in preeclampsia[2]. Proteinuria occurs in part due to impaired integrity of glomerular barrier and loss of size selectivity causing plasma proteins to leak into the urine. Preeclampsia is also associated with decreased renal blood flow and decreased uric acid secretion[2]. Cerebral edema is the most common finding in preeclampsia when the brain is involved[2]. Visual

disturbances that are most often reversible can occur in preeclamptic women[2]. Preeclampsia is also associated with a chronic disseminated intravascular coagulation indicated by platelet activation, increased thrombin-antithrombin III complexes and fibrin degradation products, and decreased platelets and antithrombin III[7,8].

Acute maternal complications of preeclampsia includes eclampsia, Hemolysis, elevated liver enzymes, low platelets (HELLP syndrome), liver rupture, pulmonary edema, renal failure, disseminated intravascular coagulopathy (DIC), hypertensive emergency, hypertensive encephalopathy and blindness[9]. Eclampsia is a life threatening condition which is characterized by the development of generalized convulsions with or without coma that cannot be explained by causes other than pregnancy[10]. HELLP syndrome is another serious complication of preeclampsia[9]. It has been estimated that 6% of women with severe preeclampsia develop one of the three clinical manifestations of this syndrome with elevated liver enzymes or low platelet count being the most common, 12% develop two of them, and 10% develop all of them. Perinatal and maternal death rates associated with preeclampsia are significantly increased when preeclampsia is complicated by HELLP syndrome[9]. Liver rupture is a severe complication of preeclampsia that occurs most frequently in multiparas of advanced age[11]. Liver rupture is rare, however, when it occurs, it is associated with high maternal and fetal mortality rate.

Pulmonary edema complicates up to 3% of preeclamptic pregnancies with up to 80% of cases occurring after delivery[12]. Acute renal failure is a rare complication of preeclampsia that is characterized by a sudden decrease in glomerular filtration rate, which causes retention of water and urea[9]. Up to 90% of the cases are due to acute tubular necrosis. In these cases, renal damage is often reversible and completely resolves after delivery, however, 10 to 29% of cases of acute renal failure as a complication of preeclampsia are due to bilateral renal cortical necrosis[9]. These cases are much more severe and associated with significantly increased maternal and fetal mortality rate.

Disseminated intravascular coagulopathy (DIC) is another possible complication of preeclampsia[9]. DIC is characterized by abnormal activation of the coagulation system which leads to widespread formation of fibrin microthrombi that can compromise adequate blood flow to the organs and cause organ failure[9]. In addition, the continuous activation of coagulation results in excessive consumption of coagulation factors and platelets, which causes bleeding tendency[13]. Thrombocytopenia (low platelet count of less than 100,000 per µl of blood), which is estimated to occur in 10% of preeclamptic women, is usually the first indication of DIC[9]. Hypertensive emergencies, which predispose to cerebrovascular accident (stroke) and hypertensive encephalopathy, may also complicate preeclampsia[14]. Hypertensive encephalopathy is characterized by neurological disturbances, such as headache, convulsions and visual disturbances, in the presence of hypertension[9]. Hypertensive encephalopathy can cause blindness in 1% to 15% of women with severe preeclampsia[15]. Although cerebrovascular accident is rare in pregnancy, it is a leading cause of death in preeclampsia and eclampsia[15].

B. Epidemiology

Preeclampsia and eclampsia are among the leading causes of obstetrical mortality and morbidity[16]. Preeclampsia occurs in approximately 6% to 8% of pregnant women and is estimated to be responsible for 15% of obstetrical deaths in the United States[17]. The incidence of preeclampsia in developed countries is estimated to be 4.5% to 11.2% of pregnancies[2]. However, the incidence of preeclampsia in developing countries is as high as 27%[18]. Preeclampsia more frequently affects pregnant women at both extremes of reproductive age, however, women who are less than 20 years old are at a higher risk[19].

Eclampsia accounts for about 15% of maternal mortality in the United States of America[20] and is the cause of approximately 10% of maternal deaths per year worldwide[21]. The incidence of eclampsia is estimated to be at 4 to 5 cases per 10,000 live births in developed countries[22] and 6 to 100 per 10,000 live births in developing countries[23].

C. Prevention and treatment

Multiple strategies have been proposed for prevention of preeclampsia[24]. These include dietary sodium restriction, dietary supplementation (fish oil, vitamin C, vitamin E and calcium), bed rest, and pharmacologic agents (diuretics, antihypertensive medications, heparin and other medications). However, none of these strategies has proven to be helpful in prevention of preeclampsia.

Meta-analysis of low-dose aspirin trials revealed that aspirin is effective in preventing preeclampsia[25,26], and its effectiveness is related to patient compliance[27]. A recent study demonstrated that supplementation during pregnancy with L- arginine, the substrate for nitric oxide synthesis, and antioxidant vitamins caused significant decrease in the incidence of preeclampsia in a high-risk population[28]. However, the same study indicated that supplementation with antioxidants alone was not effective.

To date, delivery of the fetus and placenta is the only cure for preeclampsia, which can occur at any time after 20 weeks gestation, therefore, preeclampsia is a common cause of preterm birth, low birth weight babies and increased fetal morbidity and mortality[1].

D. Pathophysiology of preeclampsia

Despite the extensive research efforts to understand the pathophysiology of preeclampsia, the exact process in not well understood, however, it has been proposed that the etiology of preeclampsia is divided into two stages where the first stage is associated with placentation issues, and the second stage involves development of maternal clinical manifestations[29].

1. Poor placentation in preeclampsia

The placenta has a fundamental role in the pathophysiology of preeclampsia because preeclampsia occurs only in the presence the placenta or placental tissue, and symptoms disappear soon after delivery of the placenta[29]. For example, a case report of a woman with abdominal pregnancy and retained placenta remained preeclamptic for months after delivery until the placenta was absorbed[30]. Also hydatidiform moles, which are masses of abnormal placental tissue, are associated with increased risk of preeclampsia[1].

Normal placentation is characterized by the invasion of spiral arterioles by a specialized subset of trophoblast cells called extravillous cytotrophoblasts. These cells replace maternal endothelium and much of the highly muscular tunica media of the spiral arterioles changing their morphology from narrow, muscular, vasoconstrictor responsive arterioles to wide, low-resistance, vasoconstrictor unresponsive canals in a process known as pseudovascularization or spiral remodeling[10]. This process extends to the inner third of the endometrium and is more or less completed by 20 weeks gestation[31]. Spiral remodeling enhances blood flow to the intervillous space where physiological exchange of nutrients and gases takes place between the maternal and the fetal circulations. In many cases of preeclampsia, invasion and remodeling of spiral arterioles by cytotrophoblasts is shallow and incomplete, a process called poor placentation, which results in reduced blood flow and placental hypoxia that is associated with placental oxidative stress due to an imbalance of increased production of reactive oxygen species and decreased

antioxidant defenses. Poor placentation, however, does not always cause preeclampsia[10], so other mechanisms are involved.

2. Neutrophil activation in preeclampsia

Neutrophils are the most abundant leukocytes in the blood comprising up to 70% of white blood cells[32]. Neutrophils are part of the innate immune system and they are highly mobile and phagocytic immune cells. Neutrophils are the first line of defense in the body against bacterial and fungal infections after physical barriers, such as skin, have been broken[32]. They are the first immune cells that extravasate to the site of inflammation in response to infection or tissue injury. Neutrophils play a key role in inflammation[32]. Beside their ability to respond to chemokines and cytokines, neutrophils can release chemokines that attract other immune cells such as dendritic cells and monocytes to sites of inflammation. Neutrophils also produce Tumor necrosis factor α (TNFα) and other cytokines that promote the differentiation and activation of dendritic cells and macrophages. Furthermore, they produce other ligands that are involved in proliferation and maturation of T and B lymphocytes. Neutrophils function against bacterial and fungal infections by isolating, phagocytizing and destroying the invading pathogens[32]. The latter is accomplished by two types of mechanisms: 1) oxidative mechanisms, which involve the production of reactive oxygen species (ROS), such as superoxide and hypochlorite ions, and 2) non-oxidative mechanisms, which involve synthesis and release of a variety of proteolytic enzymes. However, neutrophil destructive machineries are not exclusively directed against the invading pathogens and they can also destroy self-tissues. Thus, although neutrophils are generally thought to be a first line of defense for our bodies, there is a growing evidence of neutrophil involvement in a variety of inflammatory diseases that are not associated with infection[33].

Normal pregnancy is associated with neutrophil activation, which is exaggerated in preeclampsia. This was first demonstrated by measuring plasma levels of neutrophil elastase, a marker of neutrophil activation. Plasma elastase levels were significantly higher in normal pregnant women as compared to normal non-pregnant women, and were significantly higher in preeclamptic women as compared to normal pregnant women[34]. Increased neutrophil activation in preeclampsia was later confirmed by evaluating other markers of neutrophil activation such as increased intracellular free ionized calcium[35], increased plasma levels of defensins and lactoferrin[36], increased expression of CD11b[37], and increased release of intracellular reactive oxygen species[38]. Neutrophil activation in preeclampsia is limited to the maternal circulation[39]. Plasma from normal pregnant women significantly inhibited superoxide production by neutrophils from non-pregnant women, but did not inhibit superoxide production by neutrophils from preeclamptic women[40].

Neutrophil activation in preeclampsia most likely occurs as neutrophils circulate through the placental intervillous space and are exposed to increased levels of lipid peroxides[41]. Neutrophils can also be activated by syncytiotrophoblast microvillus membrane micro-particles as indicated by the induction of superoxide generation[42]. Increased levels of these micro-particles have been detected in the maternal circulation in preeclampsia[43]. Preeclampsia is also associated with increased plasma levels of small dense low-density lipoprotein, very low-density lipoprotein[44] and oxidized low-density lipoprotein[45]. Incubation of isolated neutrophils with oxidized low-density lipoprotein resulted in their activation as indicated by increased expression of CD11b and decrease expression of L-selectin suggesting an other possible cause of neutrophil activation in preeclampsia[46].

3. Endothelial Dysfunction

Endothelium is a layer of flattened cells that line the luminal surface of blood vessels. Endothelium is not an inert tissue; rather, it is involved in a variety of physiological and pathological

processes. Endothelium permits the physiological exchange of products between blood and interstitial fluid[47]. It is also involved in controlling vessel tone, and therefore blood pressure, through the production of vasoactive substances which can be vasodilators such as nitric oxide, prostacyclin and endothelial derived hyperpolarizing factor, or vasoconstrictors such as endothelium-derived contracting factors, thromboxane and endothelin[48]. Endothelium also plays an essential role in hemostasis[49] and inflammation[50].

Normal endothelial functions favor vasodilation, anti-coagulation and anti-inflammation. However, endothelial injury results in abnormal alterations in the vascular properties of endothelium characterized by a shift toward reduced vasodilation, pro-inflammation and pro-coagulation, a condition known as "endothelial dysfunction"[51]. Endothelial dysfunction is associated with cardiovascular diseases such as hypertension, coronary artery disease, chronic heart failure, peripheral artery disease, diabetes and chronic renal failure. Preeclampsia is also associated with endothelial dysfunction[52,53] demonstrated by 1) increased production of vasoconstrictors and pro-coagulants such as Von Willebrand's factor[54], endothelin-1[55], thromboxane, prostaglandin $F_2\alpha$[56] and platelet derived growth factor, and 2) decreased production of vasodilators and anti-coagulants such as prostacyclin[57,58] and nitric oxide[59]. Endothelial dysfunction precedes the clinical manifestations of preeclampsia[5] and can help explain some of them such as hypertension, proteinuria and hypercoagulation.

The cause of endothelial dysfunction in preeclampsia is thought to be of placental origin with several candidates being proposed to be released from the placenta to the maternal circulation and cause endothelial dysfunction[60]. These include TNFα, interleukin -6, interleukin -1α, interleukin -1β, oxidized lipid products, neurokinin-B, syncytiotrophoblast debris and soluble fms-like tyrosine kinase 1, a soluble receptor for vascular endothelial growth factor. These factors have been reported to induce endothelial dysfunction in *in vitro* models, however, they are not increased in all preeclamptic cases and are not sufficient by themselves to explain the complex pathophysiology of preeclampsia.

Neutrophil activation is another possible mechanism by which the placenta can cause endothelial dysfunction through the direct interaction between activated neutrophils and endothelium. Recently, neutrophil infiltration of resistance-sized systemic blood vessels associated with activation of nuclear factor-kappa B (NF-κB) and increased expression of cyclooxygenase-2 (COX-2), intercellular adhesion molecule-1 (ICAM-1) and interleukin-8 (IL-8) in endothelial and vascular smooth muscle cells was demonstrated in preeclampsia[61-63].

4. Oxidative stress

Preeclampsia is associated with an imbalance of increased lipid peroxidation along with decrease antioxidant protection leading to oxidative stress. This imbalance is present in the maternal and placental compartments[64]. Lipid peroxides are produced when polyunsaturated fatty acids interact with free radicals such as oxygen free radicals[64]. Oxygen free radicals, also called reactive oxygen species (ROS), include superoxide, hydroxyl radical, alkoxy radical, peroxyl radical, nitric oxide, and hydrogen peroxide. Although hydrogen peroxide is not a radical, it is considered as a reactive oxygen species due to its high reactivity. Sources of reactive oxygen species include mitochondria, oxidative enzymes such as xanthine oxidase, activated neutrophils, and arachidonic acid metabolism by the lipoxygenase and the cyclooxygenase pathways. In turn, lipid peroxides can generate reactive oxygen species through their interaction with molecular oxygen[64]. Once the lipid peroxidation process is initiated, it becomes self propagating, unless stopped by an antioxidant, such as vitamin E[64].

Antioxidants neutralize the toxic effects of lipid peroxides and oxygen free radicals, and limit their formation[64]. Antioxidants can be divided into extracellular (plasma) antioxidants and intracellular antioxidants. The major mechanism of action for plasma antioxidants is to bind transition metals such as iron and copper, which stimulate free radical reactions. These plasma antioxidants include transferrin,

lactoferrin, ceruloplasmin, albumin, uric acid, haptoglobin and hemopexin. Ascorbic acid, uric acid and albumin provide additional antioxidant activity in the plasma through the scavenging of water-soluble peroxyl radicals. Vitamin E is the most important lipid soluble antioxidant in plasma and cells. Because of its solubility in lipids, vitamin E becomes a part of plasma lipoproteins, cell membranes and membranes of the intracellular organelles. Vitamin E is essential in protecting against lipid peroxidation by interfering with its self propagation. Vitamin E is consumed during lipid peroxidation and its levels are decreased when lipid peroxidation is increased. Intracellular antioxidants include superoxide dismutase, which converts superoxide to hydrogen peroxide, catalase, which inactivates hydrogen peroxide, and glutathione peroxidase, which inactivates hydrogen peroxide as well as lipid peroxides.

Normal pregnancy is associated with increased maternal blood levels of lipid peroxides[65], however, several antioxidants such as vitamin E, ceruloplasmin, glutathione peroxidase activity and the net antioxidant activity are increased, which nullify the toxic effects of increased lipid peroxides. In contrast to normal pregnancy, preeclampsia is associated with a greater increase in maternal blood levels of lipid peroxides, which is not off-set by an increase in antioxidants[65]. Tissue levels and production rates of lipid peroxides are also significantly increased in the placenta[65]. Some of the lipid peroxides that are produced by placenta are stable enough to function in the maternal circulation such as oxidized polyunsaturated fatty acids in low-density lipoproteins, which have a half-life of 3 hours. In contrast to normal pregnancy, preeclampsia is associated with a significant decrease in various maternal circulating antioxidants such as vitamin E and net antioxidant activity. Vitamin E levels and the activities of glutathione peroxidase and superoxide dismutase are also significantly decreased in preeclamptic placentas[64].

Reactive oxygen species, particularly superoxide, are also abnormally increased in preeclampsia[66]. Neutrophils are a major source of superoxide[67]. Neutrophils isolated from preeclamptic women showed enhanced superoxide production in response to stimulus as compared to neutrophils from normal pregnant women[68]. Superoxide interacts with nitric oxide to form peroxynitrite[69]. Peroxynitrite

formation is increased in the placenta and in the maternal vasculature in preeclampsia[70,71]. Peroxynitrite is a potent oxidant[72] that can damage endothelial cells directly and impair their function[73]. Because nitric oxide is a potent vasodilator and platelet aggregation inhibitor that is continuously released by endothelium[74], peroxynitrite formation can result in impaired endothelium-mediated relaxation[75] observed in preeclampsia through the consumption of nitric oxide. Also, decomposition of peroxynitrite generates hydroxyl radical which is a potent free radical that can directly impair cell function and mediate vascular dysfunction[76].

Lipid peroxides and reactive oxygen species can cause a variety of effects that are relevant to the pathophysiology of preeclampsia such as endothelial dysfunction, induction of platelet aggregation and neutrophil activation[64]. Lipid peroxides increase the production of thromboxane through a cyclooxygenase dependent mechanism[77], and decrease the production of prostacyclin through the inhibition of prostacyclin synthase[78]. Preeclampsia is associated with an imbalance of increased thromboxane and decreased prostacyclin[79]. Therefore, lipid peroxides contribute to this imbalance, which can explain major manifestations in preeclampsia such as hypertension, coagulopathy and reduced uteroplacental blood flow. Preeclampsia is also associated with maternal systemic inflammation[80-82]. Increased lipid peroxides and reactive oxygen species in preeclampsia can contribute to maternal inflammation through the activation of NF-κB and induction of COX-2[83] which are hall marks of inflammation. Recently, activation of NF-κB and induction of COX-2 was demonstrated in system blood vessels of preeclamptic women[62].

5. Thromboxane / prostacyclin imbalance

Thromboxane A_2 is an unstable metabolite of arachidonic acid that is implicated in a wide range of physiological and pathological processes. Thromboxane A_2 half-life is approximately 30 seconds[84].

Therefore, thromboxane A_2 levels are measured indirectly by measuring the levels of its more stable metabolite thromboxane B_2. In addition to production by platelets, thromboxane can be produced by a variety of cells and tissues such as placenta, vascular smooth muscle cells, endothelial cells and neutrophils[84-87]. Arachidonic acid, which is released from membrane phospholipids by the action of phospholipase A_2, is metabolized by cyclooxygenase into prostaglandin H_2, which is further metabolized by thromboxane synthase into thromboxane A_2. Thromboxane A_2 acts through its receptor, thromboxane A_2 receptor or TP receptor, a G-protein coupled receptor that has a wide distribution thought the body. Thromboxane A_2 is a potent vasoconstrictor, potent stimulator of platelet activation[84] and an important inflammatory mediator[88].

Preeclampsia is also characterized by neutrophil activation[36], oxidative stress[89], increased lipid peroxidation[27], and increased plasma levels of linoleic acid[90], the fatty acid precursor of arachidonic acid. An oxidizing solution enriched with linoleic acid (OxLA), which is similar to the conditions of oxidative stress and elevated plasma linoleic acid levels in preeclampsia, significantly increased thromboxane and TNFα production by neutrophils[86]. TNFα production was thromboxane dependent because pinane thromboxane, which is an inhibitor of thromboxane synthase and an antagonist of thromboxane receptor, abolished OxLA stimulated TNFα production by neutrophils. Moreover, OxLA stimulated IL-8 production by cultured human vascular smooth muscle cells, which was attenuated by the inhibition of the cyclooxygenase pathway suggesting a role of thromboxane in IL-8 response[85]. IL-8, a potent activator and chemoattractant of neutrophils, is over expressed by vascular smooth muscle cells and endothelium in systemic vasculature of preeclamptic women[61]. Thromboxane is also involved in neutrophil generation of superoxide because pinane thromboxane significantly lowered superoxide production by neutrophils isolated from pregnant women or activated by arachidonic acid[91]. Inhibition of thromboxane receptor suppressed the expression of ICAM-I in human vascular endothelial cells that were stimulated by TNFα[92]. Preeclampsia is also associated with an increase in the expression of thromboxane synthase in trophoblasts and decidua of preeclamptic placentas[93].

Prostacyclin is another unstable metabolite of arachidonic acid that is primarily produced by endothelial cells of maternal, placental, uterine and umbilical vessels[27]. However, it can also be produced by the avascular amnion and chorion. Both thromboxane and prostacyclin are synthesized from the same precursor, which is prostaglandin H_2, by two different enzymes which are thromboxane synthase and prostacyclin synthase, respectively[94]. Production of prostacyclin can be determined by measuring its stable metabolite, 6-keto $PGF_1\alpha$. Prostacyclin is a potent vasodilator and potent inhibitor of platelet aggregation[27], and thus oppose the actions of thromboxane.

In normal pregnancy, maternal plasma levels of prostacyclin progressively increase with advancing gestation, whereas those of thromboxane progressively decrease. Therefore, the ratio of prostacyclin to thromboxane progressively increases during normal pregnancy indicating that the vasodilating and platelet inhibition actions of prostacyclin are progressively favored with advancing gestation in normal pregnancy[65]. Preeclampsia is characterized by an imbalance of increased thromboxane and decreased prostacyclin that was first described by Walsh et al in the placenta[95] and later confirmed for the maternal compartment in blood and urine[96,97]. This imbalance predates and can explain some of the main clinical manifestations of preeclampsia, such as hypertension and thrombosis. The same imbalance has been reported in other pathological conditions that involve the cardiovascular system such as atherosis[98], myocardial infarction[99] and diabetes[100].

E. Inflammation and preeclampsia

Normal pregnancy is associated with mild systemic inflammatory changes which increase as pregnancy progresses[82]. These changes include increased plasma levels of fibrinogen[101], plasminogen activator inhibitor type 1[102] ceruloplasmin[103], interleukin-6[104], and tumor necrosis factor-α[105,106]. They also include leukocytosis[35], leukocyte activation[38], increased circulating markers of oxidative stress such as

lipid peroxides and malondialdehyde[107], and hypertriglyceridemia[108]. All these inflammatory changes are exacerbated in preeclampsia[109]. Elevation in inflammatory markers predates and may contribute to the presentation of the clinical signs and symptoms of preeclampsia. Therefore, a possible explanation for preeclampsia could be the inability of the body to compensate for an exaggerated pregnancy induced systemic inflammatory response.

Recently, inflammation of the systemic vasculature was demonstrated in women with preeclampsia indicated by significant activation of NF-κB and significant increase in the expression of inflammatory markers including ICAM-1, IL-8, and COX-2 in endothelium and vascular smooth muscle[61,62]. These inflammatory changes were associated with significant neutrophil infiltration. Infiltrating neutrophils can provide plausible explanation for endothelial and vascular smooth muscle dysfunction associated with preeclampsia through their ability to release toxic substances such as ROS, TNFα, thromboxane and Matrix metalloproteinase-8.

F. Epigenetics and DNA methylation

Epigenetics is the study of heritable changes in gene expression patterns, which are mediated through mechanisms other than changes in the nucleotide sequence of the DNA[110]. Epigenetic regulation contributes to phenotype by mediating genomic adaptation to environmental changes and insults. Epigenetic mechanisms include histone modification, small interfering RNAs, DNA methylation and other mechanisms.

DNA methylation is essential for mammalian embryogenesis, genome stability, maintaining of imprinting and X chromosome inactivation[110]. DNA methylation occurs at the 5' position of a cytosine in a CpG dinucleotide context. Methylated cytosine accounts for approximately 1% of all DNA bases[111]. About 75% of CpG dinucleotides in mammalian genomes are methylated and about 88% of active

promoters are associated with CpG rich sequences. To date, four DNA methyltransferases (DNMT) have been reported which are DNMT1, DNMT2, DNMT3A and DNMT3B[112]. Except for DNMT2, which acts probably as an RNA methyltransferase, all other DNA methyltransferases are required for embryonic vitality. Unlike DNMT3A and DNMT3B which are responsible for de novo DNA methylation, DNMT1 prefers hemimethylated DNA and functions as a maintenance methyltransferase. In general, DNA methylation is associated with decreased gene transcription and DNA hypomethylation is associated with increased gene transcription[113]. DNA-methyl-binding-domain proteins, or methyl-CpG-binding proteins, and DNMTs themselves can recognize methylated DNA and bind to it. This prevents binding of transcriptional activators through steric hindrance. These proteins can also recruit transcriptional co-repressors, such as histone deacetylases and polycomb proteins, resulting in heterochromatin formation and gene silencing. Both active and passive DNA demethylation undoubtedly occurs, such as during embryonic development, however, the exact mechanisms of global and/or gene specific DNA demethylation are not well understood[114].

DNA methylation is a reversible process and DNA methylation patterns are affected by age, diet, oxidative stress and environmental stimuli[110]. In monozygotic twins, who are genetically identical, differences in DNA methylation increase with age and different environmental influences cause different patterns of DNA methylation[115]. Aging is associated with global DNA hypomethylation accompanied with hypermethylation of specific genes[116]. DNA methylation is dependent on dietary intake of folic acid[117]. Folic acid is a methyl donor required for the synthesis of S-adenosylmethionine which is the substrate for DNMTs. DNA methylation levels correlate with the availability of folic acid and the activity of enzymes involved in folic acid metabolism such as 5,10-methylenetetrahydrofolate reductase. High folic acid intake in mice results in DNA hypermethylation of an allele at the agouti locus, which determines whether a mouse coat is banded (agouti) or solid in color (non-agouti)[118]. Chemical and environmental toxins such heavy metals and aromatic compounds can also influence patterns of DNA

methylation[119,120]. Vinclozolin, which is an antiandrogenic compound, affects DNA methylation patterns in sperm and its effect can last at least for four generations[121].

Changes in DNA methylation patterns have been linked to a variety of complex diseases including cancers[122], inflammatory bowel disease[123], neural tube defects[124], schizophrenia, bipolar disorder[125], autoimmune diseases such as systemic lupus erythematosus[126] and rheumatoid arthritis[127], type II diabetes, metabolic syndrome[128] and cardiovascular diseases such as atherosclerosis[129] and ischemic heart disease and stroke[130].

DNA methyltransferases use S-adenosylmethionine as a donor of methyl group in their reactions[131]. When the methyl group is transferred, S-adenosylmethionine is converted to S-adenosylhomocysteine which is hydrolyzed, under physiological conditions, to homocysteine and adenosine. The equilibrium of this reversible reaction strongly favors S-adenosylhomocysteine synthesis rather than hydrolysis and an increase in intracellular homocysteine levels can eventually increase S-adenosylhomocysteine levels[132]. S-adenosylhomocysteine has a higher affinity to DNA methyltransferases than S-adenosylmethionine, which makes it a potent inhibitor of DNA methylation reactions[133]. One study demonstrated that increased plasma levels of total homocysteine and S-adenosylhomocysteine correlated with decreased global DNA methylation in white blood cells of patients with advance atherosclerosis[134]. Interestingly, a group of studies reported that plasma levels of homocysteine and S-adenosylhomocysteine are significantly elevated in preeclamptic women as compared to normal pregnant women[135-137].

Methylenetetrahydrofolate reductase is the enzyme that catalyzes the conversion of 5,10-methylenetetrahydrofolate to 5-methyltetrahydrofolate, which is required for re-methylation of homocysteine to methionine. Pertinent to this is a study that showed methylenetetrahydrofolate reductase knockout mice had either significantly decreased S-adenosylmethionine levels or significantly increased S-adenosylhomocysteine levels, or both, associated with global DNA hypomethylation[138].

These knockout mice also showed abnormal aortic lipid deposition similar to those observed in early atherosclerosis.

In another study, apolipoprotein E knockout mice, which are prone to atherosclerosis, showed both DNA hypermethylation and hypomethylation with slightly more but significant DNA hypomethylation in their aortae and peripheral blood cells at age of 4 weeks and 6 month[139]. These DNA methylation events were associated with the initial stages of atherogenesis. The same study also showed that relatively short stimulation of the human macrophage cell line, THP-1, with mixtures of lipoproteins of high VLDL and LDL ratio to HDL, similar to lipoprotein ratios in apolipoprotein E knockout mice, caused significant DNA hypermethylation compared to untreated cells, or cells treated with mixtures of lipoproteins of low VLDL and LDL ratio to HDL, similar to lipoprotein ratios in wild-type mice.

Another study demonstrated that a low protein diet in rats was associated with global hypomethylation[140]. Deficiency of amino acids required to generate methyl donors, such as glycine, may underline this phenomena. Supplementation of a low protein diet with glycine or folate reversed the effect on DNA methylation. The same study showed that offspring of female rats which were placed on a low protein diet during conception developed upregulation of angiotensin II receptor b1 (ATb1) in their adrenal glands and they became more responsive to angiotensin II and later developed hypertension. The proximal promoter of the AT1b gene in the adrenal glands of these rats was significantly less methylated, and in vitro experiment demonstrated that AT1b gene expression was highly correlated with its promoter methylation.

DNA methylation patterns can also be influenced by reactive oxygen species[141]. Hydroxyl radical can result in base modification, deletions, strand breakage and other DNA lesions, which can interfere with methylation of DNA by DNMTs. The presence of 8-hydroxy-2'-deoxyguanosine and O^6-methyl guanine in a CpG dinucleotide inhibits methylation of the adjacent cytosine. 8-Hydroxy-2'-deoxyguanosine and O^6-methyl guanine also decrease the binding affinity of DNA-methyl-binding-

domain proteins to methylated CpG dinucleotides attenuating the DNA methylation dependent silencing of gene transcription. Furthermore, 8-hydroxy-2'-deoxyguanosine or O^6-methyl guanine may not be recognized by the DNA proof reading enzymes and can be mispaired with thymine contributing to hypomethylation of DNA. On the other hand, single stranded DNA formation due to DNA strand breakage by ROS can stimulate de novo DNA methylation. A number of studies have shown a clear association between decreased expression of critical antioxidant enzymes and hypermethylation mediated gene silencing in tumorigenesis[122].

G. Epigenetics and preeclampsia

Little is known about the role of epigenetics in preeclampsia. It has been suggested that early epigenetic alterations in gametes and/or the embryo can result in placental defects and predispose to preeclampsia in assisted reproductive technology pregnancies, which are associated with increased risk of preeclampsia[142]. Deletion of imprinted gene p57-Kip2 in mice is associated with hypertension and proteinuria, which are the main manifestations in preeclamptic women, during pregnancy[143]. Epigenetic alterations in imprinted and non-imprinted genes were demonstrated in preeclamptic placentas. Imprinted gene H19 is a member of a group of growth regulators where the paternal allele is imprinted while the maternal allele is expressed. A study showed significantly higher percentage of preeclamptic women with loss of imprinting, and therefore biallelic expression of the H19 gene in placental tissues during the third trimester of pregnancy as compared to normal pregnant women who showed monoallelic expression in all of the cases[144]. The same study also showed that loss of imprinting of the H19 gene was associated with more severe clinical symptoms in preeclamptic women. The investigators suggested that the loss of imprinting of the H19 gene may attribute to reduce invasive capacity of trophoblasts resulting in poor placentation.

Epigenetic alterations of non-imprinting genes were also reported in preeclamptic placentas. The expression of serine protease inhibitor A3 (SERPINA3) was increased and its promoter methylation was decreased in preeclamptic placentas as compared to normal pregnant women[145]. The increased expression of SERPINA3 protease inhibitors could possibly disrupt extracellular matrix solubilization by inhibiting elastase activity. This could reduce trophoblastic invasion leading to poor placentation. Furthermore, the expression of matrix metalloproteinase-9 was increased and its promoter methylation was decreased in preeclamptic placentas as compared to normal pregnant women[146]. Increased expression was well correlated with promoter hypomethylation.

A study that investigated global DNA methylation profiles of placentas revealed promoter hypomethylation of multiple genes in early-onset preeclampsia, which is a severe form of preeclampsia, as compared to placentas from normal pregnancy[147]. Another study demonstrated that X chromosome inactivation, which is essentially maintained by DNA methylation, was extremely disturbed in peripheral blood cells collected from preeclamptic women as compared to normal pregnant women[148].

H. Thromboxane synthase

Thromboxane synthase is an inducible microsomal enzyme that catalyzes two distinct but simultaneous reaction of the same substrate, which are isomerization of PGH_2 into thromboxane A_2 and cleavage of PGH_2 into 12-L-hydroxy-5, 8, 10- heptadecatrienoic acid and malondialdehyde[149]. These reactions are extremely rapid. Therefore, the primary regulation of thromboxane A_2 production is largely dependent on the availability of thromboxane synthase and PGH_2. Both transcriptional and post-transcriptional levels of regulation for thromboxane synthase have been reported[150,151]. Epigenetic factors may influence the expression of thromboxane synthase as suggested by the distinctive methylation patterns of thromboxane synthase promoter that were found in several human cell lines expressing the

enzyme[152]. Moreover, aging is associated with increased expression of thromboxane synthase in endothelial cells which also suggest an epigenetic mechanism in the regulation of expression of this enzyme[153].

I. Matrix metalloproteinases

Matrix metalloproteinases (MMPs) are a family of more than twenty Zn-dependent endopeptidases that are involved in several physiological and pathological processes including wound healing[154], development[155], inflammation[156], atherosclerosis[157], cancer biology[158], leukocyte activation[154] and regulation of vessel tone[159,160]. MMPs can be produced by a variety of cells including neutrophils, vascular smooth muscle cells and endothelial cells[161]. Almost all components of the extracellular matrix can be cleaved and degraded by MMPs, however, MMPs process and regulate the biological activity of a large number of non-extracellular matrix proteins including growth factors such as connective tissue growth factor and transforming growth factor β, cytokines such as pro-TNFα and IL-1β, chemokines such as monocyte chemotactic protein 3, cell membrane receptors such as protease activated receptor-1 and IL-2 receptor α, vasoactive ligands such as big endothelin, serine proteinase inhibitors, lipoproteins and other MMPs[162,163]. MMPs are regulated at three major levels which are gene expression, activation of newly synthesized MMPs (pro-MMPs), and inhibition of activated MMPs by tissue inhibitors of matrix metalloproteinases (TIMPs)[161]. Several genes encoding for MMPs can be induced by a number of factors including cytokines and growth factors. On the other hand, these genes can be inhibited by other factors such as glucocorticoids and retinoids. Activation of MMPs involves the removal of the propeptide domain. This domain contains a cysteine residue that coordinates with the Zn^{++} ion in the catalytic domain and therefore inactivates it. Removal of the propeptide domain can be catalyzed by other proteases such as trypsin, plasmin and other MMPs especially membrane associated MMPs. Oxidants such peroxynitrite can also activate pro-MMPs by disrupting the cysteine- Zn interaction[162]. TIMPs act by

binding MMPs to form non covalent complexes and, thereby, mask the substrate cleavage binding sites of MMPs.

J. Matrix metalloproteinase-1

Matrix metalloproteinase-1 (MMP-1) is an interstitial collagenase that is implicated in a number of physiological and pathological processes. Recently, Estrada et al reported that MMP-1 gene and protein expression are increased in omental fat blood vessels of preeclamptic women as compared to normal pregnant women[159]. The same study also showed that MMP-1 plasma levels were also increased in preeclamptic women. Increased expression of MMP-1 in systemic blood vessels was detected in vascular smooth muscle cells, endothelial cells and infiltrating leukocytes as indicated by immunohistochemistry staining. In contrast, vascular expression of TIMP-1 and collagen 1 α 1(COL1A1), which encodes the principle component of collagen type I, were unaffected or decreased in preeclamptic women suggesting an imbalance of increased collagen degradation and decreased collagen synthesis in preeclampsia. By affecting the integrity of the blood vessel wall, these findings might explain proteinuria and edema that occur in preeclampsia.

Oxidative stress, neutrophil infiltration of systemic blood vessels and vascular inflammation which are associated with preeclampsia are likely responsible for the imbalance in collagen synthesis and degradation[159]. Treatment of primary cultures of human vascular smooth muscle cells with an oxidizing solution composed of hypoxanthine and xanthine oxidase, activated neutrophils or TNFα significantly increased MMP-1 expression and secretion but decreased or did not change the expression of TIMP-1 and COL1A1, which is similar to what was found in preeclamptic vessels.

MMP-1 expression in systemic blood vessels of preeclamptic women might explain neutrophil infiltration and vasoconstriction[159]. For example, supernatants taken from vascular smooth muscle

primary cultures treated with MMP-1 stimulated neutrophil migration in modified Boyden chambers. This was associated with increased vascular smooth muscle cell secretion of IL-8 and collagen Type I C terminal telopeptide fragment, which are known neutrophil chemoattractants. Furthermore, MMP-1 induced contraction of omental arteries in a dose dependent manner demonstrating a previously unrecognized mechanism by which MMPs can modify vessel tone. Vasoconstriction was mediated by activation of PAR-1, which was found in the same study to be overexpressed in these arteries, as indicated by the loss of contraction in response to MMP-1 in the presence of PAR-1 inhibitor.

MMP-1 may be regulated by DNA methylation. A study showed that MMP-1 expression in amnion fibroblasts is regulated by DNA methylation as indicated by a significant increase in MMP-1 gene and protein expression caused by inhibition of DNA methylation in primary cultures of amnion fibroblasts with 5-Aza-2-deoxycytidine (5-Aza)[164]. The increased MMP-1 expression was correlated with a decrease in methylation at a particular site (-1538) in the MMP-1 promoter. DNA methylation at the same site in amnion was significantly decreased in a larger percentage of preterm prematurely ruptured fetal membranes where MMP-1 expression was increased.

K. Specific Aims

1. Specific Aim 1

To determine if preeclampsia is associated with hypomethylation of CpG dinucleotides in the promoter regions of inflammatory genes associated with vascular dysfunction using global DNA methylation analysis.

Hypothesis: Preeclampsia is associated with hypomethylation of CpG sites in promoter regions of inflammatory genes associated with vascular dysfunction.

Omental arteries will be dissected of omental fat samples obtained from normal pregnant and preeclamptic women during cesarean section. DNA will be extracted from omental arteries. DNA will be bisulfite treated and then DNA methylation profiles will be investigated using the high throughput Infinium HumanMethylation27 BeadChip assay.

2. Specific Aim 2

To target genes of interest identified in Aim 1 to have hypomethylated CpG sites in their promoter regions for further study to determine if their gene and protein expression correlates with the methylation status of their promoters.

Hypothesis: Inflammatory genes identified in Specific Aim 1 to be hypomethylated are overexpressed in systemic vasculature of preeclamptic women as compared to normal pregnant women.

Omental arteries will be dissected of omental fat samples obtained from normal pregnant and preeclamptic women during C-section. Both RNA and protein will be extracted from omental arteries. Quantitative real-time polymerase chain reaction will be used to examine the gene expression of genes of interest and Western blot or ELISA will be used to examine the protein expression of these genes.

3. Specific Aim 3

To determine if gene and protein expression of genes of interest are regulated by DNA methylation in human cell culture models.

Hypothesis: Decreased DNA methylation causes increased gene and protein expression of genes of interest in cell culture models.

Cell cultures will be treated with 5-Aza which inhibits DNA methylation. After that, cells will be collected and both RNA and protein will be extracted from omental arteries. Quantitative real time polymerase chain reaction will be used to examine the gene expression and Western blot will be used to examine protein expression.

In summary, this dissertation will examine if preeclampsia is associated with differences in DNA methylation profiles of arteries of preeclamptic women as compared with normal pregnant women. It will also examine the gene and protein expression of genes that are hypomethylated in preeclamptic women to determine if the decrease in DNA methylation is associated with increased gene and protein expression. Finally, cell cultures will be used to examine the role of DNA methylation in gene expression.

L. Significance of this research

This study is the first to examine DNA methylation in systemic blood vessels of normal pregnant and preeclamptic women. If differences in DNA methylation were identified in preeclamptic women, these differences might help explain why some pregnant women develop preeclampsia and others do not. For example, decreased DNA methylation in the promoter regions of inflammatory genes might make these women more responsive to the pregnancy induced inflammatory response increasing their risk of preeclampsia. Alterations in DNA methylation might be preexisting, however, neutrophil infiltration of systemic blood vessels of preeclamptic women could also cause alterations in DNA methylation which may help explain the increased risk of cardiovascular diseases later in life in women who have had preeclampsia.

CHAPTER 2: MATERIALS AND METHODS

A. Study subjects

Omental fat biopsies (approximately 2 cm X 2cm X 2cm) were collected during cesarean section (C-section) from previously consented normal pregnant and preeclamptic women at the Medical College of Virginia (MCV) Hospitals, Virginia Commonwealth University (VCU) Medical Center, Richmond, Virginia. Biopsies were submerged in normal saline in a sterile jar and kept in a refrigerator (4˚C) until transferred to the laboratory as soon as possible for processing. Omental fat was selected for this study because it is highly vascular, accessible during a C-section and omental vessels contribute to total peripheral vascular resistance.

Women recruited for the study were 28 to 38 weeks of gestation. Women were classified by the clinicians based on their clinical signs and symptoms into normal pregnant, mild preeclamptic or severe preeclamptic women. Mild preeclampsia is diagnosed when the blood pressure is ≥ 140 mmHg systolic or ≥ 90 mmHg diastolic and 0.3 g of protein is collected in the urine within 24 hours, whereas severe preeclampsia is diagnosed when blood pressure is ≥ 160 mmHg systolic or ≥ 110 mmHg diastolic and 5 g of protein is collected in the urine within 24 hours[1]. Clinical characteristics of the patients are given in tables for each chapter. Women who were excluded from the study included those with chorioamnionitis, maternal infections, active sexually transmitted diseases (e.g. HIV), lupus or diabetes. Also, women who were obese (body mass index ≥ 30), smoked or were in labor were excluded from the study. These exclusion criteria were chosen because they are known to cause inflammation.

B. Vessel dissection

Dissection of omental arteries was done under a dissection microscope (Olympus, B061) on a silicone dissection dish pre-cooled to 4˚C (NESLAB - RTE-7 Refrigerated Bath/Circulator, Thermo Scientific, Asheville, NC). The fat biopsy was spread and pinned down on the silicone dissection dish in cold (4˚C) phosphate buffered saline (PBS, pH=7.4, Gibco, Invitrogen, Carlsbad, CA), and the dissection microscope was used to visualize the blood vessels.

Omental arteries were distinguished from omental veins based on their morphology and branching points. In general, arteries are narrower with thicker walls than veins. Also, the branching points of an artery tend to be more acute, whereas those of a vein tend to be more rounded. An artery and a vein often ran together making it easier to discern differences. Comparison was done after the fat was cleared to allow for proper inspection of the vessels. Maintaining the integrity of the vessels to keep the blood inside their lumens facilitated the localization of the vessels within the fat during dissection and the discrimination between an artery and a vein.

Vessels were fixed and gently stretched on the silicon dissection dish using two pins at either end. Initially, the fat around a vessel was cut as close as possible to the vessel wall keeping the cutting plane of the scissor (0.255 mm, Science Tools, Foster City, CA) parallel to the long axes of the vessel and the curved tip of the scissor pointing away from the vessel wall but carefully leaving about 1 mm of fat around the vessel to avoid damaging its wall. A fine tip scissor (0.075 mm, Fine Science Tools, Foster City, CA) was used for the fine dissection and final cleaning of the vessel. A Dumont #55 forceps (Science Tools, Foster City, CA) was used to hold the fat and gently pull it away from the vessel. This usually resulted in formation of a transparent zone between the vessel wall and the fat, most likely loose connective tissues that surround the tunica adventitia of the vessel. The fine tip scissor was used to cut through this zone while keeping the cutting plane parallel to the length of the vessel and the curved tip away from the wall. Adherent fat was cleaned from all sides of the vessel. Finally, the vessel was held from one end with a forceps and another forceps was used to squeeze the blood out of the vessel from the

other end. Collected arteries (10-50 mg) were kept in a 2 ml Eppendorf tube placed on ice until the end of the procedure and then frozen at -80˚C.

C. Vascular smooth muscle cell isolation and cell culture

Vascular smooth muscle cells (VSMC) were isolated from human placental chorionic plate arteries as described by Leik et al[165]. Briefly, placentas of consented normal pregnant women who delivered by C-section were collected and transferred to the lab as quick as possible. Chorionic plate arteries were identified based on the observation that these arteries cross over their counterpart veins. Arteries were dissected from the placental tissue, rinsed of blood with Hank's balanced salt solution containing 2% antibiotics and antimycotics (200 U/ml penicillin, 200 µg/ml streptomycin, 50 µg/ml amphotericin B, Gibco, Carlsbad, CA) for 3 times and cut from one side along its long axis to open the arterial lumen. Small pieces of the arterial sheet were cut and placed on their endothelial surface on 10 cm culture plates and left for few minutes to adhere to the plate surface. After that, 5 ml of Medium-199 (M-199, Gibco, Invitrogen, Carlsbad, CA) containing 10% fetal bovine serum (FBS, Gibco, Invitrogen, Carlsbad, CA), and 1% antibiotics and antimycotics (100 U/ml penicillin, 100 µg/ml streptomycin, 25µg/ml amphotericin B, Gibco, Invitrogen, Carlsbad, CA) was carefully added to the plates without disturbing the adherent explants. Explants were incubated at 37˚C with 5% CO_2 in a cell culture incubator (Thermo Fisher, Waltham, MA) and medium was replaced every 2 days. At the end of the first week, cells started to grow from the explants and after about 4 weeks cells were confluent. At this stage, cells were treated with M-199 without FBS for one day to eliminate the presence of contaminating endothelial cells and fibroblasts because, unlike smooth muscle cells, these cells cannot survive without a serum-enriched medium. Cultured VSMCs were then either passaged or frozen in liquid nitrogen for future use. Cells were used between passage 3 and 6.

D. HL-60 cells

HL-60 cells (ATCC, Manassas, VA)**,** a neutrophil-like cell line, were cultured in Iscove's Modified Dulbecco's Medium (IMDM, ATCC, Manassas, VA) supplemented with 10% fetal bovine serum (Gibco, Invitrogen, Carlsbad, CA) and 1% antibiotics and antimycotics (100 U/ml penicillin, 100 µg/ml streptomycin, 25µg/ml amphotericin B, Gibco, Invitrogen, Carlsbad, CA) as recommended by ATCC. Approximately 500,000 cells per ml were seeded in 5 ml of media in a T-25 flask for treatments.

E. Treatments of cell cultures

1. Control

Control flasks consisted of medium appropriate for the type of cells being cultured.

2. Neutrophils

a. Neutrophil isolation

Histopaque density gradient centrifugation was used for neutrophil isolation from whole blood obtained from normal nonpregnant or normal pregnant women. Five ml of Histopaque 1119 (Sigma-Aldrich, Saint-Louis, MO) were added to a 50 ml conical tube. Then, 5 ml with of Histopaque 1077 (Sigma-Aldrich, Saint-Louis, MO) were carefully layered on the top of the Histopaque 1119. After that 10 ml of fresh blood were carefully layered over the top of the Histopaque 1017. The tube was centrifuged at 700 x g for 30 minutes at room temperature. This resulted in the formation of 6 distinct

layers which are from the top to the bottom: plasma; mononuclear cell layer, which includes lymphocytes, monocytes and platelets; Histopaque 1077; granulocyte layer, which includes neutrophils; Histopaque 1119; and red blood cells (RBC). In addition to neutrophils, the granulocyte layer also includes basophils and eosinophils, however, these cells comprise only approximately 4% of the cells. The plasma, mononuclear cell layer, and Histopaque 1077 to within 0.5 cm of the granulocyte layer were carefully aspirated and discarded. The granulocyte layer cells were carefully transferred to a new 50 ml tube. To wash the cells, 10 ml of PBS were added to the cells and the tube was centrifuged at 200 x g for 10 minutes at 4˚C. The PBS was carefully aspirated and the cell pellet re-suspended in another 10 ml of PBS. The tube was centrifuged at 200 x g for 10 minutes at 4˚C to pellet the cells. To lyse the RBCs, which cause the pellet to be red in color, 3 ml of ice-cold sterile filtered double deionized water (ddH_2O) were added and the pellet was gently re-suspended. After exactly 30 seconds, 1 ml of 0.6 M potassium chloride (KCl) was added to restore tonicity, and then the tube was centrifuged at 200 x g at 4˚C for 4 minutes. The lysing step was repeated one more time if necessary. The supernatant was discarded and the pellet re-suspended in 1 ml of M-199.

b. Neutrophil counting

To count the neutrophils, 50 µl of cell suspension was added to 350 µl of trypan blue dye (Sigma-Aldrich, Saint-Louis, MO) and pipetted up and down several times to mix well. This resulted in a dilution factor of 8. Roughly 10 µl of the mixture was loaded onto a hemocytometer and neutrophils were counted in all four quadrants of the hemocytometer. The number of neutrophils in the four chambers was divided by four to get the average number of neutrophils per square. The volume of each square with the cover slip in place is 0.1 mm^3. So, to calculate the number of neutrophils in 1 ml, the average number of neutrophils per square was multiplied by 10^4 then by the dilution factor of 8.

Number of neutrophils per ml = average count per square x dilution factor x 10^4 x number of ml.

c. Neutrophil activation

Neutrophils were activated with 100 μM of arachidonic acid. Solution A was made by adding 10 μl of a 50 mg in 100 μl ethanol stock solution of arachidonic acid (Cayman Chemical, Ann Arbor, MI) to 1.08 ml of PBS. After that, 16.6 μl of solution A was added to 1 ml M-199 containing neutrophils isolated by Histopaque and the cell suspension was incubated in a rotator for 30 minutes at 37˚C.

d. Treatment with neutrophils

Neutrophils were counted on a hemocytometer and a volume containing 62,500 activated neutrophils were added to VSMCs in a T-25 flask containing 5 ml of M-199 with 10% FBS and 1% antibiotics/antimycotics.

3. ROS

Reactive oxygen species (ROS) were generated by using 0.05 mM hypoxanthine (Sigma, Saint-Louis, MO) and 0.003 U/ml xanthine oxidase (Calbiochem, Darmstadt, Germany) in M-199 with 10% FBS. A 1 mM stock solution of hypoxanthine was prepared by adding 0.003 gm of hypoxanthine (MW 136.1) into 20 ml of ddH_2O. To dissolve the hypoxanthine, the solution was sonicated for 45 minutes in a water bath sonicator. To make a 20 ml stock of the ROS generating solution with a final concentration of

0.05 mM of hypoxanthine, 1 ml of the 1 mM hypoxanthine stock solution was added to 19 ml of M-199 with 10% FBS and 1% antibiotics/anti-mycotics. Xanthine oxidase was provided as a 20 U/ml buttermilk stock solution. For a final concentration of 0.003 U/ml xanthine oxidase in the 20 ml hypoxanthine stock solution, 3 µl of the 20 U/ml xanthine oxidase stock was added. The ROS generating solution was added to VSMCs in T-25 flasks.

4. Tumor necrosis factor α (TNFα)

Ten µg of recombinant human TNFα (R&D Systems, Minneapolis, MN) was reconstituted in 1 ml of sterile PBS containing 1% bovine serum albumin, aliquoted into 0.5 µg/50 µl aliquots and stored in -80˚C. For a final concentration of 1 ng/ml of TNFα, 0.5 µl of 0.5µg/50µl aliquot was added to VSMCs in a T-25 flask containing 5 ml of medium M-199 with 10% FBS and 1% antibiotics/anti-mycotics.

5. 5-Aza-2-deoxycytidine (5-Aza)

A 25 mM stock solution was prepared by adding 0.88 ml of ddH_2O to 5 mg of 5-Aza (Sigma-Aldrich, Saint-Louis, MO). The stock was divided into 20 µl aliquots. For a final concentration of 10 µM of 5-Aza, 2 µl of the stock were added to VSMCs or HL-60 cells in a T-25 flask containing 5 ml of medium with 10% FBS and 1% antibiotics/anti-mycotics.

6. Phorbol 12-myristate 13-acetate (PMA)

A first stock solution of 8 M was made by adding 1ml of dimethyl sulfoxide (DMSO, Sigma-Aldrich, Saint-Louis, MO) to 5 mg of PMA (Sigma-Aldrich, Saint-Louis, MO). A second stock solution of 0.1 mM was made by adding 1 µl of the first stock solution to 799 µl of DMSO. First and second stock solutions were divided into 50 µl aliquots, light protected and stored at -20˚C. For a final concentration of 10^{-8} M of PMA, 0.5 µl of 0.1 mM stock was added to HL-60 cells in a T-25 flask containing 5 ml of 10% FBS medium and 1% antibiotics/anti-mycotics.

7. Linoleic acid

A 0.11 M stock solution of linoleic acid was made by adding 1,520 µl of 100% ethanol to a vial containing 50 mg of linoleic acid in 200 µl ethanol (Cayman Chemicals, Ann Arbor, MI). For a final concentration of 70 µM, 3.18 µl of the stock solution was added HL-60 cells in a T-25 flask containing 5 ml of 10% FBS medium and 1% anti-biotics/anti-mycotics.

F. Cell Collection

T-25 flasks were kept on ice during the process of cell collection. For cultured VSMCs, medium was aspirated from the attached VSMCs on the floor of a T-25 flask and either saved for future analysis or discarded. To wash the cells on the floor of the flask from residual medium, FBS and dead cells, 2 ml of ice cold sterile PBS (Gibco, Carlsbad, CA) was added to the T-25 flask and the flask was mixed for a few seconds in an orbital motion, and the PBS was aspirated. The washing step was repeated once more. After that, cells were scraped in 1 ml of ice cold PBS and transferred to a 2 ml Eppendorf tube. For HL-60 cells, a T-25 flask was mixed gently and 2 ml of media were transferred to a 2 ml Eppendorf tube. When a treatment that caused cell activation and adhesion to the bottom of the flask was performed, cells

were scraped before collecting the media. Cells were pelleted down by centrifuging the tube at 3,000 x g for 10 minutes at 4˚C. The supernatant was aspirated, and cells were either processed immediately or stored at -80˚C for later use. For HL-60 cells, media (supernatant) was either discarded or saved at -20˚C.

G. Immunohistochemistry

1. Sample preparation and formalin-fixation

Omental fat biopsies were fixed in formalin within one day from the time of collection. Fat was cut into smaller pieces (approximately 1cm X 1cm X 0.5 cm) with scissors. One to two of these pieces were placed in a tissue cassette (Tissue-Tek Uni-Cassette, Sakura, Torrance, CA). Cassette were then closed, labeled and submerged in a jar of 10% neutral buffer formalin (Sigma-Aldrich, Saint-Louis, MO). The jar was kept rotating in an Excella E24 incubator shaker (New Brunswick Scientific, Edison, NJ) at 250 rpm for five days at room temperature in order to fix the tissue. On the fifth day, cassettes were opened and tissue was inspected for proper fixation based on appearance and touch. Cassettes were then washed from formalin with running ddH_2O and placed in 100 mM phosphate buffer (pH=7.5), and then cassettes were kept in the refrigerator (4˚C) until time for paraffin embedding.

2. Paraffin embedding and tissue block preparation

For paraffin embedding, an automated tissue processor (Shandon Citadel 2000 tissue processor, Shandon Scientific limited, Cheshire, England) was used. The machine first dehydrated the samples by passing them through a graded alcohol series of 70%, 85%, 95%, 95%, 100%, and 100%. Tissues were then cleared with CitriSolv (Fisher Scientific, Malvern, PA) and finally embedded with paraffin. The paraffin embedded tissue was removed from the cassette and placed on a metal tray partially filled with

warm paraffin. The metal tray was then filled with paraffin and covered with the porous surface of the tissues cassette. More paraffin was added through the porous surface of the cassette and the metal tray and cassette unit was placed on ice so that the paraffin would cool down and solidify. Once the paraffin solidified, the tissue block was removed from the metal tray.

3. Tissue sectioning and slide preparation

Before the blocks were sectioned, paraffin that surrounded the embedded tissue was beveled with sharp blade to limit the amount of paraffin that the blade of the microtome had to cut during the sectioning process. Once the block was prepared, it was mounted on a microtome (Shandon AS325 Microtome), and the tissue was cut into 8 µm thick sections that were continuous with each other to form a ribbon. Ribbons were carefully transferred onto the surface of 37˚C ddH_2O bath (floating bath model 135, Fisher Tissue Prep, Fisher Scientific, Malvern, PA). The ribbon was carefully separated into pieces of 2 or 3 sections and each section was placed on a Superfrost plus glass slide (Fisher Scientific, Malvern, PA). To ensure firm adherence of the tissue sections on the slides, the glass slides were placed on a 37˚C slide warmer overnight.

4. Immunohistochemical staining

a. Tissue preparation

Slides were labeled and placed in a slide holder. Slides were submerged in three separate champers of Histoclear (National Diagnostics, Atlanta, GA) for 5 minutes each, to deparaffinize the tissues. Tissues were then hydrated in a graded alcohol series of 100%, 100%, 95%, 95%, 85, and 50% for 2 minutes each. After that, slides were incubated in 100 mM phosphate buffer (pH=7.5) for 10

minutes. To quench the endogenous peroxidase activity of the tissues, slides were incubated in 3% hydrogen peroxide in methanol for 30 minutes. After that, the slides were washed in 100 mM phosphate buffer (pH=7.5) for 5 minutes and then in ddH_2O for 6 minutes.

b. Antigen retrieval

For antigen retrieval, slides were place in a plastic container containing 250 ml of 10 mM citrate buffer (pH=6). The plastic container was placed in an 8-quarter programmable pressure cooker (Cook Essentials, CPE800) filled with 2-3 L of ddH2O and the slides were pressurized on low setting for 5 min. Once finished, the pressure was released and the plastic container was removed from the pressure cooker and cooled to room temperature for 15 minutes.

c. Blocking

A hydrophobic glue marker (Pap Pen, Research Products International Corp, Mt. Prospect, IL) was used to draw a hydrophobic barrier around each tissue specimen. Ten percent normal goat serum blocking solution (Invitrogen, Carlsbad, CA) was applied on each specimen and incubated for 30 minutes in a humidity chamber. Slides were then washed 3 times with phosphate buffer saline containing 0.05% Tween-20, 2 minutes each.

d. Staining

Rabbit anti-human thromboxane synthase (1:50, Proteintech group, Chicago, IL) or rabbit anti-human MMP-8 antibody (1:100, Proteintech group, Chicago, IL) were pre-diluted with 100 mM phosphate buffer (pH=7.5). Slides were placed in a humidity chamber and 100 µl of diluted antibody were added onto each tissue specimen and incubated for 1 hour. A negative control slide from a preeclamptic patient was stained along with the other slides. For the negative control slide, 100 µl of rabbit primary antibody isotype control (Invitrogen, Carlsbad, CA) was applied on each tissue specimen. Slides were then washed 3 times in 0.05% Tween-20 PBS, 2 minutes each, and placed back into the humidity chamber. After that, 2 drops (~100 µl) of horseradish peroxide polymer conjugate (SuperPicture kit, Invitrogen/Zymed laboratories, South San Francisco, CA) were applied on each specimen and incubated for 10 minutes. Slides were then washed in 0.05% Tween-20 PBS 3 times, 2 minutes each, and placed back in the humidity chamber. After that, 2 drops (~100 µl) of diaminobenzidine substrate (SuperPicture kit, Invitrogen/Zymed laboratories, South San Francisco, CA) were applied on each specimen and incubated for 5 minutes. Lastly, slides were washed in 0.05% Tween-20 PBS 3 times, 2 minutes each.

e. Counterstaining

For counterstaining, slides were dipped once in 1:5 dilution of hematoxylin (Hematoxylin QS, Vector Laboratories, Burlingame, CA) and removed quickly. This was followed immediately with two separate rinses in ddH_2O. Then the slides were dipped 5 times in 0.05% acetic acid in acetone, 2 seconds each.

5. Tissue preservation

Slides were dehydrated in graded alcohol series of 50%, 85%, 95%, 95%, 100%, and 100%, 2 minutes each, and then placed in Histoclear twice, 3 minutes each. After the slides were removed from Histoclear, 2 drops of Vectomount (Vector Laboratories, Burlingame, CA) were added onto each slide and a coverslip was carefully placed on each slide without trapping air bubbles. Slides were left to dry overnight before being analyzed under the microscope.

6. Data analysis for immunohistochemistry

Slides were analyzed under a light microscope (Olympus BH2, Opelco, Washington, DC) equipped with a digital camera (Olympus QColor5, Canada). Vessel diameter was measured by image analysis software (CellSens Digital Imaging Software, Olympus America, Center Valley, PA) and vessels between 10 μm and 200 μm in diameter were analyzed since these vessels represent resistance-sized blood vessels. An average of 35 vessels were analyzed per slide. Vessel staining for thromboxane synthase or MMP-8 was evaluated using a visual score ranging from 0 to 4 where 0 means no staining and 4 means dark and extensive staining. Visual scoring was verified by a second investigator and by measuring the optical density of staining (OD) using the image analysis software. Optical density of staining in vessels was normalized to the optical density of the background. Slides were also analyzed for percentage of vessels stained and percentage of vessels with leukocyte staining for thromboxane synthase or MMP-8. The percentage of stained vessels and the percentage of vessels with stained leukocyte were calculated by the following equations:

$$\text{Percentage of stained vessels} = \frac{\text{Number of stained vessels}}{\text{Total \# of vessels}} \times 100\%$$

Percentage of vessels with stained leukocytes = $\frac{\text{Number of vessels with stained leukocytes}}{\text{Total \# of vessels}}$ x 100%

H. DNA extraction from omental arteries or cells, and DNA concentration measurement

DNA was extracted from omental arteries or cells using QuickGene DNA tissue kit and QuickGene-Mini80 system (AutoGen, Holliston, MA) according to the manufacture's protocol. For omental arteries, about 10 mg of arteries were cut into small pieces and lysed by incubating the arteries in 180 µl of tissue lysing buffer and 20 µl of proteinase K on a rotary shaker at 55˚C for 2 hours (Eppendorf Thermomixer Shaker, Eppendorf, Hauppauge, NY). Cells (around 10^6 cells) were lysed in the same way but were incubated for 30 minutes. RNase treatment was done by adding 20 µl of RNase A (100 mg/ml, Qiagen, Valencia, CA) to the lysate and incubating the mixture for 2 minutes at room temperature. DNA was eluted in 50 µl of the elution buffer to insure a high amount of DNA at low volumes.

DNA concentration was measured and DNA quality was assisted by using the NanoDrop 1000 Spectrophotometer (Thermo Scientific, Asheville, NC). Samples with an $A_{260/280}$ ratio of 1.8 were considered to be pure and used for study.

I. Bisulfite treatment

Genomic DNA was bisulfite treated using MethylEasy™ Xceed kit (Human Genetic Signatures, Randwick, Australia) as indicated by the user manual. Bisulfite treatment of genomic DNA causes hydrolytic deamination of unmethylated cytosines resulting in their conversion into uracils. Methylated cytosines are resistant to the effect of bisulfite and remain as cytosines. The amount of starting genomic

DNA used per reaction was 1000 ng. Based on the kit standard protocol, the combined volume of DNA solution and nuclease free water was 20 µl. The minimum DNA concentration required for each sample to have 1000 ng of DNA in 20 µl is 50 ng/µl. When the DNA concentration was less than 50 ng/µl, the sample was concentrated by using Savant DNA 120 Speed Vac Concentrator (Thermo Scientific, Asheville, NC).

J. Illumina Infinium Human Methylation27 BeadChip assay

The high throughput Illumina Infinium HumanMethylation27 BeadChip assay (Illumina, San Diego, CA) was used for DNA methylation analysis. This assay allows the examination of 27,578 CpG dinucleotides located within the proximal promoters of 14,495 genes. The BeadChip was run by the Nucleic Acids Research Facility at VCU using the standard protocol provided by Illumina. In brief, 10 µl of bisulfite treated DNA (50 ng/ µl) was isothermally amplified at 37˚C for 24 hours. The amplification product was enzymatically fragmented and the fragmented DNA was purified, and applied to BeadChip for hybridization. During hybridization, DNA anneals to specific single stranded oligonucleotides, which are covalently linked to different types of beads. Each CpG site is presented by 2 types of beads, which correspond to the nucleotide identity, and thus the methylation status, of the bisulfite treated cytosine at that site. Hybridization was followed by single-base extension of the oligonucleotides where the hybridized DNA was used as a template to incorporate hapten labeled dideoxynucleotides. After that, the chip was fluorescently stained, and then scanned for the intensities of the methylated and the unmethylated bead types using the Illumina BeadArray Reader. The raw data was analyzed with the Illumina Bead Studio software. DNA methylation values (β values) were assigned to each CpG site by subtracting the background intensity of negative controls from both the methylated and unmethylated intensities and then taking the ratio of the methylated intensity to the sum of both methylated and

unmethylated intensities. Therefore, the β value can be anywhere between 0 and 1 where 0 means no methylation and 1 means full methylation.

1. Statistical analysis

Statistical analysis for the Illumina Infinium Human Methylation27 BeadChip assay was done by Dr. Kellie Archer (Department of Biostatistics, VCU). For each CpG site a two-sample t-test was performed comparing the seven severe pre-eclampsia samples to the five normal samples with respect to proportion methylated. Specifically, for CpG sites i=1,…,27,578, the hypotheses tested were:

$\mathbf{H_0}$: $\bar{\beta}_{i,pre-eclampsia} = \bar{\beta}_{i,normal}$

$\mathbf{H_A}$: $\bar{\beta}_{i,pre-eclampsia} \neq \bar{\beta}_{i,normal}$

The p-values from the two-sample t-tests were obtained for all CpG sites. The p-value is the probability of obtaining a test statistic as or more extreme as the one observed under the conditions of the null hypothesis. In most scientific endeavors, an $\alpha = 0.05$ threshold is customarily applied so that a p-value < 0.05 is considered as evidence for the alternative hypothesis, that is, $p < 0.05$ typically indicates a significant finding. However, application of an $\alpha = 0.05$ threshold to univariable tests of significance in high-throughput genomic settings will yield a large number of Type I errors simply by chance. When analyzing high-throughput genomic data, the multiple comparison problem is most often addressed through estimation of the false discovery rate (FDR). To control for multiple hypothesis testing, the p-values were subsequently used in estimating FDR using the q-value method[166]. More specifically, when testing m null hypotheses, we may want to control the number of rejected null hypotheses that are truly null (F) among all those null hypotheses that are rejected (S). The q-value is such a method that for a particular feature is defined to be the expected proportion of false positives among all features as or more

extreme than the one observed[166]. For a given p-value threshold t where $0 \leq t \leq 1$, we want to estimate $FDR(t) = E(F(t)/S(t)) \approx E(F(t))/E(S(t))$.

F(t) represents the number of false discoveries at threshold t while S (t) represents the number of null hypotheses considered significant at threshold t. Formally, FDR(t) is estimated as

$$FDR(t) = \frac{\pi_0 mt}{S(t)} = \frac{\pi_0 mt}{\sum_{g=1}^{m} I(p_g \leq t)},$$

where π_0 represents the proportion of hypotheses for which the null is true and $I(p_g \leq t)$ is 1 if the p-value for the g^{th} CpG site is less than or equal to the threshold t. For application datasets, π_0 is typically unknown and so is estimated using the distribution of raw p-values using either a smoothing or bootstrap method. In this study CpG sites with a FDR < 10% were considered significant.

2. Gene Ontology terms

For CpG sites identified as significant, the CpG sites were mapped to Gene Ontology terms, molecular function (MF) and biological process (BP), and a hypergeometric test was performed to determine whether any term was over-represented among those CpG sites identified as significant compared to the number of CpG sites mapping to that term on the entire array. For MF and BP terms, a p-value of less than 0.05 was considered significant

3. Canonical pathway and network identification

Genes with statistically differentially methylated CpG sites were imported into Ingenuity Pathways Analysis software (IPA, v9; Ingenuity Systems, Redwood City, CA) to identify canonical pathways and gene-to-gene interaction networks within our dataset. Canonical pathways and gene networks were algorithmically constructed based on published literature in the Ingenuity Knowledge Base, where each relation was supported by at least one reference.

K. Bisulfite Sequencing

The bisulfite treated DNA was amplified with primers that flank the region of interest (first round primers). Another set of primers (second round or nested primers) was used to amplify a region within the first PCR product, which included the CpG dinucleotides that were studied. The second round (nested) PCR was performed to reduce the contamination caused by nonspecific primer annealing and to increase the amount of the desired product. Methyl Primer Express Software (Applied Biosystems) was used to design the first round primers and the sound round (nested) primers. Primers were synthesized by Integrated DNA Technologies (IDT) and provided in a lyophilized form. The lyophilized primers were reconstituted with nuclease free water. The volume of the added nuclease free water was calculated to have a final concentration of 150 pMol/µl of the primers. The first round PCR was prepared with 12.5 µl of 2 X PCR master mixes (AmpiTaq Gold PCR master, Applied Biosystems), 5 µl of the bisulfite treated DNA (20ng/µl), 2 µl of the first round primers and 5.5 µl of nuclease free water. The following thermal cycling profile was used: 1 cycle of 95˚C for 3 minutes for initial denaturation and polymerase activation; 30 cycles of 95˚C for 1 minute for denaturation, 58˚C for 2 minutes for annealing, and 72˚C for 2 minutes for elongation; and 1 cycle of 72˚C for 10 minutes for final elongation. The first round PCR product was purified using QIAquick PCR Purification kit (Qiagen, Valencia, CA), and then subjected to a second round of PCR using the nested primers. The second round PCR was prepared with 12.5 µl of master mix

(FastStart High Fidelity PCR System, Roche), 2 µl of nested primers, 2 µl of the first round PCR product, and 8.5 µl of nuclease free water. The following thermal cycling program was used: one cycle of 95˚C for 2 minutes for initial denaturation and polymerase activation; 35 cycles of 95˚C for 30 seconds for denaturation, and 58˚C for 30 seconds for annealing, and 72˚ C for 3 minutes for final elongation; and 72˚C for 7 minutes for final elongation. A Mastercycler ep Thermal Cycler (Eppendorf, Hauppauge, NY) was used to run the first and the second round PCR reactions.

Before purifying the second PCR product, 5 µl of the second PCR product was mixed with 1 µl of Gel Loading Dye Blue (6X) (New England BioLabs, Ipswich, MA) and loaded on 2% Tris-Acetate-EDTA (TAE) agarose gel. To make 2% agarose gel, 0.2 g of agarose (Invitrogen, Carlsbad, CA) were added to 10 ml of 1X TAE buffer (Cellgro, Manassas, VA) and microwaved for 1 minute. The solution was left to cool for a few minutes, and then poured into gel casters. Gels were left to solidify for 20 minutes and used immediately or soaked in 1X TAE buffer and stored at 4˚C until used. To determine the size of the bands on the gel, 6 µl of 1kb DNA Ladder (New England BioLabs, Ipswich, MA) were loaded into the first lane. The gel was run in 1X TAE buffer at 100 V for 45 minutes. The gel was stained with ethidium bromide by soaking it in 100 ml of 1X TAE buffer containing 10 µl ethidium bromide (Invitrogen, Carlsbad, CA) for 20 minutes and then destained by soaking it in 100 ml of 1X TAE buffer without ethidium bromide for 5 minutes. After that, the gel was scanned and viewed with Molecular Imager Gel Doc XR+ System (Bio-Rad Laboratories, Hercules, CA).

MethylEasy™ Xceed kit is provided with a control sample of untreated genomic DNA (control sample 1), a control sample of bisulfite treated DNA (control sample 2), control first round PCR primers (3A), and control second round PCR primers (3B) for nested PCR. Control Sample 1 and a no template control sample were processed in parallel with the test samples. Control Primers 3A and 3B are validated PCR primers that are specific for converted DNA. These primers were used to check the integrity of the recovered DNA. Treated control sample 1, control sample 2, treated no template control sample, and selected treated test samples were amplified with control primers 3A and 3B, and the second round PCR

products were run on 2% agarose gel. The expected amplicon size for the control second round PCR primers was 240 base pair. Second round PCR product was purified using QIAquick PCR Purification kit (Qiagen, Valencia, CA).

The second round PCR product was cloned using TOPO TA Cloning kit (Invitrogen, Carlsbad, CA). In brief, 1µl of the second round PCR product was added to 1 µl of TOPO cloning vector and the mixture was incubated for 10 minutes. TOPO cloning vector is a linearized vector with a single overhanging 3´ thymidine (T) residue on each end. The enzyme blend used in the FastStart High Fidelity PCR System used in the second round PCR has a non-template-dependent terminal transferase activity that results in the addition of a single adenosine (A) residue to the 3´ end of the PCR product, making this system compatible for T/A cloning. This allows PCR inserts to ligate efficiently with the vector. After ligation, competent E.coli bacteria provided by the kit were transformed and then plated on selective Lysogeny broth (LB) agar plates. To make LB Agar plates, 40 g of LB agar and 20 g of LB broth (Fisher Scientific, Pittsburgh, PA) were added to 1 L of ddH_2O and stirred with a magnetic stirrer on a hot plate (70°C) until dissolved. The suspension was transferred to a bottle and autoclaved. After that, 2 ml of 25 mg/ml ampicillin (Fisher Scientific, Pittsburgh, PA) were added to the suspension, which was gently swirled to mix. Before adding the ampicillin, the suspension was cooled down to avoid damaging the ampicillin with high temperature. Ten ml of the suspension was add into a sterile petri dish (Fisher Scientific, Pittsburgh, PA) and evenly distributed by gentle agitation. Plates were left to cool and solidify and then stored in a sterile bag at 4˚C until used. Before culturing the bacteria on LB agar, 20 µl of IPTG/X-Gal solution (Fisher Scientific, Pittsburgh, PA) was added to each plate and evenly distributed. X-gal was added for blue/white screening of colonies. Blue color results when the X-gal is cleaved by the β-galactosidase enzyme encoded by a gene engineered into the plasmid. Insertion of the clone DNA disturbs the reading frame of the β- galactosidase gene making the bacteria unable to cleave X-gal which results in the white colony. Ten white colonies were randomly selected and each was cultured in 1.5 ml of LB media at 37˚C overnight. LB media was prepared by following the same protocol for LB agar palettes,

except no agar was added to the suspension. Plasmid was purified using QIAprep Spin Miniprep Kit (Qiagen, Valencia, CA) and screened with M13 primer system provided by TOPO TA Cloning kit. PCR products were run on 2% agarose gel to verify the presence of the insert in the vector. Clones were sent to VCU nucleic acid research facilities for sequencing. Sequencing data were analyzed using MacVector software (MacVector, Cary, North Carolina). The following formula was used to calculate the percentage of methylation:

$$\text{Percentage of methylation of a given CpG site} = \frac{\text{\# of clones where that site was methylated}}{\text{\# of total clones}} \times 100\%$$

L. RNA extraction, cDNA synthesis and quantitative real time PCR (qRT-PCR)

RNA was extracted from omental arteries using RiboPure kit (Ambion, Austin, TX) according to the manufacturer's method. About 25 mg of arteries were cut into small pieces with a scissor and homogenized in 1 ml of the TRI reagent solution with a rotor stator homogenizer (PRO 200, PRO Scientific, Germantown, TN) at 200 rpm for 30 seconds divided into six 5 seconds intervals. Processed samples were loaded into spin columns, washed 3 times and RNA was eluted in 50 μl of the elution buffer. DNase treatment was performed after the first washing step by adding 40 μl of DNase solution (TURBO DNase, Ambion, Austin, TX) to each spin column and incubating for 5 minutes.

For cultured VSMC or HL-60 cells, RNA was extracted using QuickGene RNA cultured cell HC kit and Quick gene Mini-80 (AutoGen, Holliston, MA) according to the manufacturer protocol. For DNase treatment, 40 μl of DNase solution (TURBO DNase, Ambion, Austin, TX) were add to each cartridge and incubated for 5 minutes. RNA was eluted in 50 μl of the elution buffer.

RNA concentration was measured and RNA quality was assessed by using the NanoDrop 1000 Spectrophotometer (Thermo Scientific, Asheville, NC). Samples with an $A_{260/280}$ ratio of 1.8 - 2 were considered pure and used for cDNA synthesis. RNA was reverse transcribed to cDNA using the iScript cDNA Synthesis Kit (Bio-Rad Laboratories, Hercules, CA). Quantitative RT-PCR reactions were performed with RT² SYBR® Green qPCR Mastermix (SABiosciences, Frederick, MD) on Mastercycler ep realplex S thermal cycler (Eppendorf, Hauppauge, NY). As recommended by SABiosciences, 8 ng of cDNA was used for each qRT-PCR reaction. Glyceraldehyde 3-phosphate dehydrogenase (*GAPDH*) gene was used as a housekeeping gene. qRT-PCR primers are listed in Table 1. Melting curve analysis was used to verify there was no DNA contamination, which is indicated by the presence of more than one peak leading to false positive data. Fold changes were calculated by the ΔΔCT method using Microsoft Excel.

M. Microarrays

The expression of 84 transcription factor genes was assessed by using Human Transcription Factors PCR Array (Qiagen, Valencia, CA) according to the manufacturer's instructions. Data analysis was performed by using the Excel based RT² Profiler PCR Array Data Analysis Template v3.3 provided Qiagen.

N. Protein extraction from blood vessels

Radio Immuno Precipitation Assay buffer (RIPA) containing 150 mM sodium chloride, 1.0% NP-40, 0.5% sodium deoxycholate, 0.1% sodium dodecyl sulphate (SDS) was used as a lysing buffer. For each 1 ml of RIPA buffer, 10 µl of Halt protease and phosphatase inhibitor cocktail (Pierce, Rockford, IL)

was added before use. Fresh or frozen omental arteries (40-50 mg) were cut into small pieces to avoid trapping the vessels between the blades of the rotor stator homogenizer. Arteries were cut with a clean curved tip scissor while keeping the tissue on ice. RIPA buffer (100-150 µl) was added to the cut arteries. Arteries were then homogenized by a rotor stator homogenizer (PRO 200, PRO Scientific, Germantown, TN) for 1 minute at a speed of 300 rpm while keeping them on ice. The homogenate was consistently agitated for 2 hours at 4˚C using an orbital shaker (Orbit LS, Labnet, Edison, NJ) then centrifuged at 14000 x g for 10 minutes at 4˚C. Supernatant was transferred to a new microcentrifuge tube and stored at -20˚C.

O. Protein extraction from cells

RIPA buffer (50 µl) containing Halt protease and phosphatase inhibitor cocktail was added to the cell pellet and the cells were lysed by sonicating the pellet for 2 seconds for 10 times with a sonicator probe (1/8" Microtip, EpiShear Sonicator, Active Motif, Carlsbad, CA). Lysate was constantly agitated for 30 minutes at 4˚C using an orbital shaker (Orbit LS, Labnet, Edison, NJ) then centrifuged at 14000 x g for 10 minutes at 4˚C. Supernatant was transferred to a new microcentrifuge tube and stored at -20˚C.

P. Measurement of protein concentration

Protein concentrations were measured using the bicinchoninic acid (BCA) protein assay (Thermo Scientific, Asheville, NC) in plate format. Absorbance measurements were captured with FLUOstar OPTIMA plate reader (BMG Labtech, Cary, NC). Using MARS software provided with the machine, the standard samples were used to derive a standard curve of absorbance versus micrograms of protein and the protein concentrations of the unknown samples were determined from the standard curve in µg/ml.

Q. Western blot

1. Gel Casting

Bio-Rad casting apparatus and 1.5 mm combs were used to cast Tris-Glycine SDS gels of standard size (3" x 5" x 0.2"). Each gel consisted of 2 parts: An upper part of about 2 cm of stacking gel and a lower part of resolving gel. Ten ml of 10% resolving gel were made by mixing 4 ml of ddH_2O, 3.3 ml of 30% acrylamide mix (Bio-Rad, Hercules, CA), 2.5 ml of 1.5 M Tris-HCL (pH 8.8) (Bio-Rad, Hercules, CA), 100 µl of 10% SDS (Bio-Rad, Hercules, CA), and 100 µl of 10% ammonium persulfate (Fisher Scientific, Fair Lawn, NJ). To initiate the polymerization process of the mixture, 10 µl of N, N, N', N'- teramethylethylenediamine (TEMED, Sigma-Aldrich, Saint Louis, MO) were added and then about 8 ml of the mixture were poured into the gel caster, leaving about 2 cm of space for the stacking gel. The mixture was layered with a few drops of 1-butanol (Sigma-Aldrich, Saint-Louis, MO) and allowed to set. To make 10 ml of (4%) stacking gel, 3.4 of ml H_2O, 850 µl of 30% acrylamide mix, 625 µl 1.5 Tris (pH 8.8) (Bio-Rad, Hercules, CA), 50 µl 10% SDS and 10 µl 10% ammonium persulfate were mixed together and 10 µl of TEMED was added. The mixture was poured into the gel caster on the top of the resolving gel until the space that was left over was filled, and then a comb was inserted to form the wells and define the lanes in the gel. The gel was left to set for 15 minutes, and then it was either used immediately or soaked in PBS and stored in 4˚C overnight to be used in the next day.

2. Sample preparation and loading

Fermentas protein loading buffer pack (Thermo Scientific, Asheville, NC) was used for sample loading. A total volume of 50 µl was loaded per lane. This included: the volume of lysate required to get 50 or 100 µg of protein per lane (calculated for each sample), 2.5 µl ($1/20^{th}$ of the final volume) of 20X

Fermentas reducing agent, 10 µl (1/5th of final volume) of 5X Fermentas loading buffer, and the volume of ddH_2O required to bring the final volume to 50 µl. Samples were vortexed for a few seconds, flash spined, and boiled at 95-100˚C for 5 minutes. Samples were cooled to room temperature and then loaded into the wells of the gel using gel loading pipette tips. Ten µl of precision plus all blue protein standards (Bio-Rad, Hercules, CA) were used to determine the molecular weight of the detected bands. They also served as a positive control for the electrophoresis and transfer steps.

3. Gel electrophoresis

The XCell SureLock Mini-Cell system (Invitrogen, Carlsbad, CA) was used for gel electrophoresis. The comb was removed and the wells were rinsed with ddH_2O, then with running buffer and the gel was assembled with the other parts of the electrophoresis cell. A 1X dilution of 10x Tris/Glycine/SDS buffer (Bio-Rad, Hercules, CA) was used as the running buffer. The inner chamber of the cell assembly was filled with running buffer so that the buffer level was above the level of the wells, and checked for any leak. After loading the samples into the gel, the outer chamber was filled with about 650 ml of running buffer and the cell was hooked to a power supply (PowerEase 500, Invitrogen, Carlsbad, CA) inside a refrigerator. The gel was run at 120 V for 1.5 hour, or until the dye front reached the bottom of the gel. A magnetic stirrer was used to constantly move the buffer in the outer chamber to enhance heat dissipation.

4. Preparation of the transfer membrane, plotting pads and filter papers

Polyvinylidene Fluoride (PVDF) membrane (0.2 µ pore size, Millipore) was pre-wetted in 100% methanol for 30 seconds, or until the membrane became translucent gray in color, rinsed in ddH_2O and

soaked in ice cold 40% methanol transfer buffer for 15-20 minutes for equilibration. The blotting pads were also soaked in ice cold 40% methanol transfer buffer and pressed to remove air bubbles. Filter papers were soaked briefly in ice cold 40% methanol transfer buffer immediately before their use.

5. Protein Transfer

XCell II Blot Module along with XCell SureLock Mini-Cell (Invitrogen, Carlsbad, CA) was used for protein transfer. A 25X tris-glycine transfer buffer was made by dissolving 18.2 g (12 mM final concentration) of tris base (Research Organics, Cleveland, Ohio) and 90.0 g (96 mM final concentration) of glycine (Caledon, Georgetown, Ontario, Canada) in 500 ml of ddH_2O. On the day before the run, 1L of 40% methanol 1X tris-glycine transfer buffer was made by mixing 40 ml of 25X tris-glycine transfer buffer, 200 ml of methanol and 760 ml of ddH_2O. The 40% methanol 1X tris-glycine transfer buffer was kept in the refrigerator overnight to cool it down to 4˚C before use. The gel was transferred immediately without soaking it into transfer buffer. The gel, along with the blotting pads, filter papers and PVDF membrane were assembled in the XCell II Blot Module as indicated by the user manual, and then the XCell Blot Module was placed into the XCell SureLock Mini-Cell. The inner chamber was filled with about 200 ml of the 40% methanol 1X tris-glycine transfer buffer and checked for any leaks. The outer chamber was filled with approximately 650 ml of ddH_2O. The cell was hooked to PowerEase 500 power supply placed inside a refrigerator and the gel was run at 25 V for 2 hours. A magnetic stirrer was used to constantly move the buffer in the outer chamber to enhance heat dissipation.

6. Blotting

The Odyssey blotting system (Li-cor, Lincoln, NE) was used for blotting of the membrane. The face of the membrane in approximation with the gel was marked. The membrane was blocked with 10 ml of 1:1 solution of Odyssey Blocking buffer (Li-cor, Lincoln, NE) and PBS for 1 hour at room temperature in a 50 ml conical tube placed on a rotator (Labquake rotator, Barnstead, Dubuque, IA). The membrane was then washed three times with PBS containing 0.1% Tween-20 for 5 minutes each.

The primary antibody was diluted in 10 ml of Odyssey buffer containing 0.1% Tween-20. After that, the membrane was incubated with the primary antibody solution overnight at 4˚C in 50 ml conical tube placed on the rotator. The membrane was then washed 4 times for 5 minutes each with 0.1% Tween-20 PBS. Secondary antibodies were diluted in 10 ml of 0.1% Tween-20 Odyssey blocking buffer in an amber 50 ml conical tube. Because the secondary antibodies are light sensitive, the membrane was protected from light from this step on. The membrane was incubated with the secondary antibody solution for 45 min at 4˚C. After that, the membrane was washed 4 times for 5 minutes each with 0.1% Tween-20 PBS. Then the membrane was washed 4 times for 5 minutes each with PBS alone and 4 times 5 minutes each with ddH_2O. Primary and secondary antibodies used are shown in Table 2.

7. Image analysis

The Odyssey infrared imaging system (Li-cor, Lincoln, NE) was used for scanning the membrane to detect and analyze immune reactive proteins on the blot. Before placing the membrane on the Odyssey scanner, the glass and silicon mat were carefully cleaned from dust. The scanning parameters were adjusted to obtain the highest possible image quality. Each band was surrounded by a rectangle and the intensity value of the band was calculated by multiplying the average intensity of the band by the area of the rectangle. The intensity value of a target protein band was divided by the intensity value of the corresponding β-actin band to normalize for loading errors. Normalized intensity value of the control

experiment was set as 100% and the change in the intensity of the target protein for each treatment was calculated relative to the control.

R. Enzyme-linked immunosorbent assay (ELISA)

Commercial ELISA kits were used to quantify total MMP-1 (pro-MMP-1 and active MMP-1) and TIMP-1 in VSMC culture medium. Medium was not concentrated, diluted or filtered before it was used in ELISA. Amersham human MMP-1 ELISA Biotrak System kit (GE Healthcare, Piscataway, NJ) was used for measuring total MMP-1, and Amersham human TIMP-1 ELISA Biotrak system kit (GE Healthcare, Piscataway, NJ) was used for measuring TIMP-1. Absorbance measurements were captured with FLUOstar OPTIMA plate reader (BMG Labtech, Ortenberg, Germany). MARS data analysis software was used to derive a standard curve of absorbance versus ng/ml of protein from the standard samples and determine the protein concentration (ng/ml) of the unknown samples from the curve. At the time of media collection, cells from the same T-25 flask were collected and processed for DNA extraction as explained above. For normalization, the total amount of MMP-1 or TIMP-1 protein (ng) in 5ml (volume of medium used in a T-25 flask) was divided by the total amount of DNA (μg) extracted from the cells of the same flask.

S. Enzyme immunoassay (EIA)

Thromboxane B_2 (TXB_2) Enzyme Immunoassay kit (Assay Designs, Ann Arbor, MI) was used to measure thromboxane B_2 in media as indicated by the manufacturer's protocol. Media was diluted by a factor of 1:1 before it was used in the assay. Absorbance measurements were captured using FLUOstar OPTIMA plate reader (BMG Labtech, Ortenberg, Germany) and thromboxane B_2 concentrations were

calculated in pg/ml using MARS data analysis software. For normalization, the total amount TXB_2 (pg) in 5ml (volume of medium used in a T-25 flask) was divided by the total amount of DNA (μg) extracted from the cells of the same flask.

Table 1: List of qRT-PCR primes used for gene expression.

Gene	Forward primer	Reversed primer
MMP1	SA Biosciences, Frederick, MD	
MMP8	SA Biosciences, Frederick, MD	
TBXAS1	SA Biosciences, Frederick, MD	
COL1A1	ACG AAG ACATCCCACCAA TCAC	CGTTGTCGCAGACGCAGA
GAPDH	GATTCCACCCATGGCAAATT	AGATGGTGATGGGATTTCCATT
TIMP1	CTGTGGCTCCCTGGAACA	CCAACAGTGTAGGTCTTGGTGAAG

Table 2: List of primary and secondary antibodies used for protein expression.

Protein	Primary antibody	Secondary antibodies
TBXAS1	Rabbit anti-human TBXAS1 (1:1000, Proteintech, Chicago, IL)	Alexa Fluor 680 donkey anti-rabbit (1:10,000, Invitrogen, Carlsbad, CA)
MMP-1	Goat anti-human MMP-1 (0.2 μg/ml, R&D Systems, Minneapolis, MN)	IRDye800 donkey anti-goat (1:20,000, Rockland, Gilbertsville, PA)
MMP-8	Rabbit anti-human MMP-8 (1:500, Proteintech, Chicago, IL)	Alexa Fluor 680 donkey anti-rabbit (1:20,000, Invitrogen, Carlsbad, CA)
COL1A1	Goat anti-human COL1A1 (1:1,000, Santa Cruz Biotechnology, Santa Cruz, CA)	IRDye800 donkey anti-goat (1:20,000, Rockland, Gilbertsville, PA)
β-actin	Rabbit anti-human β-actin (1:1,000, Sigma, Saint Louis, MO)	Alexa Fluor 680 donkey anti-rabbit (1:20,000, Invitrogen, Carlsbad, CA)
β-actin	Mouse anti-human β-actin (1:1,000, Sigma, Saint Louis, MO)	IRDye800 goat anti-mouse (1:20,000, Rockland, Gilbertsville, PA)

CHAPTER 3: DNA METHYLATION IS ALTERED IN MATERNAL BLOOD VESSELS OF PREECLAMPTIC WOMEN

A. Abstract

Methylation of cytosine in genomic DNA, especially cytosines clustered in gene promoters (CpG islands), is a major epigenetic alteration controlling gene expression. In general, hypomethylation of cytosines is associated with increased gene expression, whereas hypermethylation is associated with reduced gene expression. Little is known about the role of DNA methylation in preeclampsia. We analyzed 27,578 CpG sites that map to 14,495 genes in omental arteries of normal pregnant and preeclamptic women for DNA methylation status using the Illumina platform. We found 1,685 genes with a significant difference in DNA methylation at a false discovery rate of < 10% with many inflammatory genes having reduced methylation. Unsupervised hierarchical clustering revealed natural clustering by diagnosis and methylation status. Of the genes with significant methylation differences, 236 were significant at a false discovery rate of < 5%. When data were analyzed more stringently to a false discovery rate of < 5% and difference in methylation of > 0.10, 65 genes were identified, all of which showed reduced methylation in preeclampsia. When these genes were mapped to Gene Ontology for Molecular Functions and Biological Processes, 75 molecular functions and 149 biological processes were over-represented in the preeclamptic vessels. These included smooth muscle contraction, thrombosis, inflammation, redox homeostasis, sugar metabolism and amino acid metabolism. We speculate that reduced methylation may contribute to the pathogenesis of preeclampsia, and that alterations in DNA methylation resulting from preeclampsia may increase maternal risk of cardiovascular disease later in life.

B. Introduction

Preeclampsia is a pregnancy disorder that remains a worldwide health problem and a leading cause of preterm delivery and of maternal and infant mortality and morbidity[1]. It is a complex, multisystem disease which is diagnosed clinically by new onset of hypertension and proteinuria that occur after twenty weeks gestation in pregnant women who are otherwise healthy[1]. Preeclampsia is often associated with other end organ problems, such as cerebral, pulmonary and systemic edema, activation of the coagulation system, reduced utero-placental blood flow and intrauterine growth restriction. The pathophysiology of preeclampsia is not well understood. It has been considered as a two-stage disease where the first stage is poor placentation and the second stage is development of exaggerated maternal systemic inflammatory response[167].

Many studies have reported possible genetic contribution to preeclampsia based on inheritance patterns or mutations in candidate genes[168,169], however, few studies have examined the possible contribution of epigenetic mechanisms. Epigenetics is the study of changes in gene expression, which are mediated through mechanisms that do not involve changes in the DNA sequence. DNA methylation is the best characterized epigenetic mechanism[170]. It refers to the reversible addition of a methyl group (CH_3) at the 5' carbon of a cytosine in a CpG dinucleotide context. DNA methylation patterns can change in response to age, environmental stimuli, diet and oxidative stress[110,116,141]. The pattern of DNA methylation is maintained by DNA methyltransferase enzymes during future cell divisions[110]. In general, DNA hypomethylation is associated with increased gene expression whereas DNA hypermethylation is associated with decreased gene expression[171]. DNA methylation is involved in important biological processes such as tissue-specific gene regulation during development, X-chromosome inactivation and genomic imprinting[172].

Changes in DNA methylation patterns have been detected in a growing number of complex diseases including cancer[173], schizophrenia[174], neural tube defect[175] and cardiovascular diseases such as

atherosclerosis[129], ischemic heart disease and stroke[130]. Little information is available regarding DNA methylation in preeclampsia, but it might be an important pathologic mechanism because preeclampsia is associated with oxidative stress[41,89] and obesity[176], both of which can influence DNA methylation. It has been suggested the increased risk of preeclampsia in assisted reproductive technology pregnancies may be due to early epigenetic changes in gametes and/or embryos that contributes to abnormal placentation and development of preeclampsia[177]. Epigenetic changes associated with imprinted and non-imprinted genes have been demonstrated in preeclamptic placentas[144,145,178] and deletion of imprinted gene p57-Kip2 in mice is associated with hypertension and proteinuria[143], which are manifestations of preeclampsia[1]. In a study that investigated global DNA methylation profiles of placentas using Illumina GoldenGate Methylation Cancer panel I array, investigators reported promoter hypomethylation of 34 CpG sites in early-onset preeclampsia[147].

To date, there have been no reports dealing with DNA methylation in systemic blood vessels of the mother with preeclampsia. In this study, we used the Illumina HumanMethylation27 platform to simultaneously profile more than 27,000 CpG sites representing more than 14,000 genes in samples of omental fat arteries isolated from normal pregnant and preeclamptic women. Omental arteries were used because these arteries are a component of maternal systemic vasculature, and they play a role in blood pressure regulation by contributing to total peripheral vascular resistance.

C. Materials and methods

1. Study subjects

Omental fat biopsies of approximately 2 cm x 2 cm x 0.5 cm in size were collected from normal pregnant (n = 5) and preeclamptic (n = 7) women during medically indicated cesarean sections performed at MCV Hospital, Virginia Commonwealth University Medical Center, Richmond, VA. Once obtained,

the biopsy was placed in a sterile container on ice and transferred to the lab for processing as soon as possible. Preeclampsia was diagnosed in gravid females by new onset of hypertension (systolic blood pressure of ≥ 140 mmHg and/or diastolic blood pressure ≥ 90mmHg) and proteinuria (300 mg or more of protein in the urine per 24 h collection) that occurred in women who were otherwise normal [1]. Women with chorioamnionitis, maternal infections, active sexually transmitted diseases, lupus, or diabetes, and women who were smokers or in labor were excluded because these conditions are associated with inflammatory changes. Patient clinical data are shown in Table 3. All subjects gave informed consent. The Office of Research Subjects Protection at Virginia Commonwealth University approved this study.

2. Sample processing, DNA extraction, and bisulfite treatment

Fat biopsies from normal pregnant and preeclamptic women were dissected for omental arteries under a dissection microscope. Arteries and veins were distinguished from each other based on their morphology. In general, arteries were thicker, narrower and their branching points were more acute as compared to veins. Omental arteries were dissected and cleared carefully of adhering fat. DNA was extracted from the arteries (~10 mg in weight) using QuickGene DNA tissue kit S kit and QuickGene-Mini80 system (AutoGen, Holliston, MA) as recommended by the user manual. RNase treatment was performed with RNase A (Qiagen, Valencia, CA). DNA concentration was measured and its quality was assessed using NanoDrop 2000 spectrophotometer (Thermo Scientific, Wilmington, DE). DNA samples with $A_{260/280}$ ratio of 1.8 were considered to be pure and used in the study. DNA (1µg) was bisulfite treated using MethylEasy Exceed kit (Human Genetic Signatures, Randwick, Australia). DNA was eluted in 20 µl elution buffer for a final concentration of 50 ng/µl

3. Methylation assay

The high throughput Illumina Infinium HumanMethylation27 BeadChip assay (Illumina, San Diego, CA) was used for DNA methylation analysis. This assay allows the examination of 27,578 CpG dinucleotides located within the proximal promoters of 14,495 genes. The BeadChip was run by the Nucleic Acids Research Facilities at VCU using the standard protocol provided by Illumina. In brief, 10 µl of bisulfite treated DNA (50 ng/µl) was isothermally amplified at 37˚C for 24 h. The amplification product was enzymatically fragmented and the fragmented DNA was purified, and applied to the BeadChip for hybridization. During hybridization, DNA anneals to specific single stranded oligonucleotides, which are covalently linked to different types of beads. Each CpG site is presented by 2 types of beads, which corresponds to the nucleotide identity, and thus the methylation status, of the bisulfite treated cytosine at that site. Hybridization was followed by single-base extension of the oligonucleotides where the hybridized DNA was used as a template to incorporate hapten labeled dideoxynucleotides. After that, the BeadChip was fluorescently stained, and then scanned for the intensities of the methylated and the unmethylated bead types using the Illumina BeadArray Reader. The scanned arrays were processed using Illumina's GenomeStudio Methylation Analysis Module to obtain the β values for each CpG site, where β_{ij} represents proportion methylated for the i^{th} CpG site and the j^{th} array, and where β = 1 would indicate complete methylation and β = 0 would indicate no methylation. Validation of the BeadChip assay was performed by evaluating the quality of the hybridizations for six X-linked genes, and by using COBRA[179-181] for the -1538 CpG site upstream from the transcription start site for the matrix metalloproteinase-1 gene as we previously described[164].

4. Statistical analysis

For each CpG site a two-sample t-test was performed comparing the seven severe preeclampsia samples to the five normal samples with respect to proportion methylated. Specifically, for CpG sites i = 1,…,27,578, the hypotheses tested were:

H_0: $\bar{\beta}_{i,pre-eclampsia} = \bar{\beta}_{i,normal}$

H_A: $\bar{\beta}_{i,pre-eclampsia} \neq \bar{\beta}_{i,normal}$

The p-values from the two-sample t-tests were obtained for all CpG sites. The p-value is the probability of obtaining a test statistic as or more extreme as the one observed under the conditions of the null hypothesis. In most scientific endeavors, an $\alpha = 0.05$ threshold is customarily applied so that a p-value < 0.05 is considered as evidence for the alternative hypothesis, that is, $p < 0.05$ typically indicates a significant finding. However, application of $\alpha = 0.05$ threshold to univariable tests of significance in high-throughput genomic settings will yield a large number of Type I errors simply by chance. When analyzing high-throughput genomic data, the multiple comparison problem is most often addressed through estimation of the false discovery rate (FDR). To control for multiple hypothesis testing, the p-values were subsequently used in estimating FDR using the q-value method[166]. More specifically, when testing m null hypotheses, we may want to control the number of rejected null hypotheses that are truly null (F) among all those null hypotheses that are rejected (S). The q-value is such a method that for a particular feature is defined to be the expected proportion of false positives among all features as or more extreme than the one observed[166]. For a given p-value threshold t where $0 \leq t \leq 1$, we want to estimate $FDR(t) = E(F(t)/S(t)) \approx E(F(t))/E(S(t))$. F(t) represents the number of false discoveries at threshold t while S (t) represents the number of null hypotheses considered significant at threshold t. Formally, FDR(t) is estimated as

$$FDR(t) = \frac{\pi_0 mt}{S(t)} = \frac{\pi_0 mt}{\sum_{g=1}^{m} I(p_g \le t)}$$

where π_0 represents the proportion of hypotheses for which the null is true and $I(p_g \le t)$ is 1 if the p-value for the g^{th} CpG site is less than or equal to the threshold t. For application datasets, π_0 is typically unknown and so is estimated using the distribution of raw p-values using either a smoothing or bootstrap method. In this study CpG sites with a FDR < 10% were considered significant.

For CpG sites identified as significant, the CpG sites were mapped to Gene Ontology terms (molecular function (MF), biological process (BP)) and a hypergeometric test was performed to determine whether any term was over-represented among those CpG sites identified as significant compared to the number of CpG sites mapping to that term on the entire array. For MF and BP terms, a p-value < 0.05 was considered significant.

5. Canonical pathway and network identification

Genes with statistically differentially methylated CpG sites were imported into Ingenuity Pathways Analysis software (IPA, v9; Ingenuity systems, Redwood City, CA) to identify canonical pathways and gene-to-gene interaction networks within our dataset. Canonical pathways and gene networks were algorithmically constructed based on published literature in the Ingenuity Knowledge Base, where each relation was supported by at least one reference.

D. Results

Due to the role of methylation in X-chromosome inactivation, differential methylation patterns between males and females have been observed for CpG sites of genes located on the X chromosome, and are used as quality control checks[182]. Therefore, the quality of the hybridizations was examined by plotting the proportion methylated for the six X-linked genes (*EFNB1*, *ELK1*, *FMR1*, *G6PD*, *GPC3*, *GLA*), which are expected to show hemi-methylation for females as an indication of good quality[183]. Based upon this examination, there were no quality concerns for the twelve samples included in this study (Figure 1). As an additional validation, COBRA quantification of methylation was used for the -1538 CpG site in the matrix metalloproteinase-1 (*MMP1*) promoter, which we previously showed to have reduced methylation associated with increased expression of MMP-1 in amnions of patients with preterm premature rupture of the membranes[164]. COBRA quantification was similar to the BeadChip assay. Methylation by COBRA of an omental artery from a normal pregnant woman was 63% and methylation of an omental artery from a preeclamptic woman was 52% for a $\Delta\beta$ of -0.11. This compared favorably with the BeadChip analysis of the -1298 CpG site for *MMP1* of 81.6% for normal pregnancy versus 73.6% for preeclamptic pregnancy for a $\Delta\beta$ of -0.08 ($p = 0.016$, FDR = 0.1069). Although the methylation percentage of the -1538 CpG site varied from that of the -1298 CpG site, this is not unexpected because methylation percentage varies for CpG sites in the *MMP1* promoter[164].

Unsupervised hierarchical clustering using Euclidean distance and Ward's method was applied to determine whether the samples naturally clustered by diagnosis. The methylation matrix was filtered to include CpG sites having a mean $\beta > 0.15$ and a standard deviation among the top 90% of standard deviations, leaving 1,233 CpG sites. Unsupervised hierarchical clustering (Figure 2) revealed natural clustering of the samples by diagnosis, normal pregnant versus preeclamptic and natural clustering of the CpG sites by methylation status, reduced methylated versus relatively more methylated.

Statistical analysis revealed 4,184 CpG sites, corresponding to 3,736 genes, with significant differential methylation when comparing between normal pregnant and preeclamptic omental arteries at P-value of less than 0.05. This is considerably greater than what is expected by chance alone. Of these

CpG sites, 1,771 CpG sites, mapped to 1,685 genes, had a FDR of less than 10% (Table 4) and 237 CpG sites, representing 236 genes, had a FDR of less than 5%. Interestingly, many of these genes were related to inflammation. Of the 237 CpG sites, 155 CpG sites (~65%) had reduced methylation in preeclamptic omental arteries. For each CpG detected in the BeadChip, the distance from the transcription start site (TSS), and whether it was located within a CpG island, was provided by Illumina. Transcription factor binding sites are often located within the nucleosome free region of the gene promoter[184]. The position of the CpG sites relative to nucleosomes was not provided in this assay. However, one could infer that the nucleosome free region is most likely 200 base pairs upstream of the TSS[185]. The median distance from TSS for the 237 CpG sites was -299. Also, of these CpG sites, 112 CpG sites (~47%) were located within CpG islands. Interestingly, 67% of CpG sites that had significantly reduced methylation were not located in CpG islands whereas 91% of CpG sites that were significantly more methylated were located in CpG islands. When data were analyzed more stringently to a FDR of less than 5% and difference in methylation of more than 0.10, 65 genes were identified, all of which were less methylated in preeclamptic women.

To visualize the distribution of the CpG sites based on their biological and statistical significance, a volcano plot was created by plotting the difference between average proportion methylated for normal pregnant and preeclamptic women for all 27,578 CpG sites analyzed by the BeadChip on the X axes, and the negative $\log_{10}$ transformed P-values from the two class comparison analysis performed for each CpG site on the Y axis. The plot was divided into four quadrants by the line X=0 which divided the CpG sites into CpG sites that are less methylated in preeclamptic omental arteries compared to normal pregnant counterparts on the left and CpG sites that were more methylated in preeclamptic omental arteries on the right, and the line Y= $-\log_{10}$ (P-value equivalent to FDR of 10%) which divided the CpG sites that were significantly differentially methylated above that line and CpG site with no significant difference in methylation below the line (Figure 3). The larger population of CpG sites that was observed in the upper

left quadrant of the plot indicated preeclamptic samples had a significant decrease in their DNA methylation compared to normal pregnant.

When genes with differentially methylated CpG sites at FDR cut-off of 0.05 were mapped to Gene Ontology for Molecular Functions (MF) and Biological Processes (BP), 75 MFs and 149 BPs were over-represented in the preeclamptic vessels ($p < 0.05$), many of which were pertinent to the pathophysiology of preeclampsia (Table 5).

Genes with differentially methylated CpG sites at FDR cut-off of 0.1 were analyzed with IPA software to assess the interconnectivity between these genes and other related genes within a canonical pathway or a gene-to-gene interaction network which may indicate functional importance of these genes in the biology of the disease. Twenty-five significant canonical pathways ($p < 0.05$) were identified (Table 6). Some of these pathways were associated with inflammation, such as retinoid X receptor (RXR) inhibition, peroxisome proliferator-activated receptor (PPAR) signaling and high mobility group box chromosomal protein 1 (HMGB1) signaling. Using IPA network analysis, 50 gene-to-gene interaction networks were identified. Four of them included inflammatory response, hematological disease, inflammatory disease and/or cardiovascular disease among their top three associated biological functions ($p < 0.005$). A network is shown in Figure 4 for inflammatory genes.

E. Discussion

In this study, we used a high throughput assay to investigate the global DNA methylation profiles in omental arteries from normal pregnant women and women with severe preeclampsia. We identified 3,736 genes with significantly differentially methylated CpG sites between the two groups, which is significantly greater than expected by chance alone. Unsupervised hierarchical clustering revealed natural clustering by diagnosis demonstrating that DNA methylation profiles distinguished each group. Volcano

plot demonstrated that the most significant differences in DNA methylation of CpG sites were "hypomethylated" genes in preeclamptic women. Of genes with significant methylation differences, 236 were significant at a FDR of less than 5%. When data were analyzed more stringently to FDR of 5% and difference in methylation of more than 0.10, 65 genes were identified, all of which had lower levels of methylation in preeclampsia.

DNA methylation is maintained by the action of DNA methyltransferases, which use S-adenosylmethionine as a donor of methyl group in their reactions[131]. When the methyl group is transferred, S-adenosylmethionine is converted to S-adenosylhomocysteine, which is hydrolyzed under physiological conditions to homocysteine and adenosine. The equilibrium of this reversible reaction strongly favors S-adenosylhomocysteine synthesis rather than hydrolysis and an increase in intracellular homocysteine levels can increase S-adenosylhomocysteine levels [132]. S-adenosylhomocysteine has a higher affinity to DNA methyltransferases than S-adenosylmethionine does, which makes it a potent inhibitor of DNA methylation reactions[133]. A number of studies reported that plasma levels of homocysteine and S-adenosylhomocysteine are significantly elevated in preeclamptic women as compared to normal pregnant women[135-137]. The relationship between hyperhomocysteinemia and DNA methylation has been studied in cardiovascular diseases such as atherosclerosis. For example, increased plasma levels of total homocysteine and S-adenosylhomocysteine were correlated with decreased global DNA methylation in white blood cells of patients with advance atherosclerosis[134]. Methylenetetrahydrofolate reductase is the enzyme that catalyzes the conversion of 5,10-methylenetetrahydrofolate to 5-methyltetrahydrofolate, which is required for the re-methylation homocysteine to methionine. A study using methylenetetrahydrofolate reductase knockout mice found that decreased S-adenosylmethionine levels or significantly increased S-adenosylhomocysteine levels, or both, correlated with global DNA hypomethylation[138]. Knockout mice also showed abnormal aortic lipid deposition similar to those observed in early atherosclerosis. Our study showed that preeclampsia is associated with changes in DNA methylation patterns in maternal systemic vasculature. Preeclampsia is

associated with increased risk of cardiovascular diseases, such as hypertension, atherosclerosis, ischemic heart disease and stroke later in life[186]. The exact role of DNA methylation in the etiology of these diseases with respect to preeclampsia remains to be determined.

The thromboxane synthase gene (*TBXAS1*) was the most hypomethylated gene in preeclamptic women. *TBXAS1* encodes an enzyme that catalyzes the isomerization of prostaglandin H_2 into thromboxane[94]. Preeclampsia is associated with an imbalance of increased thromboxane and decreased prostacyclin, which was first described in placenta[95] and later confirmed for maternal blood[96] and maternal urine[97]. This imbalance can provide a plausible explanation for hypertension, reduced uteroplacental blood flow and hypercoagulopathy observed in women with preeclampsia because thromboxane is a potent vasoconstrictor and platelet activator, whereas prostacyclin is a potent vasodilator and inhibitor of platelet activation[27]. Our findings suggest an epigenetic regulation of the *TBXAS1* gene because we found that its reduced methylation is associated with its increased expression in omental arteries of preeclamptic women[187].

Another gene that was significantly less methylated in our analysis was *MMP1* ($p = 0.016$, FDR = 0.1069, $\Delta\beta = 0.08$). This gene also appears to be epigenetically regulated because its reduced methylation is associated with its increased expression in omental arteries of preeclamptic women [159] and experimentally induced hypomethylation results in its increased expression in human vascular smooth muscle cells in culture[188]. Interestingly, increased expression of MMP-1 is also associated with reduced DNA methylation in amnion of patients with preterm premature rupture of the membranes [164].

Normal pregnancy is associated with mild systemic inflammatory changes which increase as pregnancy progresses[82]. These changes include increased plasma levels of fibrinogen[101], plasminogen activator inhibitor type 1[102] ceruloplasmin[103], interleukin-6[104], and tumor necrosis factor-α[105,106]. They also include leukocytosis[189], leukocyte activation[38,190,191], increased circulating markers of oxidative stress such as lipid hydroperoxides and malondialdehyde[192], and hypertriglyceridemia[108]. All these inflammatory

changes are exacerbated in preeclampsia[109]. The differences between normal pregnancy and preeclampsia in terms of systemic inflammation are less striking than those between normal pregnancy and the nonpregnant state[82]. This suggests that preeclampsia may arise due to an inability of maternal homeostasis to adapt to a pregnancy induced systemic inflammation. In our study, many inflammation-related genes were significantly hypomethylated in preeclamptic women as compared to normal pregnant women. DNA hypomethylation is generally associated with increased gene expression, so reduced methylation may place a woman in a more responsive state to inflammatory stimuli.

Ingenuity pathway analysis (IPA) demonstrated that genes with significant changes in methylation in preeclamptic women were associated with multiple canonical pathways related to inflammation and immune response. These pathways included inhibition of RXR function and PPAR signaling. PPARs and RXRs help regulate inflammatory responses in endothelial and vascular smooth muscle cells. Activation of these receptors results in the formation of PPAR/RXR heterodimers which exert anti-inflammatory effects in these cells[193]. Preeclampsia is associated with inflammation and dysfunction of maternal systemic endothelial and vascular smooth muscle cells[62], so the inhibition of these pathways may contribute to the pathophysiology of preeclampsia. HMGB1 signaling is another canonical pathway identified by IPA software in our dataset. HMGB1 is a nuclear transcription factor which possesses potent cytokine activity when released from innate immune cells, mediating the late response to inflammation[194] through toll-like receptors 4 and 2[195]. HMGB1 is also released from cultured human vascular smooth muscle cells in response to C-reactive protein[196], which is elevated in preeclampsia[197,198]. HMGB1 causes increased expression of intercellular adhesion molecule-1 (ICAM-1) and interleukin-8 (IL-8) in cultured human endothelial cells[199] and increases expression of C-reactive protein, MMP-2 and MMP-9 in cultured human vascular smooth muscles[196]. These changes are similar to what is found in preeclampsia where the expression of ICAM-1 and IL-8 are increased in endothelial cells of maternal systemic blood vessels[61], and levels of C-reactive protein[197,198], MMP-2[200] and MMP-9[201] are elevated in the plasma. This suggests that hypomethylation related to HMGB1 signaling may be involved

in the pathophysiology of preeclampsia. IPA analysis also indicated that genes in our dataset were involved in gene-to-gene interaction networks, which had inflammatory response, inflammatory disease and cardiovascular disease among their top associated biological functions. These relationships suggest that DNA methylation may contribute to preeclampsia by influencing multiple pathways and gene-to-gene networks related to inflammation in a woman's systemic blood vessels.

When genes with an FDR of less than 5% were mapped for Molecular Functions and Biological Processes, 75 Molecular Functions and 149 Biological Process were over-represented in preeclampsia representing functions and pathways pertinent to pathophysiology. These included smooth muscle contraction, thrombosis, inflammation, redox homeostasis, sugar metabolism and amino acid metabolism. These are particularly relevant to preeclampsia because it is associated with increased vascular resistance, increased arterial pressure[202], reduced uteroplacental blood flow[203], hypercoagulopathy[204], inflammation[109], oxidative stress[89] and altered carbohydrate and amino acid metabolism[205].

Our study had some methodological limitations. The number of samples analyzed was limited due to the difficulty in obtaining omental arterial samples. In addition, although the Illumina Human Methylation27 platform is a reliable way to assess the methylation status of large numbers of CpG sites in the promoter region of genes[183], it does not cover all CpG sites in the human genome. Methylation of CpG sites outside of the gene promoter regions are also likely important. Consequently, some important epigenetic alterations may have been overlooked in our analysis. Another limitation is the cellular heterogeneity of omental arteries, which did not allow us to specify the cell type where methylation changes were occurring. Because of the extensive infiltration of neutrophils into the mother's blood vessels in preeclampsia[61-63], neutrophils are just as likely to be the source of the DNA methylation changes as are endothelial or vascular smooth muscle cells.

Our study is the first to compare DNA methylation profiles in systemic blood vessels of normal pregnant and preeclamptic women. Reduced methylation of inflammatory genes was prominent in

omental arteries of preeclamptic women. Genes with significant differential methylation were involved in multiple pathways and gene-to-gene networks pertinent to the clinical features of preeclampsia. We speculate that reduced methylation prior to pregnancy may increase the risk of getting preeclampsia, whereas reduced methylation caused by oxidative stress during preeclampsia may contribute to increasing the risk of cardiovascular disease later in life[186].

Our study may have clinical implications for the treatment of preeclampsia. Folate is an essential vitamin for the synthesis of methyl donors utilized by methyltransferases to methylate DNA. Therefore, dietary supplementation with folate might restore reduced methylation in inflammatory genes, and protect against development of preeclampsia. In this regard, a large study of almost 3,000 pregnant women found supplementation with multivitamins containing folic acid was associated with reduced risk of preeclampsia[206].

Table 3: Clinical Characteristics of Patient Groups.

Variable	Normal Pregnant (n = 5)	Preeclamptic (n = 7)
Maternal age (y)	23.0 ± 1.7	24.9 ± 1.4
Pre-pregnancy BMI (kg/m^2)	24.4 ± 1.5	29.9 ± 2.9
Systolic blood pressure (mmHg)	115.0 ± 3.2	168.0 ± 2.8*
Diastolic blood pressure (mmHg)	69.6 ± 1.3	91.1 ± 3.9**
Proteinuria (mg/24 h)	ND	307.8 ± 26.7 (n = 4)
Dipstick	ND	2.3 ± 0.9 (n = 3)
Parity		
Primiparous	2	2
Multiparous	3	5
Gestational age (wk)	39.2 ± 0.2	34.1 ± 1.7*
Infant birth weight (g)	3424 ± 110	2304 ± 393

Values are presented as mean ± SEM.

*$p < 0.05$, **$p < 0.01$, *** $p < 0.001$ by t-test.

ND, not detectable.

Table 4: List of differentially methylated CpG sites at false discovery rate (FDR) < 10%. NP = normal pregnant, PE = preeclamptic, β = methylation values where 0≤ β≤1, 0 = no methylation and 1 = full methylation. Δβ = difference in methylation. Minus values indicate less methylation and positive values more methylation in preeclamptic arteries as compared to normal pregnant arteries.

Symbol	Gene ID	Gene Description	Mean β PE	Mean β NP	Δβ	FDR
A2ML1	144568	alpha-2-macroglobulin-like 1	0.68	0.83	-0.15	0.042
A4GNT	51146	alpha-1,4-N-acetylglucosaminyltransferase	0.71	0.84	-0.13	0.063
AAAS	8086	achalasia, adrenocortical insufficiency, alacrimia (Allgrove, triple-A)	0.20	0.14	0.06	0.080
AANAT	15	arylalkylamine N-acetyltransferase	0.94	0.91	0.03	0.065
ABCA4	24	ATP-binding cassette, sub-family A (ABC1), member 4	0.71	0.80	-0.09	0.080
ABCB4	5244	ATP-binding cassette, sub-family B (MDR/TAP), member 4	0.83	0.79	0.04	0.089
ABCC5	10057	ATP-binding cassette, sub-family C (CFTR/MRP), member 5	0.02	0.01	0.01	0.086
ABCG1	9619	ATP-binding cassette, sub-family G (WHITE), member 1	0.68	0.79	-0.11	0.047
ABCG5	64240	ATP-binding cassette, sub-family G (WHITE), member 5	0.81	0.89	-0.08	0.066
ABHD2	11057	abhydrolase domain containing 2	0.08	0.05	0.03	0.080
ABO	28	ABO blood group (transferase A, alpha 1-3-N-acetylgalactosaminyltransferase; transferase B, alpha 1-3-galactosyltransferase)	0.94	0.89	0.04	0.087
ABR	29	active BCR-related gene	0.02	0.01	0.01	0.073
ACAT2	39	acetyl-Coenzyme A acetyltransferase 2	0.40	0.19	0.21	0.067
ACO1	48	aconitase 1, soluble	0.02	0.01	0.01	0.079

Symbol	Gene ID	Gene Description	Mean β PE	Mean β NP	Δβ	FDR
ACRBP	84519	acrosin binding protein	0.72	0.80	-0.08	0.099
ACSBG2	81616	acyl-CoA synthetase bubblegum family member 2	0.85	0.89	-0.05	0.051
ACSL4	2182	acyl-CoA synthetase long-chain family member 4	0.73	0.83	-0.10	0.061
ACSL5	51703	acyl-CoA synthetase long-chain family member 5	0.66	0.75	-0.10	0.069
ACSL5	51703	acyl-CoA synthetase long-chain family member 5	0.84	0.92	-0.08	0.085
ACTL7A	10881	actin-like 7A	0.73	0.79	-0.06	0.074
ACTL7B	10880	actin-like 7B	0.94	0.96	-0.02	0.089
ACTR1B	10120	ARP1 actin-related protein 1 homolog B, centractin beta (yeast)	0.04	0.02	0.02	0.090
ACTRT1	139741	actin-related protein T1	0.69	0.60	0.09	0.072
ACY1	95	aminoacylase 1	0.91	0.96	-0.05	0.089
ADA	100	adenosine deaminase	0.80	0.69	0.11	0.073
ADAMTS6	11174	ADAM metallopeptidase with thrombospondin type 1 motif, 6	0.04	0.02	0.02	0.067
ADAMTS9	56999	ADAM metallopeptidase with thrombospondin type 1 motif, 9	0.02	0.01	0.00	0.065
ADAMTSL3	57188	ADAMTS-like 3	0.03	0.02	0.01	0.061
ADC	113451	arginine decarboxylase	0.05	0.03	0.01	0.086
ADH1A	124	alcohol dehydrogenase 1A (class I), alpha polypeptide	0.23	0.31	-0.08	0.099
ADORA2B	136	adenosine A2b receptor	0.61	0.78	-0.16	0.053
AES	166	amino-terminal enhancer of split	0.12	0.19	-0.07	0.084
AFF2	2334	AF4/FMR2 family, member 2	0.87	0.90	-0.04	0.042
AFF2	2334	AF4/FMR2 family, member 2	0.70	0.82	-0.12	0.080
AFM	173	afamin	0.46	0.58	-0.12	0.084

Symbol	Gene ID	Gene Description	Mean β PE	Mean β NP	Δβ	FDR
AGBL2	79841	ATP/GTP binding protein-like 2	0.28	0.35	-0.08	0.066
AGTR1	185	angiotensin II receptor, type 1	0.05	0.03	0.02	0.047
AGTRAP	57085	angiotensin II receptor-associated protein	0.05	0.03	0.02	0.078
AKAP5	9495	A kinase (PRKA) anchor protein 5	0.13	0.09	0.04	0.099
AKT3	10000	v-akt murine thymoma viral oncogene homolog 3 (protein kinase B, gamma)	0.94	0.97	-0.03	0.075
ALDH1A3	220	aldehyde dehydrogenase 1 family, member A3	0.60	0.72	-0.12	0.094
ALDH3A1	218	aldehyde dehydrogenase 3 family, memberA1	0.37	0.30	0.07	0.059
ALDOB	229	aldolase B, fructose-bisphosphate	0.79	0.87	-0.08	0.064
ALG1	56052	asparagine-linked glycosylation 1, beta-1,4-mannosyltransferase homolog (S. cerevisiae)	0.18	0.10	0.08	0.077
ALG5	29880	asparagine-linked glycosylation 5, dolichyl-phosphate beta-glucosyltransferase homolog (S. cerevisiae)	0.05	0.03	0.02	0.094
ALPK1	80216	alpha-kinase 1	0.95	0.98	-0.02	0.086
ALS2CR12	130540	amyotrophic lateral sclerosis 2 (juvenile) chromosome region, candidate 12	0.85	0.91	-0.05	0.053
ALX4	60529	ALX homeobox 4	0.76	0.70	0.07	0.088
AMBP	259	alpha-1-microglobulin/bikunin precursor	0.81	0.90	-0.09	0.054
AMDHD1	144193	amidohydrolase domain containing 1	0.84	0.91	-0.08	0.039
AMHR2	269	anti-Mullerian hormone receptor, type II	0.88	0.93	-0.05	0.083
AMY2B	280	amylase, alpha 2B (pancreatic)	0.29	0.35	-0.06	0.076
ANK1	286	ankyrin 1, erythrocytic	0.73	0.85	-0.11	0.063

Symbol	Gene ID	Gene Description	Mean β PE	Mean β NP	Δβ	FDR
ANKRD10	55608	ankyrin repeat domain 10	0.07	0.05	0.03	0.074
ANKRD35	148741	ankyrin repeat domain 35	0.02	0.01	0.01	0.077
ANKRD37	353322	ankyrin repeat domain 37	0.02	0.01	0.01	0.090
ANKRD38	163782	KN motif and ankyrin repeat domains 4	0.96	0.98	-0.01	0.053
ANKRD7	56311	ankyrin repeat domain 7	0.81	0.88	-0.07	0.064
ANPEP	290	alanyl (membrane) aminopeptidase	0.81	0.90	-0.09	0.047
ANXA8	244	annexin A8-like 2	0.60	0.72	-0.13	0.085
AP2S1	1175	adaptor-related protein complex 2, sigma 1 subunit	0.55	0.69	-0.14	0.074
APC	324	adenomatous polyposis coli	0.04	0.03	0.01	0.044
APEH	327	N-acylaminoacyl-peptide hydrolase	0.09	0.05	0.04	0.098
API5	8539	API5-like 1; apoptosis inhibitor 5	0.15	0.11	0.04	0.057
APLP2	334	amyloid beta (A4) precursor-like protein 2	0.09	0.07	0.03	0.076
APOBEC1	339	apolipoprotein B mRNA editing enzyme, catalytic polypeptide 1	0.75	0.85	-0.10	0.055
APOBEC4	403314	apolipoprotein B mRNA editing enzyme, catalytic polypeptide-like 4 (putative)	0.64	0.73	-0.09	0.080
APOC4	346	apolipoprotein C-IV	0.33	0.52	-0.19	0.053
APOD	347	apolipoprotein D	0.67	0.77	-0.11	0.080
APOH	350	apolipoprotein H (beta-2-glycoprotein I)	0.44	0.57	-0.13	0.074
APOL1	8542	apolipoprotein L, 1	0.92	0.90	0.02	0.086
APOL3	80833	apolipoprotein L, 3	0.20	0.31	-0.12	0.042
AQP8	343	aquaporin 8	0.50	0.62	-0.12	0.083
ARD1A	8260	ARD1 homolog A, N-acetyltransferase (S. cerevisiae)	0.97	0.98	-0.01	0.087

Symbol	Gene ID	Gene Description	Mean β PE	Mean β NP	Δβ	FDR
ARF3	377	ADP-ribosylation factor 3	0.05	0.02	0.02	0.088
ARFRP1	10139	ADP-ribosylation factor related protein 1	0.90	0.95	-0.05	0.073
ARHGAP9	64333	Rho GTPase activating protein 9	0.91	0.87	0.04	0.073
ARHGEF16	27237	Rho guanine exchange factor (GEF) 16	0.88	0.83	0.05	0.077
ARID1A	8289	AT rich interactive domain 1A (SWI-like)	0.02	0.01	0.01	0.077
ARIH2	10425	ariadne homolog 2 (Drosophila)	0.62	0.75	-0.13	0.053
ARL11	115761	ADP-ribosylation factor-like 11	0.83	0.90	-0.07	0.042
ARL13B	200894	ADP-ribosylation factor-like 13B	0.04	0.02	0.02	0.039
ARL13B	200894	ADP-ribosylation factor-like 13B	0.87	0.92	-0.06	0.053
ARL2	402	ADP-ribosylation factor-like 2	0.04	0.02	0.02	0.090
ARL6	84100	ADP-ribosylation factor-like 6	0.05	0.03	0.02	0.070
ARMC2	84071	armadillo repeat containing 2	0.67	0.79	-0.11	0.063
ARP10	164668	apolipoprotein B mRNA editing enzyme, catalytic polypeptide-like 3H	0.84	0.88	-0.05	0.091
ASAH1	427	N-acylsphingosine amidohydrolase (acid ceramidase) 1	0.02	0.01	0.01	0.053
ASB14	142686	ankyrin repeat and SOCS box-containing 14	0.81	0.90	-0.08	0.042
ASB2	51676	ankyrin repeat and SOCS box-containing 2	0.69	0.80	-0.12	0.053
ASB3	51130	ankyrin repeat and SOCS box-containing 3	0.13	0.08	0.04	0.055
ASB4	51666	ankyrin repeat and SOCS box-containing 4	0.72	0.79	-0.07	0.055
ASB5	140458	ankyrin repeat and SOCS box-containing 5	0.88	0.92	-0.04	0.089

Symbol	Gene ID	Gene Description	Mean β PE	Mean β NP	Δβ	FDR
ASB8	140461	ankyrin repeat and SOCS box-containing 8	0.04	0.03	0.01	0.077
ASCL3	56676	achaete-scute complex homolog 3 (Drosophila)	0.86	0.93	-0.06	0.059
ASPA	443	aspartoacylase (Canavan disease)	0.49	0.63	-0.14	0.082
ASZ1	136991	ankyrin repeat, SAM and basic leucine zipper domain containing 1	0.90	0.94	-0.04	0.090
ATF7	11016	activating transcription factor 7	0.05	0.03	0.01	0.094
ATF7IP2	80063	activating transcription factor 7 interacting protein 2	0.45	0.62	-0.17	0.060
ATG10	83734	ATG10 autophagy related 10 homolog (S. cerevisiae)	0.04	0.02	0.01	0.094
ATG7	10533	ATG7 autophagy related 7 homolog (S. cerevisiae)	0.39	0.48	-0.09	0.099
ATP10A	57194	ATPase, class V, type 10A	0.50	0.68	-0.17	0.042
ATP10A	57194	ATPase, class V, type 10A	0.86	0.93	-0.07	0.047
ATP10A	57194	ATPase, class V, type 10A	0.74	0.83	-0.09	0.064
ATP10A	57194	ATPase, class V, type 10A	0.88	0.92	-0.05	0.082
ATP2B1	490	ATPase, Ca++ transporting, plasma membrane 1	0.86	0.91	-0.05	0.067
ATP6V0D1	9114	ATPase, H+ transporting, lysosomal 38kDa, V0 subunit d1	0.02	0.01	0.00	0.094
ATP6V1A	523	ATPase, H+ transporting, lysosomal 70kDa, V1 subunit A	0.09	0.05	0.04	0.064
ATP6V1C2	245973	ATPase, H+ transporting, lysosomal 42kDa, V1 subunit C2	0.04	0.02	0.02	0.093
ATP6V1F	9296	ATPase, H+ transporting, lysosomal 14kDa, V1 subunit F	0.04	0.02	0.02	0.074
ATP9A	10079	ATPase, class II, type 9A	0.79	0.89	-0.10	0.047
ATP9B	374868	ATPase, class II, type 9B	0.02	0.01	0.01	0.047

Symbol	Gene ID	Gene Description	Mean β PE	Mean β NP	Δβ	FDR
ATPBD1C	51184	GPN-loop GTPase 3	0.06	0.03	0.03	0.057
AVPR1A	552	arginine vasopressin receptor 1A	0.72	0.80	-0.08	0.096
AVPR2	554	arginine vasopressin receptor 2	0.84	0.78	0.06	0.076
B3GALT1	8708	UDP-Gal:betaGlcNAc beta 1,3-galactosyltransferase, polypeptide 1	0.86	0.92	-0.06	0.080
B3GALT7	374907	UDP-GlcNAc:betaGal beta-1,3-N-acetylglucosaminyltransferase 8	0.49	0.62	-0.13	0.093
B3GNT1	10678	UDP-GlcNAc:betaGal beta-1,3-N-acetylglucosaminyltransferase 1	0.80	0.91	-0.11	0.046
BANF1	8815	barrier to autointegration factor 1	0.74	0.68	0.06	0.073
BAPX1	579	NK3 homeobox 2	0.03	0.02	0.01	0.090
BASP1	10409	brain abundant, membrane attached signal protein 1	0.04	0.02	0.02	0.086
BAT2D1	23215	BAT2 domain containing 1	0.05	0.03	0.02	0.062
BAZ2B	29994	bromodomain adjacent to zinc finger domain, 2B	0.77	0.86	-0.08	0.066
BCAS2	10286	breast carcinoma amplified sequence 2	0.04	0.02	0.02	0.094
BCL10	8915	B-cell CLL/lymphoma 10	0.80	0.73	0.06	0.090
BCL2A1	597	BCL2-related protein A1	0.38	0.49	-0.12	0.056
BCL2L13	23786	BCL2-like 13 (apoptosis facilitator)	0.03	0.02	0.02	0.066
BFSP2	8419	beaded filament structural protein 2, phakinin	0.56	0.65	-0.08	0.089
BIRC8	112401	baculoviral IAP repeat-containing 8	0.69	0.79	-0.10	0.094
BLOC1S2	282991	biogenesis of lysosomal organelles complex-1, subunit 2	0.07	0.04	0.02	0.066
BNIPL	149428	BCL2/adenovirus E1B 19kD interacting protein like	0.51	0.63	-0.12	0.066
BRCA1	672	breast cancer 1, early onset	0.73	0.83	-0.10	0.059
BRCA1	672	breast cancer 1, early onset	0.85	0.91	-0.06	0.073

Symbol	Gene ID	Gene Description	Mean β PE	Mean β NP	Δβ	FDR
BRCA1	672	breast cancer 1, early onset	0.25	0.35	-0.09	0.077
BRIP1	83990	BRCA1 interacting protein C-terminal helicase 1	0.08	0.05	0.03	0.024
BRSK1	84446	BR serine/threonine kinase 1	0.93	0.95	-0.03	0.055
BRWD1	54014	bromodomain and WD repeat domain containing 1	0.04	0.01	0.03	0.083
BTN2A1	11120	butyrophilin, subfamily 2, member A1	0.87	0.91	-0.05	0.056
BTNL8	79908	butyrophilin-like 8	0.68	0.76	-0.08	0.095
BXDC1	84154	ribosome production factor 2 homolog (S. cerevisiae)	0.04	0.02	0.02	0.073
C10orf10	11067	chromosome 10 open reading frame 10	0.64	0.75	-0.11	0.071
C10orf111	221060	chromosome 10 open reading frame 111	0.65	0.81	-0.16	0.047
C10orf32	119032	chromosome 10 open reading frame 32	0.03	0.02	0.01	0.094
C10orf63	219670	enkurin, TRPC channel interacting protein	0.05	0.03	0.02	0.087
C10orf70	55847	CDGSH iron sulfur domain 1	0.03	0.02	0.01	0.073
C11orf30	56946	chromosome 11 open reading frame 30	0.03	0.02	0.01	0.066
C11orf44	283171	chromosome 11 open reading frame 44	0.87	0.84	0.04	0.082
C11orf49	79096	chromosome 11 open reading frame 49	0.06	0.04	0.02	0.084
C11orf54	28970	chromosome 11 open reading frame 54	0.03	0.02	0.01	0.063
C12orf30	80018	chromosome 12 open reading frame 30	0.03	0.02	0.01	0.065
C12orf31	84298	LLP homolog, long-term synaptic facilitation (Aplysia)	0.05	0.04	0.02	0.050

Symbol	Gene ID	Gene Description	Mean β PE	Mean β NP	Δβ	FDR
C12orf36	283422	chromosome 12 open reading frame 36	0.85	0.91	-0.06	0.081
C12orf47	51275	chromosome 12 open reading frame 47	0.03	0.02	0.01	0.088
C14orf112	51241	COX16 cytochrome c oxidase assembly homolog (S. cerevisiae)	0.05	0.03	0.02	0.080
C14orf166B	145497	chromosome 14 open reading frame 166B	0.09	0.10	-0.02	0.094
C14orf29	145447	abhydrolase domain containing 12B	0.67	0.80	-0.14	0.042
C14orf48	256369	chromosome 14 open reading frame 48	0.79	0.89	-0.10	0.040
C14orf68	283600	chromosome 14 open reading frame 68	0.97	0.98	-0.01	0.094
C14orf8	122664	tubulin polymerization-promoting protein family member 2	0.61	0.71	-0.10	0.089
C15orf15	51187	ribosomal L24 domain containing 1	0.01	0.01	0.00	0.052
C15orf24	56851	chromosome 15 open reading frame 24	0.65	0.76	-0.11	0.076
C15orf24	56851	chromosome 15 open reading frame 24	0.91	0.94	-0.03	0.087
C15orf27	123591	chromosome 15 open reading frame 27	0.05	0.03	0.02	0.070
C15orf32	145858	chromosome 15 open reading frame 32	0.78	0.83	-0.05	0.068
C16orf34	90861	hematological and neurological expressed 1-like	0.03	0.02	0.01	0.053
C16orf46	123775	chromosome 16 open reading frame 46	0.08	0.04	0.04	0.074
C16orf47	388289	chromosome 16 open reading frame 47	0.63	0.75	-0.11	0.077
C16orf60	55839	centromere protein N	0.03	0.02	0.01	0.062

Symbol	Gene ID	Gene Description	Mean β PE	Mean β NP	Δβ	FDR
C16orf61	56942	chromosome 16 open reading frame 61	0.10	0.08	0.03	0.086
C17orf61	254863	chromosome 17 open reading frame 61	0.02	0.01	0.01	0.065
C18orf1	753	chromosome 18 open reading frame 1	0.02	0.01	0.01	0.042
C18orf20	221241	chromosome 18 open reading frame 20	0.67	0.81	-0.13	0.038
C18orf20	221241	chromosome 18 open reading frame 20	0.77	0.86	-0.10	0.052
C18orf45	85019	chromosome 18 open reading frame 45	0.05	0.03	0.02	0.084
C19orf12	83636	chromosome 19 open reading frame 12	0.05	0.03	0.02	0.090
C19orf18	147685	chromosome 19 open reading frame 18	0.64	0.76	-0.13	0.068
C19orf6	91304	chromosome 19 open reading frame 6	0.05	0.03	0.02	0.081
C1orf105	92346	chromosome 1 open reading frame 105	0.80	0.88	-0.07	0.065
C1orf107	27042	chromosome 1 open reading frame 107	0.11	0.04	0.06	0.085
C1orf128	57095	chromosome 1 open reading frame 128	0.03	0.02	0.01	0.081
C1orf128	57095	chromosome 1 open reading frame 128	0.04	0.03	0.01	0.094
C1orf150	148823	chromosome 1 open reading frame 150	0.73	0.81	-0.07	0.080
C1orf162	128346	chromosome 1 open reading frame 162	0.74	0.83	-0.09	0.039
C1orf188	148646	chromosome 1 open reading frame 188	0.74	0.80	-0.06	0.081
C1orf198	84886	chromosome 1 open reading frame 198	0.13	0.07	0.06	0.074

Symbol	Gene ID	Gene Description	Mean β PE	Mean β NP	Δβ	FDR
C1orf201	90529	chromosome 1 open reading frame 201	0.89	0.94	-0.05	0.065
C1orf59	113802	chromosome 1 open reading frame 59	0.06	0.03	0.03	0.077
C1orf62	254268	chromosome 1 open reading frame 62	0.62	0.79	-0.17	0.038
C1orf62	254268	chromosome 1 open reading frame 62	0.62	0.75	-0.13	0.054
C1orf74	148304	chromosome 1 open reading frame 74	0.03	0.03	0.01	0.065
C1orf83	127428	chromosome 1 open reading frame 83	0.04	0.02	0.02	0.038
C1QTNF4	114900	C1q and tumor necrosis factor related protein 4	0.49	0.65	-0.16	0.073
C1RL	51279	complement component 1, r subcomponent-like	0.03	0.02	0.01	0.053
C1S	716	complement component 1, s subcomponent	0.41	0.34	0.07	0.092
C20orf114	92747	chromosome 20 open reading frame 114	0.83	0.77	0.05	0.090
C20orf116	65992	DDRGK domain containing 1	0.87	0.93	-0.06	0.053
C20orf135	140701	chromosome 20 open reading frame 135	0.64	0.77	-0.13	0.085
C20orf173	140873	chromosome 20 open reading frame 173	0.80	0.86	-0.06	0.080
C20orf179	140836	barrier to autointegration factor 2	0.75	0.82	-0.07	0.074
C20orf20	55257	chromosome 20 open reading frame 20	0.07	0.03	0.03	0.086
C20orf31	55741	ER degradation enhancer, mannosidase alpha-like 2	0.04	0.02	0.02	0.076
C20orf38	55304	serine palmitoyltransferase, long chain base subunit 3	0.11	0.07	0.03	0.086
C20orf52	140823	reactive oxygen species modulator 1	0.06	0.03	0.03	0.050
C20orf54	113278	chromosome 20 open reading frame 54	0.74	0.84	-0.09	0.093

Symbol	Gene ID	Gene Description	Mean β PE	Mean β NP	Δβ	FDR
C20orf70	140683	chromosome 20 open reading frame 70	0.52	0.64	-0.12	0.058
C20orf79	140856	chromosome 20 open reading frame 79	0.71	0.85	-0.14	0.083
C21orf6	10069	RWD domain containing 2B	0.06	0.14	-0.08	0.050
C21orf77	55264	chromosome 21 open reading frame 77	0.70	0.74	-0.04	0.086
C21orf99	149992	chromosome 21 open reading frame 99	0.28	0.19	0.09	0.060
C22orf18	79019	centromere protein M	0.03	0.01	0.01	0.098
C2orf7	84279	chromosome 2 open reading frame 7	0.92	0.94	-0.02	0.082
C3orf24	115795	chromosome 3 open reading frame 24	0.87	0.94	-0.07	0.047
C3orf45	132228	chromosome 3 open reading frame 45	0.77	0.90	-0.13	0.024
C5orf20	140947	chromosome 5 open reading frame 20	0.56	0.67	-0.11	0.065
C5orf3	10827	family with sequence similarity 114, member A2	0.02	0.01	0.01	0.059
C6orf108	10591	chromosome 6 open reading frame 108	0.08	0.04	0.03	0.080
C6orf111	25957	splicing factor, arginine/serine-rich 18	0.63	0.77	-0.13	0.053
C6orf141	135398	chromosome 6 open reading frame 141	0.15	0.10	0.06	0.050
C6orf15	29113	chromosome 6 open reading frame 15	0.76	0.85	-0.09	0.045
C6orf151	154007	small nuclear ribonucleoprotein 48kDa (U11/U12)	0.05	0.03	0.02	0.076
C6orf204	387119	chromosome 6 open reading frame 204	0.52	0.64	-0.13	0.074
C6orf32	9750	family with sequence similarity 65, member B	0.88	0.83	0.05	0.046
C6orf72	116254	chromosome 6 open reading frame 72	0.02	0.01	0.01	0.066
C6orf81	221481	chromosome 6 open reading frame 81	0.69	0.77	-0.08	0.081

Symbol	Gene ID	Gene Description	Mean β PE	Mean β NP	Δβ	FDR
C6orf89	221477	chromosome 6 open reading frame 89	0.08	0.05	0.03	0.081
C7orf16	10842	chromosome 7 open reading frame 16	0.62	0.76	-0.14	0.063
C7orf23	79161	chromosome 7 open reading frame 23	0.05	0.03	0.02	0.050
C7orf33	202865	chromosome 7 open reading frame 33	0.75	0.87	-0.12	0.090
C7orf9	64111	neuropeptide VF precursor	0.77	0.85	-0.08	0.090
C8A	731	complement component 8, alpha polypeptide	0.82	0.91	-0.09	0.053
C8B	732	complement component 8, beta polypeptide	0.66	0.77	-0.11	0.047
C8orf17	56988	chromosome 8 open reading frame 17	0.92	0.96	-0.04	0.038
C8ORFK32	51059	family with sequence similarity 135, member B	0.62	0.70	-0.08	0.093
C9orf10	23196	family with sequence similarity 120A	0.03	0.02	0.01	0.056
C9orf138	158297	family with sequence similarity 154, member A	0.86	0.79	0.07	0.083
C9orf23	138716	chromosome 9 open reading frame 23	0.06	0.05	0.02	0.085
C9orf24	84688	chromosome 9 open reading frame 24	0.73	0.82	-0.09	0.047
C9orf40	55071	chromosome 9 open reading frame 40	0.07	0.04	0.03	0.047
C9orf45	81571	chromosome 9 open reading frame 45	0.76	0.89	-0.12	0.038
C9orf48	347240	kinesin family member 24	0.76	0.84	-0.08	0.075
C9orf48	347240	kinesin family member 24	0.81	0.86	-0.05	0.078
C9orf64	84267	chromosome 9 open reading frame 64	0.46	0.36	0.10	0.080
C9orf72	203228	chromosome 9 open reading frame 72	0.03	0.02	0.01	0.085
CA4	762	carbonic anhydrase IV	0.06	0.02	0.04	0.090
CA6	765	carbonic anhydrase VI	0.81	0.93	-0.12	0.074
CABYR	26256	calcium binding tyrosine-(Y)-phosphorylation regulated	0.04	0.02	0.02	0.045

Symbol	Gene ID	Gene Description	Mean β PE	Mean β NP	Δβ	FDR
CACNG1	786	calcium channel, voltage-dependent, gamma subunit 1	0.09	0.13	-0.04	0.093
CALCA	796	calcitonin-related polypeptide alpha	0.08	0.05	0.03	0.077
CAMK2A	815	calcium/calmodulin-dependent protein kinase II alpha	0.58	0.75	-0.18	0.052
CAMSAP1	157922	calmodulin regulated spectrin-associated protein 1	0.61	0.68	-0.07	0.063
CAMSAP1	157922	calmodulin regulated spectrin-associated protein 1	0.50	0.63	-0.13	0.085
CANT1	124583	calcium activated nucleotidase 1	0.03	0.02	0.01	0.063
CAPN6	827	calpain 6	0.14	0.10	0.05	0.100
CAPS	828	calcyphosine	0.84	0.88	-0.04	0.090
CASC3	22794	cancer susceptibility candidate 3	0.05	0.03	0.02	0.079
CASP3	836	caspase 3, apoptosis-related cysteine peptidase	0.87	0.92	-0.05	0.080
CASP8AP2	9994	caspase 8 associated protein 2	0.03	0.02	0.01	0.086
CASQ1	844	calsequestrin 1 (fast-twitch, skeletal muscle)	0.91	0.95	-0.04	0.081
CASZ1	54897	castor zinc finger 1	0.03	0.02	0.01	0.099
CATSPER1	117144	cation channel, sperm associated 1	0.72	0.83	-0.11	0.066
CATSPER2	117155	cation channel, sperm associated 2	0.66	0.79	-0.13	0.063
CBWD1	55871	COBW domain containing 1	0.05	0.03	0.02	0.099
CCAR1	55749	cell division cycle and apoptosis regulator 1	0.03	0.02	0.01	0.087
CCBP2	1238	chemokine binding protein 2	0.93	0.95	-0.03	0.084
CCDC17	149483	coiled-coil domain containing 17	0.62	0.71	-0.09	0.064
CCDC41	51134	coiled-coil domain containing 41	0.04	0.02	0.02	0.075
CCDC48	79825	coiled-coil domain containing 48	0.84	0.90	-0.06	0.083
CCDC55	84081	coiled-coil domain containing 55	0.90	0.93	-0.03	0.074

Symbol	Gene ID	Gene Description	Mean β PE	Mean β NP	Δβ	FDR
CCKAR	886	cholecystokinin A receptor	0.47	0.57	-0.11	0.081
CCL1	6346	chemokine (C-C motif) ligand 1	0.77	0.85	-0.08	0.069
CCL13	6357	chemokine (C-C motif) ligand 13	0.89	0.93	-0.05	0.062
CCL21	6366	chemokine (C-C motif) ligand 21	0.72	0.80	-0.08	0.065
CCL22	6367	chemokine (C-C motif) ligand 22	0.86	0.93	-0.07	0.046
CCL23	6368	chemokine (C-C motif) ligand 23	0.46	0.61	-0.15	0.052
CCL5	6352	chemokine (C-C motif) ligand 5	0.70	0.82	-0.12	0.087
CCNC	892	cyclin C	0.03	0.01	0.01	0.081
CCND1	595	cyclin D1	0.81	0.88	-0.07	0.070
CCND2	894	cyclin D2	0.16	0.08	0.08	0.055
CCND2	894	cyclin D2	0.19	0.11	0.08	0.073
CCNL1	57018	cyclin L1	0.06	0.04	0.02	0.100
CCR8	1237	chemokine (C-C motif) receptor 8	0.88	0.92	-0.04	0.081
CD160	11126	CD160 molecule	0.92	0.95	-0.03	0.074
CD2BP2	10421	CD2 (cytoplasmic tail) binding protein 2	0.05	0.02	0.03	0.058
CD300LG	146894	CD300 molecule-like family member g	0.86	0.77	0.09	0.089
CD38	952	CD38 molecule	0.67	0.80	-0.12	0.043
CD3D	915	CD3d molecule, delta (CD3-TCR complex)	0.91	0.88	0.03	0.053
CD3G	917	CD3g molecule, gamma (CD3-TCR complex)	0.78	0.85	-0.07	0.080
CD99L2	83692	CD99 molecule-like 2	0.74	0.87	-0.13	0.042
CDC14A	8556	CDC14 cell division cycle 14 homolog A (S. cerevisiae)	0.02	0.01	0.01	0.047
CDCA1	83540	NUF2, NDC80 kinetochore complex component, homolog (S. cerevisiae)	0.01	0.02	-0.01	0.090

Symbol	Gene ID	Gene Description	Mean β PE	Mean β NP	Δβ	FDR
CDCA8	55143	cell division cycle associated 8	0.05	0.02	0.03	0.088
CDH1	999	cadherin 1, type 1, E-cadherin (epithelial)	0.44	0.61	-0.16	0.039
CDH26	60437	cadherin-like 26	0.67	0.80	-0.12	0.046
CDH3	1001	cadherin 3, type 1, P-cadherin (placental)	0.90	0.94	-0.04	0.099
CDK2	1017	cyclin-dependent kinase 2	0.04	0.02	0.02	0.073
CDK2AP1	8099	cyclin-dependent kinase 2 associated protein 1	0.03	0.02	0.01	0.077
CDK3	1018	cyclin-dependent kinase 3	0.04	0.07	-0.03	0.081
CDR1	1038	cerebellar degeneration-related protein 1, 34kDa	0.74	0.85	-0.11	0.042
CDS2	8760	CDP-diacylglycerol synthase (phosphatidate cytidylyltransferase) 2	0.36	0.47	-0.11	0.079
CDSN	1041	corneodesmosin	0.93	0.97	-0.04	0.063
CDX1	1044	caudal type homeobox 1	0.93	0.96	-0.03	0.097
CEACAM19	56971	carcinoembryonic antigen-related cell adhesion molecule 19	0.67	0.77	-0.11	0.065
CEACAM7	1087	carcinoembryonic antigen-related cell adhesion molecule 7	0.84	0.91	-0.07	0.073
CEACAM8	1088	carcinoembryonic antigen-related cell adhesion molecule 8	0.27	0.37	-0.10	0.038
CEBPZ	10153	CCAAT/enhancer binding protein (C/EBP), zeta	0.03	0.02	0.01	0.080
CECR5	27440	cat eye syndrome chromosome region, candidate 5	0.64	0.75	-0.11	0.041
CECR5	27440	cat eye syndrome chromosome region, candidate 5	0.70	0.83	-0.14	0.053
CEL	1056	carboxyl ester lipase (bile salt-stimulated lipase)	0.90	0.95	-0.04	0.065
CEP350	9857	centrosomal protein 350kDa	0.04	0.03	0.01	0.074

Symbol	Gene ID	Gene Description	Mean β PE	Mean β NP	Δβ	FDR
CEPT1	10390	choline/ethanolamine phosphotransferase 1	0.05	0.03	0.02	0.063
CHCHD8	51287	coiled-coil-helix-coiled-coil-helix domain containing 8	0.03	0.02	0.01	0.094
CHD2	1106	chromodomain helicase DNA binding protein 2	0.92	0.95	-0.03	0.074
CHFR	55743	checkpoint with forkhead and ring finger domains	0.77	0.86	-0.09	0.053
CHKA	1119	choline kinase alpha	0.07	0.03	0.04	0.073
CHMP4B	128866	chromatin modifying protein 4B	0.83	0.90	-0.07	0.054
CHMP5	51510	chromatin modifying protein 5	0.07	0.05	0.02	0.055
CHN1	1123	chimerin (chimaerin) 1	0.05	0.03	0.02	0.074
CHRM5	1133	cholinergic receptor, muscarinic 5	0.54	0.68	-0.14	0.055
CHRNA1	1134	cholinergic receptor, nicotinic, alpha 1 (muscle)	0.88	0.93	-0.05	0.077
CHRNA3	1136	cholinergic receptor, nicotinic, alpha 3	0.13	0.22	-0.09	0.082
CHRNA4	1137	cholinergic receptor, nicotinic, alpha 4	0.19	0.29	-0.10	0.074
CHRNA9	55584	cholinergic receptor, nicotinic, alpha 9	0.85	0.90	-0.05	0.080
CHRND	1144	cholinergic receptor, nicotinic, delta	0.86	0.81	0.04	0.089
CHST10	9486	carbohydrate sulfotransferase 10	0.08	0.05	0.03	0.087
CHST11	50515	carbohydrate (chondroitin 4) sulfotransferase 11	0.55	0.76	-0.21	0.093
CHST12	55501	carbohydrate (chondroitin 4) sulfotransferase 12	0.64	0.73	-0.09	0.099
CIB3	117286	calcium and integrin binding family member 3	0.82	0.89	-0.07	0.040
CIDEC	63924	cell death-inducing DFFA-like effector c	0.85	0.81	0.04	0.085
CINP	51550	cyclin-dependent kinase 2-interacting protein	0.02	0.01	0.01	0.067

Symbol	Gene ID	Gene Description	Mean β PE	Mean β NP	Δβ	FDR
CIP29	84324	SAP domain containing ribonucleoprotein	0.03	0.02	0.01	0.089
CIR	9541	corepressor interacting with RBPJ	0.51	0.69	-0.19	0.056
CLC	1178	Charcot-Leyden crystal protein	0.81	0.88	-0.07	0.059
CLCA2	9635	chloride channel accessory 2	0.74	0.82	-0.08	0.093
CLCN3	1182	chloride channel 3	0.05	0.03	0.02	0.099
CLDN10	9071	claudin 10	0.78	0.88	-0.10	0.076
CLDN18	51208	claudin 18	0.63	0.77	-0.14	0.074
CLDN18	51208	claudin 18	0.64	0.82	-0.18	0.077
CLDN20	49861	claudin 20	0.71	0.82	-0.10	0.084
CLDN8	9073	claudin 8	0.80	0.90	-0.10	0.042
CLEC2D	29121	C-type lectin domain family 2, member D	0.75	0.81	-0.06	0.090
CLMN	79789	calmin (calponin-like, transmembrane)	0.04	0.03	0.01	0.099
CLPX	10845	ClpX caseinolytic peptidase X homolog (E. coli)	0.05	0.03	0.02	0.085
CLTA	1211	clathrin, light chain (Lca)	0.05	0.02	0.03	0.066
CLUL1	27098	clusterin-like 1 (retinal)	0.08	0.05	0.03	0.046
CMTM5	116173	CKLF-like MARVEL transmembrane domain containing 5	0.93	0.96	-0.03	0.066
CNN1	1264	calponin 1, basic, smooth muscle	0.37	0.54	-0.17	0.053
CNOT8	9337	CCR4-NOT transcription complex, subunit 8	0.05	0.04	0.01	0.088
CNR1	1268	cannabinoid receptor 1 (brain)	0.69	0.80	-0.12	0.074
COCH	1690	coagulation factor C homolog, cochlin (Limulus polyphemus)	0.07	0.04	0.02	0.072
COL11A2	1302	collagen, type XI, alpha 2	0.08	0.05	0.03	0.094
COMMD2	51122	COMM domain containing 2	0.03	0.02	0.01	0.066

Symbol	Gene ID	Gene Description	Mean β PE	Mean β NP	Δβ	FDR
COPS5	10987	COP9 constitutive photomorphogenic homolog subunit 5 (Arabidopsis)	0.03	0.02	0.01	0.069
COPS6	10980	COP9 constitutive photomorphogenic homolog subunit 6 (Arabidopsis)	0.04	0.03	0.02	0.098
COPS7B	64708	COP9 constitutive photomorphogenic homolog subunit 7B (Arabidopsis)	0.22	0.13	0.09	0.065
CORO1C	23603	coronin, actin binding protein, 1C	0.06	0.04	0.02	0.055
CORO2B	10391	coronin, actin binding protein, 2B	0.89	0.92	-0.03	0.075
CP110	9738	CP110 protein	0.06	0.04	0.02	0.094
CPA2	1358	carboxypeptidase A2 (pancreatic)	0.63	0.72	-0.09	0.080
CPA2	1358	carboxypeptidase A2 (pancreatic)	0.54	0.69	-0.14	0.080
CPA4	51200	carboxypeptidase A4	0.88	0.91	-0.03	0.054
CPB2	1361	carboxypeptidase B2 (plasma)	0.89	0.92	-0.03	0.083
CPNE4	131034	copine IV	0.74	0.85	-0.11	0.024
CPO	130749	carboxypeptidase O	0.72	0.82	-0.10	0.053
CPO	130749	carboxypeptidase O	0.85	0.92	-0.07	0.054
CREBL1	1388	activating transcription factor 6 beta	0.03	0.02	0.02	0.063
CRH	1392	corticotropin releasing hormone	0.51	0.67	-0.17	0.042
CRMP1	1400	collapsin response mediator protein 1	0.07	0.06	0.02	0.090
CRSP6	9440	mediator complex subunit 17	0.02	0.01	0.01	0.096
CRTAM	56253	cytotoxic and regulatory T cell molecule	0.50	0.67	-0.17	0.046
CRYBA1	1411	crystallin, beta A1	0.77	0.86	-0.09	0.063
CRYBA1	1411	crystallin, beta A1	0.91	0.95	-0.05	0.073
CRYGC	1420	crystallin, gamma C	0.73	0.88	-0.14	0.074
CSH2	1443	chorionic somatomammotropin hormone 2	0.94	0.91	0.03	0.053
CST4	1472	cystatin S	0.82	0.91	-0.08	0.042

Symbol	Gene ID	Gene Description	Mean β PE	Mean β NP	Δβ	FDR
CST8	10047	cystatin 8 (cystatin-related epididymal specific)	0.72	0.82	-0.10	0.059
CTCF	10664	CCCTC-binding factor (zinc finger protein)	0.03	0.02	0.01	0.070
CTNNA3	29119	catenin (cadherin-associated protein), alpha 3	0.14	0.10	0.04	0.091
CTPS	1503	CTP synthase	0.87	0.92	-0.05	0.065
CTSE	1510	cathepsin E	0.75	0.88	-0.13	0.054
CTTNBP2NL	55917	CTTNBP2 N-terminal like	0.10	0.04	0.06	0.055
CTXN1	404217	cortexin 1	0.75	0.66	0.09	0.073
CUEDC1	404093	CUE domain containing 1	0.60	0.69	-0.09	0.081
CUL5	8065	cullin 5	0.08	0.05	0.04	0.064
CUZD1	50624	CUB and zona pellucida-like domains 1	0.27	0.36	-0.09	0.063
CWF19L2	143884	CWF19-like 2, cell cycle control (S. pombe)	0.83	0.90	-0.07	0.053
CX62	84694	gap junction protein, alpha 10, 62kDa	0.76	0.84	-0.08	0.086
CXCL16	58191	chemokine (C-X-C motif) ligand 16	0.97	0.98	-0.01	0.099
CXCR3	2833	chemokine (C-X-C motif) receptor 3	0.52	0.61	-0.09	0.040
CXorf15	55787	chromosome X open reading frame 15	0.05	0.02	0.03	0.047
CXorf20	139105	BEN domain containing 2	0.53	0.66	-0.13	0.088
CXorf45	79868	asparagine-linked glycosylation 13 homolog (S. cerevisiae)	0.54	0.67	-0.12	0.099
CXorf9	54440	SAM and SH3 domain containing 3	0.63	0.70	-0.07	0.085
CYCS	54205	cytochrome c, somatic	0.06	0.04	0.02	0.089
CYP17A1	1586	cytochrome P450, family 17, subfamily A, polypeptide 1	0.60	0.71	-0.11	0.055
CYP19A1	1588	cytochrome P450, family 19, subfamily A, polypeptide 1	0.82	0.90	-0.08	0.063

Symbol	Gene ID	Gene Description	Mean β PE	Mean β NP	Δβ	FDR
CYP2R1	120227	cytochrome P450, family 2, subfamily R, polypeptide 1	0.04	0.02	0.01	0.050
CYP3A7	1551	cytochrome P450, family 3, subfamily A, polypeptide 7	0.73	0.81	-0.08	0.094
CYP4F2	8529	cytochrome P450, family 4, subfamily F, polypeptide 2	0.63	0.74	-0.11	0.087
CYP4Z1	199974	cytochrome P450, family 4, subfamily Z, polypeptide 1	0.56	0.66	-0.09	0.079
CYP7B1	9420	cytochrome P450, family 7, subfamily B, polypeptide 1	0.71	0.85	-0.14	0.041
CYSLTR2	57105	cysteinyl leukotriene receptor 2	0.78	0.87	-0.09	0.061
DAO	1610	D-amino-acid oxidase	0.88	0.92	-0.04	0.050
DAPK1	1612	death-associated protein kinase 1	0.59	0.73	-0.14	0.074
DAPK3	1613	death-associated protein kinase 3	0.03	0.02	0.01	0.089
DBT	1629	dihydrolipoamide branched chain transacylase E2	0.04	0.02	0.02	0.081
DCAKD	79877	dephospho-CoA kinase domain containing	0.82	0.87	-0.06	0.065
DCC	1630	deleted in colorectal carcinoma	0.09	0.06	0.04	0.038
DCHS1	8642	dachsous 1 (Drosophila)	0.82	0.78	0.05	0.065
DCLRE1C	64421	DNA cross-link repair 1C (PSO2 homolog, S. cerevisiae)	0.01	0.01	0.01	0.087
DCST1	149095	DC-STAMP domain containing 1	0.84	0.91	-0.07	0.074
DCST1	149095	DC-STAMP domain containing 1	0.15	0.20	-0.05	0.090
DCTN4	51164	dynactin 4 (p62)	0.03	0.02	0.01	0.079
DDX10	1662	DEAD (Asp-Glu-Ala-Asp) box polypeptide 10	0.05	0.03	0.01	0.094
DDX19A	55308	DEAD (Asp-Glu-Ala-As) box polypeptide 19A	0.03	0.02	0.01	0.089

Symbol	Gene ID	Gene Description	Mean β PE	Mean β NP	Δβ	FDR
DDX6	1656	DEAD (Asp-Glu-Ala-Asp) box polypeptide 6	0.09	0.06	0.02	0.084
DEFA1	1667	defensin, alpha 1	0.58	0.69	-0.11	0.065
DEFB1	1672	defensin, beta 1	0.62	0.53	0.09	0.089
DEFB125	245938	defensin, beta 125	0.67	0.76	-0.09	0.067
DEFB129	140881	defensin, beta 129	0.71	0.80	-0.09	0.074
DENND2C	163259	DENN/MADD domain containing 2C	0.03	0.01	0.01	0.065
DENND4C	55667	DENN/MADD domain containing 4C	0.55	0.68	-0.14	0.075
DEPDC2	80243	phosphatidylinositol-3,4,5-trisphosphate-dependent Rac exchange factor 2	0.05	0.04	0.01	0.087
DERL1	79139	Der1-like domain family, member 1	0.04	0.02	0.01	0.080
DHDH	27294	dihydrodiol dehydrogenase (dimeric)	0.77	0.88	-0.12	0.052
DHRS8	51170	hydroxysteroid (17-beta) dehydrogenase 11	0.05	0.03	0.02	0.087
DHTKD1	55526	dehydrogenase E1 and transketolase domain containing 1	0.07	0.04	0.03	0.100
DHX16	8449	DEAH (Asp-Glu-Ala-His) box polypeptide 16	0.04	0.02	0.02	0.097
DHX37	57647	DEAH (Asp-Glu-Ala-His) box polypeptide 37	0.83	0.92	-0.09	0.065
DHX57	90957	DEAH (Asp-Glu-Ala-Asp/His) box polypeptide 57	0.36	0.49	-0.12	0.066
DIPA	11007	coiled-coil domain containing 85B	0.05	0.03	0.02	0.063
DIRAS3	9077	DIRAS family, GTP-binding RAS-like 3	0.27	0.42	-0.14	0.074
DKFZp434N035	84222	transmembrane protein 191A	0.84	0.92	-0.08	0.047
DKFZp434O0527	255101	coiled-coil domain containing 108	0.86	0.78	0.08	0.064

Symbol	Gene ID	Gene Description	Mean β PE	Mean β NP	Δβ	FDR
DKFZp727G131	221786	chromosome 7 open reading frame 38	0.07	0.04	0.03	0.090
DLK1	8788	delta-like 1 homolog (Drosophila)	0.04	0.02	0.01	0.066
DLX5	1749	distal-less homeobox 5	0.07	0.03	0.04	0.046
DLX5	1749	distal-less homeobox 5	0.03	0.02	0.01	0.097
DMBX1	127343	diencephalon/mesencephalon homeobox 1	0.40	0.55	-0.16	0.088
DNAH10	196385	dynein, axonemal, heavy chain 10	0.82	0.89	-0.07	0.065
DNAH5	1767	dynein, axonemal, heavy chain 5	0.78	0.87	-0.09	0.042
DNAH8	1769	dynein, axonemal, heavy chain 8	0.78	0.86	-0.07	0.080
DNAHL1	284176	dynein, axonemal, heavy chain like 1	0.90	0.94	-0.04	0.063
DNAI2	64446	dynein, axonemal, intermediate chain 2	0.83	0.92	-0.09	0.042
DNAJA4	55466	DnaJ (Hsp40) homolog, subfamily A, member 4	0.81	0.89	-0.08	0.066
DNAJC11	55735	DnaJ (Hsp40) homolog, subfamily C, member 11	0.71	0.80	-0.09	0.084
DNAJC12	56521	DnaJ (Hsp40) homolog, subfamily C, member 12	0.85	0.89	-0.04	0.080
DNAJC5G	285126	DnaJ (Hsp40) homolog, subfamily C, member 5 gamma	0.73	0.82	-0.09	0.099
DNASE1	1773	deoxyribonuclease I	0.87	0.93	-0.06	0.053
DNM1L	10059	dynamin 1-like	0.87	0.92	-0.05	0.063
DNMBP	23268	dynamin binding protein	0.73	0.82	-0.09	0.098
DNTT	1791	deoxynucleotidyltransferase, terminal	0.56	0.71	-0.15	0.038
DNTT	1791	deoxynucleotidyltransferase, terminal	0.61	0.70	-0.09	0.099
DOCK1	1793	dedicator of cytokinesis 1	0.93	0.91	0.02	0.047
DOM3Z	1797	dom-3 homolog Z (C. elegans)	0.87	0.92	-0.05	0.080

Symbol	Gene ID	Gene Description	Mean β PE	Mean β NP	Δβ	FDR
DPF1	8193	D4, zinc and double PHD fingers family 1	0.11	0.06	0.04	0.065
DPF1	8193	D4, zinc and double PHD fingers family 1	0.16	0.09	0.07	0.073
DPM2	8818	dolichyl-phosphate mannosyltransferase polypeptide 2, regulatory subunit	0.03	0.02	0.01	0.065
DPP6	1804	dipeptidyl-peptidase 6	0.77	0.84	-0.07	0.098
DQX1	165545	DEAQ box RNA-dependent ATPase 1	0.06	0.08	-0.02	0.076
DQX1	165545	DEAQ box RNA-dependent ATPase 1	0.79	0.87	-0.08	0.093
DRD2	1813	dopamine receptor D2	0.91	0.94	-0.03	0.075
DRP2	1821	dystrophin related protein 2	0.52	0.61	-0.10	0.073
DSCR10	259234	Down syndrome critical region gene 10	0.85	0.91	-0.06	0.052
DSU	55686	melanoregulin	0.05	0.02	0.03	0.094
DTNBP1	84062	dystrobrevin binding protein 1	0.72	0.84	-0.11	0.052
DUS2L	54920	dihydrouridine synthase 2-like, SMM1 homolog (S. cerevisiae)	0.02	0.01	0.01	0.068
DUSP13	51207	dual specificity phosphatase 13	0.31	0.42	-0.11	0.065
DUSP3	1845	dual specificity phosphatase 3	0.03	0.02	0.01	0.065
DUSP4	1846	dual specificity phosphatase 4	0.04	0.03	0.01	0.075
DYNC1LI2	1783	dynein, cytoplasmic 1, light intermediate chain 2	0.02	0.01	0.01	0.081
DYNLT1	6993	dynein, light chain, Tctex-type 1	0.07	0.04	0.02	0.067
DYRK4	8798	dual-specificity tyrosine-(Y)-phosphorylation regulated kinase 4	0.79	0.85	-0.06	0.067
E2F5	1875	E2F transcription factor 5, p130-binding	0.03	0.02	0.01	0.090
EAF2	55840	ELL associated factor 2	0.02	0.01	0.01	0.084

Symbol	Gene ID	Gene Description	Mean β PE	Mean β NP	Δβ	FDR
EBNA1BP2	10969	EBNA1 binding protein 2	0.05	0.03	0.02	0.071
ECH1	1891	enoyl Coenzyme A hydratase 1, peroxisomal	0.03	0.01	0.01	0.059
EDG7	23566	lysophosphatidic acid receptor 3	0.64	0.76	-0.12	0.099
EDG8	53637	sphingosine-1-phosphate receptor 5	0.05	0.04	0.02	0.098
EDN1	1906	endothelin 1	0.04	0.03	0.01	0.040
EDNRB	1910	endothelin receptor type B	0.42	0.53	-0.11	0.100
EEF1G	1937	eukaryotic translation elongation factor 1 gamma	0.03	0.02	0.01	0.080
EFCAB1	79645	EF-hand calcium binding domain 1	0.83	0.89	-0.06	0.066
EFHD1	80303	EF-hand domain family, member D1	0.11	0.07	0.04	0.090
EFNB1	1947	ephrin-B1	0.22	0.31	-0.10	0.090
EGFL7	51162	EGF-like-domain, multiple 7	0.45	0.60	-0.15	0.065
EI24	9538	etoposide induced 2.4 mRNA	0.16	0.06	0.11	0.067
EIF2AK1	27102	eukaryotic translation initiation factor 2-alpha kinase 1	0.03	0.02	0.01	0.074
EIF2B3	8891	eukaryotic translation initiation factor 2B, subunit 3 gamma, 58kDa	0.02	0.01	0.01	0.065
ELA2	1991	elastase, neutrophil expressed	0.56	0.68	-0.11	0.042
ELAC1	55520	elaC homolog 1 (E. coli)	0.72	0.82	-0.10	0.082
ELOF1	84337	elongation factor 1 homolog (S. cerevisiae)	0.76	0.86	-0.09	0.069
ENDOGL1	9941	endo/exonuclease (5'-3'), endonuclease G-like	0.60	0.73	-0.14	0.047
ENPP3	5169	ectonucleotide pyrophosphatase/phosphodiesterase 3	0.70	0.79	-0.09	0.065
ENPP5	59084	ectonucleotide pyrophosphatase/phosphodiesterase 5 (putative function)	0.04	0.03	0.01	0.074

Symbol	Gene ID	Gene Description	Mean β PE	Mean β NP	Δβ	FDR
ENTPD4	9583	ectonucleoside triphosphate diphosphohydrolase 4	0.82	0.86	-0.05	0.094
ENTPD7	57089	ectonucleoside triphosphate diphosphohydrolase 7	0.05	0.03	0.02	0.099
ENY2	56943	enhancer of yellow 2 homolog (Drosophila)	0.02	0.01	0.01	0.095
EPB49	2039	erythrocyte membrane protein band 4.9 (dematin)	0.68	0.78	-0.09	0.065
EPPB9	27077	B9 protein domain 1	0.64	0.76	-0.12	0.082
EPS8L1	54869	EPS8-like 1	0.83	0.89	-0.06	0.070
EPS8L3	79574	EPS8-like 3	0.20	0.27	-0.06	0.066
EPS8L3	79574	EPS8-like 3	0.90	0.87	0.03	0.094
ERAF	51327	erythroid associated factor	0.70	0.77	-0.07	0.074
ERBB2	2064	v-erb-b2 erythroblastic leukemia viral oncogene homolog 2, neuro/glioblastoma derived oncogene homolog (avian)	0.08	0.06	0.02	0.065
ERBB2	2064	v-erb-b2 erythroblastic leukemia viral oncogene homolog 2, neuro/glioblastoma derived oncogene homolog (avian)	0.04	0.02	0.01	0.081
ERBB2IP	55914	erbb2 interacting protein	0.07	0.04	0.03	0.063
ERCC1	2067	excision repair cross-complementing rodent repair deficiency, complementation group 1 (includes overlapping antisense sequence)	0.15	0.11	0.05	0.099
ERCC6	2074	excision repair cross-complementing rodent repair deficiency, complementation group 6	0.03	0.02	0.01	0.070
ERH	2079	enhancer of rudimentary homolog (Drosophila)	0.03	0.02	0.01	0.065
ERMAP	114625	erythroblast membrane-associated protein (Scianna blood group)	0.04	0.02	0.02	0.025

Symbol	Gene ID	Gene Description	Mean β PE	Mean β NP	Δβ	FDR
ERV3	2086	endogenous retroviral sequence 3 (includes zinc finger protein H-plk/HPF9)	0.89	0.93	-0.04	0.039
ERVWE1	30816	endogenous retroviral family W, env(C7), member 1	0.73	0.85	-0.12	0.047
ETS1	2113	v-ets erythroblastosis virus E26 oncogene homolog 1 (avian)	0.03	0.02	0.02	0.066
ETS1	2113	v-ets erythroblastosis virus E26 oncogene homolog 1 (avian)	0.03	0.02	0.01	0.067
EVI5	7813	ecotropic viral integration site 5	0.87	0.92	-0.05	0.068
EVPL	2125	envoplakin	0.06	0.10	-0.04	0.064
EWSR1	2130	Ewing sarcoma breakpoint region 1	0.03	0.01	0.01	0.087
EXOC1	55763	exocyst complex component 1	0.02	0.01	0.01	0.079
EXOSC6	118460	exosome component 6	0.71	0.82	-0.11	0.042
EXOSC9	5393	exosome component 9	0.04	0.02	0.02	0.046
F12	2161	coagulation factor XII (Hageman factor)	0.86	0.91	-0.04	0.063
F2	2147	coagulation factor II (thrombin)	0.82	0.87	-0.06	0.061
F8A1	8263	coagulation factor VIII-associated (intronic transcript) 1	0.79	0.72	0.07	0.084
FABP1	2168	fatty acid binding protein 1, liver	0.60	0.71	-0.11	0.047
FABP4	2167	fatty acid binding protein 4, adipocyte	0.41	0.58	-0.16	0.050
FAIM2	23017	Fas apoptotic inhibitory molecule 2	0.87	0.94	-0.07	0.042
FALZ	2186	bromodomain PHD finger transcription factor	0.03	0.01	0.02	0.099
FAM113A	64773	family with sequence similarity 113, member A	0.84	0.92	-0.09	0.045
FAM71B	153745	family with sequence similarity 71, member B	0.66	0.80	-0.15	0.065

Symbol	Gene ID	Gene Description	Mean β PE	Mean β NP	Δβ	FDR
FAM76A	199870	family with sequence similarity 76, member A	0.03	0.01	0.01	0.094
FAM83A	84985	family with sequence similarity 83, member A	0.54	0.67	-0.14	0.053
FAM86A	196483	family with sequence similarity 86, member A	0.02	0.01	0.01	0.078
FAM9A	171482	family with sequence similarity 9, member A	0.92	0.94	-0.02	0.065
FBLN1	2192	fibulin 1	0.82	0.86	-0.04	0.088
FBP1	2203	fructose-1,6-bisphosphatase 1	0.11	0.07	0.04	0.074
FBXL19	54620	F-box and leucine-rich repeat protein 19	0.82	0.87	-0.06	0.074
FBXO15	201456	F-box protein 15	0.09	0.05	0.05	0.071
FBXO28	23219	F-box protein 28	0.02	0.01	0.01	0.066
FBXO28	23219	F-box protein 28	0.04	0.02	0.02	0.074
FBXO44	93611	F-box protein 44	0.84	0.89	-0.05	0.080
FBXO5	26271	F-box protein 5	0.03	0.01	0.01	0.085
FCGR2A	2212	Fc fragment of IgG, low affinity IIa, receptor (CD32)	0.86	0.91	-0.06	0.053
FCN3	8547	ficolin (collagen/fibrinogen domain containing) 3 (Hakata antigen)	0.92	0.89	0.03	0.088
FCRL3	115352	Fc receptor-like 3	0.57	0.69	-0.12	0.086
FDPS	2224	farnesyl diphosphate synthase (farnesyl pyrophosphate synthetase, dimethylallyltranstransferase, geranyltranstransferase)	0.03	0.02	0.01	0.074
FECH	2235	ferrochelatase (protoporphyria)	0.07	0.03	0.04	0.074
FEN1	2237	flap structure-specific endonuclease 1	0.03	0.02	0.01	0.065
FEN1	2237	flap structure-specific endonuclease 1	0.06	0.02	0.04	0.074
FERD3L	222894	Fer3-like (Drosophila)	0.07	0.04	0.03	0.080

Symbol	Gene ID	Gene Description	Mean β PE	Mean β NP	Δβ	FDR
FGF19	9965	fibroblast growth factor 19	0.55	0.45	0.09	0.090
FGF21	26291	fibroblast growth factor 21	0.90	0.86	0.04	0.074
FHIT	2272	fragile histidine triad gene	0.29	0.21	0.08	0.063
FHL1	2273	four and a half LIM domains 1	0.75	0.85	-0.10	0.065
FHL3	2275	four and a half LIM domains 3	0.06	0.03	0.04	0.098
FKBP4	2288	FK506 binding protein 4, 59kDa	0.85	0.91	-0.06	0.056
FKBP5	2289	FK506 binding protein 5	0.67	0.75	-0.08	0.042
FKSG2	59347	apoptosis inhibitor	0.89	0.92	-0.04	0.094
FLJ10379	55133	S1 RNA binding domain 1	0.73	0.81	-0.08	0.089
FLJ10916	55258	threonine synthase-like 2 (S. cerevisiae)	0.64	0.79	-0.15	0.066
FLJ13614	84142	family with sequence similarity 175, member A	0.05	0.03	0.02	0.081
FLJ14437	84665	myopalladin	0.76	0.85	-0.09	0.067
FLJ14437	84665	myopalladin	0.59	0.74	-0.15	0.074
FLJ20130	54830	nucleoporin 62kDa C-terminal like	0.75	0.65	0.10	0.065
FLJ20364	54908	coiled-coil domain containing 99	0.04	0.03	0.02	0.074
FLJ20718	55027	HEAT repeat containing 3	0.83	0.89	-0.06	0.073
FLJ21103	79607	family with sequence similarity 118, member B	0.71	0.80	-0.10	0.074
FLJ21736	79984	esterase 31	0.58	0.68	-0.10	0.074
FLJ21827	56912	chromosome 11 open reading frame 60	0.07	0.03	0.03	0.047
FLJ21908	79657	RNA polymerase II associated protein 3	0.07	0.04	0.02	0.094
FLJ22222	79701	chromosome 17 open reading frame 101	0.07	0.04	0.02	0.080
FLJ22555	79568	chromosome 2 open reading frame 47	0.84	0.89	-0.05	0.073

Symbol	Gene ID	Gene Description	Mean β PE	Mean β NP	Δβ	FDR
FLJ22624	79866	chromosome 13 open reading frame 34	0.05	0.03	0.03	0.081
FLJ23322	80020	FAD-dependent oxidoreductase domain containing 2	0.77	0.87	-0.10	0.075
FLJ23356	84197	protein kinase-like protein SgK196	0.03	0.02	0.02	0.086
FLJ25006	124923	uncharacterized serine/threonine-protein kinase SgK494	0.61	0.75	-0.13	0.094
FLJ25067	149840	chromosome 20 open reading frame 196	0.15	0.12	0.04	0.067
FLJ25084	151516	aspartic peptidase, retroviral-like 1	0.61	0.70	-0.09	0.068
FLJ25369	200523	chromosome 2 open reading frame 51	0.78	0.85	-0.07	0.065
FLJ25530	220296	hepatic and glial cell adhesion molecule	0.69	0.81	-0.12	0.047
FLJ25976	283579	chromosome 14 open reading frame 178	0.51	0.65	-0.14	0.082
FLJ30294	130827	transmembrane protein 182	0.65	0.74	-0.09	0.047
FLJ32028	201799	transmembrane protein 154	0.63	0.77	-0.15	0.053
FLJ32065	201283	hypothetical protein FLJ32065	0.03	0.02	0.01	0.054
FLJ32065	201283	hypothetical protein FLJ32065	0.81	0.91	-0.10	0.065
FLJ32206	149421	chromosome 1 open reading frame 215	0.58	0.73	-0.15	0.081
FLJ32894	144360	chromosome 12 open reading frame 67	0.77	0.85	-0.08	0.088
FLJ33534	285150	hypothetical LOC285150	0.52	0.67	-0.15	0.067
FLJ33790	283212	kelch-like 35 (Drosophila)	0.04	0.03	0.02	0.048
FLJ35784	374877	chromosome 19 open reading frame 45	0.78	0.85	-0.07	0.043
FLJ35785	283796	golgin A8 family, member I, pseudogene	0.74	0.80	-0.06	0.090

Symbol	Gene ID	Gene Description	Mean β PE	Mean β NP	Δβ	FDR
FLJ35801	150291	chromosome 22 open reading frame 27	0.64	0.52	0.12	0.081
FLJ35894	283847	coiled-coil domain containing 79	0.90	0.94	-0.04	0.073
FLJ37078	222183	hypothetical protein FLJ37078	0.47	0.57	-0.10	0.088
FLJ37587	283446	myosin IH	0.74	0.83	-0.09	0.042
FLJ37587	283446	myosin IH	0.77	0.71	0.06	0.053
FLJ38379	285097	hypothetical FLJ38379	0.47	0.62	-0.14	0.047
FLJ38451	126375	zinc finger protein 792	0.86	0.93	-0.07	0.053
FLJ40142	400073	chromosome 12 open reading frame 76	0.93	0.96	-0.03	0.054
FLJ40288	286023	hypothetical FLJ40288	0.53	0.74	-0.21	0.086
FLJ40919	144809	chromosome 13 open reading frame 30	0.70	0.78	-0.08	0.079
FLJ41131	284325	chromosome 19 open reading frame 54	0.03	0.02	0.01	0.086
FLJ42291	346547	hypothetical LOC346547	0.49	0.61	-0.12	0.073
FLJ43582	389649	chromosome 8 open reading frame 86	0.95	0.97	-0.02	0.056
FLJ44186	346689	killer cell lectin-like receptor subfamily G, member 2	0.67	0.79	-0.12	0.038
FLJ44691	345193	leucine-rich repeat, immunoglobulin-like and transmembrane domains 3	0.71	0.85	-0.13	0.057
FLJ45909	126432	Ras and Rab interactor-like	0.67	0.79	-0.12	0.072
FLJ90650	206338	laeverin	0.74	0.83	-0.09	0.050
FLJ90805	284339	transmembrane protein 145	0.10	0.07	0.03	0.094
FLT3LG	2323	fms-related tyrosine kinase 3 ligand	0.05	0.02	0.02	0.094
FMO1	2326	flavin containing monooxygenase 1	0.66	0.72	-0.07	0.080
FMO3	2328	flavin containing monooxygenase 3	0.87	0.91	-0.05	0.080
FMO5	2330	flavin containing monooxygenase 5	0.07	0.04	0.03	0.090

Symbol	Gene ID	Gene Description	Mean β PE	Mean β NP	Δβ	FDR
FNDC3B	64778	fibronectin type III domain containing 3B	0.88	0.93	-0.05	0.065
FNDC3B	64778	fibronectin type III domain containing 3B	0.81	0.93	-0.12	0.065
FNDC8	54752	fibronectin type III domain containing 8	0.73	0.81	-0.08	0.050
FNDC8	54752	fibronectin type III domain containing 8	0.15	0.10	0.06	0.089
FNTB	2342	farnesyltransferase, CAAX box, beta	0.06	0.03	0.03	0.066
FOLR2	2350	folate receptor 2 (fetal)	0.80	0.88	-0.08	0.073
FOS	2353	v-fos FBJ murine osteosarcoma viral oncogene homolog	0.01	0.01	0.01	0.074
FOXD4L4	349334	forkhead box D4-like 4	0.04	0.06	-0.02	0.062
FOXN1	8456	forkhead box N1	0.85	0.94	-0.09	0.025
FRMD4A	55691	FERM domain containing 4A	0.69	0.58	0.12	0.077
FSIP1	161835	fibrous sheath interacting protein 1	0.07	0.04	0.03	0.070
FTMT	94033	ferritin mitochondrial	0.80	0.91	-0.12	0.066
FURIN	5045	furin (paired basic amino acid cleaving enzyme)	0.33	0.39	-0.06	0.099
FUT5	2527	fucosyltransferase 5 (alpha (1,3) fucosyltransferase)	0.67	0.77	-0.10	0.065
FXC1	26515	fracture callus 1 homolog (rat)	0.80	0.91	-0.11	0.042
FYTTD1	84248	forty-two-three domain containing 1	0.05	0.03	0.02	0.046
FZD4	8322	frizzled homolog 4 (Drosophila)	0.03	0.02	0.01	0.089
G1P2	9636	ISG15 ubiquitin-like modifier	0.04	0.02	0.02	0.094
GABPA	2551	GA binding protein transcription factor, alpha subunit 60kDa	0.05	0.02	0.03	0.065
GABRA5	2558	gamma-aminobutyric acid (GABA) A receptor, alpha 5	0.20	0.30	-0.11	0.042

Symbol	Gene ID	Gene Description	Mean β PE	Mean β NP	Δβ	FDR
GALNT13	114805	UDP-N-acetyl-alpha-D-galactosamine:polypeptide N-acetylgalactosaminyltransferase 13 (GalNAc-T13)	0.32	0.51	-0.19	0.054
GALNT6	11226	UDP-N-acetyl-alpha-D-galactosamine:polypeptide N-acetylgalactosaminyltransferase 6 (GalNAc-T6)	0.81	0.88	-0.07	0.042
GAP43	2596	growth associated protein 43	0.03	0.02	0.01	0.065
GAS7	8522	growth arrest-specific 7	0.06	0.04	0.02	0.075
GAS8	2622	growth arrest-specific 8	0.02	0.02	0.01	0.074
GATA1	2623	GATA binding protein 1 (globin transcription factor 1)	0.65	0.78	-0.13	0.047
GATA5	140628	GATA binding protein 5	0.90	0.86	0.04	0.094
GCA	25801	grancalcin, EF-hand calcium binding protein	0.06	0.04	0.03	0.086
GCDH	2639	glutaryl-Coenzyme A dehydrogenase	0.03	0.02	0.01	0.050
GCK	2645	glucokinase (hexokinase 4)	0.85	0.91	-0.06	0.087
GCNT2	2651	glucosaminyl (N-acetyl) transferase 2, I-branching enzyme (I blood group)	0.67	0.76	-0.09	0.065
Gcom1	145781	GRINL1A complex locus	0.10	0.15	-0.05	0.088
GFRA2	2675	GDNF family receptor alpha 2	0.90	0.96	-0.06	0.074
GGA2	23062	golgi associated, gamma adaptin ear containing, ARF binding protein 2	0.05	0.03	0.02	0.065
GGPS1	9453	geranylgeranyl diphosphate synthase 1	0.10	0.06	0.04	0.065
GIMAP7	168537	GTPase, IMAP family member 7	0.78	0.86	-0.08	0.064
GIPR	2696	gastric inhibitory polypeptide receptor	0.65	0.78	-0.12	0.056
GJB1	2705	gap junction protein, beta 1, 32kDa	0.86	0.90	-0.05	0.053
GJB6	10804	gap junction protein, beta 6, 30kDa	0.71	0.81	-0.10	0.081
GK	2710	glycerol kinase	0.73	0.80	-0.06	0.089

Symbol	Gene ID	Gene Description	Mean β PE	Mean β NP	Δβ	FDR
GLI3	2737	GLI family zinc finger 3	0.03	0.02	0.01	0.064
GLO1	2739	glyoxalase I	0.03	0.02	0.01	0.047
GLT28D1	55849	asparagine-linked glycosylation 13 homolog (S. cerevisiae)	0.89	0.92	-0.03	0.081
GLTSCR1	29998	glioma tumor suppressor candidate region gene 1	0.76	0.85	-0.09	0.050
GLTSCR1	29998	glioma tumor suppressor candidate region gene 1	0.74	0.82	-0.08	0.096
GLULD1	51557	lengsin, lens protein with glutamine synthetase domain	0.89	0.93	-0.04	0.050
GMCL1L	64396	germ cell-less homolog 1 (Drosophila)	0.81	0.89	-0.07	0.050
GNAO1	2775	guanine nucleotide binding protein (G protein), alpha activating activity polypeptide O	0.03	0.02	0.01	0.089
GNAS	2778	GNAS complex locus	0.25	0.36	-0.11	0.048
GNAS	2778	GNAS complex locus	0.46	0.56	-0.11	0.093
GNB1L	54584	guanine nucleotide binding protein (G protein), beta polypeptide 1-like	0.02	0.01	0.01	0.074
GNG4	2786	guanine nucleotide binding protein (G protein), gamma 4	0.10	0.05	0.05	0.067
GNG7	2788	guanine nucleotide binding protein (G protein), gamma 7	0.53	0.67	-0.14	0.056
GOLGA2L1	55592	golgi autoantigen, golgin subfamily a, 2-like 1	0.91	0.94	-0.03	0.085
GOLPH2	51280	golgi membrane protein 1	0.10	0.05	0.05	0.099
GORASP1	64689	golgi reassembly stacking protein 1, 65kDa	0.08	0.04	0.04	0.065
GOSR2	9570	golgi SNAP receptor complex member 2	0.06	0.04	0.03	0.064
GOSR2	9570	golgi SNAP receptor complex member 2	0.02	0.01	0.01	0.093

Symbol	Gene ID	Gene Description	Mean β PE	Mean β NP	Δβ	FDR
GP1BA	2811	glycoprotein Ib (platelet), alpha polypeptide	0.69	0.81	-0.12	0.063
GP2	2813	glycoprotein 2 (zymogen granule membrane)	0.62	0.73	-0.11	0.094
GP5	2814	glycoprotein V (platelet)	0.82	0.89	-0.07	0.063
GPAA1	8733	glycosylphosphatidylinositol anchor attachment protein 1 homolog (yeast)	0.04	0.02	0.02	0.064
GPATC2	55105	G patch domain containing 2	0.60	0.74	-0.14	0.052
GPC4	2239	glypican 4	0.85	0.91	-0.06	0.076
GPR1	2825	G protein-coupled receptor 1	0.65	0.79	-0.14	0.042
GPR115	221393	G protein-coupled receptor 115	0.17	0.29	-0.11	0.094
GPR12	2835	G protein-coupled receptor 12	0.59	0.70	-0.10	0.074
GPR137B	7107	G protein-coupled receptor 137B	0.02	0.01	0.01	0.093
GPR15	2838	G protein-coupled receptor 15	0.78	0.87	-0.09	0.082
GPR156	165829	G protein-coupled receptor 156	0.23	0.34	-0.11	0.055
GPR173	54328	G protein-coupled receptor 173	0.89	0.94	-0.05	0.050
GPR175	131601	G protein-coupled receptor 175	0.91	0.95	-0.03	0.068
GPR3	2827	G protein-coupled receptor 3	0.05	0.03	0.02	0.095
GPR31	2853	G protein-coupled receptor 31	0.89	0.92	-0.03	0.074
GPR37L1	9283	G protein-coupled receptor 37 like 1	0.81	0.86	-0.05	0.089
GPR61	83873	G protein-coupled receptor 61	0.80	0.87	-0.08	0.064
GPRC5D	55507	G protein-coupled receptor, family C, group 5, member D	0.55	0.67	-0.12	0.097
GPSM1	26086	G-protein signaling modulator 1 (AGS3-like, C. elegans)	0.21	0.28	-0.07	0.046
GPSM1	26086	G-protein signaling modulator 1 (AGS3-like, C. elegans)	0.79	0.88	-0.09	0.046
GPSN2	9524	glycoprotein, synaptic 2	0.13	0.09	0.04	0.042

Symbol	Gene ID	Gene Description	Mean β PE	Mean β NP	Δβ	FDR
GPSN2	9524	glycoprotein, synaptic 2	0.08	0.05	0.02	0.079
GPT	2875	glutamic-pyruvate transaminase (alanine aminotransferase)	0.04	0.05	-0.01	0.097
GRLF1	2909	glucocorticoid receptor DNA binding factor 1	0.93	0.96	-0.03	0.095
GRTP1	79774	growth hormone regulated TBC protein 1	0.93	0.97	-0.04	0.067
GSG1	83445	germ cell associated 1	0.89	0.94	-0.05	0.053
GSTM4	2948	glutathione S-transferase mu 4	0.89	0.94	-0.05	0.038
GSTP1	2950	glutathione S-transferase pi 1	0.85	0.91	-0.06	0.067
GUCY2C	2984	guanylate cyclase 2C (heat stable enterotoxin receptor)	0.64	0.76	-0.12	0.050
GYG1	2992	glycogenin 1	0.06	0.03	0.03	0.099
GYPA	2993	glycophorin A (MNS blood group)	0.90	0.88	0.02	0.065
GYS2	2998	glycogen synthase 2 (liver)	0.80	0.90	-0.10	0.038
H19	283120	H19, imprinted maternally expressed transcript (non-protein coding)	0.87	0.81	0.06	0.071
H19	283120	H19, imprinted maternally expressed transcript (non-protein coding)	0.89	0.85	0.04	0.088
H1F0	3005	H1 histone family, member 0	0.76	0.85	-0.09	0.074
H1T2	341567	H1 histone family, member N, testis-specific	0.22	0.28	-0.06	0.070
HAL	3034	histidine ammonia-lyase	0.83	0.90	-0.07	0.053
HAO1	54363	hydroxyacid oxidase (glycolate oxidase) 1	0.56	0.66	-0.10	0.074
HAPLN2	60484	hyaluronan and proteoglycan link protein 2	0.49	0.39	0.10	0.078
HBB	3043	hemoglobin, beta	0.68	0.79	-0.11	0.053
HBII-437	338427	small nucleolar RNA, C/D box 108	0.79	0.87	-0.08	0.067

Symbol	Gene ID	Gene Description	Mean β PE	Mean β NP	Δβ	FDR
HCLS1	3059	hematopoietic cell-specific Lyn substrate 1	0.59	0.70	-0.11	0.080
HCRTR1	3061	hypocretin (orexin) receptor 1	0.67	0.82	-0.15	0.052
HDAC9	9734	histone deacetylase 9	0.07	0.05	0.02	0.086
HES1	3280	hairy and enhancer of split 1, (Drosophila)	0.03	0.02	0.01	0.050
HGFAC	3083	HGF activator	0.45	0.57	-0.13	0.065
HHLA1	10086	HERV-H LTR-associating 1	0.90	0.82	0.08	0.025
HHLA3	11147	HERV-H LTR-associating 3	0.04	0.02	0.02	0.053
HINT1	3094	histidine triad nucleotide binding protein 1	0.06	0.04	0.02	0.062
HINT2	84681	histidine triad nucleotide binding protein 2	0.03	0.01	0.01	0.066
HIPK4	147746	homeodomain interacting protein kinase 4	0.76	0.72	0.04	0.093
HIST1H2AH	85235	histone cluster 1, H2a	0.04	0.02	0.02	0.087
HIST1H2AM	8336	histone cluster 1, H2am	0.03	0.02	0.01	0.086
HIST1H2BD	3017	histone cluster 1, H2bd	0.06	0.04	0.02	0.065
HIST1H3B	8358	histone cluster 1, H3b	0.02	0.02	0.01	0.063
HIST1H3H	8357	histone cluster 1, H4d	0.08	0.05	0.04	0.040
HIST1H4D	8360	histone cluster 1, H3h	0.05	0.03	0.02	0.075
HK1	3098	hexokinase 1	0.63	0.71	-0.07	0.073
HKR1	284459	GLI-Kruppel family member HKR1	0.94	0.96	-0.02	0.055
HMG20B	10362	high-mobility group 20B	0.97	0.98	-0.01	0.080
HMGCL	3155	3-hydroxymethyl-3-methylglutaryl-Coenzyme A lyase	0.95	0.97	-0.02	0.085
HMP19	51617	HMP19 protein	0.01	0.01	0.00	0.062
HNF4A	3172	hepatocyte nuclear factor 4, alpha	0.90	0.87	0.04	0.060

Symbol	Gene ID	Gene Description	Mean β PE	Mean β NP	Δβ	FDR
HNRPA3	220988	heterogeneous nuclear ribonucleoprotein A3	0.03	0.02	0.01	0.057
HNRPC	3183	heterogeneous nuclear ribonucleoprotein C (C1/C2)	0.04	0.02	0.02	0.040
HNRPLL	92906	heterogeneous nuclear ribonucleoprotein L-like	0.04	0.03	0.01	0.095
HNRPM	4670	heterogeneous nuclear ribonucleoprotein M	0.05	0.03	0.03	0.063
HOMER3	9454	homer homolog 3 (Drosophila)	0.77	0.71	0.05	0.094
HOXA2	3199	homeobox A2	0.44	0.33	0.11	0.090
HOXD10	3236	homeobox D10	0.33	0.24	0.09	0.084
H-plk	51351	zinc finger protein 117	0.61	0.71	-0.10	0.086
HPR	3250	haptoglobin-related protein	0.77	0.85	-0.08	0.090
HPS3	84343	Hermansky-Pudlak syndrome 3	0.04	0.01	0.02	0.087
HPSE2	60495	heparanase 2	0.07	0.03	0.04	0.038
HRASLS2	54979	HRAS-like suppressor 2	0.42	0.54	-0.12	0.044
HRB2	11103	KRR1, small subunit (SSU) processome component, homolog (yeast)	0.05	0.02	0.02	0.063
HSD17B1	3292	hydroxysteroid (17-beta) dehydrogenase 1	0.68	0.81	-0.14	0.044
HSD17B1	3292	hydroxysteroid (17-beta) dehydrogenase 1	0.67	0.74	-0.08	0.085
HSP90B1	7184	heat shock protein 90kDa beta (Grp94), member 1	0.05	0.03	0.02	0.067
HSPA2	3306	heat shock 70kDa protein 2	0.91	0.95	-0.04	0.047
HSPA2	3306	heat shock 70kDa protein 2	0.91	0.96	-0.05	0.065
HSPA2	3306	heat shock 70kDa protein 2	0.78	0.88	-0.09	0.081
HSPB6	126393	heat shock protein, alpha-crystallin-related, B6	0.91	0.96	-0.05	0.077

Symbol	Gene ID	Gene Description	Mean β PE	Mean β NP	Δβ	FDR
HSPBAP1	79663	HSPB (heat shock 27kDa) associated protein 1	0.04	0.03	0.02	0.090
HTR3C	170572	5-hydroxytryptamine (serotonin) receptor 3, family member C	0.53	0.64	-0.11	0.065
HTR3D	200909	5-hydroxytryptamine (serotonin) receptor 3 family member D	0.85	0.78	0.07	0.056
HTR7	3363	5-hydroxytryptamine (serotonin) receptor 7 (adenylate cyclase-coupled)	0.05	0.03	0.02	0.089
HYMAI	57061	hydatidiform mole associated and imprinted (non-protein coding)	0.62	0.73	-0.11	0.059
HYPK	25764	chromosome 15 open reading frame 63	0.11	0.07	0.04	0.087
IARS	3376	isoleucyl-tRNA synthetase	0.05	0.04	0.01	0.072
IBRDC1	154214	ring finger protein 217	0.88	0.92	-0.04	0.075
IDH3B	3420	isocitrate dehydrogenase 3 (NAD+) beta	0.03	0.02	0.01	0.089
IFIT1	3434	interferon-induced protein with tetratricopeptide repeats 1	0.08	0.06	0.02	0.091
IFITM1	8519	interferon induced transmembrane protein 1 (9-27)	0.67	0.75	-0.08	0.063
IFITM2	10581	interferon induced transmembrane protein 2 (1-8D)	0.97	0.98	-0.01	0.089
IFNA16	3449	interferon, alpha 16	0.61	0.73	-0.12	0.073
IFNA21	3452	interferon, alpha 21	0.65	0.76	-0.11	0.080
IFT57	55081	intraflagellar transport 57 homolog (Chlamydomonas)	0.04	0.03	0.01	0.095
IGFBP7	3490	insulin-like growth factor binding protein 7	0.06	0.04	0.02	0.089
IGSF10	285313	immunoglobulin superfamily, member 10	0.83	0.90	-0.07	0.063
IGSF6	10261	immunoglobulin superfamily, member 6	0.81	0.89	-0.08	0.047

Symbol	Gene ID	Gene Description	Mean β PE	Mean β NP	Δβ	FDR
IL10	3586	interleukin 10	0.78	0.88	-0.10	0.086
IL17	3605	interleukin 17A	0.59	0.70	-0.11	0.074
IL17E	64806	interleukin 25	0.42	0.55	-0.14	0.042
IL18RAP	8807	interleukin 18 receptor accessory protein	0.17	0.22	-0.05	0.094
IL1A	3552	interleukin 1, alpha	0.75	0.84	-0.09	0.040
IL1F10	84639	interleukin 1 family, member 10 (theta)	0.67	0.77	-0.10	0.070
IL1F9	56300	interleukin 1 family, member 9	0.78	0.87	-0.10	0.042
IL1RAP	3556	interleukin 1 receptor accessory protein	0.03	0.01	0.01	0.087
IL1RL1	9173	interleukin 1 receptor-like 1	0.81	0.88	-0.07	0.039
IL1RL1	9173	interleukin 1 receptor-like 1	0.57	0.69	-0.12	0.053
IL20RA	53832	interleukin 20 receptor, alpha	0.93	0.96	-0.04	0.076
IL24	11009	interleukin 24	0.91	0.96	-0.05	0.074
IL27	246778	interleukin 27	0.65	0.78	-0.13	0.065
IL2RB	3560	interleukin 2 receptor, beta	0.84	0.89	-0.06	0.065
IL4	3565	interleukin 4	0.91	0.96	-0.04	0.050
IL5	3567	interleukin 5 (colony-stimulating factor, eosinophil)	0.53	0.68	-0.15	0.065
IL7	3574	interleukin 7	0.04	0.02	0.02	0.074
IMPACT	55364	Impact homolog (mouse)	0.96	0.98	-0.02	0.094
INGX	27160	inhibitor of growth family, X-linked, pseudogene	0.71	0.82	-0.11	0.078
INPP5F	22876	inositol polyphosphate-5-phosphatase F	0.06	0.04	0.02	0.090
INSIG2	51141	insulin induced gene 2	0.04	0.03	0.02	0.066
INSL4	3641	insulin-like 4 (placenta)	0.79	0.87	-0.09	0.067

Symbol	Gene ID	Gene Description	Mean β PE	Mean β NP	Δβ	FDR
IQCF1	132141	IQ motif containing F1	0.72	0.84	-0.12	0.044
IQCG	84223	IQ motif containing G	0.07	0.04	0.02	0.064
IQCH	64799	IQ motif containing H	0.58	0.69	-0.11	0.086
ISG20L1	64782	apoptosis enhancing nuclease	0.03	0.02	0.01	0.042
ITGA11	22801	integrin, alpha 11	0.04	0.02	0.01	0.095
ITGA8	8516	integrin, alpha 8	0.92	0.95	-0.03	0.087
ITGAE	3682	integrin, alpha E (antigen CD103, human mucosal lymphocyte antigen 1; alpha polypeptide)	0.56	0.65	-0.09	0.083
ITGB4BP	3692	eukaryotic translation initiation factor 6	0.06	0.03	0.02	0.053
ITK	3702	IL2-inducible T-cell kinase	0.79	0.87	-0.09	0.049
ITSN1	6453	intersectin 1 (SH3 domain protein)	0.04	0.02	0.02	0.074
ITSN2	50618	intersectin 2	0.08	0.04	0.04	0.050
IVL	3713	involucrin	0.80	0.88	-0.08	0.065
IZUMO1	284359	izumo sperm-egg fusion 1	0.04	0.03	0.01	0.094
JMJD2A	9682	lysine (K)-specific demethylase 4A	0.12	0.07	0.04	0.083
JMY	133746	junction mediating and regulatory protein, p53 cofactor	0.66	0.80	-0.13	0.047
JOSD3	79101	TATA box binding protein (TBP)-associated factor, RNA polymerase I, D, 41kDa	0.73	0.83	-0.10	0.089
JTV1	7965	aminoacyl tRNA synthetase complex-interacting multifunctional protein 2	0.61	0.73	-0.12	0.075
KCNE1L	23630	KCNE1-like	0.54	0.68	-0.14	0.073
KCNJ11	3767	potassium inwardly-rectifying channel, subfamily J, member 11	0.06	0.03	0.03	0.097
KCNQ1	3784	potassium voltage-gated channel, KQT-like subfamily, member 1	0.81	0.86	-0.05	0.070

Symbol	Gene ID	Gene Description	Mean β PE	Mean β NP	Δβ	FDR
KCNS1	3787	potassium voltage-gated channel, delayed-rectifier, subfamily S, member 1	0.30	0.22	0.08	0.042
KCNT2	343450	potassium channel, subfamily T, member 2	0.08	0.06	0.02	0.073
KCNV2	169522	potassium channel, subfamily V, member 2	0.52	0.67	-0.15	0.074
KIAA0141	9812	KIAA0141	0.89	0.94	-0.05	0.076
KIAA0174	9798	KIAA0174	0.03	0.01	0.01	0.054
KIAA0179	23076	ribosomal RNA processing 1 homolog B (S. cerevisiae)	0.79	0.86	-0.07	0.087
KIAA0247	9766	KIAA0247	0.06	0.03	0.03	0.053
KIAA0652	9776	KIAA0652	0.56	0.70	-0.14	0.068
KIAA0676	23061	TBC1 domain family, member 9B (with GRAM domain)	0.93	0.97	-0.04	0.042
KIAA0703	9914	ATPase, Ca++ transporting, type 2C, member 2	0.97	0.98	-0.01	0.086
KIAA0738	9747	family with sequence similarity 115, member A	0.87	0.92	-0.06	0.070
KIAA0889	25781	KIAA0889	0.86	0.91	-0.06	0.038
KIAA1008	22894	DIS3 mitotic control homolog (S. cerevisiae)	0.02	0.01	0.01	0.085
KIAA1128	54462	KIAA1128	0.64	0.75	-0.11	0.095
KIAA1143	57456	KIAA1143	0.06	0.03	0.02	0.063
KIAA1244	57221	KIAA1244	0.63	0.76	-0.13	0.071
KIAA1704	55425	KIAA1704	0.74	0.87	-0.12	0.065
KIAA1754	85450	inositol 1,4,5-triphosphate receptor interacting protein	0.59	0.71	-0.12	0.064
KIF22	3835	kinesin family member 22	0.05	0.02	0.03	0.095

Symbol	Gene ID	Gene Description	Mean β PE	Mean β NP	Δβ	FDR
KIR3DL2	3812	killer cell immunoglobulin-like receptor, three domains, long cytoplasmic tail, 2	0.52	0.63	-0.11	0.065
KLB	152831	klotho beta	0.70	0.79	-0.09	0.094
KLC4	89953	kinesin light chain 4	0.92	0.96	-0.04	0.047
KLF12	11278	Kruppel-like factor 12	0.03	0.01	0.01	0.073
KLHDC4	54758	kelch domain containing 4	0.04	0.02	0.02	0.099
KLHL20	27252	kelch-like 20 (Drosophila)	0.03	0.01	0.01	0.055
KLHL3	26249	kelch-like 3 (Drosophila)	0.11	0.08	0.04	0.041
KLHL8	57563	kelch-like 8 (Drosophila)	0.01	0.01	0.01	0.065
KLK11	11012	kallikrein-related peptidase 11	0.85	0.88	-0.03	0.077
KLK14	43847	kallikrein-related peptidase 14	0.83	0.91	-0.07	0.040
KLRG1	10219	killer cell lectin-like receptor subfamily G, member 1	0.66	0.78	-0.12	0.075
KRT10	3858	keratin 10	0.87	0.93	-0.06	0.096
KRT24	192666	keratin 24	0.28	0.46	-0.18	0.063
KRT25C	342574	keratin 27	0.72	0.81	-0.09	0.082
KRT2A	3849	keratin 2	0.63	0.72	-0.09	0.080
KRTAP1-1	81851	keratin associated protein 1-1	0.64	0.79	-0.15	0.050
KRTAP13-4	284827	keratin associated protein 13-4	0.80	0.87	-0.07	0.076
KRTAP17-1	83902	keratin associated protein 17-1	0.80	0.90	-0.09	0.025
KRTAP19-2	337969	keratin associated protein 19-2	0.56	0.67	-0.12	0.065
KRTAP19-3	337970	keratin associated protein 19-3	0.63	0.73	-0.10	0.070
KRTAP4-4	84616	keratin associated protein 4-4	0.78	0.88	-0.09	0.065
KRTAP6-2	337967	keratin associated protein 6-2	0.89	0.92	-0.03	0.099
KRTAP9-3	83900	keratin associated protein 9-3	0.82	0.88	-0.07	0.042
KRTCAP2	200185	keratinocyte associated protein 2	0.06	0.04	0.02	0.078

Symbol	Gene ID	Gene Description	Mean β PE	Mean β NP	Δβ	FDR
KRTHA3A	3883	keratin 33A	0.79	0.84	-0.06	0.086
KRTHA4	3885	keratin 34	0.73	0.81	-0.08	0.082
KRTHA4	3885	keratin 34	0.86	0.93	-0.07	0.090
KRTHA5	3886	keratin 35	0.81	0.87	-0.06	0.065
KRTHA8	8687	keratin 38	0.47	0.60	-0.13	0.077
KRTHB2	3888	keratin 82	0.74	0.83	-0.10	0.042
KSP37	83888	fibroblast growth factor binding protein 2	0.49	0.64	-0.15	0.049
KTN1	3895	kinectin 1 (kinesin receptor)	0.08	0.04	0.04	0.075
LACE1	246269	lactation elevated 1	0.02	0.01	0.01	0.070
LAG3	3902	lymphocyte-activation gene 3	0.47	0.56	-0.09	0.047
LAIR2	3904	leukocyte-associated immunoglobulin-like receptor 2	0.95	0.98	-0.02	0.080
LAMP1	3916	lysosomal-associated membrane protein 1	0.10	0.05	0.05	0.094
LANCL1	10314	LanC lantibiotic synthetase component C-like 1 (bacterial)	0.03	0.02	0.01	0.088
LASS2	29956	LAG1 homolog, ceramide synthase 2	0.03	0.02	0.01	0.075
LATS1	9113	LATS, large tumor suppressor, homolog 1 (Drosophila)	0.02	0.01	0.01	0.100
LCN6	158062	lipocalin 6	0.75	0.83	-0.08	0.073
LCT	3938	lactase	0.81	0.89	-0.08	0.046
LEMD3	23592	LEM domain containing 3	0.06	0.03	0.03	0.082
LETM2	137994	leucine zipper-EF-hand containing transmembrane protein 2	0.07	0.04	0.03	0.061
LGALS2	3957	lectin, galactoside-binding, soluble, 2	0.33	0.44	-0.11	0.055
LGALS4	3960	lectin, galactoside-binding, soluble, 4	0.27	0.34	-0.07	0.053
LHFP	10186	lipoma HMGIC fusion partner	0.02	0.01	0.01	0.047

Symbol	Gene ID	Gene Description	Mean β PE	Mean β NP	Δβ	FDR
LIG4	3981	ligase IV, DNA, ATP-dependent	0.03	0.02	0.01	0.081
LILRB2	10288	leukocyte immunoglobulin-like receptor, subfamily B (with TM and ITIM domains), member 2	0.67	0.79	-0.12	0.054
LILRB2	10288	leukocyte immunoglobulin-like receptor, subfamily B (with TM and ITIM domains), member 2	0.78	0.87	-0.10	0.088
LILRB4	11006	leukocyte immunoglobulin-like receptor, subfamily B (with TM and ITIM domains), member 4	0.51	0.62	-0.11	0.075
LIN10	80262	chromosome 16 open reading frame 70	0.02	0.01	0.01	0.050
LIPH	200879	lipase, member H	0.70	0.78	-0.08	0.080
LMAN2L	81562	lectin, mannose-binding 2-like	0.07	0.04	0.03	0.038
LMX1A	4009	LIM homeobox transcription factor 1, alpha	0.91	0.94	-0.03	0.084
LOC112714	112714	tubulin, alpha 3e	0.88	0.93	-0.05	0.063
LOC120379	120379	PIH1 domain containing 2	0.52	0.68	-0.16	0.074
LOC122258	122258	chromosome 13 open reading frame 28	0.62	0.71	-0.09	0.056
LOC133957	133957	coiled-coil domain containing 127	0.05	0.03	0.02	0.084
LOC196549	196549	eukaryotic translation elongation factor 1 delta pseudogene 3	0.56	0.70	-0.14	0.056
LOC202459	202459	oligosaccharyltransferase complex subunit-like	0.81	0.88	-0.07	0.050
LOC253012	253012	HEPACAM family member 2	0.88	0.92	-0.05	0.089
LOC283377	283377	SPRY domain containing 4	0.05	0.03	0.02	0.072
LOC284361	284361	chromosome 19 open reading frame 63	0.82	0.91	-0.09	0.044
LOC339524	339524	hypothetical LOC339524	0.07	0.05	0.02	0.086
LOC339789	339789	chromosome 2 open reading frame 46	0.78	0.87	-0.08	0.038

Symbol	Gene ID	Gene Description	Mean β PE	Mean β NP	Δβ	FDR
LOC340061	340061	transmembrane protein 173	0.05	0.03	0.02	0.099
LOC346673	346673	stimulated by retinoic acid gene 8 homolog (mouse)	0.70	0.80	-0.10	0.043
LOC346673	346673	stimulated by retinoic acid gene 8 homolog (mouse)	0.80	0.89	-0.09	0.047
LOC51136	51136	ring finger protein, transmembrane 1	0.04	0.02	0.02	0.058
LOC54103	54103	pigeon homolog (Drosophila)	0.79	0.90	-0.11	0.066
LOC57146	57146	transmembrane protein 159	0.02	0.01	0.01	0.038
LOC57146	57146	transmembrane protein 159	0.04	0.02	0.02	0.087
LOC81691	81691	exonuclease NEF-sp	0.61	0.73	-0.12	0.085
LOC84661	84661	dpy-30 homolog (C. elegans)	0.03	0.02	0.01	0.067
LOC90580	90580	chromosome 19 open reading frame 52	0.83	0.89	-0.06	0.074
LOC90826	90826	protein arginine methyltransferase 10 (putative)	0.04	0.03	0.01	0.075
LPAL2	80350	lipoprotein, Lp(a)-like 2	0.32	0.40	-0.08	0.089
LPPR4	9890	plasticity related gene 1	0.08	0.05	0.03	0.059
LPXN	9404	leupaxin	0.80	0.89	-0.09	0.081
LRP2	4036	low density lipoprotein-related protein 2	0.06	0.03	0.03	0.056
LRP3	4037	low density lipoprotein receptor-related protein 3	0.80	0.86	-0.07	0.086
LRRC25	126364	leucine rich repeat containing 25	0.83	0.90	-0.07	0.048
LRRC44	127255	leucine-rich repeats and IQ motif containing 3	0.12	0.09	0.03	0.091
LRRC8B	23507	leucine rich repeat containing 8 family, member B	0.07	0.10	-0.04	0.038
LSP1	4046	lymphocyte-specific protein 1	0.39	0.52	-0.13	0.074

Symbol	Gene ID	Gene Description	Mean β PE	Mean β NP	Δβ	FDR
LTA	4049	lymphotoxin alpha (TNF superfamily, member 1)	0.33	0.49	-0.16	0.046
LTB	4050	lymphotoxin beta (TNF superfamily, member 3)	0.92	0.95	-0.03	0.078
LTBP4	8425	latent transforming growth factor beta binding protein 4	0.66	0.75	-0.09	0.050
LTK	4058	leukocyte receptor tyrosine kinase	0.76	0.86	-0.10	0.076
LY6E	4061	lymphocyte antigen 6 complex, locus E	0.05	0.02	0.02	0.099
LY6G6C	80740	lymphocyte antigen 6 complex, locus G6C	0.89	0.85	0.04	0.094
LYNX1	66004	Ly6/neurotoxin 1	0.04	0.03	0.02	0.087
LYSMD4	145748	LysM, putative peptidoglycan-binding, domain containing 4	0.91	0.87	0.04	0.053
LYZL2	119180	lysozyme-like 2	0.77	0.85	-0.07	0.086
MAGEA10	4109	melanoma antigen family A, 10	0.19	0.26	-0.07	0.065
MAGEA2B	266740	melanoma antigen family A, 2B	0.74	0.84	-0.10	0.038
MAGEA4	4103	melanoma antigen family A, 4	0.48	0.56	-0.08	0.087
MAGEC2	51438	melanoma antigen family C, 2	0.83	0.77	0.06	0.094
MAK	4117	male germ cell-associated kinase	0.09	0.14	-0.05	0.093
MAK	4117	male germ cell-associated kinase	0.85	0.88	-0.03	0.093
MAP1LC3A	84557	microtubule-associated protein 1 light chain 3 alpha	0.60	0.71	-0.11	0.066
MAP2K5	5607	mitogen-activated protein kinase kinase 5	0.03	0.02	0.02	0.080
MAP3K11	4296	mitogen-activated protein kinase kinase kinase 11	0.07	0.04	0.03	0.065
MAP3K14	9020	mitogen-activated protein kinase kinase kinase 14	0.94	0.91	0.03	0.082
MAPK13	5603	mitogen-activated protein kinase 13	0.50	0.61	-0.11	0.094

Symbol	Gene ID	Gene Description	Mean β PE	Mean β NP	Δβ	FDR
MAPK4	5596	mitogen-activated protein kinase 4	0.93	0.95	-0.02	0.080
MAPRE1	22919	microtubule-associated protein, RP/EB family, member 1	0.07	0.04	0.03	0.080
MARCH8	220972	membrane-associated ring finger (C3HC4) 8	0.08	0.05	0.03	0.066
MARK3	4140	MAP/microtubule affinity-regulating kinase 3	0.02	0.01	0.01	0.053
MAS1L	116511	MAS1 oncogene-like	0.61	0.74	-0.12	0.073
MASTL	84930	microtubule associated serine/threonine kinase-like	0.04	0.02	0.02	0.047
MASTL	84930	microtubule associated serine/threonine kinase-like	0.03	0.02	0.01	0.086
MBTD1	54799	mbt domain containing 1	0.37	0.50	-0.13	0.063
MC2R	4158	melanocortin 2 receptor (adrenocorticotropic hormone)	0.77	0.85	-0.08	0.050
MCFD2	90411	multiple coagulation factor deficiency 2	0.11	0.06	0.05	0.088
MCM4	4173	minichromosome maintenance complex component 4	0.05	0.03	0.02	0.100
MCM5	4174	minichromosome maintenance complex component 5	0.12	0.15	-0.03	0.080
MCTS1	28985	malignant T cell amplified sequence 1	0.75	0.84	-0.09	0.067
MECP2	4204	methyl CpG binding protein 2 (Rett syndrome)	0.56	0.71	-0.15	0.061
METAP1	23173	methionyl aminopeptidase 1	0.88	0.92	-0.04	0.080
MFAP3	4238	microfibrillar-associated protein 3	0.70	0.78	-0.08	0.086
MFAP4	4239	microfibrillar-associated protein 4	0.22	0.32	-0.10	0.066
MFN1	55669	mitofusin 1	0.02	0.01	0.01	0.053
MFSD2	84879	major facilitator superfamily domain containing 2	0.05	0.02	0.02	0.094

Symbol	Gene ID	Gene Description	Mean β PE	Mean β NP	Δβ	FDR
MGC11257	84310	chromosome 7 open reading frame 50	0.93	0.96	-0.03	0.090
MGC11266	79172	centromere protein O	0.03	0.01	0.01	0.046
MGC13024	93129	ORAI calcium release-activated calcium modulator 3	0.02	0.01	0.01	0.062
MGC13034	134288	transmembrane protein 174	0.82	0.88	-0.07	0.079
MGC13096	84306	programmed cell death 2-like	0.02	0.01	0.01	0.098
MGC16169	93627	TBC domain-containing protein kinase-like	0.05	0.03	0.02	0.047
MGC16943	112479	exoribonuclease 2	0.03	0.02	0.01	0.074
MGC17330	113791	phosphoinositide-3-kinase interacting protein 1	0.03	0.02	0.01	0.094
MGC22001	197196	transmembrane protein 148	0.77	0.84	-0.08	0.097
MGC2463	79037	poliovirus receptor related immunoglobulin domain containing	0.84	0.81	0.03	0.087
MGC32020	91442	chromosome 19 open reading frame 40	0.04	0.02	0.02	0.083
MGC3265	78991	prenylcysteine oxidase 1 like	0.02	0.01	0.01	0.064
MGC33302	256471	major facilitator superfamily domain containing 8	0.09	0.05	0.05	0.075
MGC33530	222008	V-set and transmembrane domain containing 2A	0.05	0.03	0.02	0.085
MGC33839	125875	claudin domain containing 2	0.80	0.87	-0.07	0.073
MGC34646	157807	retinaldehyde binding protein 1-like 1	0.07	0.04	0.03	0.050
MGC34830	120196	chromosome 11 open reading frame 69	0.51	0.65	-0.14	0.065
MGC34830	120196	chromosome 11 open reading frame 69	0.73	0.80	-0.07	0.077
MGC35043	255119	chromosome 4 open reading frame 22	0.03	0.01	0.01	0.045
MGC35048	124152	IQ motif containing K	0.80	0.84	-0.04	0.057

Symbol	Gene ID	Gene Description	Mean β PE	Mean β NP	Δβ	FDR
MGC35154	165100	chromosome 2 open reading frame 57	0.90	0.85	0.05	0.039
MGC35169	121793	chromosome 13 open reading frame 16	0.55	0.66	-0.12	0.053
MGC35308	285800	proline rich 18	0.77	0.82	-0.05	0.084
MGC4618	84286	transmembrane protein 175	0.68	0.63	0.05	0.089
MGC48595	399671	HEAT repeat containing 4	0.60	0.75	-0.14	0.053
MGC50372	253143	chromosome 22 open reading frame 30	0.87	0.91	-0.04	0.074
MGC7036	196383	Rab interacting lysosomal protein-like 2	0.03	0.02	0.01	0.065
MGMT	4255	O-6-methylguanine-DNA methyltransferase	0.90	0.95	-0.05	0.042
MGMT	4255	O-6-methylguanine-DNA methyltransferase	0.93	0.97	-0.04	0.042
MGMT	4255	O-6-methylguanine-DNA methyltransferase	0.88	0.95	-0.07	0.055
MGMT	4255	O-6-methylguanine-DNA methyltransferase	0.80	0.86	-0.05	0.073
MGMT	4255	O-6-methylguanine-DNA methyltransferase	0.77	0.84	-0.07	0.074
MGMT	4255	O-6-methylguanine-DNA methyltransferase	0.09	0.14	-0.05	0.084
MGMT	4255	O-6-methylguanine-DNA methyltransferase	0.78	0.86	-0.08	0.089
MGMT	4255	O-6-methylguanine-DNA methyltransferase	0.91	0.93	-0.02	0.099
MGST3	4259	microsomal glutathione S-transferase 3	0.02	0.01	0.01	0.073
MINPP1	9562	multiple inositol polyphosphate histidine phosphatase, 1	0.04	0.02	0.02	0.070
MIP	4284	major intrinsic protein of lens fiber	0.80	0.88	-0.08	0.041

Symbol	Gene ID	Gene Description	Mean β PE	Mean β NP	Δβ	FDR
MKRN1	23608	makorin ring finger protein 1	0.12	0.09	0.03	0.085
MKRN3	7681	makorin ring finger protein 3	0.61	0.78	-0.16	0.080
MLANA	2315	melan-A	0.65	0.78	-0.13	0.079
MLH1	4292	mutL homolog 1, colon cancer, nonpolyposis type 2 (E. coli)	0.04	0.03	0.01	0.063
MLL4	9757	myeloid/lymphoid or mixed-lineage leukemia 4	0.03	0.02	0.01	0.055
MLSTD1	55711	fatty acyl CoA reductase 2	0.77	0.86	-0.09	0.066
MME	4311	membrane metallo-endopeptidase	0.04	0.02	0.02	0.085
MMS19L	64210	MMS19 nucleotide excision repair homolog (S. cerevisiae)	0.06	0.04	0.02	0.073
MON1B	22879	MON1 homolog B (yeast)	0.03	0.02	0.01	0.079
MORC1	27136	MORC family CW-type zinc finger 1	0.85	0.92	-0.07	0.080
MORF4L1	10933	mortality factor 4 like 1	0.81	0.88	-0.07	0.053
MPDZ	8777	multiple PDZ domain protein	0.92	0.95	-0.04	0.055
MPI	4351	mannose phosphate isomerase	0.92	0.94	-0.02	0.074
MPL	4352	myeloproliferative leukemia virus oncogene	0.84	0.88	-0.04	0.077
MPPED1	758	metallophosphoesterase domain containing 1	0.74	0.85	-0.10	0.059
MPPED2	744	metallophosphoesterase domain containing 2	0.92	0.97	-0.04	0.067
MPZL1	9019	myelin protein zero-like 1	0.83	0.91	-0.08	0.046
MPZL1	9019	myelin protein zero-like 1	0.07	0.04	0.03	0.084
MRPL15	29088	mitochondrial ribosomal protein L15	0.03	0.02	0.01	0.056
MRPL35	51318	mitochondrial ribosomal protein L35	0.02	0.01	0.01	0.091
MRPL4	51073	mitochondrial ribosomal protein L4	0.03	0.02	0.01	0.077
MRPL44	65080	mitochondrial ribosomal protein L44	0.04	0.03	0.02	0.090

Symbol	Gene ID	Gene Description	Mean β PE	Mean β NP	Δβ	FDR
MRPL51	51258	mitochondrial ribosomal protein L51	0.06	0.04	0.02	0.083
MRPS10	55173	mitochondrial ribosomal protein S10	0.02	0.01	0.01	0.066
MRPS22	56945	mitochondrial ribosomal protein S22	0.02	0.01	0.01	0.061
MRPS34	65993	mitochondrial ribosomal protein S34	0.04	0.02	0.02	0.062
MRRF	92399	mitochondrial ribosome recycling factor	0.03	0.01	0.01	0.087
MRS2L	57380	MRS2 magnesium homeostasis factor homolog (S. cerevisiae)	0.03	0.01	0.02	0.061
MS4A10	341116	membrane-spanning 4-domains, subfamily A, member 10	0.61	0.73	-0.12	0.087
MSH6	2956	mutS homolog 6 (E. coli)	0.04	0.02	0.02	0.069
MSMB	4477	microseminoprotein, beta-	0.62	0.77	-0.15	0.061
MSN	4478	moesin	0.78	0.87	-0.09	0.042
MSR1	4481	macrophage scavenger receptor 1	0.88	0.93	-0.05	0.065
MT	27349	malonyl CoA:ACP acyltransferase (mitochondrial)	0.02	0.01	0.01	0.084
MT1B	4490	metallothionein 1B	0.81	0.89	-0.08	0.044
MTAP	4507	methylthioadenosine phosphorylase	0.18	0.12	0.06	0.095
MTCP1	4515	mature T-cell proliferation 1	0.54	0.67	-0.13	0.070
MTMR1	8776	myotubularin related protein 1	0.75	0.82	-0.07	0.094
MUC1	4582	mucin 1, cell surface associated	0.70	0.81	-0.11	0.044
MUC13	56667	mucin 13, cell surface associated	0.81	0.86	-0.05	0.094
MYBPC1	4604	myosin binding protein C, slow type	0.77	0.85	-0.07	0.078
MYBPC2	4606	myosin binding protein C, fast type	0.76	0.85	-0.09	0.047
MYBPC3	4607	myosin binding protein C, cardiac	0.58	0.66	-0.08	0.053
MYBPC3	4607	myosin binding protein C, cardiac	0.91	0.89	0.02	0.073
MYBPH	4608	myosin binding protein H	0.77	0.85	-0.09	0.054

Symbol	Gene ID	Gene Description	Mean β PE	Mean β NP	Δβ	FDR
MYBPH	4608	myosin binding protein H	0.43	0.59	-0.17	0.093
MYCBP	26292	c-myc binding protein	0.05	0.03	0.02	0.089
MYD88	4615	myeloid differentiation primary response gene (88)	0.04	0.03	0.02	0.063
MYH4	4622	myosin, heavy chain 4, skeletal muscle	0.78	0.85	-0.07	0.089
MYLPF	29895	myosin light chain, phosphorylatable, fast skeletal muscle	0.63	0.74	-0.11	0.086
MYO18B	84700	myosin XVIIIB	0.87	0.93	-0.05	0.099
MYO1F	4542	myosin IF	0.09	0.05	0.04	0.099
MYO5A	4644	myosin VA (heavy chain 12, myoxin)	0.02	0.01	0.01	0.061
MYO5A	4644	myosin VA (heavy chain 12, myoxin)	0.03	0.02	0.01	0.097
MYO9B	4650	myosin IXB	0.05	0.07	-0.02	0.086
MYOM2	9172	myomesin (M-protein) 2, 165kDa	0.17	0.11	0.06	0.080
MYST4	23522	MYST histone acetyltransferase (monocytic leukemia) 4	0.90	0.95	-0.05	0.038
MYST4	23522	MYST histone acetyltransferase (monocytic leukemia) 4	0.69	0.78	-0.09	0.071
N4BP2	55728	NEDD4 binding protein 2	0.93	0.90	0.03	0.074
NALP4	147945	NLR family, pyrin domain containing 4	0.89	0.93	-0.04	0.094
NALP5	126206	NLR family, pyrin domain containing 5	0.76	0.84	-0.08	0.077
NALP7	199713	NLR family, pyrin domain containing 7	0.66	0.75	-0.08	0.094
NALP8	126205	NLR family, pyrin domain containing 8	0.71	0.83	-0.12	0.064
NAPRT1	93100	nicotinate phosphoribosyltransferase domain containing 1	0.89	0.93	-0.04	0.065
NARG2	79664	NMDA receptor regulated 2	0.03	0.02	0.01	0.083

Symbol	Gene ID	Gene Description	Mean β PE	Mean β NP	Δβ	FDR
NARS	4677	asparaginyl-tRNA synthetase	0.81	0.89	-0.08	0.042
NAT5	51126	N-acetyltransferase 5 (GCN5-related, putative)	0.03	0.02	0.01	0.088
NBL1	4681	neuroblastoma, suppression of tumorigenicity 1	0.75	0.88	-0.13	0.099
NBPF3	84224	neuroblastoma breakpoint family, member 3	0.02	0.02	0.01	0.081
NCL	4691	nucleolin	0.94	0.92	0.02	0.084
NDRG3	57446	NDRG family member 3	0.05	0.03	0.02	0.065
NDUFA13	51079	NADH dehydrogenase (ubiquinone) 1 alpha subcomplex, 13	0.83	0.90	-0.07	0.089
NDUFA3	4696	NADH dehydrogenase (ubiquinone) 1 alpha subcomplex, 3, 9kDa	0.05	0.02	0.03	0.076
NDUFA4	4697	NADH dehydrogenase (ubiquinone) 1 alpha subcomplex, 4, 9kDa	0.03	0.02	0.01	0.061
NDUFA4	4697	NADH dehydrogenase (ubiquinone) 1 alpha subcomplex, 4, 9kDa	0.04	0.02	0.02	0.080
NDUFB6	4712	NADH dehydrogenase (ubiquinone) 1 beta subcomplex, 6, 17kDa	0.04	0.02	0.02	0.055
NDUFC1	4717	NADH dehydrogenase (ubiquinone) 1, subcomplex unknown, 1, 6kDa	0.03	0.02	0.01	0.052
NECAP1	25977	NECAP endocytosis associated 1	0.82	0.91	-0.08	0.044
NEFL	4747	neurofilament, light polypeptide	0.06	0.04	0.02	0.076
NEK10	152110	NIMA (never in mitosis gene a)-related kinase 10	0.92	0.96	-0.04	0.070
NEU2	4759	sialidase 2 (cytosolic sialidase)	0.13	0.16	-0.04	0.086
NEURL	9148	neuralized homolog (Drosophila)	0.69	0.59	0.10	0.067
NEUROD2	4761	neurogenic differentiation 2	0.91	0.96	-0.05	0.078
NEUROD4	58158	neurogenic differentiation 4	0.08	0.05	0.03	0.067

Symbol	Gene ID	Gene Description	Mean β PE	Mean β NP	Δβ	FDR
NFKB2	4791	nuclear factor of kappa light polypeptide gene enhancer in B-cells 2 (p49/p100)	0.03	0.02	0.01	0.075
NFKBIE	4794	nuclear factor of kappa light polypeptide gene enhancer in B-cells inhibitor, epsilon	0.59	0.72	-0.13	0.063
NFRKB	4798	nuclear factor related to kappaB binding protein	0.91	0.94	-0.03	0.087
NMNAT2	23057	nicotinamide nucleotide adenylyltransferase 2	0.02	0.01	0.01	0.086
NNAT	4826	neuronatin	0.89	0.93	-0.04	0.090
NOLA3	55505	NOP10 ribonucleoprotein homolog (yeast)	0.05	0.03	0.02	0.067
NOPE	57722	immunoglobulin superfamily, DCC subclass, member 4	0.14	0.09	0.05	0.063
NOS3	4846	nitric oxide synthase 3 (endothelial cell)	0.79	0.86	-0.07	0.066
NPBWR1	2831	neuropeptides B/W receptor 1	0.04	0.02	0.02	0.038
NPFF	8620	neuropeptide FF-amide peptide precursor	0.90	0.93	-0.03	0.099
NPFFR2	10886	neuropeptide FF receptor 2	0.66	0.77	-0.11	0.053
NPM3	10360	nucleophosmin/nucleoplasmin, 3	0.06	0.04	0.02	0.070
NQO2	4835	NAD(P)H dehydrogenase, quinone 2	0.02	0.02	0.01	0.085
NR0B1	190	nuclear receptor subfamily 0, group B, member 1	0.66	0.75	-0.09	0.087
NR0B2	8431	nuclear receptor subfamily 0, group B, member 2	0.95	0.97	-0.02	0.055
NR0B2	8431	nuclear receptor subfamily 0, group B, member 2	0.85	0.92	-0.08	0.055
NR1D1	9572	nuclear receptor subfamily 1, group D, member 1	0.08	0.04	0.03	0.077

Symbol	Gene ID	Gene Description	Mean β PE	Mean β NP	Δβ	FDR
NR1H2	7376	nuclear receptor subfamily 1, group H, member 2	0.04	0.03	0.01	0.075
NR1I2	8856	nuclear receptor subfamily 1, group I, member 2	0.58	0.67	-0.09	0.094
NRAP	4892	nebulin-related anchoring protein	0.86	0.89	-0.04	0.045
NRTN	4902	neurturin	0.81	0.75	0.06	0.064
NSDHL	50814	NAD(P) dependent steroid dehydrogenase-like	0.78	0.85	-0.07	0.039
NSUN5C	260294	NOL1/NOP2/Sun domain family, member 5C	0.87	0.93	-0.06	0.042
NSUN6	221078	NOL1/NOP2/Sun domain family, member 6	0.03	0.02	0.01	0.074
NT5C3L	115024	5'-nucleotidase, cytosolic III-like	0.65	0.76	-0.11	0.061
NUDT1	4521	nudix (nucleoside diphosphate linked moiety X)-type motif 1	0.88	0.93	-0.05	0.051
NUMB	8650	numb homolog (Drosophila)	0.09	0.05	0.04	0.065
NUP93	9688	nucleoporin 93kDa	0.87	0.92	-0.04	0.088
NUT	256646	chromosome 15 open reading frame 55	0.77	0.88	-0.11	0.061
NXF3	56000	nuclear RNA export factor 3	0.36	0.43	-0.06	0.086
NYD-SP18	84691	family with sequence similarity 71, member F1	0.85	0.89	-0.04	0.067
OACT5	10162	lysophosphatidylcholine acyltransferase 3	0.03	0.01	0.02	0.073
OBP2B	29989	odorant binding protein 2B	0.89	0.95	-0.05	0.044
OCM	4951	oncomodulin 2	0.72	0.82	-0.10	0.053
OKL38	29948	oxidative stress induced growth inhibitor 1	0.79	0.87	-0.08	0.042
OLFM1	10439	olfactomedin 1	0.66	0.77	-0.10	0.064

Symbol	Gene ID	Gene Description	Mean β PE	Mean β NP	Δβ	FDR
OPA3	80207	optic atrophy 3 (autosomal recessive, with chorea and spastic paraplegia)	0.02	0.01	0.01	0.070
OR1A1	8383	olfactory receptor, family 1, subfamily A, member 1	0.56	0.72	-0.16	0.042
OR1D2	4991	olfactory receptor, family 1, subfamily D, member 2	0.32	0.46	-0.14	0.053
OR1F1	4992	olfactory receptor, family 1, subfamily F, member 1	0.39	0.46	-0.08	0.090
OR2F1	26211	olfactory receptor, family 2, subfamily F, member 1	0.72	0.79	-0.06	0.058
OR2K2	26248	olfactory receptor, family 2, subfamily K, member 2	0.84	0.91	-0.07	0.061
OR2V2	285659	olfactory receptor, family 2, subfamily V, member 2	0.83	0.88	-0.05	0.065
OR3A1	4994	olfactory receptor, family 3, subfamily A, member 1	0.94	0.91	0.03	0.065
OR3A1	4994	olfactory receptor, family 3, subfamily A, member 1	0.02	0.03	-0.01	0.085
OR7A17	26333	olfactory receptor, family 7, subfamily A, member 17	0.45	0.63	-0.18	0.046
OSBPL5	114879	oxysterol binding protein-like 5	0.22	0.30	-0.08	0.070
OSBPL5	114879	oxysterol binding protein-like 5	0.22	0.28	-0.06	0.075
OTUD4	54726	OTU domain containing 4	0.80	0.86	-0.06	0.084
OTUD6B	51633	OTU domain containing 6B	0.03	0.02	0.02	0.042
OTUD7	161725	OTU domain containing 7A	0.79	0.88	-0.09	0.063
OXA1L	5018	oxidase (cytochrome c) assembly 1-like	0.06	0.04	0.03	0.100
OXSM	54995	3-oxoacyl-ACP synthase, mitochondrial	0.02	0.01	0.01	0.093
OXT	5020	oxytocin, prepropeptide	0.17	0.26	-0.09	0.047
OXT	5020	oxytocin, prepropeptide	0.80	0.86	-0.05	0.064

Symbol	Gene ID	Gene Description	Mean β PE	Mean β NP	Δβ	FDR
P11	8909	26 serine protease	0.69	0.83	-0.14	0.044
P2RX4	5025	purinergic receptor P2X, ligand-gated ion channel, 4	0.85	0.92	-0.08	0.065
P2RXL1	9127	purinergic receptor P2X, ligand-gated ion channel, 6	0.80	0.90	-0.10	0.064
P2RY11	5032	purinergic receptor P2Y, G-protein coupled, 11	0.63	0.75	-0.12	0.090
P2RY2	5029	purinergic receptor P2Y, G-protein coupled, 2	0.11	0.05	0.05	0.065
P2RY6	5031	pyrimidinergic receptor P2Y, G-protein coupled, 6	0.76	0.84	-0.08	0.094
PAGE1	8712	P antigen family, member 1 (prostate associated)	0.57	0.68	-0.11	0.074
PAIP2	51247	poly(A) binding protein interacting protein 2	0.02	0.01	0.01	0.039
PAIP2	51247	poly(A) binding protein interacting protein 2	0.08	0.06	0.02	0.095
PAK6	56924	p21 protein (Cdc42/Rac)-activated kinase 6	0.67	0.78	-0.11	0.055
PAK6	56924	p21 protein (Cdc42/Rac)-activated kinase 6	0.02	0.01	0.01	0.073
PANX1	24145	pannexin 1	0.17	0.12	0.05	0.095
PAQR5	54852	progestin and adipoQ receptor family member V	0.87	0.93	-0.05	0.065
PAQR8	85315	progestin and adipoQ receptor family member VIII	0.06	0.03	0.03	0.068
PARK7	11315	Parkinson disease (autosomal recessive, early onset) 7	0.08	0.06	0.03	0.071
PARP16	54956	poly (ADP-ribose) polymerase family, member 16	0.07	0.04	0.03	0.085
PARP4	143	poly (ADP-ribose) polymerase family, member 4	0.01	0.01	0.01	0.090

Symbol	Gene ID	Gene Description	Mean β PE	Mean β NP	Δβ	FDR
PARP9	83666	poly (ADP-ribose) polymerase family, member 9	0.83	0.90	-0.07	0.067
PARS2	25973	prolyl-tRNA synthetase 2, mitochondrial (putative)	0.01	0.01	0.01	0.098
PARVB	29780	parvin, beta	0.83	0.90	-0.07	0.073
PC	5091	pyruvate carboxylase	0.76	0.83	-0.07	0.099
PCAF	8850	K(lysine) acetyltransferase 2B	0.08	0.05	0.03	0.095
PCBP3	54039	poly(rC) binding protein 3	0.76	0.85	-0.09	0.063
PCDH20	64881	protocadherin 20	0.05	0.04	0.01	0.082
PCDHB2	56133	protocadherin beta 2	0.07	0.05	0.02	0.098
PCNA	5111	proliferating cell nuclear antigen	0.05	0.03	0.02	0.082
PCOLCE	5118	procollagen C-endopeptidase enhancer	0.72	0.83	-0.12	0.065
PCSK2	5126	proprotein convertase subtilisin/kexin type 2	0.03	0.02	0.01	0.087
PDCD7	10081	programmed cell death 7	0.04	0.02	0.02	0.047
PDE4D	5144	phosphodiesterase 4D, cAMP-specific (phosphodiesterase E3 dunce homolog, Drosophila)	0.92	0.94	-0.02	0.094
PDE6H	5149	phosphodiesterase 6H, cGMP-specific, cone, gamma	0.89	0.94	-0.04	0.087
PDP2	57546	pyruvate dehyrogenase phosphatase catalytic subunit 2	0.03	0.02	0.01	0.084
PDXK	8566	pyridoxal (pyridoxine, vitamin B6) kinase	0.81	0.86	-0.05	0.065
PDZRN4	29951	PDZ domain containing ring finger 4	0.63	0.75	-0.12	0.050
PEG10	23089	paternally expressed 10	0.49	0.63	-0.14	0.065
PEG10	23089	paternally expressed 10	0.91	0.95	-0.04	0.073
PELI1	57162	pellino homolog 1 (Drosophila)	0.41	0.50	-0.09	0.090
PER2	8864	period homolog 2 (Drosophila)	0.07	0.05	0.03	0.073

Symbol	Gene ID	Gene Description	Mean β PE	Mean β NP	Δβ	FDR
PER3	8863	period homolog 3 (Drosophila)	0.96	0.94	0.02	0.065
PERP	64065	PERP, TP53 apoptosis effector	0.05	0.03	0.02	0.086
PES1	23481	pescadillo homolog 1, containing BRCT domain (zebrafish)	0.03	0.02	0.01	0.065
PEX11A	8800	peroxisomal biogenesis factor 11 alpha	0.06	0.03	0.03	0.050
PEX11B	8799	peroxisomal biogenesis factor 11 beta	0.02	0.01	0.01	0.025
PEX14	5195	peroxisomal biogenesis factor 14	0.05	0.04	0.02	0.065
PEX19	5824	peroxisomal biogenesis factor 19	0.03	0.02	0.01	0.046
PEX5L	51555	peroxisomal biogenesis factor 5-like	0.01	0.01	0.00	0.099
PF4V1	5197	platelet factor 4 variant 1	0.93	0.94	-0.02	0.070
PFC	5199	complement factor properdin	0.64	0.70	-0.06	0.089
PFDN4	5203	prefoldin subunit 4	0.04	0.01	0.02	0.071
PFDN5	5204	prefoldin subunit 5	0.07	0.04	0.03	0.068
PFKFB2	5208	6-phosphofructo-2-kinase/fructose-2,6-biphosphatase 2	0.03	0.02	0.01	0.075
PFTK1	5218	PFTAIRE protein kinase 1	0.41	0.61	-0.20	0.025
PGAM1	5223	phosphoglycerate mutase 1 (brain)	0.03	0.02	0.01	0.047
PGBD4	161779	piggyBac transposable element derived 4	0.08	0.04	0.04	0.042
PGBD5	79605	piggyBac transposable element derived 5	0.81	0.88	-0.08	0.090
PGCP	10404	plasma glutamate carboxypeptidase	0.16	0.10	0.06	0.089
PGPEP1	54858	pyroglutamyl-peptidase I	0.96	0.98	-0.02	0.074
PHC2	1912	polyhomeotic homolog 2 (Drosophila)	0.52	0.70	-0.17	0.069
PHTF1	10745	putative homeodomain transcription factor 1	0.28	0.17	0.12	0.071
PHYH2	26061	2-hydroxyacyl-CoA lyase 1	0.04	0.03	0.01	0.077

Symbol	Gene ID	Gene Description	Mean β PE	Mean β NP	Δβ	FDR
PIGF	5281	phosphatidylinositol glycan anchor biosynthesis, class F	0.04	0.02	0.01	0.086
PIGL	9487	phosphatidylinositol glycan anchor biosynthesis, class L	0.07	0.04	0.03	0.089
PIGV	55650	phosphatidylinositol glycan anchor biosynthesis, class V	0.04	0.02	0.02	0.098
PIK4CA	5297	phosphatidylinositol 4-kinase, catalytic, alpha	0.88	0.92	-0.04	0.100
PIP5K1A	8394	phosphatidylinositol-4-phosphate 5-kinase, type I, alpha	0.02	0.01	0.01	0.065
PIP5KL1	138429	phosphatidylinositol-4-phosphate 5-kinase-like 1	0.06	0.03	0.03	0.040
PKD1	5310	polycystic kidney disease 1 (autosomal dominant)	0.90	0.94	-0.04	0.059
PKHD1	5314	polycystic kidney and hepatic disease 1 (autosomal recessive)	0.56	0.68	-0.12	0.075
PKIB	5570	protein kinase (cAMP-dependent, catalytic) inhibitor beta	0.04	0.02	0.02	0.073
PLA1A	51365	phospholipase A1 member A	0.88	0.91	-0.04	0.065
PLA2G3	50487	phospholipase A2, group III	0.63	0.55	0.08	0.098
PLA2R1	22925	phospholipase A2 receptor 1, 180kDa	0.03	0.01	0.01	0.038
PLAC4	191585	placenta-specific 4	0.62	0.71	-0.10	0.085
PLAGL2	5326	pleiomorphic adenoma gene-like 2	0.03	0.06	-0.03	0.095
PLCG2	5336	phospholipase C, gamma 2 (phosphatidylinositol-specific)	0.47	0.65	-0.17	0.071
PLCXD2	257068	phosphatidylinositol-specific phospholipase C, X domain containing 2	0.04	0.02	0.02	0.074
PLEKHA9	51054	pleckstrin homology domain containing, family A (phosphoinositide binding specific) member 9	0.05	0.03	0.02	0.073

Symbol	Gene ID	Gene Description	Mean β PE	Mean β NP	Δβ	FDR
PLEKHH2	130271	pleckstrin homology domain containing, family H (with MyTH4 domain) member 2	0.55	0.65	-0.11	0.068
PLIN	5346	perilipin	0.82	0.92	-0.10	0.039
PLK2	10769	polo-like kinase 2 (Drosophila)	0.03	0.02	0.02	0.063
PLSCR1	5359	phospholipid scramblase 1	0.31	0.43	-0.12	0.088
PLSCR2	57047	phospholipid scramblase 2	0.64	0.71	-0.08	0.063
PLXNB3	5365	plexin B3	0.73	0.80	-0.07	0.090
PMCHL2	5370	pro-melanin-concentrating hormone-like 2	0.75	0.86	-0.11	0.038
PMM2	5373	phosphomannomutase 2	0.84	0.90	-0.06	0.087
PMM2	5373	phosphomannomutase 2	0.83	0.87	-0.04	0.094
PNKD	25953	paroxysmal nonkinesigenic dyskinesia	0.52	0.64	-0.12	0.076
PNLIPRP1	5407	pancreatic lipase-related protein 1	0.55	0.72	-0.18	0.055
PNLIPRP2	5408	pancreatic lipase-related protein 2	0.82	0.91	-0.09	0.040
PNN	5411	pinin, desmosome associated protein	0.04	0.02	0.02	0.093
POLE3	54107	polymerase (DNA directed), epsilon 3 (p17 subunit)	0.75	0.83	-0.08	0.081
POLN	353497	polymerase (DNA directed) nu	0.58	0.70	-0.12	0.089
POLR1C	9533	polymerase (RNA) I polypeptide C, 30kDa	0.75	0.85	-0.10	0.087
POLR1C	9533	polymerase (RNA) I polypeptide C, 30kDa	0.78	0.85	-0.07	0.091
POLR2B	5431	polymerase (RNA) II (DNA directed) polypeptide B, 140kDa	0.05	0.04	0.02	0.062
POLR2C	5432	polymerase (RNA) II (DNA directed) polypeptide C, 33kDa	0.03	0.02	0.01	0.073
POLR3E	55718	polymerase (RNA) III (DNA directed) polypeptide E (80kD)	0.07	0.04	0.03	0.099

Symbol	Gene ID	Gene Description	Mean β PE	Mean β NP	Δβ	FDR
POLR3H	171568	polymerase (RNA) III (DNA directed) polypeptide H (22.9kD)	0.83	0.90	-0.07	0.055
POMT1	10585	protein-O-mannosyltransferase 1	0.04	0.02	0.02	0.074
PON2	5445	paraoxonase 2	0.05	0.03	0.02	0.072
PPHLN1	51535	periphilin 1	0.05	0.03	0.02	0.067
PPIE	10450	peptidylprolyl isomerase E (cyclophilin E)	0.05	0.03	0.02	0.087
PPM1D	8493	protein phosphatase 1D magnesium-dependent, delta isoform	0.03	0.02	0.01	0.063
PPME1	51400	protein phosphatase methylesterase 1	0.05	0.02	0.02	0.064
PPME1	51400	protein phosphatase methylesterase 1	0.03	0.02	0.01	0.089
PPP4C	5531	protein phosphatase 4 (formerly X), catalytic subunit	0.04	0.02	0.02	0.040
PRAME	23532	preferentially expressed antigen in melanoma	0.71	0.62	0.09	0.055
PRCP	5547	prolylcarboxypeptidase (angiotensinase C)	0.08	0.05	0.04	0.051
PRDM2	7799	PR domain containing 2, with ZNF domain	0.64	0.77	-0.13	0.055
PRH1	5554	proline-rich protein HaeIII subfamily 1	0.38	0.51	-0.14	0.091
PRH2	5555	proline-rich protein HaeIII subfamily 2	0.83	0.91	-0.08	0.056
PRH2	5555	proline-rich protein HaeIII subfamily 2	0.73	0.79	-0.05	0.094
PRKAA2	5563	protein kinase, AMP-activated, alpha 2 catalytic subunit	0.03	0.02	0.01	0.055
PRKACG	5568	protein kinase, cAMP-dependent, catalytic, gamma	0.89	0.94	-0.05	0.073
PRKD3	23683	protein kinase D3	0.71	0.80	-0.09	0.080
PRMT3	10196	protein arginine methyltransferase 3	0.04	0.02	0.02	0.083
PROC	5624	protein C (inactivator of coagulation factors Va and VIIIa)	0.89	0.93	-0.04	0.078

Symbol	Gene ID	Gene Description	Mean β PE	Mean β NP	Δβ	FDR
PROC	5624	protein C (inactivator of coagulation factors Va and VIIIa)	0.86	0.90	-0.04	0.086
PROM1	8842	prominin 1	0.90	0.96	-0.06	0.061
PRPF3	9129	PRP3 pre-mRNA processing factor 3 homolog (S. cerevisiae)	0.08	0.05	0.03	0.076
PRPF39	55015	PRP39 pre-mRNA processing factor 39 homolog (S. cerevisiae)	0.11	0.07	0.04	0.065
PRPF8	10594	PRP8 pre-mRNA processing factor 8 homolog (S. cerevisiae)	0.05	0.03	0.02	0.081
PRPS1L1	221823	phosphoribosyl pyrophosphate synthetase 1	0.60	0.74	-0.14	0.069
PRSSL1	400668	protease, serine-like 1	0.91	0.95	-0.04	0.053
PSCD1	9267	cytohesin 1	0.05	0.02	0.03	0.042
PSCD4	27128	cytohesin 4	0.90	0.94	-0.04	0.074
PSEN1	5663	presenilin 1	0.03	0.02	0.01	0.094
PSF1	9837	GINS complex subunit 1 (Psf1 homolog)	0.91	0.94	-0.03	0.065
PSMA3	5684	proteasome (prosome, macropain) subunit, alpha type, 3	0.05	0.03	0.02	0.089
PSMB6	5694	proteasome (prosome, macropain) subunit, beta type, 6	0.06	0.03	0.03	0.046
PSMB7	5695	proteasome (prosome, macropain) subunit, beta type, 7	0.05	0.02	0.03	0.090
PSMC2	5701	proteasome (prosome, macropain) 26S subunit, ATPase, 2	0.05	0.03	0.02	0.065
PSMD14	10213	proteasome (prosome, macropain) 26S subunit, non-ATPase, 14	0.03	0.02	0.01	0.093
PSMD9	5715	proteasome (prosome, macropain) 26S subunit, non-ATPase, 9	0.03	0.01	0.01	0.063
PSMF1	9491	proteasome (prosome, macropain) inhibitor subunit 1 (PI31)	0.54	0.72	-0.17	0.089

Symbol	Gene ID	Gene Description	Mean β PE	Mean β NP	Δβ	FDR
PSRC1	84722	proline/serine-rich coiled-coil 1	0.03	0.02	0.01	0.047
PTAFR	5724	platelet-activating factor receptor	0.74	0.79	-0.04	0.086
PTBP2	58155	polypyrimidine tract binding protein 2	0.02	0.01	0.01	0.063
PTCD2	79810	pentatricopeptide repeat domain 2	0.52	0.68	-0.15	0.053
PTER	9317	phosphotriesterase related	0.07	0.04	0.03	0.067
PTGS2	5743	prostaglandin-endoperoxide synthase 2 (prostaglandin G/H synthase and cyclooxygenase)	0.03	0.01	0.02	0.048
PTK6	5753	PTK6 protein tyrosine kinase 6	0.90	0.85	0.04	0.055
PTK7	5754	PTK7 protein tyrosine kinase 7	0.03	0.01	0.01	0.066
PTP4A1	7803	protein tyrosine phosphatase type IVA, member 1	0.03	0.02	0.01	0.053
PTP4A3	11156	protein tyrosine phosphatase type IVA, member 3	0.55	0.70	-0.16	0.068
PTPN3	5774	protein tyrosine phosphatase, non-receptor type 3	0.82	0.88	-0.06	0.053
PTPRD	5789	protein tyrosine phosphatase, receptor type, D	0.92	0.96	-0.03	0.063
PTPRN2	5799	protein tyrosine phosphatase, receptor type, N polypeptide 2	0.03	0.02	0.02	0.074
PTTG2	10744	pituitary tumor-transforming 2	0.92	0.94	-0.02	0.066
PUM2	23369	pumilio homolog 2 (Drosophila)	0.38	0.46	-0.07	0.095
PUS7L	83448	pseudouridylate synthase 7 homolog (S. cerevisiae)-like	0.88	0.95	-0.07	0.038
PVRL3	25945	poliovirus receptor-related 3	0.04	0.02	0.01	0.067
PVT1	5820	Pvt1 oncogene (non-protein coding)	0.91	0.95	-0.03	0.063
PWCR1	63968	#N/A	0.74	0.83	-0.09	0.088
PXT1	222659	peroxisomal, testis specific 1	0.76	0.83	-0.08	0.094
PYGM	5837	phosphorylase, glycogen, muscle	0.92	0.96	-0.04	0.055

Symbol	Gene ID	Gene Description	Mean β PE	Mean β NP	Δβ	FDR
PYY2	23615	peptide YY, 2 (seminalplasmin)	0.77	0.87	-0.10	0.055
QARS	5859	glutaminyl-tRNA synthetase	0.04	0.02	0.01	0.071
QRSL1	55278	glutaminyl-tRNA synthase (glutamine-hydrolyzing)-like 1	0.01	0.01	0.01	0.087
RAB34	83871	RAB34, member RAS oncogene family	0.94	0.97	-0.02	0.084
RAB3C	115827	RAB3C, member RAS oncogene family	0.08	0.04	0.04	0.060
RAB3IL1	5866	RAB3A interacting protein (rabin3)-like 1	0.02	0.01	0.01	0.055
RAB4A	5867	RAB4A, member RAS oncogene family	0.13	0.09	0.04	0.081
RAB5A	5868	RAB5A, member RAS oncogene family	0.10	0.06	0.03	0.063
RAB5B	5869	RAB5B, member RAS oncogene family	0.05	0.02	0.03	0.038
RAB8A	4218	RAB8A, member RAS oncogene family	0.81	0.72	0.09	0.066
RABGGTA	5875	Rab geranylgeranyltransferase, alpha subunit	0.87	0.83	0.04	0.086
RACGAP1	29127	Rac GTPase activating protein 1	0.87	0.92	-0.06	0.099
RAD23A	5886	RAD23 homolog A (S. cerevisiae)	0.34	0.47	-0.13	0.087
RAD52	5893	RAD52 homolog (S. cerevisiae)	0.05	0.03	0.03	0.065
RAI16	64760	family with sequence similarity 160, member B2	0.86	0.92	-0.05	0.063
RAI17	57178	zinc finger, MIZ-type containing 1	0.80	0.87	-0.07	0.076
RALBP1	10928	ralA binding protein 1	0.16	0.12	0.04	0.064
RANBP2	5903	RAN binding protein 2	0.04	0.02	0.02	0.045
RAPGEF1	2889	Rap guanine nucleotide exchange factor (GEF) 1	0.50	0.61	-0.11	0.042

Symbol	Gene ID	Gene Description	Mean β PE	Mean β NP	Δβ	FDR
RASA1	5921	RAS p21 protein activator (GTPase activating protein) 1	0.05	0.03	0.02	0.042
RASGRP3	25780	RAS guanyl releasing protein 3 (calcium and DAG-regulated)	0.43	0.57	-0.14	0.081
RB1	5925	retinoblastoma 1	0.82	0.74	0.08	0.065
RB1	5925	retinoblastoma 1	0.94	0.91	0.03	0.083
RB1	5925	retinoblastoma 1	0.57	0.68	-0.11	0.084
RBAF600	23352	ubiquitin protein ligase E3 component n-recognin 4	0.03	0.02	0.01	0.070
RBBP4	5928	retinoblastoma binding protein 4	0.57	0.68	-0.11	0.073
RBBP7	5931	retinoblastoma binding protein 7	0.85	0.89	-0.05	0.053
RBKS	64080	ribokinase	0.14	0.09	0.05	0.074
RBM10	8241	RNA binding motif protein 10	0.69	0.79	-0.11	0.080
RBM12	10137	RNA binding motif protein 12	0.02	0.01	0.01	0.073
RBM21	64852	terminal uridylyl transferase 1, U6 snRNA-specific	0.03	0.02	0.02	0.085
RBP2	5948	retinol binding protein 2, cellular	0.45	0.57	-0.12	0.098
RC74	55756	integrator complex subunit 9	0.03	0.01	0.01	0.066
RCD-8	23644	enhancer of mRNA decapping 4	0.04	0.02	0.01	0.076
RDH11	51109	retinol dehydrogenase 11 (all-trans/9-cis/11-cis)	0.02	0.01	0.01	0.067
RDS	5961	peripherin 2 (retinal degeneration, slow)	0.66	0.77	-0.11	0.085
REG1A	5967	regenerating islet-derived 1 alpha	0.81	0.89	-0.08	0.065
REG1A	5967	regenerating islet-derived 1 alpha	0.49	0.62	-0.13	0.070
REPIN1	29803	replication initiator 1	0.52	0.69	-0.17	0.063
REXO2	25996	REX2, RNA exonuclease 2 homolog (S. cerevisiae)	0.04	0.02	0.01	0.063

Symbol	Gene ID	Gene Description	Mean β PE	Mean β NP	Δβ	FDR
RFC1	5981	replication factor C (activator 1) 1, 145kDa	0.05	0.03	0.02	0.059
Rgr	266747	ral guanine nucleotide dissociation stimulator-like 4	0.77	0.87	-0.10	0.063
Rgr	266747	ral guanine nucleotide dissociation stimulator-like 4	0.80	0.84	-0.04	0.073
RGS13	6003	regulator of G-protein signaling 13	0.06	0.11	-0.05	0.063
RGS3	5998	regulator of G-protein signaling 3	0.80	0.88	-0.07	0.098
RGS6	9628	regulator of G-protein signaling 6	0.14	0.10	0.04	0.086
RGSL1	353299	regulator of G-protein signaling like 1	0.81	0.89	-0.08	0.042
RHO	6010	rhodopsin	0.08	0.10	-0.02	0.094
RHOBTB3	22836	Rho-related BTB domain containing 3	0.02	0.01	0.01	0.074
RHOD	29984	ras homolog gene family, member D	0.25	0.16	0.09	0.095
RIMBP2	23504	RIMS binding protein 2	0.63	0.75	-0.12	0.093
RIMS3	9783	regulating synaptic membrane exocytosis 3	0.80	0.73	0.07	0.086
RIOK2	55781	RIO kinase 2 (yeast)	0.06	0.04	0.02	0.098
RIPK3	11035	receptor-interacting serine-threonine kinase 3	0.50	0.64	-0.14	0.053
RIT1	6016	Ras-like without CAAX 1	0.06	0.04	0.03	0.087
RLN3	117579	relaxin 3	0.59	0.74	-0.15	0.055
RNASEH2A	10535	ribonuclease H2, subunit A	0.83	0.89	-0.07	0.072
RNASEH2A	10535	ribonuclease H2, subunit A	0.05	0.03	0.02	0.100
RND3	390	Rho family GTPase 3	0.07	0.04	0.03	0.094
RNF113A	7737	ring finger protein 113A	0.78	0.86	-0.09	0.094
RNF14	9604	ring finger protein 14	0.70	0.79	-0.10	0.090
RNF170	81790	ring finger protein 170	0.08	0.04	0.04	0.053
RNF185	91445	ring finger protein 185	0.09	0.06	0.04	0.071

Symbol	Gene ID	Gene Description	Mean β PE	Mean β NP	Δβ	FDR
RNF185	91445	ring finger protein 185	0.07	0.05	0.03	0.072
RNF2	6045	ring finger protein 2	0.02	0.01	0.01	0.084
RNF41	10193	ring finger protein 41	0.40	0.46	-0.06	0.086
RNF41	10193	ring finger protein 41	0.02	0.01	0.01	0.092
RNGTT	8732	RNA guanylyltransferase and 5'-phosphatase	0.06	0.04	0.02	0.088
ROR1	4919	receptor tyrosine kinase-like orphan receptor 1	0.05	0.03	0.02	0.087
RPL18	6141	ribosomal protein L18	0.72	0.80	-0.09	0.076
RPL18A	6142	ribosomal protein L18a	0.08	0.04	0.04	0.063
RPL21	6144	ribosomal protein L21 pseudogene	0.04	0.02	0.02	0.070
RPL22	6146	ribosomal protein L22	0.05	0.03	0.02	0.074
RPL38	6169	ribosomal protein L38	0.06	0.03	0.03	0.081
RPL5	6125	ribosomal protein L5	0.04	0.02	0.02	0.055
RPP21	79897	ribonuclease P/MRP 21kDa subunit	0.90	0.95	-0.05	0.063
RPP38	10557	ribonuclease P/MRP 38kDa subunit	0.02	0.01	0.01	0.074
RPS19	6223	ribosomal protein S19	0.02	0.01	0.01	0.077
RPS24	6229	ribosomal protein S24	0.05	0.03	0.02	0.082
RPS6KA1	6195	ribosomal protein S6 kinase, 90kDa, polypeptide 1	0.66	0.74	-0.08	0.056
RPS8	6202	ribosomal protein S8	0.03	0.02	0.01	0.082
RPS9	6203	ribosomal protein S9	0.05	0.03	0.02	0.039
RQCD1	9125	RCD1 required for cell differentiation1 homolog (S. pombe)	0.05	0.03	0.02	0.081
RRAGB	10325	Ras-related GTP binding B	0.68	0.75	-0.07	0.065
RRAS	6237	related RAS viral (r-ras) oncogene homolog	0.03	0.02	0.01	0.070
RTBDN	83546	retbindin	0.77	0.87	-0.10	0.047

Symbol	Gene ID	Gene Description	Mean β PE	Mean β NP	Δβ	FDR
RTN3	10313	reticulon 3	0.03	0.02	0.01	0.070
RTN4RL2	349667	reticulon 4 receptor-like 2	0.07	0.05	0.03	0.067
RUNX3	864	runt-related transcription factor 3	0.88	0.92	-0.04	0.070
RUNX3	864	runt-related transcription factor 3	0.06	0.09	-0.03	0.087
RUNX3	864	runt-related transcription factor 3	0.81	0.89	-0.08	0.094
S100A1	6271	S100 calcium binding protein A1	0.87	0.92	-0.04	0.089
S100A11	6282	S100 calcium binding protein A11	0.03	0.02	0.01	0.065
S100A16	140576	S100 calcium binding protein A16	0.79	0.84	-0.06	0.090
S100P	6286	S100 calcium binding protein P	0.59	0.65	-0.07	0.077
SACS	26278	spastic ataxia of Charlevoix-Saguenay (sacsin)	0.69	0.83	-0.14	0.046
SAG	6295	retina and pineal gland (arrestin)	0.48	0.60	-0.11	0.055
SAGE1	55511	sarcoma antigen 1	0.70	0.81	-0.12	0.053
SAMD12	401474	sterile alpha motif domain containing 12	0.02	0.01	0.01	0.074
SAP18	10284	Sin3A-associated protein, 18kDa	0.04	0.02	0.02	0.063
SART3	9733	squamous cell carcinoma antigen recognized by T cells 3	0.02	0.02	0.01	0.100
SAS10	57050	UTP3, small subunit (SSU) processome component, homolog (S. cerevisiae)	0.04	0.02	0.02	0.080
SBNO1	55206	strawberry notch homolog 1 (Drosophila)	0.12	0.20	-0.08	0.053
SBNO1	55206	strawberry notch homolog 1 (Drosophila)	0.84	0.89	-0.05	0.072
SBP1	90198	chromosome 19 open reading frame 49	0.80	0.91	-0.11	0.050
SC5DL	6309	sterol-C5-desaturase (ERG3 delta-5-desaturase homolog, S. cerevisiae)-like	0.05	0.02	0.03	0.058

Symbol	Gene ID	Gene Description	Mean β PE	Mean β NP	Δβ	FDR
SCAMP2	10066	secretory carrier membrane protein 2	0.04	0.02	0.02	0.074
SCAMP3	10067	secretory carrier membrane protein 3	0.10	0.07	0.03	0.098
SCDR10	374875	hydroxysteroid (11-beta) dehydrogenase 1-like	0.04	0.03	0.01	0.087
SCEL	8796	sciellin	0.66	0.80	-0.14	0.055
SCML1	6322	sex comb on midleg-like 1 (Drosophila)	0.72	0.83	-0.10	0.055
SCN7A	6332	sodium channel, voltage-gated, type VII, alpha	0.88	0.92	-0.03	0.065
SCRN1	9805	secernin 1	0.80	0.88	-0.07	0.098
SCRN3	79634	secernin 3	0.04	0.02	0.02	0.065
SCTR	6344	secretin receptor	0.28	0.39	-0.11	0.075
SCUBE1	80274	signal peptide, CUB domain, EGF-like 1	0.12	0.07	0.06	0.085
SDCCAG1	9147	serologically defined colon cancer antigen 1	0.04	0.02	0.02	0.068
SDCCAG33	10194	teashirt zinc finger homeobox 1	0.77	0.87	-0.10	0.085
SDF2	6388	stromal cell-derived factor 2	0.05	0.04	0.02	0.094
SDHA	6389	succinate dehydrogenase complex, subunit A, flavoprotein (Fp)	0.87	0.89	-0.03	0.094
SEC10L1	10640	exocyst complex component 5	0.10	0.06	0.05	0.081
SEMA6B	10501	sema domain, transmembrane domain (TM), and cytoplasmic domain, (semaphorin) 6B	0.66	0.56	0.10	0.094
SEPHS1	22929	selenophosphate synthetase 1	0.08	0.05	0.03	0.064
SEPT2	4735	septin 2	0.04	0.03	0.01	0.074
SERF2	10169	small EDRK-rich factor 2	0.02	0.01	0.01	0.057
SERPINA7	6906	serpin peptidase inhibitor, clade A (alpha-1 antiproteinase, antitrypsin), member 7	0.11	0.18	-0.08	0.074

Symbol	Gene ID	Gene Description	Mean β PE	Mean β NP	Δβ	FDR
SERPINB4	6318	serpin peptidase inhibitor, clade B (ovalbumin), member 4	0.40	0.54	-0.14	0.050
SERPINB7	8710	serpin peptidase inhibitor, clade B (ovalbumin), member 7	0.58	0.72	-0.14	0.042
SERPINB7	8710	serpin peptidase inhibitor, clade B (ovalbumin), member 7	0.82	0.90	-0.08	0.053
SERPINF1	5176	serpin peptidase inhibitor, clade F (alpha-2 antiplasmin, pigment epithelium derived factor), member 1	0.81	0.76	0.05	0.094
SERPINI1	5274	serpin peptidase inhibitor, clade I (neuroserpin), member 1	0.78	0.87	-0.08	0.046
SERTAD1	29950	SERTA domain containing 1	0.02	0.01	0.01	0.086
SETBP1	26040	SET binding protein 1	0.85	0.91	-0.06	0.055
SETBP1	26040	SET binding protein 1	0.09	0.12	-0.04	0.065
SFRP2	6423	secreted frizzled-related protein 2	0.13	0.09	0.04	0.067
SFRP5	6425	secreted frizzled-related protein 5	0.14	0.08	0.07	0.064
SFRS16	11129	splicing factor, arginine/serine-rich 16	0.75	0.86	-0.11	0.080
SFRS5	6430	splicing factor, arginine/serine-rich 5	0.05	0.02	0.03	0.077
SFTPB	6439	surfactant protein B	0.82	0.77	0.05	0.099
SFXN2	118980	sideroflexin 2	0.05	0.03	0.02	0.040
SH2D4B	387694	SH2 domain containing 4B	0.95	0.97	-0.02	0.086
SH3KBP1	30011	SH3-domain kinase binding protein 1	0.60	0.73	-0.14	0.089
SH3RF2	153769	SH3 domain containing ring finger 2	0.09	0.06	0.03	0.098
SHCBP1	79801	SHC SH2-domain binding protein 1	0.06	0.03	0.02	0.089
SHFM1	7979	split hand/foot malformation (ectrodactyly) type 1	0.05	0.03	0.02	0.074
SIAE	54414	sialic acid acetylesterase	0.71	0.81	-0.10	0.041
SIN3A	25942	SIN3 homolog A, transcription regulator (yeast)	0.04	0.02	0.02	0.091

Symbol	Gene ID	Gene Description	Mean β PE	Mean β NP	Δβ	FDR
SIRT1	23411	sirtuin (silent mating type information regulation 2 homolog) 1 (S. cerevisiae)	0.88	0.92	-0.04	0.087
SITPEC	51295	ECSIT homolog (Drosophila)	0.02	0.02	0.01	0.065
SLAMF8	56833	SLAM family member 8	0.11	0.23	-0.12	0.054
SLC12A1	6557	solute carrier family 12 (sodium/potassium/chloride transporters), member 1	0.91	0.95	-0.04	0.067
SLC12A3	6559	solute carrier family 12 (sodium/chloride transporters), member 3	0.53	0.61	-0.08	0.087
SLC12A9	56996	solute carrier family 12 (potassium/chloride transporters), member 9	0.10	0.05	0.05	0.081
SLC13A4	26266	solute carrier family 13 (sodium/sulfate symporters), member 4	0.68	0.75	-0.07	0.076
SLC14A1	6563	solute carrier family 14 (urea transporter), member 1 (Kidd blood group)	0.39	0.53	-0.13	0.086
SLC16A6	9120	solute carrier family 16, member 6 (monocarboxylic acid transporter 7)	0.01	0.01	0.00	0.095
SLC17A2	10246	solute carrier family 17 (sodium phosphate), member 2	0.77	0.84	-0.08	0.087
SLC17A6	57084	solute carrier family 17 (sodium-dependent inorganic phosphate cotransporter), member 6	0.08	0.03	0.05	0.067
SLC19A3	80704	solute carrier family 19, member 3	0.03	0.02	0.01	0.056
SLC1A7	6512	solute carrier family 1 (glutamate transporter), member 7	0.91	0.94	-0.03	0.083
SLC25A12	8604	solute carrier family 25 (mitochondrial carrier, Aralar), member 12	0.06	0.03	0.03	0.099
SLC25A13	10165	solute carrier family 25, member 13 (citrin)	0.08	0.05	0.02	0.050

Symbol	Gene ID	Gene Description	Mean β PE	Mean β NP	Δβ	FDR
SLC25A16	8034	solute carrier family 25 (mitochondrial carrier; Graves disease autoantigen), member 16	0.92	0.95	-0.03	0.063
SLC25A2	83884	solute carrier family 25 (mitochondrial carrier; ornithine transporter) member 2	0.80	0.88	-0.08	0.066
SLC25A20	788	solute carrier family 25 (carnitine/acylcarnitine translocase), member 20	0.59	0.73	-0.14	0.063
SLC25A35	399512	solute carrier family 25, member 35	0.81	0.77	0.05	0.080
SLC28A2	9153	solute carrier family 28 (sodium-coupled nucleoside transporter), member 2	0.67	0.79	-0.13	0.073
SLC28A2	9153	solute carrier family 28 (sodium-coupled nucleoside transporter), member 2	0.81	0.75	0.06	0.075
SLC29A2	3177	solute carrier family 29 (nucleoside transporters), member 2	0.06	0.04	0.02	0.047
SLC29A4	222962	solute carrier family 29 (nucleoside transporters), member 4	0.74	0.84	-0.10	0.074
SLC2A10	81031	solute carrier family 2 (facilitated glucose transporter), member 10	0.86	0.90	-0.04	0.095
SLC2A7	155184	solute carrier family 2 (facilitated glucose transporter), member 7	0.79	0.87	-0.08	0.073
SLC2A7	155184	solute carrier family 2 (facilitated glucose transporter), member 7	0.94	0.96	-0.02	0.094
SLC31A1	1317	solute carrier family 31 (copper transporters), member 1	0.09	0.04	0.05	0.095
SLC33A1	9197	solute carrier family 33 (acetyl-CoA transporter), member 1	0.04	0.02	0.02	0.078
SLC34A1	6569	solute carrier family 34 (sodium phosphate), member 1	0.67	0.76	-0.10	0.086
SLC35C1	55343	solute carrier family 35, member C1	0.68	0.76	-0.08	0.094
SLC35E3	55508	solute carrier family 35, member E3	0.02	0.01	0.01	0.055

Symbol	Gene ID	Gene Description	Mean β PE	Mean β NP	Δβ	FDR
SLC35F2	54733	solute carrier family 35, member F2	0.02	0.01	0.01	0.076
SLC36A3	285641	solute carrier family 36 (proton/amino acid symporter), member 3	0.68	0.77	-0.09	0.067
SLC39A11	201266	solute carrier family 39 (metal ion transporter), member 11	0.08	0.06	0.03	0.059
SLC39A12	221074	solute carrier family 39 (zinc transporter), member 12	0.60	0.73	-0.14	0.065
SLC39A8	64116	solute carrier family 39 (zinc transporter), member 8	0.06	0.04	0.02	0.099
SLC3A1	6519	solute carrier family 3 (cystine, dibasic and neutral amino acid transporters, activator of cystine, dibasic and neutral amino acid transport), member 1	0.77	0.89	-0.12	0.054
SLC4A1	6521	solute carrier family 4, anion exchanger, member 1 (erythrocyte membrane protein band 3, Diego blood group)	0.62	0.75	-0.12	0.071
SLC4A5	57835	solute carrier family 4, sodium bicarbonate cotransporter, member 5	0.71	0.85	-0.14	0.063
SLC4A5	57835	solute carrier family 4, sodium bicarbonate cotransporter, member 5	0.58	0.68	-0.10	0.094
SLC5A2	6524	solute carrier family 5 (sodium/glucose cotransporter), member 2	0.57	0.68	-0.11	0.053
SLC5A2	6524	solute carrier family 5 (sodium/glucose cotransporter), member 2	0.80	0.89	-0.09	0.064
SLC5A6	8884	solute carrier family 5 (sodium-dependent vitamin transporter), member 6	0.07	0.04	0.03	0.056
SLC5A7	60482	solute carrier family 5 (choline transporter), member 7	0.89	0.86	0.03	0.090

Symbol	Gene ID	Gene Description	Mean β PE	Mean β NP	Δβ	FDR
SLC7A11	23657	solute carrier family 7, (cationic amino acid transporter, y+ system) member 11	0.12	0.17	-0.05	0.077
SLITRK1	114798	SLIT and NTRK-like family, member 1	0.03	0.02	0.01	0.098
SLITRK4	139065	SLIT and NTRK-like family, member 4	0.84	0.89	-0.05	0.094
SLPI	6590	secretory leukocyte peptidase inhibitor	0.90	0.94	-0.04	0.066
SMAD9	4093	SMAD family member 9	0.92	0.94	-0.02	0.099
SMARCD3	6604	SWI/SNF related, matrix associated, actin dependent regulator of chromatin, subfamily d, member 3	0.07	0.04	0.03	0.065
SMARCD3	6604	SWI/SNF related, matrix associated, actin dependent regulator of chromatin, subfamily d, member 3	0.05	0.02	0.03	0.066
SMC2L1	10592	structural maintenance of chromosomes 2	0.05	0.03	0.02	0.050
SMCP	4184	sperm mitochondria-associated cysteine-rich protein	0.15	0.24	-0.08	0.065
SMEK2	57223	SMEK homolog 2, suppressor of mek1 (Dictyostelium)	0.04	0.03	0.01	0.065
SMNDC1	10285	survival motor neuron domain containing 1	0.04	0.03	0.02	0.092
SMR3A	26952	submaxillary gland androgen regulated protein 3A	0.74	0.84	-0.10	0.064
SNAI1	6615	snail homolog 1 (Drosophila)	0.05	0.02	0.03	0.076
SNAPAP	23557	SNAP-associated protein	0.71	0.82	-0.11	0.067
SNCA	6622	synuclein, alpha (non A4 component of amyloid precursor)	0.02	0.01	0.01	0.066
SNF1LK2	23235	salt-inducible kinase 2	0.08	0.05	0.03	0.040
SNRPA	6626	small nuclear ribonucleoprotein polypeptide A	0.78	0.87	-0.10	0.065

Symbol	Gene ID	Gene Description	Mean β PE	Mean β NP	Δβ	FDR
SNTA1	6640	syntrophin, alpha 1 (dystrophin-associated protein A1, 59kDa, acidic component)	0.06	0.04	0.02	0.064
SNTB1	6641	syntrophin, beta 1 (dystrophin-associated protein A1, 59kDa, basic component 1)	0.87	0.93	-0.06	0.073
SNURF	8926	SNRPN upstream reading frame	0.67	0.77	-0.10	0.094
SNX14	57231	sorting nexin 14	0.04	0.02	0.02	0.046
SOCS2	8835	suppressor of cytokine signaling 2	0.03	0.02	0.01	0.095
SORBS2	8470	sorbin and SH3 domain containing 2	0.70	0.76	-0.06	0.073
SOX3	6658	SRY (sex determining region Y)-box 3	0.75	0.85	-0.09	0.086
SPACA4	171169	sperm acrosome associated 4	0.36	0.49	-0.13	0.053
SPAG4L	140732	sperm associated antigen 4-like	0.80	0.85	-0.05	0.094
SPAM1	6677	sperm adhesion molecule 1 (PH-20 hyaluronidase, zona pellucida binding)	0.88	0.94	-0.06	0.046
SPAM1	6677	sperm adhesion molecule 1 (PH-20 hyaluronidase, zona pellucida binding)	0.85	0.88	-0.03	0.074
SPAST	6683	spastin	0.03	0.02	0.01	0.055
SPATA1	64173	spermatogenesis associated 1	0.08	0.03	0.05	0.053
SPATA3	130560	spermatogenesis associated 3	0.66	0.73	-0.07	0.073
SPATA8	145946	spermatogenesis associated 8	0.90	0.93	-0.03	0.077
SPDEF	25803	SAM pointed domain containing ets transcription factor	0.78	0.85	-0.07	0.064
SPIN	10927	spindlin 1	0.04	0.02	0.02	0.040
SPIN	10927	spindlin 1	0.02	0.01	0.01	0.098
SPINLW1	57119	serine peptidase inhibitor-like, with Kunitz and WAP domains 1 (eppin)	0.58	0.70	-0.12	0.094
SPRR2A	6700	small proline-rich protein 2A	0.51	0.61	-0.10	0.094
SPTBN2	6712	spectrin, beta, non-erythrocytic 2	0.86	0.92	-0.06	0.055

Symbol	Gene ID	Gene Description	Mean β PE	Mean β NP	Δβ	FDR
SRC	6714	v-src sarcoma (Schmidt-Ruppin A-2) viral oncogene homolog (avian)	0.65	0.74	-0.09	0.077
SRP54	6729	signal recognition particle 54kDa	0.03	0.01	0.01	0.067
SRP54	6729	signal recognition particle 54kDa	0.06	0.04	0.03	0.082
SSNA1	8636	Sjogren syndrome nuclear autoantigen 1	0.93	0.88	0.05	0.064
SSR2	6746	signal sequence receptor, beta (translocon-associated protein beta)	0.06	0.03	0.02	0.075
SSX1	6756	synovial sarcoma, X breakpoint 1	0.86	0.79	0.07	0.098
ST3GAL5	8869	ST3 beta-galactoside alpha-2,3-sialyltransferase 5	0.02	0.01	0.01	0.074
ST8SIA4	7903	ST8 alpha-N-acetyl-neuraminide alpha-2,8-sialyltransferase 4	0.05	0.03	0.02	0.075
STARD6	147323	StAR-related lipid transfer (START) domain containing 6	0.70	0.84	-0.15	0.047
STCH	6782	heat shock protein 70kDa family, member 13	0.05	0.03	0.02	0.038
STIM2	57620	stromal interaction molecule 2	0.03	0.02	0.01	0.065
STIP1	10963	stress-induced-phosphoprotein 1	0.04	0.03	0.02	0.055
STK31	56164	serine/threonine kinase 31	0.76	0.84	-0.08	0.095
STOML1	9399	stomatin (EPB72)-like 1	0.06	0.03	0.03	0.067
STON1	11037	stonin 1	0.92	0.90	0.02	0.086
STRN	6801	striatin, calmodulin binding protein	0.01	0.01	0.01	0.074
STX17	55014	syntaxin 17	0.04	0.02	0.02	0.038
STX17	55014	syntaxin 17	0.03	0.02	0.01	0.078
STX6	10228	syntaxin 6	0.05	0.03	0.02	0.098
SULT1A1	6817	sulfotransferase family, cytosolic, 1A, phenol-preferring, member 1	0.13	0.03	0.10	0.058

Symbol	Gene ID	Gene Description	Mean β PE	Mean β NP	Δβ	FDR
SULT1B1	27284	sulfotransferase family, cytosolic, 1B, member 1	0.60	0.71	-0.11	0.066
SUMO2	6613	SMT3 suppressor of mif two 3 homolog 2 (S. cerevisiae)	0.02	0.01	0.01	0.070
SUPT5H	6829	suppressor of Ty 5 homolog (S. cerevisiae)	0.07	0.04	0.03	0.067
SUPV3L1	6832	suppressor of var1, 3-like 1 (S. cerevisiae)	0.01	0.01	0.00	0.090
SYCP3	50511	synaptonemal complex protein 3	0.97	0.98	-0.01	0.079
SYT6	148281	synaptotagmin VI	0.02	0.02	0.01	0.095
TAAR1	134864	trace amine associated receptor 1	0.60	0.71	-0.11	0.070
TAAR5	9038	trace amine associated receptor 5	0.83	0.69	0.14	0.066
TACC2	10579	transforming, acidic coiled-coil containing protein 2	0.65	0.74	-0.09	0.089
TADA1L	117143	transcriptional adaptor 1 (HFI1 homolog, yeast)-like	0.03	0.02	0.01	0.065
TAF13	6884	TAF13 RNA polymerase II, TATA box binding protein (TBP)-associated factor, 18kDa	0.03	0.01	0.02	0.084
TAF1B	9014	TATA box binding protein (TBP)-associated factor, RNA polymerase I, B, 63kDa	0.04	0.02	0.02	0.047
TAL2	6887	T-cell acute lymphocytic leukemia 2	0.76	0.85	-0.09	0.074
TAPBP	6892	TAP binding protein (tapasin)	0.12	0.07	0.04	0.067
TAS2R48	259294	taste receptor, type 2, member 19	0.48	0.65	-0.17	0.055
TAS2R5	54429	taste receptor, type 2, member 5	0.49	0.57	-0.08	0.086
TAS2R5	54429	taste receptor, type 2, member 5	0.20	0.31	-0.11	0.094
TBC1D10C	374403	TBC1 domain family, member 10C	0.83	0.87	-0.04	0.099
TBC1D7	51256	TBC1 domain family, member 7	0.67	0.75	-0.08	0.089

Symbol	Gene ID	Gene Description	Mean β PE	Mean β NP	Δβ	FDR
TBRG4	9238	transforming growth factor beta regulator 4	0.05	0.02	0.03	0.046
TBXAS1	6916	thromboxane A synthase 1 (platelet)	0.43	0.67	-0.24	0.042
TCEA1	6917	transcription elongation factor A (SII), 1	0.04	0.02	0.02	0.063
TCEB3B	51224	transcription elongation factor B polypeptide 3B (elongin A2)	0.62	0.72	-0.10	0.088
TCEB3C	162699	transcription elongation factor B polypeptide 3C-like	0.79	0.84	-0.05	0.098
TCIRG1	10312	T-cell, immune regulator 1, ATPase, H+ transporting, lysosomal V0 subunit A3	0.91	0.88	0.03	0.057
TCP10L	140290	t-complex 10 (mouse)-like	0.54	0.67	-0.12	0.069
TCP11L1	55346	t-complex 11 (mouse)-like 1	0.08	0.04	0.04	0.038
TDRD1	56165	tudor domain containing 1	0.65	0.77	-0.12	0.086
TEAD1	7003	TEA domain family member 1 (SV40 transcriptional enhancer factor)	0.79	0.89	-0.09	0.058
TEAD2	8463	TEA domain family member 2	0.06	0.04	0.02	0.074
TEKT2	27285	tektin 2 (testicular)	0.26	0.36	-0.10	0.076
TENC1	23371	tensin like C1 domain containing phosphatase (tensin 2)	0.02	0.01	0.01	0.069
TFPI2	7980	tissue factor pathway inhibitor 2	0.03	0.02	0.01	0.065
TFPT	29844	TCF3 (E2A) fusion partner (in childhood Leukemia)	0.60	0.71	-0.11	0.079
TG	7038	thyroglobulin	0.59	0.75	-0.17	0.090
TGM4	7047	transglutaminase 4 (prostate)	0.86	0.91	-0.05	0.098
THEDC1	55301	oleoyl-ACP hydrolase	0.57	0.68	-0.10	0.085
THEM5	284486	thioesterase superfamily member 5	0.71	0.81	-0.10	0.047
THRAP5	10025	mediator complex subunit 16	0.02	0.01	0.01	0.094

Symbol	Gene ID	Gene Description	Mean β PE	Mean β NP	Δβ	FDR
THRSP	7069	thyroid hormone responsive (SPOT14 homolog, rat)	0.41	0.57	-0.15	0.065
THSD1	55901	thrombospondin, type I, domain containing 1	0.08	0.06	0.02	0.066
THSD4	79875	thrombospondin, type I, domain containing 4	0.89	0.94	-0.05	0.066
TIAF1	9220	TGFB1-induced anti-apoptotic factor 1	0.72	0.79	-0.07	0.053
TICAM1	148022	toll-like receptor adaptor molecule 1	0.87	0.93	-0.05	0.055
TICAM1	148022	toll-like receptor adaptor molecule 1	0.89	0.96	-0.07	0.089
TIGD2	166815	tigger transposable element derived 2	0.73	0.86	-0.13	0.025
TJP3	27134	tight junction protein 3 (zona occludens 3)	0.75	0.68	0.07	0.047
TJP3	27134	tight junction protein 3 (zona occludens 3)	0.87	0.94	-0.07	0.094
TLK1	9874	tousled-like kinase 1	0.05	0.03	0.02	0.087
TLOC1	7095	SEC62 homolog (S. cerevisiae)	0.02	0.01	0.01	0.094
TLR4	7099	toll-like receptor 4	0.06	0.04	0.02	0.065
TLR6	10333	toll-like receptor 6	0.74	0.86	-0.12	0.077
TLX1	3195	T-cell leukemia homeobox 1	0.64	0.80	-0.15	0.055
TM4SF19	116211	transmembrane 4 L six family member 19	0.90	0.94	-0.03	0.060
TMC1	117531	transmembrane channel-like 1	0.84	0.89	-0.06	0.074
TMCC1	23023	transmembrane and coiled-coil domain family 1	0.38	0.49	-0.11	0.068
TMED6	146456	transmembrane emp24 protein transport domain containing 6	0.56	0.70	-0.13	0.053
TMEM113	80335	WD repeat domain 82	0.45	0.56	-0.11	0.066
TMEM125	128218	transmembrane protein 125	0.07	0.04	0.03	0.065

Symbol	Gene ID	Gene Description	Mean β PE	Mean β NP	Δβ	FDR
TMEM23	259230	sphingomyelin synthase 1	0.07	0.04	0.03	0.038
TMEM25	84866	transmembrane protein 25	0.05	0.03	0.02	0.066
TMEM30A	55754	transmembrane protein 30A	0.05	0.04	0.01	0.066
TMEM39A	55254	transmembrane protein 39A	0.03	0.02	0.01	0.063
TMEM41A	90407	transmembrane protein 41A	0.84	0.90	-0.06	0.090
TMEM42	131616	transmembrane protein 42	0.21	0.13	0.08	0.076
TMEM45A	55076	transmembrane protein 45A	0.04	0.02	0.02	0.045
TMEM55B	90809	transmembrane protein 55B	0.03	0.02	0.01	0.079
TMEM66	51669	transmembrane protein 66	0.04	0.03	0.01	0.074
TMEM81	388730	transmembrane protein 81	0.07	0.13	-0.07	0.047
TMEM9	252839	transmembrane protein 9	0.03	0.02	0.01	0.066
TMEM9	252839	transmembrane protein 9	0.04	0.03	0.02	0.086
TMOD1	7111	tropomodulin 1	0.83	0.89	-0.06	0.095
TMOD4	29765	tropomodulin 4 (muscle)	0.73	0.84	-0.11	0.039
TMPRSS11D	9407	transmembrane protease, serine 11D	0.57	0.66	-0.09	0.050
TMPRSS3	64699	transmembrane protease, serine 3	0.68	0.80	-0.12	0.073
TMTC4	84899	transmembrane and tetratricopeptide repeat containing 4	0.81	0.89	-0.08	0.067
TNFAIP8L2	79626	tumor necrosis factor, alpha-induced protein 8-like 2	0.75	0.86	-0.10	0.055
TNFRSF17	608	tumor necrosis factor receptor superfamily, member 17	0.16	0.23	-0.08	0.089
TNFRSF25	8718	tumor necrosis factor receptor superfamily, member 25	0.80	0.86	-0.06	0.098
TNNT2	7139	troponin T type 2 (cardiac)	0.87	0.92	-0.05	0.042
TNNT3	7140	troponin T type 3 (skeletal, fast)	0.78	0.86	-0.08	0.067
TOB1	10140	transducer of ERBB2, 1	0.03	0.02	0.01	0.081

Symbol	Gene ID	Gene Description	Mean β PE	Mean β NP	Δβ	FDR
TOR2A	27433	torsin family 2, member A	0.74	0.85	-0.11	0.064
TP53BP1	7158	tumor protein p53 binding protein 1	0.03	0.01	0.02	0.075
TP73	7161	tumor protein p73	0.89	0.93	-0.04	0.057
TP73	7161	tumor protein p73	0.76	0.85	-0.09	0.067
TP73	7161	tumor protein p73	0.86	0.90	-0.04	0.091
TRAPPC6B	122553	trafficking protein particle complex 6B	0.03	0.02	0.01	0.053
TRIAD3	54476	ring finger protein 216	0.87	0.93	-0.05	0.066
TRIM16	10626	tripartite motif-containing 16	0.65	0.74	-0.10	0.074
TRIM17	51127	tripartite motif-containing 17	0.13	0.08	0.05	0.047
TRIM24	8805	tripartite motif-containing 24	0.07	0.04	0.03	0.055
TRIM29	23650	tripartite motif-containing 29	0.89	0.92	-0.03	0.099
TRIM41	90933	tripartite motif-containing 41	0.06	0.03	0.02	0.086
TRIM42	287015	tripartite motif-containing 42	0.88	0.93	-0.05	0.050
TRIM9	114088	tripartite motif-containing 9	0.05	0.03	0.02	0.038
TRIP4	9325	thyroid hormone receptor interactor 4	0.04	0.03	0.01	0.084
TRPC4AP	26133	transient receptor potential cation channel, subfamily C, member 4 associated protein	0.06	0.03	0.03	0.066
TRPM6	140803	transient receptor potential cation channel, subfamily M, member 6	0.86	0.93	-0.07	0.045
TRPM8	79054	transient receptor potential cation channel, subfamily M, member 8	0.78	0.89	-0.11	0.038
TRPV6	55503	transient receptor potential cation channel, subfamily V, member 6	0.78	0.86	-0.08	0.074
TSC2	7249	tuberous sclerosis 2	0.74	0.81	-0.07	0.086
TSCOT	57864	solute carrier family 46, member 2	0.83	0.89	-0.06	0.086
TSKS	60385	testis-specific serine kinase substrate	0.87	0.92	-0.05	0.064
TSPAN15	23555	tetraspanin 15	0.05	0.03	0.02	0.070

Symbol	Gene ID	Gene Description	Mean β PE	Mean β NP	Δβ	FDR
TSPAN2	10100	tetraspanin 2	0.03	0.01	0.01	0.074
TSPAN9	10867	tetraspanin 9	0.06	0.02	0.04	0.064
TSSK2	23617	testis-specific serine kinase 2	0.90	0.93	-0.03	0.094
TSSK4	283629	testis-specific serine kinase 4	0.78	0.89	-0.11	0.038
TSSK6	83983	testis-specific serine kinase 6	0.86	0.91	-0.04	0.084
TTC13	79573	tetratricopeptide repeat domain 13	0.90	0.94	-0.04	0.038
TTF2	8458	transcription termination factor, RNA polymerase II	0.03	0.02	0.01	0.075
TTK	7272	TTK protein kinase	0.04	0.02	0.01	0.087
TTLL2	83887	tubulin tyrosine ligase-like family, member 2	0.51	0.59	-0.08	0.080
TTLL6	284076	tubulin tyrosine ligase-like family, member 6	0.59	0.73	-0.14	0.045
TUBB1	81027	tubulin, beta 1	0.60	0.77	-0.17	0.063
TUG1	55000	taurine upregulated 1 (non-protein coding)	0.06	0.03	0.03	0.063
TULP1	7287	tubby like protein 1	0.94	0.92	0.02	0.066
TXNDC2	84203	thioredoxin domain containing 2 (spermatozoa)	0.56	0.65	-0.09	0.063
TXNDC6	347736	thioredoxin domain containing 6	0.02	0.01	0.01	0.074
UBADC1	10422	UBA domain containing 1	0.05	0.03	0.02	0.080
UBD	10537	ubiquitin D	0.71	0.76	-0.06	0.074
UBE1DC1	79876	ubiquitin-like modifier activating enzyme 5	0.04	0.02	0.02	0.045
UBE1L2	55236	ubiquitin-like modifier activating enzyme 6	0.02	0.01	0.01	0.071
UBE2B	7320	ubiquitin-conjugating enzyme E2B (RAD6 homolog)	0.03	0.02	0.01	0.052

Symbol	Gene ID	Gene Description	Mean β PE	Mean β NP	Δβ	FDR
UBE2B	7320	ubiquitin-conjugating enzyme E2B (RAD6 homolog)	0.05	0.03	0.02	0.081
UBE2D3	7323	ubiquitin-conjugating enzyme E2D 3 (UBC4/5 homolog, yeast)	0.02	0.02	0.01	0.098
UBE2E1	7324	ubiquitin-conjugating enzyme E2E 1 (UBC4/5 homolog, yeast)	0.76	0.84	-0.08	0.047
UBE2U	148581	ubiquitin-conjugating enzyme E2U (putative)	0.71	0.81	-0.10	0.053
UBTF	7343	upstream binding transcription factor, RNA polymerase I	0.04	0.03	0.01	0.098
UCN2	90226	urocortin 2	0.71	0.84	-0.13	0.066
UGT1A1	54658	UDP glucuronosyltransferase 1 family, polypeptide A1	0.88	0.92	-0.04	0.089
UGT2A3	79799	UDP glucuronosyltransferase 2 family, polypeptide A3	0.78	0.90	-0.12	0.066
UGT2B4	7363	UDP glucuronosyltransferase 2 family, polypeptide B4	0.87	0.90	-0.03	0.094
UNC5CL	222643	unc-5 homolog C (C. elegans)-like	0.81	0.89	-0.08	0.063
UNQ9391	203074	tryptophan/serine protease	0.90	0.85	0.04	0.080
UPP2	151531	uridine phosphorylase 2	0.82	0.91	-0.08	0.086
UQCRH	7388	ubiquinol-cytochrome c reductase hinge protein-like	0.12	0.07	0.06	0.098
USF2	7392	upstream transcription factor 2, c-fos interacting	0.07	0.04	0.03	0.095
USP29	57663	ubiquitin specific peptidase 29	0.78	0.88	-0.09	0.065
USP32	84669	ubiquitin specific peptidase 32	0.05	0.04	0.01	0.088
USP54	159195	ubiquitin specific peptidase 54	0.76	0.84	-0.08	0.047
UTP11L	51118	UTP11-like, U3 small nucleolar ribonucleoprotein, (yeast)	0.05	0.03	0.02	0.057
UVRAG	7405	UV radiation resistance associated gene	0.03	0.02	0.01	0.073

Symbol	Gene ID	Gene Description	Mean β PE	Mean β NP	Δβ	FDR
VAMP8	8673	vesicle-associated membrane protein 8 (endobrevin)	0.59	0.70	-0.11	0.063
VAV1	7409	vav 1 guanine nucleotide exchange factor	0.50	0.66	-0.16	0.046
VBP1	7411	von Hippel-Lindau binding protein 1	0.77	0.85	-0.08	0.065
VDR	7421	vitamin D (1,25- dihydroxyvitamin D3) receptor	0.08	0.06	0.02	0.066
VGLL4	9686	vestigial like 4 (Drosophila)	0.06	0.04	0.02	0.042
VHL	7428	von Hippel-Lindau tumor suppressor	0.66	0.81	-0.15	0.047
VHL	7428	von Hippel-Lindau tumor suppressor	0.74	0.84	-0.10	0.077
VNN3	55350	vanin 3	0.40	0.68	-0.28	0.090
VRK2	7444	vaccinia related kinase 2	0.03	0.02	0.01	0.063
VRK3	51231	vaccinia related kinase 3	0.06	0.03	0.03	0.040
WBP2	23558	WW domain binding protein 2	0.02	0.01	0.01	0.070
WBSCR19	285955	speedy homolog E6 (Xenopus laevis)	0.78	0.68	0.10	0.042
WDR21A	26094	WD repeat domain 21A	0.50	0.62	-0.12	0.080
WDR21C	138009	WD repeat domain 21C	0.66	0.81	-0.14	0.047
WDR34	89891	WD repeat domain 34	0.02	0.01	0.01	0.067
WDR36	134430	WD repeat domain 36	0.03	0.02	0.01	0.086
WDR39	9391	cytosolic iron-sulfur protein assembly 1 homolog (S. cerevisiae)	0.94	0.97	-0.03	0.056
WDR4	10785	WD repeat domain 4	0.02	0.01	0.01	0.064
WDR40B	139170	WD repeat domain 40B	0.87	0.79	0.08	0.061
WDR47	22911	WD repeat domain 47	0.12	0.09	0.03	0.079
WDR65	149465	WD repeat domain 65	0.59	0.70	-0.10	0.100
WDR7	23335	WD repeat domain 7	0.04	0.02	0.02	0.092
WDTC1	23038	WD and tetratricopeptide repeats 1	0.09	0.04	0.05	0.096

Symbol	Gene ID	Gene Description	Mean β PE	Mean β NP	Δβ	FDR
WFDC10B	280664	WAP four-disulfide core domain 10B	0.76	0.86	-0.09	0.057
WFDC5	149708	WAP four-disulfide core domain 5	0.86	0.81	0.05	0.065
WFDC6	140870	WAP four-disulfide core domain 6	0.95	0.98	-0.03	0.068
WFDC8	90199	WAP four-disulfide core domain 8	0.86	0.93	-0.08	0.073
WHSC1	7468	Wolf-Hirschhorn syndrome candidate 1	0.72	0.85	-0.14	0.075
WHSC1L1	54904	Wolf-Hirschhorn syndrome candidate 1-like 1	0.03	0.02	0.01	0.073
WT1	7490	Wilms tumor 1	0.85	0.77	0.07	0.058
XAGE5	170627	X antigen family, member 5	0.79	0.85	-0.06	0.074
XCR1	2829	chemokine (C motif) receptor 1	0.52	0.64	-0.12	0.069
XYLB	9942	xylulokinase homolog (H. influenzae)	0.85	0.92	-0.06	0.075
YES1	7525	v-yes-1 Yamaguchi sarcoma viral oncogene homolog 1	0.11	0.07	0.05	0.071
YIPF5	81555	Yip1 domain family, member 5	0.10	0.06	0.04	0.065
YY2	404281	YY2 transcription factor	0.66	0.76	-0.09	0.094
ZBED3	84327	zinc finger, BED-type containing 3	0.03	0.02	0.01	0.063
ZC3H10	84872	zinc finger CCCH-type containing 10	0.03	0.02	0.01	0.074
ZD52F10	93099	dermokine	0.76	0.85	-0.09	0.071
ZD52F10	93099	dermokine	0.88	0.91	-0.03	0.082
ZDHHC12	84885	zinc finger, DHHC-type containing 12	0.07	0.05	0.02	0.072
ZFAND2A	90637	zinc finger, AN1-type domain 2A	0.03	0.01	0.01	0.065
ZFP42	132625	zinc finger protein 42 homolog (mouse)	0.09	0.04	0.05	0.083
ZFYVE19	84936	zinc finger, FYVE domain containing 19	0.85	0.91	-0.06	0.055
ZFYVE19	84936	zinc finger, FYVE domain containing 19	0.33	0.47	-0.13	0.065

Symbol	Gene ID	Gene Description	Mean β PE	Mean β NP	Δβ	FDR
ZFYVE9	9372	zinc finger, FYVE domain containing 9	0.06	0.04	0.02	0.040
ZHX3	23051	zinc fingers and homeoboxes 3	0.72	0.77	-0.05	0.086
ZIM2	23619	zinc finger, imprinted 2	0.68	0.63	0.05	0.055
ZNF114	163071	zinc finger protein 114	0.06	0.04	0.02	0.089
ZNF157	7712	zinc finger protein 157	0.76	0.86	-0.10	0.062
ZNF169	169841	zinc finger protein 169	0.62	0.77	-0.14	0.063
ZNF22	7570	zinc finger protein 22 (KOX 15)	0.84	0.91	-0.06	0.076
ZNF23	7571	zinc finger protein 23 (KOX 16)	0.07	0.04	0.03	0.075
ZNF235	9310	zinc finger protein 235	0.08	0.04	0.04	0.094
ZNF263	10127	zinc finger protein 263	0.02	0.01	0.01	0.065
ZNF267	10308	zinc finger protein 267	0.06	0.03	0.02	0.055
ZNF277	11179	zinc finger protein 277	0.97	0.98	-0.01	0.047
ZNF318	24149	zinc finger protein 318	0.02	0.01	0.01	0.074
ZNF322B	387328	zinc finger protein 322B	0.87	0.91	-0.05	0.058
ZNF326	284695	zinc finger protein 326	0.85	0.92	-0.07	0.066
ZNF331	55422	zinc finger protein 331	0.12	0.07	0.05	0.063
ZNF333	84449	zinc finger protein 333	0.03	0.02	0.01	0.074
ZNF385	25946	zinc finger protein 385A	0.82	0.89	-0.07	0.050
ZNF408	79797	zinc finger protein 408	0.79	0.88	-0.09	0.071
ZNF436	80818	zinc finger protein 436	0.89	0.94	-0.05	0.052
ZNF439	90594	zinc finger protein 439	0.70	0.83	-0.13	0.042
ZNF499	84878	zinc finger and BTB domain containing 45	0.05	0.03	0.02	0.074
ZNF511	118472	zinc finger protein 511	0.64	0.55	0.09	0.089
ZNF511	118472	zinc finger protein 511	0.21	0.16	0.06	0.090

Symbol	Gene ID	Gene Description	Mean β PE	Mean β NP	Δβ	FDR
ZNF512	84450	zinc finger protein 512	0.07	0.04	0.03	0.063
ZNF512	84450	zinc finger protein 512	0.10	0.04	0.06	0.088
ZNF512	84450	zinc finger protein 512	0.18	0.14	0.04	0.089
ZNF558	148156	zinc finger protein 558	0.71	0.79	-0.09	0.060
ZNF577	84765	zinc finger protein 577	0.11	0.05	0.05	0.043
ZNF610	162963	zinc finger protein 610	0.70	0.85	-0.15	0.046
ZNF614	80110	zinc finger protein 614	0.08	0.04	0.04	0.039
ZNF615	284370	zinc finger protein 615	0.07	0.04	0.03	0.025
ZNF619	285267	zinc finger protein 619	0.54	0.69	-0.15	0.050
ZNF623	9831	zinc finger protein 623	0.83	0.88	-0.05	0.046
ZNF660	285349	zinc finger protein 660	0.02	0.01	0.00	0.069
ZNF678	339500	zinc finger protein 678	0.04	0.03	0.02	0.074
ZNF678	339500	zinc finger protein 678	0.76	0.81	-0.05	0.077
ZNF80	7634	zinc finger protein 80	0.94	0.96	-0.03	0.053
ZPBP	11055	zona pellucida binding protein	0.08	0.05	0.03	0.093
ZPLD1	131368	zona pellucida-like domain containing 1	0.16	0.23	-0.08	0.082
ZZZ3	26009	zinc finger, ZZ-type containing 3	0.03	0.02	0.01	0.065
SNORD109A	338428	small nucleolar RNA, C/D box 109A	0.83	0.91	-0.08	0.038
CKS1BP7	137529	CDC28 protein kinase regulatory subunit 1A pseudogene	0.12	0.23	-0.10	0.085

Note: Gene descriptions were obtained by using DAVID algorithm, National Institute of Allergy and Infectious Diseases (NIAID), NIH.

Table 5: List of Molecular Functions and Biological Processes that were over-represented in preeclamptic blood vessels and are pertinent to the pathophysiology of preeclampsia.

Biological Processes	Molecular Functions
activation of Rac GTPase activity	amino acid transmembrane transporter activity
cellular glucan metabolic process	beta-galactosidase activity
GDP-L-fucose metabolic process	CCR chemokine receptor binding
GDP-mannose metabolic process	CCR2 chemokine receptor binding
glucan metabolic process	CXCR chemokine receptor binding
glycogen metabolic process	cyclase inhibitor activity
Hemostasis	galactose binding
histidine catabolic process	galactosidase activity
inactivation of MAPK activity	GDP-mannose 4,6-dehydratase activity
L-amino acid transport	glycogen (starch) synthase activity
leukocyte migration during inflammatory response	glycogen phosphorylase activity
negative regulation of cGMP production	glycosylceramidase activity
negative regulation of MAP kinase activity	GTPase regulator activity
negative regulation of nitric oxide production	guanylate cyclase inhibitor activity
negative regulation of phosphoinositide 3-kinase cascade	heparanase activity
negative regulation of vasodilation	interferon-gamma receptor activity
positive regulation of calcium ion transport	interleukin-8 receptor binding
positive regulation of calcium ion transport into cytosol	lactase activity
positive regulation of GTPase activity	phosphoprotein phosphatase inhibitor activity

Biological Processes	Molecular Functions
positive regulation of interferon-alpha production	vitamin E binding
positive regulation of interferon-beta production	
positive regulation of Rac GTPase activity	
positive regulation of vasoconstriction	
vitamin E metabolic process	

Table 6: Canonical pathways identified by Ingenuity Pathway Analysis software at a p-value < 0.05.

Ingenuity Canonical Pathways	Molecules
LPS/IL-1 Mediated Inhibition of RXR Function	IL18RAP, ABCG5, IL1RL1, APOC4, GSTA5, ABCG1, FMO5, NR0B2, ALDH1A3, NR1I2, CYP3A7, ACSL5, GSTM4, FABP1, CHST11, FABP4, ACSL4, CHST10, FMO1, ALDH3A1, IL1RAP, FMO3, MYD88, MGMT, CHST12, IL1R1, ACSBG2, ALDH9A1, TLR4, NR1H2, MGST2, SULT1A1, CPT2, SULT1B1, MGST3
Role of Cytokines in Mediating Communication between Immune Cells	IL1A, IL5, IFNA8, IL10, IL27, IL1F10, IFNA16, IL24, IL25, IL17A, IL1F9, IFNA21, IL4
IL-10 Signaling	IL18RAP, MAP3K14, IL1A, IL1RL1, IL10, FCGR2A, NFKBIE, IL1F10, MAPK13, IL1R1, NFKB2, FOS, IL1F9, SP1, IL1RAP
LXR/RXR Activation	IL18RAP, ABCG5, IL1A, MSR1, IL1RL1, APOC4, ABCG1, NFKB2, IL1F10, IL1R1, TLR4, IL1F9, NR1H2, PTGS2, NCOR2, IL1RAP
Mismatch Repair in Eukaryotes	PCNA, MSH6, FEN1, RFC1, MLH1, EXO1
Aryl Hydrocarbon Receptor Signaling	SRC, IL1A, TP73, NQO2, GSTA5, NFKB2, CCND1, ALDH9A1, AHRR, FOS, RB1, HSP90B1, CCND2, SP1, MGST2, NR0B2, ALDH1A3, GSTM4, NCOR2, ALDH3A1, CDK2, MGST3
PPAR Signaling	IL18RAP, MAP3K14, IL1A, IL1RL1, RRAS, NFKBIE, CREBBP, IL1F10, IL1R1, NFKB2, FOS, HSP90B1, IL1F9, NR0B2, PTGS2, NCOR2, IL1RAP
Altered T Cell and B Cell Signaling in Rheumatoid Arthritis	MAP3K14, IL1A, IL10, LTB, IL1F10, NFKB2, TNFRSF17, IL17A, TLR4, IL1F9, LTA, TLR6, CCL21, FCER1G, IL4
Xenobiotic Metabolism Signaling	IL1A, MAP3K11, NQO2, GSTA5, MAPK13, FMO5, CEL, HSP90B1, CAMK2A, UGT2B4, NR1I2, CYP3A7, ALDH1A3, GSTM4, CHST11, CHST10, FMO1, PRKD3, ALDH3A1, MAP3K14, FMO3, RRAS, MGMT, CREBBP, CHST12, NFKB2, UGT1A1, ALDH9A1, AHRR, MGST2, SULT1A1, NCOR2, MAP2K5, SULT1B1, MGST3
Glycosphingolipid Biosynthesis - Neolactoseries	ST8SIA4, FUT5, ABO, UGT2A3, GCNT2, B3GNT1, ST3GAL5

Ingenuity Canonical Pathways	Molecules
IL-1 Signaling	MAP3K14, IL1A, MYD88, NFKBIE, MAPK13, IL1R1, NFKB2, GNG7, FOS, GNAT2, PRKACG, GNAO1, GNB1L, IL1RAP, GNG4
HMGB1 Signaling	IL1A, RRAS, DIRAS3, RBBP7, MAPK13, IL1R1, NFKB2, FOS, TLR4, KAT2B, RND3, SP1, RHOD, AKT3, MAP2K5
Hepatic Cholestasis	IL18RAP, MAP3K14, CYP7B1, ABCG5, IL1A, IL1RL1, MYD88, NFKBIE, NFKB2, IL1F10, IL1R1, TLR4, IL1F9, ABCB4, NR0B2, NR1I2, PRKACG, HNF4A, IL1RAP, PRKD3, FGF19
Starch and Sucrose Metabolism	PLA2R1, ENPP5, MTAP, UGT1A1, LTK, GYS2, ENPP3, HK1, DDX6, PYGM, UGT2B4, GCK, SLC3A1, AMY2B
CCR5 Signaling in Macrophages	CD3G, FOS, PLCG2, FCER1G, MAPK13, CCL5, GNB1L, PRKD3, CD3D, GNG4, GNG7
Parkinson's Signaling	CASP3, PARK7, CYCS, MAPK13, SNCA
FXR/RXR Activation	IL1A, ABCG5, CREBBP, IL1F10, IL1F9, UGT2B4, ABCB4, NR0B2, CYP19A1, NR1I2, AKT3, FBP1, HNF4A, FGF19
Biosynthesis of Steroids	FDPS, CYP7B1, NQO2, FNTB, SC5DL, GGPS1
DNA Methylation and Transcriptional Repression Signaling	MECP2, RBBP7, SIN3A, SAP18, RBBP4
Role of Hypercytokinemia/hyperchemokinemia in the Pathogenesis of Influenza	IL1F9, IL1A, IFNA8, IFNA21, IL1F10, CCL5, IFNA16, IL17A
Nicotinate and Nicotinamide Metabolism	DAPK1, CDK7, ENPP5, QPRT, TTK, VNN3, BRAF, ENPP3, NAPRT1, VNN2, PRKAA2, NMNAT2, CD38, MAK, CDK2
Role of Macrophages, Fibroblasts and Endothelial Cells in Rheumatoid Arthritis	IL18RAP, IL1A, SFRP2, IL1RL1, NFKBIE, MMP13, LTB, IL1F10, CCL5, CCND1, KLK11, IL1F9, CAMK2A, TMPRSS3, SFRP5, AKT3, IL1RAP, PRKD3, MMP1, KLK10, SRC, MAP3K14, IL10, RRAS, MYD88, C1S, IL1R1, NFATC4, IL7, APC, IL17A, PLCZ1, TLR4, FOS, FZD4, LTA, PLCG2, GNAO1, TLR6
Assembly of RNA Polymerase I Complex	POLR1C, UBTF, TAF1B

Ingenuity Canonical Pathways	Molecules
Fructose and Mannose Metabolism	HK1, ALDOB, UGT2A3, GCK, FBP1, PFKFB2, LTK, PMM2, MPI
Airway Inflammation in Asthma	IL5, IL4

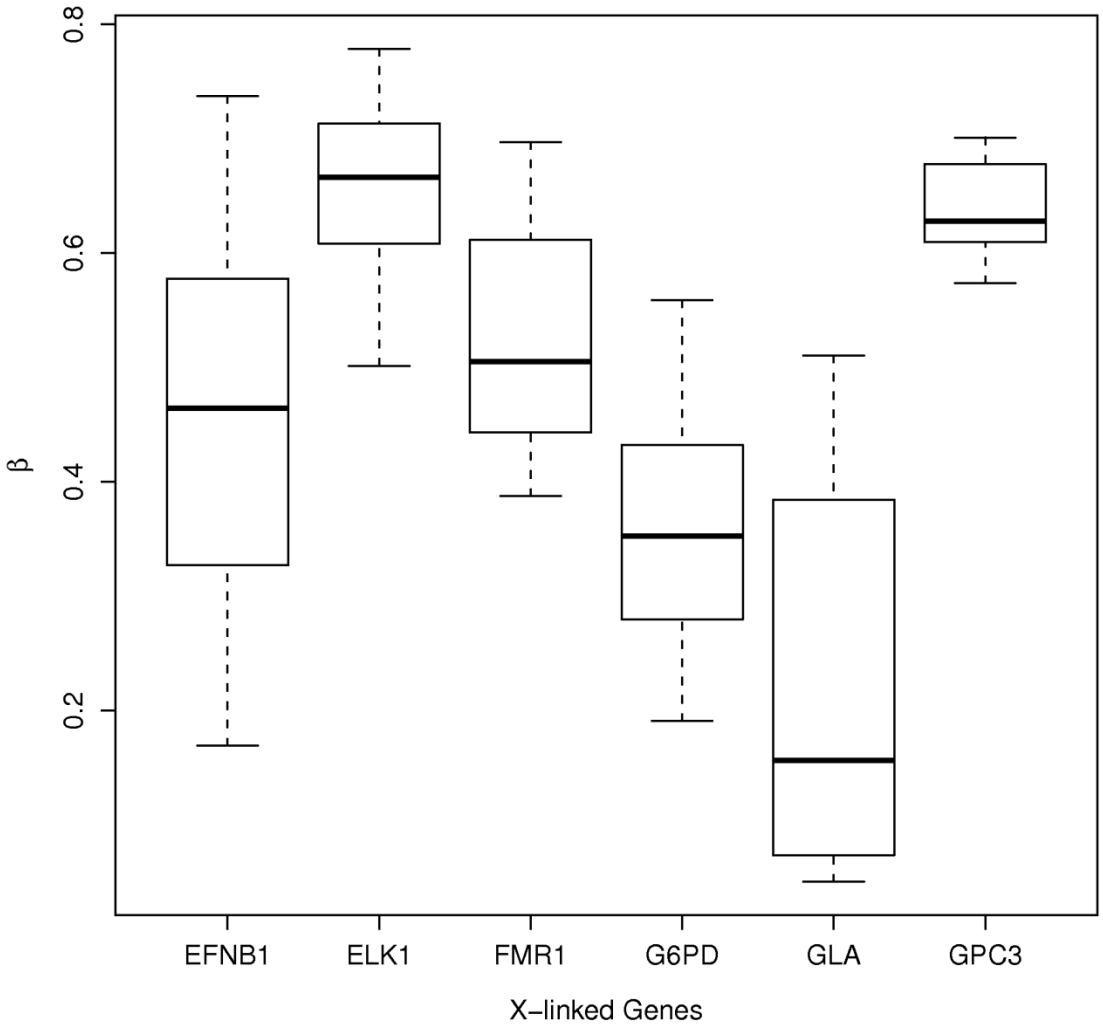

Figure 1: Boxplots of β-values for the six X-linked genes examined for quality assessment of hybridization. There were no quality concerns.

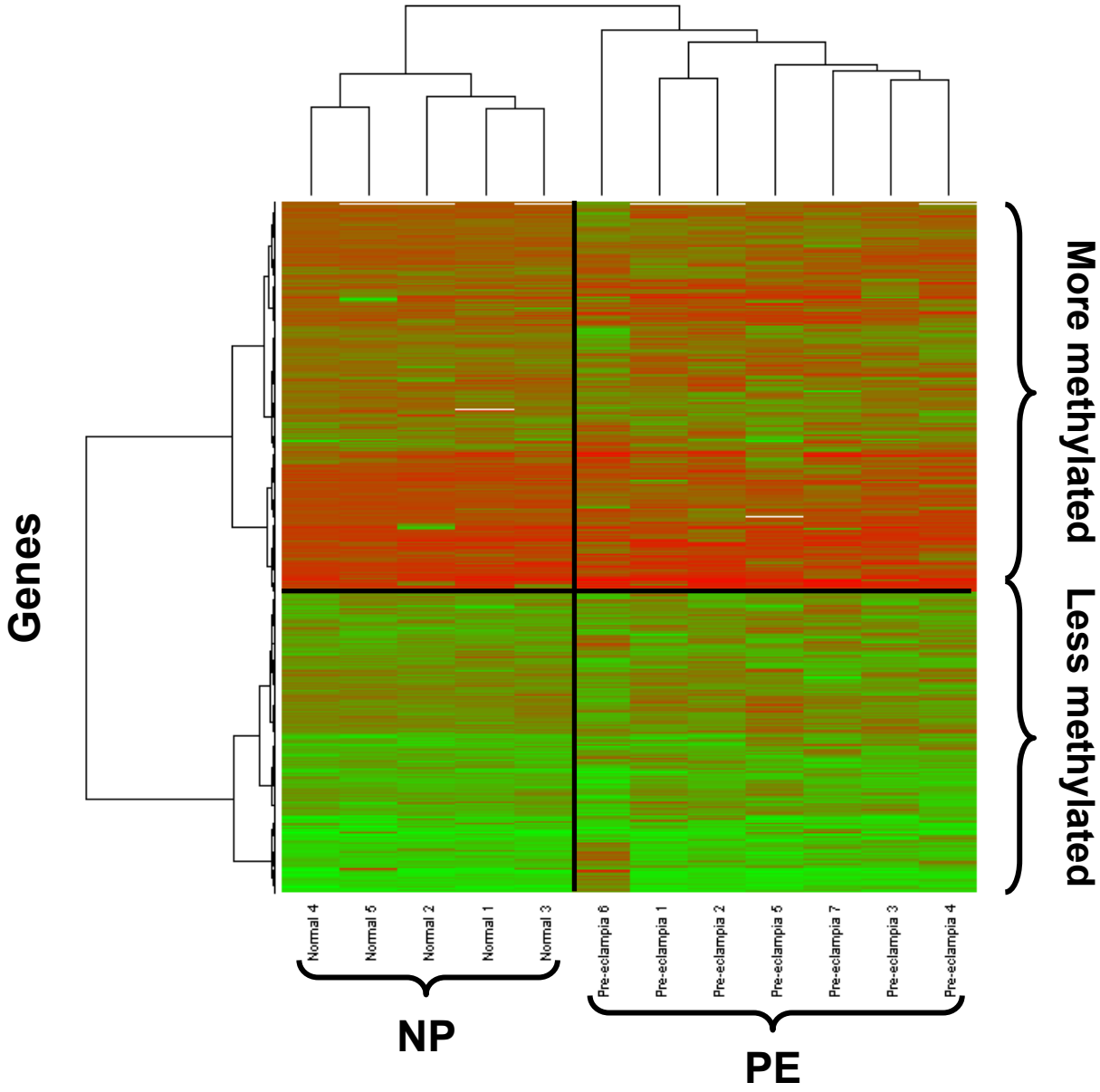

Figure 2: Heatmap of unsupervised hierarchical clustering. Unsupervised hierarchical clustering revealed natural grouping by diagnosis and methylation status. NP = normal pregnant, PE = preeclampsia, red indicates hypermethylated CpG sites, green indicates hypomethylated CpG sites.

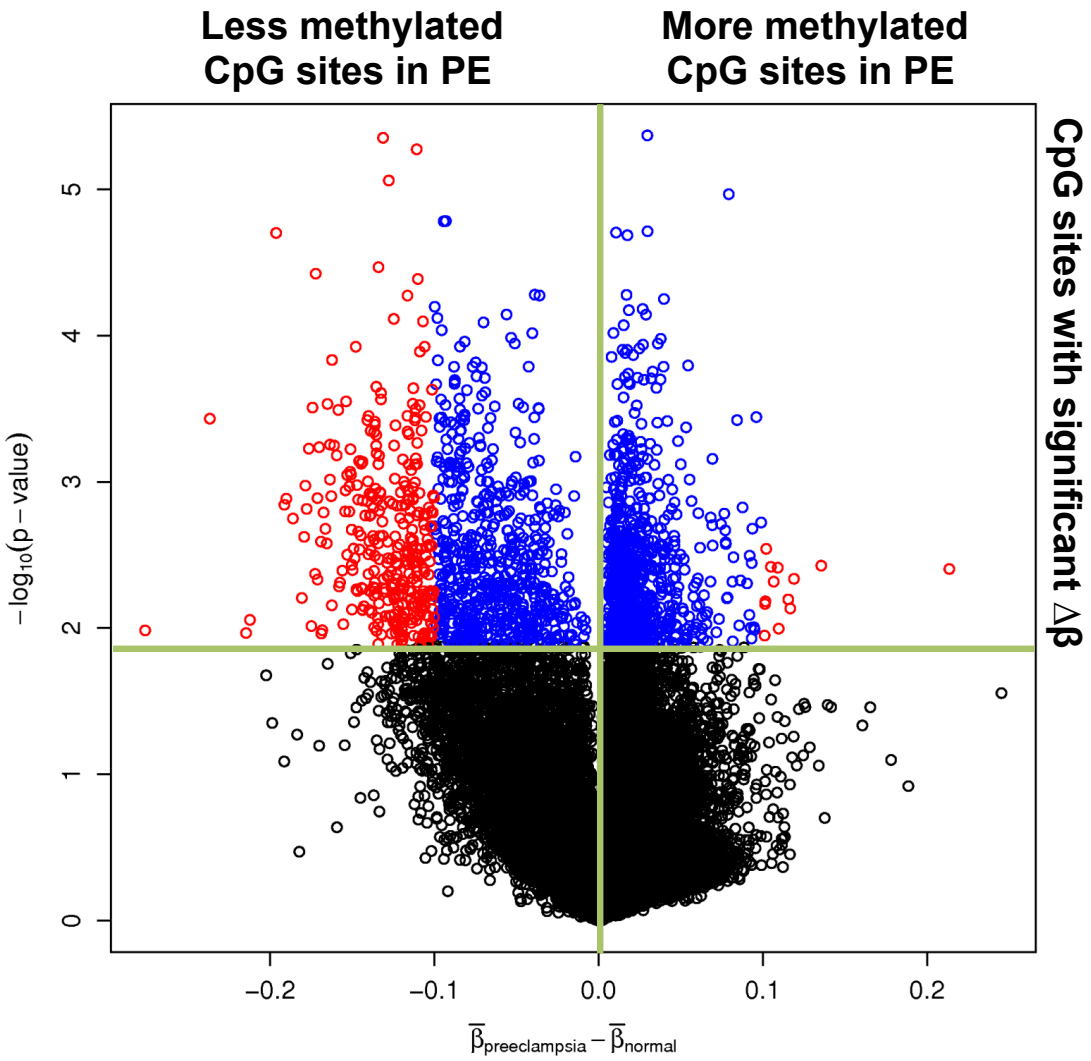

Figure 3: Volcano plot comparing severe preeclampsia vs normal pregnancy. The difference in average proportion methylated between severe preeclampsia and normal pregnancy is plotted on the x-axis and $-\log_{10}$(p-value) is plotted on the y-axis. Blue points represent CpG sites significant using a FDR of 10%; red points represent CpG sites significant using a FDR of 10% and having a difference between the two groups exceeding |0.10|.

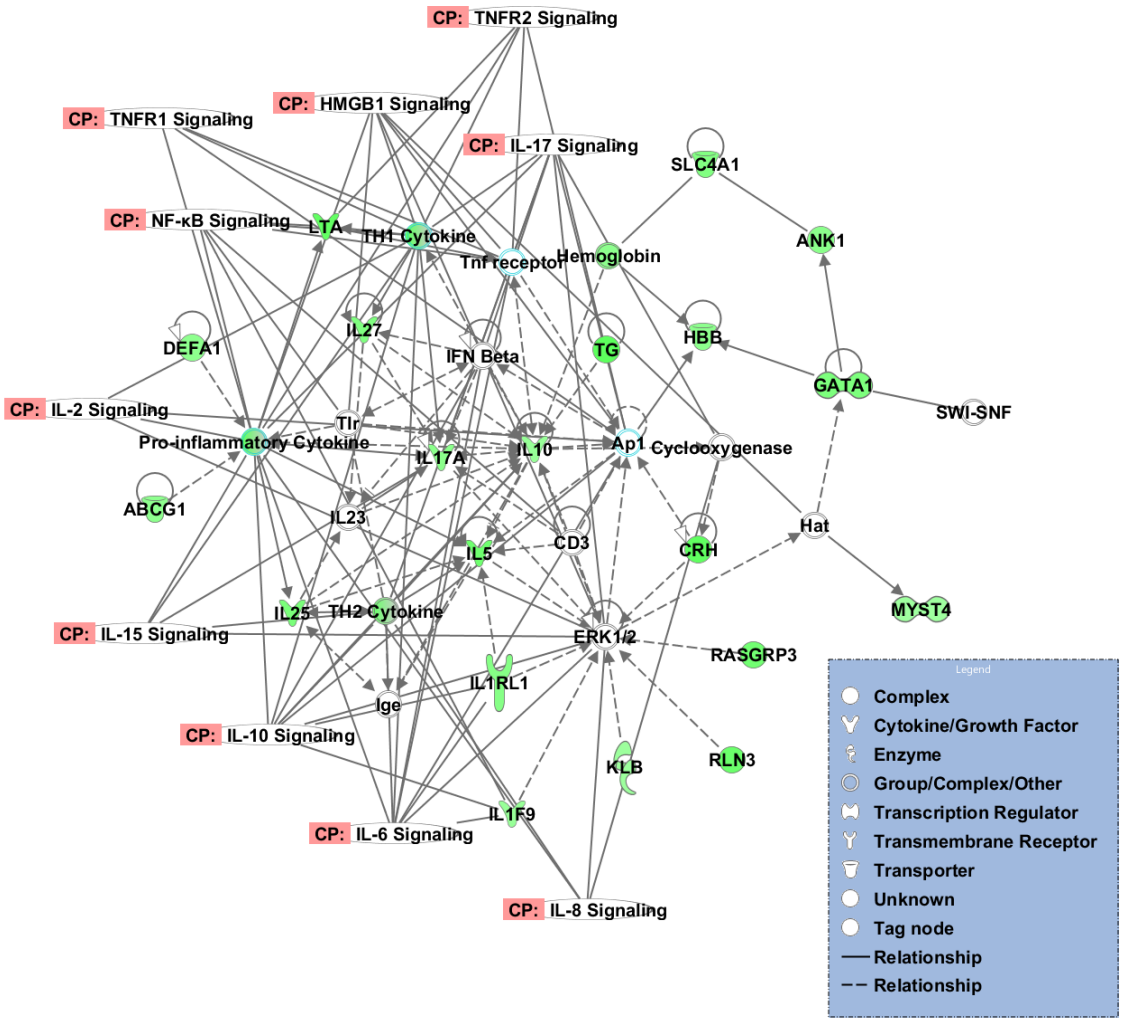

Figure 4: A gene-to-gene network identified by IPA analysis in our data set. The network includes multiple inflammatory genes which were hypomethylated in preeclampsia (green) and show the direct (indicated by solid line) and indirect (indicated by broken line) interaction between these genes and other genes in the network. The Figure also shows the interaction between genes in the network with canonical pathways related to inflammation.

CHAPTER 4: REDUCED METHYLATION OF THROMBOXANE SYNTHASE GENE IS CORRELATED WITH ITS INCREASED VASCULAR EXPRESSION IN PREECLAMPSIA

A. Abstract

Preeclampsia is characterized by increased thromboxane and decreased prostacyclin levels, which predate symptoms and can explain some of the clinical manifestations of preeclampsia, including hypertension and thrombosis. In this study, we examined DNA methylation of the promoter region of the thromboxane synthase gene (*TBXAS1*) and the expression of thromboxane synthase in systemic blood vessels of normal pregnant and preeclamptic women. Thromboxane synthase is responsible for the synthesis of thromboxane A_2, a potent vasoconstrictor and activator of platelets. We also examined the effect of experimentally induced DNA hypomethylation on the expression of thromboxane synthase in a neutrophil-like cell line (HL-60 cells), and in cultured vascular smooth muscle and endothelial cells. We found that DNA methylation of the *TBXAS1* promoter was decreased, and thromboxane synthase expression was increased in omental arteries of preeclamptic women as compared to normal pregnant women. Increased thromboxane synthase expression was observed in vascular smooth muscles cells, endothelial cells and infiltrating neutrophils. Experimentally induced DNA hypomethylation increased the expression of thromboxane synthase in a neutrophil-like cell line, whereas TNFα, a neutrophil product, increased its expression in cultured vascular smooth muscle cells. Our study suggests that epigenetic mechanisms and release of TNFα by infiltrating neutrophils could contribute to the increased expression of thromboxane synthase in systemic blood vessels, contributing to the hypertension and coagulation abnormalities associated with preeclampsia.

B. Introduction

Preeclampsia occurs in 5-7% of pregnancies, and is a leading cause of maternal and infant mortality and morbidity[1]. It is diagnosed clinically by the onset of hypertension and proteinuria, usually occurring after twenty weeks gestation. Preeclampsia is also associated with increased activation of the coagulation system evidenced by an increase in formation of fibrin, activation of the fibrinolytic system, activation of platelets and a decrease in platelet count[204].

In 1985, increased thromboxane and decreased prostacyclin levels were reported in placentas of women with preeclampsia[95] and later confirmed for maternal blood[96] and maternal urine[97]. The imbalance in thromboxane, a potent vasoconstrictor and activator of platelets, and prostacyclin, a vasodilator and inhibitor of platelet activation, could explain hypertension, reduced uteroplacental blood flow and hypercoagulopathy observed in women with preeclampsia [27].

Thromboxane and prostacyclin have a common precursor, prostaglandin H_2, but are synthesized by different enzymes[207]. Thromboxane synthase is the enzyme that catalyzes the isomerization of prostaglandin H_2 into thromboxane[94]. An increase in thromboxane synthase has been demonstrated in trophoblast and decidua cells of placentas of preeclamptic women[93] but increased expression in maternal tissue has heretofore not been shown. If thromboxane synthase was increased in maternal blood vessels, vasoconstriction and platelet activation could result due to increased thromboxane.

Increased thromboxane production in preeclampsia could be related to altered expression of the *TBXAS1* gene resulting from genomic variation or transcriptional activation. The latter could encompass epigenetic regulation, including DNA methylation. DNA methylation is a major epigenetic mechanism controlling gene expression[110]. In general, hypomethylation is associated with increased gene expression, whereas hypermethylation is associated with decreased gene expression. It has been reported that DNA methylation is involved in the regulation of thromboxane synthase gene (*TBXAS1*)[152]. Thus, reduced

methylation of the *TBXAS1* gene could result in increased thromboxane synthase and increased thromboxane A_2 production. DNA methylation status in preeclampsia may be related to oxidative stress. Oxidation of DNA causes loss of methylation[141,208,209] and preeclampsia is associated with oxidative stress[89]. Consistent with this notion is a preliminary report that found increased urinary levels of 8-hydroxy-2-deoxyguanosine, an indicator of DNA oxidation, in preeclamptic women[210].

In the present study, we tested the hypothesis that reduced DNA methylation of the *TBXAS1* gene leads to increased vascular expression of thromboxane synthase in preeclampsia. To test this, we examined the DNA methylation status of the *TBXAS1* gene and correlated it with gene and protein expression of thromboxane synthase in omental arteries obtained from preeclamptic and normal pregnant women. We then experimentally induced hypomethylation in vascular smooth muscle and endothelial cells and in a neutrophil-like cell line and determined gene and protein expression of thromboxane synthase. We examined the expression of thromboxane synthase in omental arteries because these arteries are a component of the maternal systemic vasculature, and they play a role in blood pressure regulation by contributing to the total peripheral vascular resistance. We examined the effect of hypomethylation in the neutrophil-like cell line because of the extensive vascular infiltration of neutrophils that occurs in preeclampsia[61-63] and neutrophils are a source of thromboxane[86].

C. Materials and methods

1. Study subjects

Omental fat biopsies of approximately 2 cm x 2cm x 2cm in size were collected from normal pregnant (n=16) and preeclamptic (n=22) women (28-38 weeks of gestation) during cesarean section at MCV Hospital, Virginia Commonwealth University Medical Center, Richmond, VA. Preeclampsia was diagnosed by new onset of hypertension (systolic blood pressure of ≥ 140 mm Hg and/or diastolic blood

pressure ≥ 90 mm Hg) and proteinuria (300 mg or more of protein in the urine per 24 hours collection) that occur in women who are otherwise normal[1]. Women with chorioamnionitis, infections, active sexually transmitted diseases, lupus or diabetes, and women who were smokers or in labor were excluded because these conditions are associated with inflammatory changes. Patient's clinical data are shown in Table 7. All subjects gave informed consent. This study was approved by the Office of Research Subjects Protection, Virginia Commonwealth University, Richmond, VA.

2. Methylation assay

Omental arteries from 5 normal pregnant and 7 preeclamptic women were processed for DNA extraction. DNA was extracted from the arteries (~10 mg by weight) using QuickGene DNA tissue kit and QuickGene-Mini80 system (AutoGen, Holliston, MA). DNA was treated with RNase A (Qiagen, Valencia, CA). DNA (1µg) was bisulfite treated and used in Illumina Infinium HumanMethylation27 BeadChip assay (Illumina, San Diego, CA) for DNA methylation analysis. The BeadChip was run by the Nucleic Acids Research Facilities at VCU using the protocol provided by Illumina.

3. Immunohistochemistry

Omental fat samples from 4 normal pregnant and 5 preeclamptic women were cut into small pieces approximately 0.5 cm x 0.5 cm x 0.5 cm in size, fixed immediately in 10% neutral buffered formalin and embedded in paraffin. Tissues were cut into 8 µm sections. Tissue slides were stained for rabbit antihuman polyclonal antibody specific for thromboxane synthase (1:50 titer, Proteintech, Chicago, IL). Rabbit primary antibody isotype control (Invitrogen, Camarillo, CA) was used as a negative control. A kit was used for immunohistochemical staining (SuperPicTure Polymer Detection Kit Broad Spectrum

(DAB), Invitrogen, Camarillo, CA). To quench endogenous tissue peroxidase activity, slides were incubated in 3% hydrogen peroxide in methanol for 30 minutes. For antigen retrieval, slides were heat treated in 10 mM citrate buffer for 5 minutes with a pressure cooker. Tissue slides were counterstained with 1:5 dilution of hematoxylin QS (Vector Laboratories, Burlingame, CA).

For data analysis, vessels between 10 μm and 200 μm were examined. An average of 35 vessels was analyzed per slide. Vessel staining for thromboxane synthase was evaluated using a visual intensity score of 0, 1, 2, 3 or 4 where 0 was assigned for no staining and 4 for dark and extensive staining. Visual scoring was verified by a second investigator and by measuring the optical density of staining (OD) using image analysis software (cellSens Imaging Software, Olympus America, Center Valley, PA) as previously described[61,62]. Optical density of staining for thromboxane synthase in vessels was normalized to the optical density of the background. Slides were also analyzed for percentage of vessels stained and percentage of vessels with leukocyte staining for thromboxane synthase.

4. HL-60 cells

HL-60 cells (ATCC, Manassas, VA), a neutrophil-like cell line, were used to evaluate the effect of DNA hypomethylation on the expression of thromboxane synthase. Cells were cultured in Iscove's Modified Dulbecco's Medium (IMDM, ATCC, Manassas, VA) supplemented with 10% fetal bovine serum (Gibco, Invitrogen, Carlsbad, CA) and 1% antibiotics and antimycotics (100 U/ml penicillin, 100 μg/ml streptomycin, 25 μg/ml amphotericin B, Gibco, Invitrogen, Carlsbad, CA) as recommended by ATCC. Approximately 500,000 cells per ml were seeded in 5 ml of media in a T-25 flask for treatments. Cell treatments were: 1) 10 μM 5-Aza-2-deoxycytidine (5-Aza, Sigma-Aldrich, Saint-Louis, MO), an agent that inhibits DNA methylation when incorporated into DNA during cell division, for 48 hours followed by 10-8 M of phorbol 12-myristate 13-acetate (PMA, an activator of protein kinase C, Sigma-

Aldrich, Saint-Louis, MO) for 24 hours; 2) 10 μM 5-Aza for 48 hours followed by no treatment for 24 hours; 3) no treatment for 48 hours followed by 10-8 M PMA for 24 hours; or 4) no treatment for 72 hours without treatment to serve as control. To study the effect of these treatments on the production of thromboxane B2, cells were also treated with 70 μM linoleic acid (Cayman Chemical, Ann Arbor, MI). Cells were collected for DNA, RNA or protein extraction and media was saved for enzyme immunoassay.

5. Vascular Smooth Muscle and Endothelial Cell Culture and Treatments

Human vascular smooth muscle cells (VSMC) were cultured from chorionic plate arteries of placentas collected at cesarean section from healthy pregnant women at term deliveries as previously described[165]. Human umbilical vein endothelial cells were purchased from Lifeline Cell Technology (Grand Island, NY) and cultured in T-25 flasks according to their protocol with their medium. VSMCs were cultured in T-25 flasks using Medium-199 (M-199, Gibco, Invitrogen, Carlsbad, CA) with 10% fetal bovine serum (FBS, Gibco, Invitrogen, Carlsbad, CA) and 1% antibiotics and antimycotics (100 U/ml penicillin, 100 μg/ml streptomycin, 25 μg/ml amphotericin B, Gibco, Invitrogen, Carlsbad, CA). Cells were treated with 1 ng/ml of human recombinant TNFα (R&D Systems, Minneapolis, MN) or with 5-Aza for 48 hours. Control flasks contained M-199 media with 10% FBS and 1% antibiotics and antimycotics. Treatments were refreshed every day. Cells were 50% confluent at the time of treatment and 100% confluent at the time of harvesting. Cells were washed with PBS and harvested for RNA and protein extraction.

6. Quantitative RT-PCR

Omental arteries (25-30 mg) from 5 normal pregnant and 8 preeclamptic patients were homogenized with a rotor stator homogenizer (PRO200, PRO Scientific, Oxford, CT) and total RNA was extracted using Tri-reagent with spin columns (RiboPure kit, Ambion, Austin, TX). For cell cultures, RNA extraction was performed using QuickGene RNA cultured cell kit with QuickGene Mini-80 system (AutoGen, Holliston, MA). DNase treatment was performed using Turbo DNAse kit (Ambion, Austin, TX). RNA (0.25-1 μg) was reverse transcribed to cDNA using the IScript cDNA Synthesis Kit (Bio-Rad Laboratories, Hercules, CA). Quantitative RT-PCR reactions were performed with RT² SYBR® Green qPCR Mastermix (SABiosciences, Frederick, MD) on Eppendorf Realplex Thermal Cycler. For each reaction, 8 ng of cDNA was used. Glyceraldehyde 3-phosphate dehydrogenase (*GAPDH*) was used as a housekeeping gene. For *TBXAS1* gene, commercial primers were used (SABiosciences, Frederick, MD) and for *GAPDH* gene the following primers were used: forward primer: GATTCCACCCATGGCAAATT; reverse primer: AGATGGTGATGGGATTTCCATT. *GAPDH* primers were synthesized by Integrated DNA Technologies (IDT, Coralville, IA). Data were normalized to *GAPDH* by the ΔΔCt method. Melting curve analysis confirmed specificity of the primers.

7. Western blotting

Omental arterials (45-50 mg) from 4 normal pregnant and 6 preeclamptic patients were homogenized in RIPA buffer containing 150 mM sodium chloride, 1.0% NP-40, 0.5% sodium deoxycholate, 0.1% sodium dodecyl sulphate, 50 mM Tris (pH 8.0), and 1X Halt protease inhibitor (Thermo Scientific, Pittsburgh, PA) using a rotor stator homogenizer (PRO200, PRO Scientific, Oxford, CT) at 300 rpm for 1 min. VSMC or HL-60 cells were homogenized in the same buffer using a probe sonicator (EpiShear Probe Sonicator, Active Motif, Carlsbad, CA) at 25% amplitude for 10 one sec bursts. Protein concentrations were measured using BCA assay (Thermo Fisher Scientific, Rockford, IL). Denatured protein lysates (50-100 μg) were resolved by electrophoresis on sodium dodecyl sulphate

polyacrylamide gel and electrotransferred to polyvinylidene fluoride membrane (Immobilon-FL, Millipore, Billerica, MA). Membranes were probed for thromboxane synthase and β-actin. Primary antibodies used were rabbit anti-human thromboxane synthase (1:1000, Proteintech, Chicago, IL); mouse anti-human β-actin (1:1,000, Sigma, Saint Louis, MO). Secondery antibodies used included: Alexa Fluor 680 donkey anti-rabbit (1:10,000, Invitrogen, Carlsbad, CA) for the detection of thromboxane synthase and IRDye800 goat anti-mouse (1:20,000, Rockland Immunochemicals, Gilbertsville, PA) for the detection of β-actin. LI-COR Odyssey Infrared Imaging System (Thermo Scientific, Pittsburgh, PA) was used to detect and analyze the immunoreactive proteins. Density values of protein bands were measured by multiplying the intensity of the bands by their area. Density values for thromboxane synthase bands were normalized by dividing them by the density values of their corresponding β-actin bands. The normalized thromboxane synthase density value of the reference group (control or normal pregnant) was considered 100% and changes in other groups were represented as relative to the reference group.

8. Enzyme immunoassay

The Thromboxane B_2 (TXB_2) Enzyme Immunoassay kit (Assay Designs, Ann Arbor, MI) was used to measure TXB_2 secretion into the media. TXB_2 is the stable metabolite of thromboxane A_2[211]. The procedure for the assay was done as recommended by the manufacturer. Media was diluted by a factor of 1:1 before it was used in the assay. TXB_2 concentrations were measured in pg/ml using FLUOstar OPTIMA plate reader (BMG Labtech, Ortenberg, Germany). For normalization, the total amount of TXB_2 (pg) in 5ml (volume of medium used in a T-25 flask) was divided by the total amount of DNA (μg) extracted from the cells of the same flask. DNA was extracted as described above.

9. Statistical analysis

Data analysis of the HumanMethylation27 BeadChip assay was performed using the beadarray package in R programming environment[212]. To control for multiple hypothesis testing, the p-values were subsequently used in estimating the false discovery rates (FDR) using the q-value method[166]. Methylation values (β values) are expressed as range from 0 to 1 where 0 means not methylated and 1 means fully methylated. Δβ-values indicate the difference in methylation between normal pregnant and preeclamptic women.

Student's t test was used to make comparisons of parameters between two groups and one-way ANOVA with Newman-Keuls test was used to make comparisons of parameters between more than two groups for normally distributed data. Mann-Whitney U test was used for visual intensity score data. Quantitative results were presented as mean ± SEM. We considered a p-value of < 0.05 statistically significant. A statistical software program was used for data analysis (GraphPad Prism version 4.0, San Diego, CA).

D. Results

The Illumina Infinium HumanMethylation27 BeadChip assay revealed 4,184 CpG sites, corresponding to 3,736 genes, with significant differential methylation when comparing between normal pregnant and preeclamptic omental arteries at p-value of less than 0.05[213]. Many of these genes were genes involved in inflammation. Of these genes, thromboxane synthase (*TBXAS1*) was the most significantly less methylated with an average difference in methylation (Δβ) of 0.24 at p-value of 0.00037 corresponding to a false discovery rate (FDR) of 0.042. There was no overlap in the methylation values

(β-values) between the two groups demonstrating that all preeclamptic samples were less methylated as compared to normal pregnant samples (Figure 5).

Representative staining images for thromboxane synthase are shown in Figure 6. Negative controls showed no staining for thromboxane synthase (Panel A). There was little or no staining in vessels of normal pregnant women (Panel B). However, preeclamptic vessels showed significant staining for thromboxane synthase (Panels C, D, E and F). Staining for thromboxane synthase in preeclamptic vessels was present in endothelium, vascular smooth muscle and in leukocytes, which were in the lumen, adherent to the endothelium and infiltrated into the walls of the vessels (Panel F).

The staining intensity score for thromboxane synthase was significantly greater for preeclamptic women as compared to normal pregnant women (3.0 ± 0.1 vs 0.5 ± 0.1, respectively, $p < 0.001$, Figure 7A), as was optical density (OD) of staining (88.0 ± 6.0 vs 19.0 ± 2.0 OD, respectively, $p < 0.001$, Figure 7B). Staining intensity scores and ODs were highly correlated ($r = 0.93$). The percentage of vessels with staining for thromboxane synthase was significantly greater for preeclamptic women than for normal pregnant women (95.0 ± 2.0% vs 25.0 ± 4.0% respectively, $p < 0.001$, Figure 7C), as was the percentage of vessels with leukocytes stained for thromboxane synthase (80.0 ± 2.0% vs 12.0 ± 3.0% respectively, $p <0.001$, Figure 7D).

To verify the immunohistochemistry results, we examined *TBXAS1* gene expression in omental arteries of normal pregnant and preeclamptic women. *TBXAS1* gene expression was 2.5-fold higher in omental arteries of preeclamptic women as compared to normal pregnant women (2.6 ± 0.2 vs 1.0 ± 0.1 respectively, $p < 0.01$, Figure 8). Western blotting confirmed that increased gene expression for *TBXAS1* was associated with increased thromboxane synthase protein (Figure 9, A and B). Thromboxane synthase protein expression was 3-fold greater in preeclamptic arteries as compared to normal pregnant arteries as determined by Western blot density measurements ($p < 0.01$).

To examine the role of DNA methylation in regulating the expression of thromboxane synthase in neutrophils, it was necessary to use a neutrophil-like cell line (HL-60) because neutrophils isolated from patients do not divide and therefore the 5-Aza-2-deoxycytidine (5-Aza) could not be incorporated into the genomic DNA to induce hypomethylation. Treatment of HL-60 cells with 5-Aza resulted in a significant increase in *TBXAS1* gene expression (2.6 ± 0.2-fold, $p < 0.001$). Treatment with PMA to activate the cells resulted in a 1.4 ± 0.1-fold increase in *TBXAS1*. Activation of the cells by PMA was evidenced by cell clumping and adhesion to the floor of the flask. Combining 5-Aza treatment with PMA resulted in a significant increase in *TBXAS1* gene expression as compared to control (3.8 ± 0.4-fold, $p < 0.001$), PMA alone ($p < 0.001$) or 5-Aza alone ($p < 0.001$) (Figure 10). Western blotting confirmed that protein expression was altered in concert with gene expression (Figure 11, A and B). Treatment with 5-Aza significantly increased thromboxane synthase protein expression (347 ± 11% average density measurement of Western blot as compared to control, $p < 0.001$). Combining 5-Aza treatment with PMA resulted in significantly increased thromboxane synthase protein expression (515 ± 15% of control, $p < 0.001$), PMA alone ($p < 0.001$) or 5-Aza alone ($p < 0.001$).

To evaluate the effect of the same treatments on the production of thromboxane by the neutrophil-like HL-60 cells, cells were cultured with 70 μM linoleic acid, the precursor of arachidonic acid. Treatment with 5-Aza significantly increased the production of TXB_2, the stable metabolite of TXA_2, as compared to controls (619 ± 32 vs 115 ± 20 ng/μg DNA, respectively, $p < 0.001$, Figure 12). PMA treatment caused a significant increase in the production of TXB_2 as compared to control (745 ± 36 vs 115 ± 20 ng/μg DNA, respectively, $p < 0.001$). Combining 5-Aza and PMA treatments caused an even greater increase in the production of TXB_2 (1228 ± 140 ng/μg DNA, $p < 0.001$).

In contrast to HL-60 cells, 5-Aza treatment increased *TBXAS1* gene expression by only 40% in cultured VSMCs and only 13% in cultured human umbilical vein endothelial cells, which were not statistically significant (data not shown). However, treatment of VSMCs with TNFα, a neutrophil product, significantly increased *TBXAS1* gene expression as compared to controls (3.0 ± 0.2-fold, $p < 0.001$,

Figure 13). Western blotting confirmed increased protein expression induced by TNFα (Figure 14, A and B). TNFα resulted in a 2.6-fold increase in thromboxane synthase protein in VSMCs (263 ± 37% average density of control, $P < 0.01$).

E. Discussion

In this study we report a significant reduction in DNA methylation in the promoter region of the *TBXAS1* gene associated with a significant increase in thromboxane synthase expression in omental fat arteries of preeclamptic women as compared to normal pregnant women. Increased expression of thromboxane synthase was observed in the endothelium, in the vascular smooth muscle cells and in leukocytes, which were flattened and adhered to the endothelium and infiltrated into the wall of the vessel. Increased expression of thromboxane synthase would lead to increased production of thromboxane A_2 locally in the vessel, which could explain hypertension and coagulation abnormalities in preeclamptic patients because thromboxane is a potent vasoconstrictor and platelet activator[84].

Leukocyte infiltration requires leukocyte activation, which most likely occurs as they circulate through the intervillous space and are exposed to increased lipid peroxides secreted by the placenta[41]. The infiltrating leukocytes are most likely neutrophils because neutrophils normally comprise approximately 60%-70% of all leukocytes[33] , their numbers increase 2.5-fold by 30 weeks of gestation[214] and their numbers are further increased in preeclampsia[215]. In addition, we previously reported that neutrophils, but not lymphocytes or monocytes, infiltrate systemic blood vessels of preeclamptic women[61-63,216].

To study the role of DNA methylation in the regulation of thromboxane synthase, we experimentally induced DNA hypomethylation in a neutrophil-like cell line and in cultured human VSMCs. Hypomethylation resulted in increased expression of thromboxane synthase in both cell types, however, the increase was only significant in the neutrophil-like cell line. Increased expression of

thromboxane synthase in the neutrophil-like cell line was associated with a parallel increase in the production of the stable metabolite of TXA_2, TXB_2. These data suggest that DNA methylation is important in regulating thromboxane synthase expression in neutrophils but not in vascular smooth muscle cells. However, treatment of vascular smooth muscle cells with TNFα, a neutrophil product, did significantly increase thromboxane synthase, so increased expression of thromboxane synthase in vascular tissue of preeclamptic women may be due to inflammation caused by neutrophil infiltration. Reduced DNA methylation in leukocytes has been reported in other diseases involving the cardiovascular system such as atherosclerosis[134], ischemic heart disease and stroke[130].

Pertinent to our findings of increased expression of thromboxane synthase are previous findings of increased levels of serum arachidonic acid in preeclamptic women[217] and significant activation of nuclear factor kappa B (NF-κB) and increased expression of cyclooxygenase-2 (COX-2) in preeclamptic blood vessels[62]. Similar to thromboxane synthase expression, activation of NF-κB and increased expression of COX-2 were observed in the endothelium, vascular smooth muscle and infiltrating neutrophils[62]. A possible scenario in preeclamptic blood vessels is that increased COX-2 converts increased arachidonic acid into prostaglandin H_2 and increased thromboxane synthase then converts prostaglandin H_2 into thromboxane.

Preeclampsia is associated with oxidative stress[41] and increased plasma levels of linoleic acid, the fatty acid precursor of arachidonic acid[218]. Neutrophils from normal pregnant women exposed to an oxidizing solution enriched with linoleic acid showed increased production of TNFα and thromboxane[86]. Also, exposure of cultured VSMCs to an oxidizing solution enriched with linoleic acid increased production of thromboxane[85].

Our study has several limitations. First, our findings are correlative in that they show reduced methylation is associated with increased expression of thromboxane synthase in omental arteries of preeclamptic women, but they do not prove cause and effect. In addition, we were not able to determine

the cell types where methylation changes were occurring in the omental arteries because of cellular heterogeneity, including endothelial cells, vascular smooth muscle cells and infiltrated neutrophils. Another limitation is that we cannot prove that reduced methylation in the *TBXAS1* gene promoter per se is responsible for increased expression, as opposed to changes in the expression of other factors that regulate *TBXAS1* (e.g., transcription factors or other regulatory factors) whose levels might be altered by changes in DNA methylation. However, by experimentally inducing hypomethylation in vascular smooth muscle cells and a neutrophil-like cell line we were able to demonstrate a strong association between DNA methylation status and thromboxane synthase expression in neutrophils, which have the highest thromboxane synthase content per cell in the vessels, but not in vascular smooth muscle cells, which have a lower content.

In summary, we found that reduced methylation in the promoter region of *TBXAS1* is correlated with increased gene and protein expression of thromboxane synthase in systemic blood vessels of preeclamptic women. Increased expression was present in endothelium, vascular smooth muscle cells and infiltrating neutrophils. We also showed that experimentally induced DNA hypomethylation increases the expression of thromboxane synthase in a neutrophil-like cell line and that TNFα a neutrophil product, increases thromboxane synthase expression in culture vascular smooth muscle cells. These data suggest that reduced DNA methylation is responsible for increased expression of thromboxane synthase in neutrophils that infiltrate maternal systemic blood vessels in preeclampsia, and that vascular inflammation caused by infiltrating neutrophils is responsible of increased expression of thromboxane synthase in the endothelium and vascular smooth muscle. Increased expression of thromboxane synthase in systemic vasculature of preeclamptic women may help explain hypertension and coagulation abnormalities.

These findings suggest possible treatments for preeclampsia involving inhibition of thromboxane synthase, blockade of thromboxane receptors, or dietary supplementation with folate to increase methylation donors to protect against adverse changes in DNA methylation that affect thromboxane

synthase expression. In this regard, a large study of almost 3,000 pregnant women found supplementation with multivitamins containing folic acid was associated with reduced risk of preeclampsia[206].

Table 7: Clinical Characteristics of Patient Groups.

Variable	Normal Pregnant (n=16)	Preeclamptic (n=22)
Maternal age (y)	26.8 ± 1.6	25.6 ± 1.0
Pre-pregnancy BMI (kg/m^2)	24.4 ± 0.8	30.2 ± 1.6
Systolic blood pressure (mmHg)	114.2 ± 2.2	169.5 ± 3.2***
Diastolic blood pressure (mmHg)	70.0 ± 2.0	96.1 ± 2.4***
Proteinuria (mg/24 h)	ND	260.1 ± 31.2 (n=11)
Dipstick	ND	2.6 ± 1.4 (n=11)
Parity		
Primiparous	3	12
Multiparous	13	10
Gestational age (wk)	38.8 ± 0.2	33.0 ± 0.84***
Infant birth weight (g)	3226 ± 80.5	2060 ± 185.3***

Values are presented as mean ± SEM.

***$p < 0.001$ by t-test.

ND, not detectable.

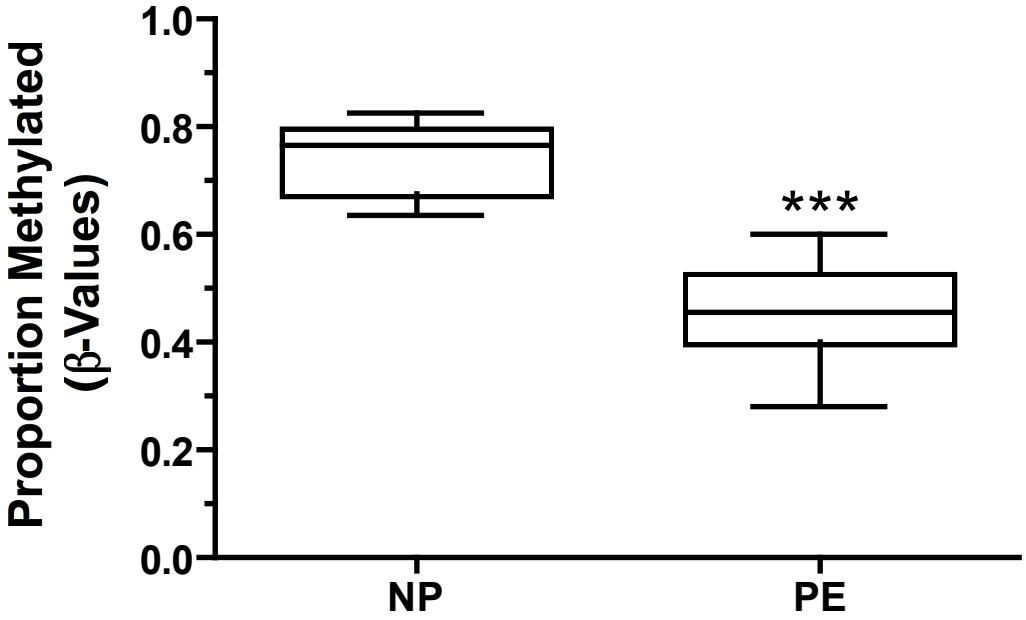

Figure 5: Boxplot of proportion methylated in omental arteries by subject group for TBXAS1 gene. Methylation was significantly lower in preeclamptic patients (n=7) than in normal pregnant patients (n=5) with no overlap between the groups. ***p< 0.001

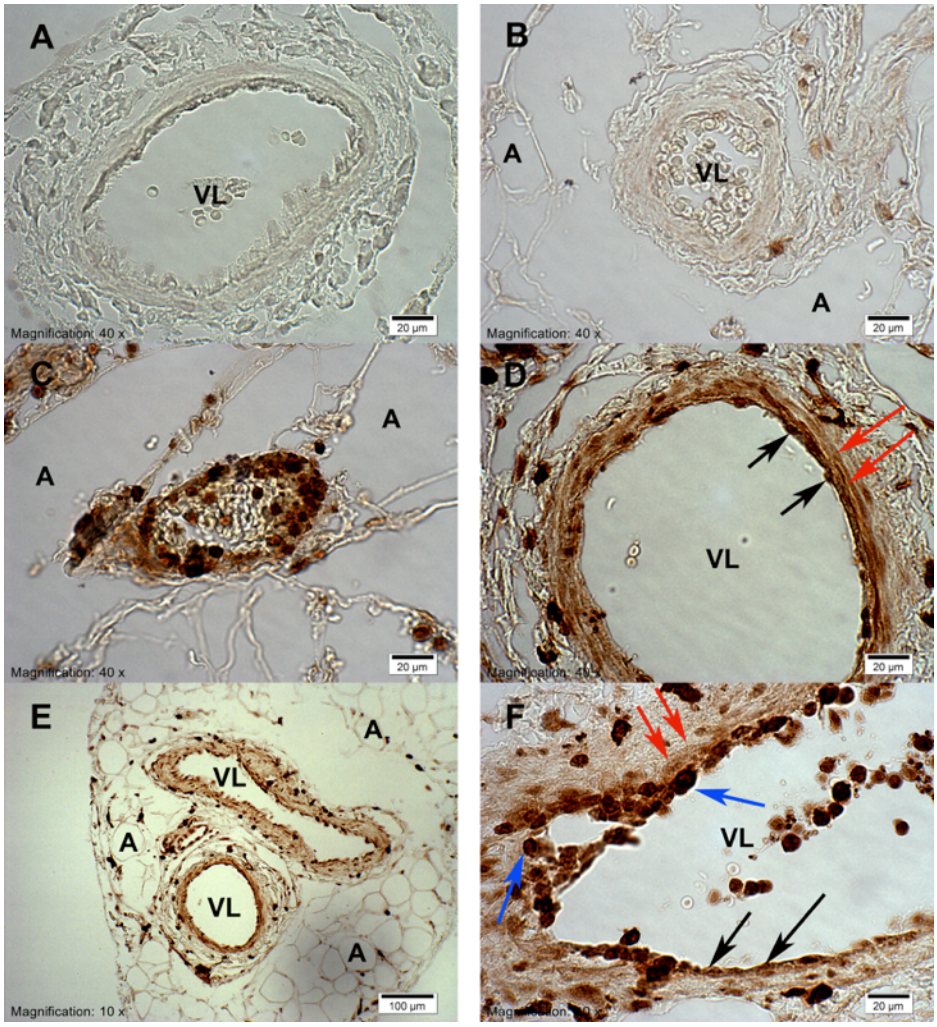

Figure 6: Representative sections for blood vessels in omental fat from normal pregnant and preeclamptic women immunostained for thromboxane synthase. A) There was no brown staining for thromboxane synthase in negative control sections. B) Blood vessels of normal pregnant women showed little or no staining for thromboxane synthase. Vessels of preeclamptic women showed significant brown staining for thromboxane synthase. Staining for thromboxane synthase in preeclamptic blood vessels was observed in endothelium (red arrows), vascular smooth muscle cells (blue arrows), and neutrophils (black arrows), which were either adhered to the endothelium or infiltrated into the wall of the vessel (F). A: adipocyte; VL: vessel lumen. Magnification and scale bar are shown on each image.

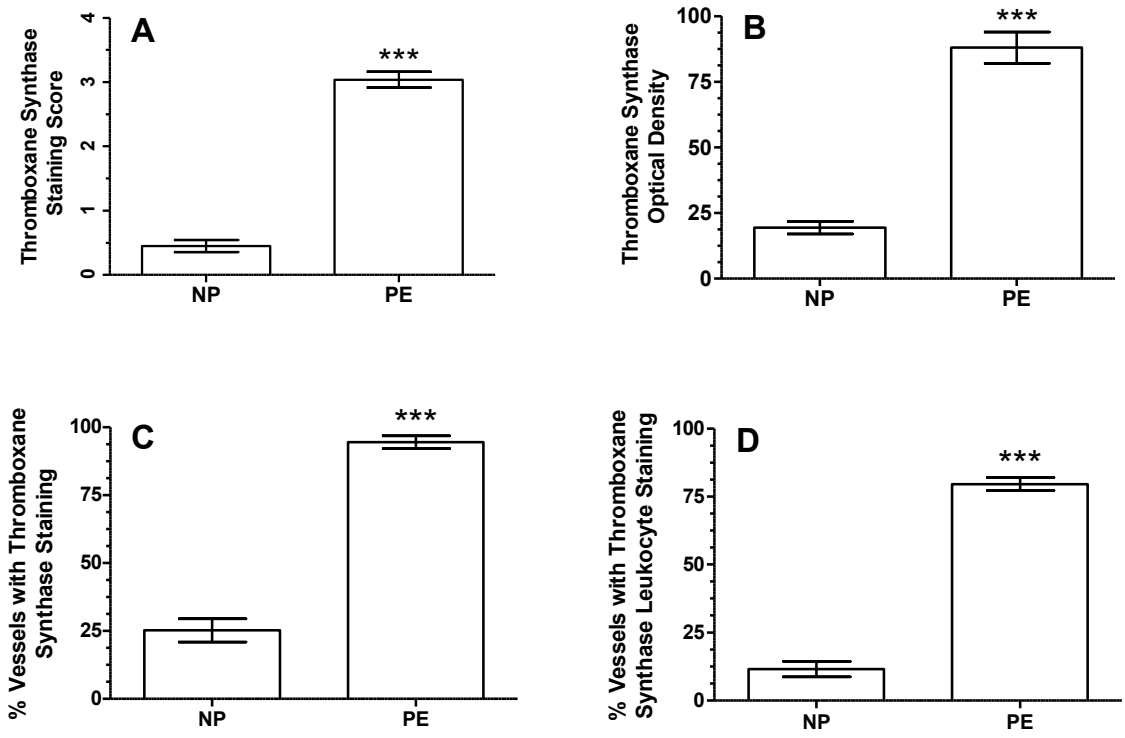

Figure 7: Results for immunohistochemical staining for thromboxane synthase in omental blood vessels from normal pregnant (NP) and preeclamptic (PE) women. A) Visual staining score for thromboxane synthase was significantly higher in blood vessels of preeclamptic women as compared to normal pregnant women. B) Optical density of staining for thromboxane synthase was also significantly higher in preeclamptic blood vessels and significantly correlated with the visual score (r=0.93). C) Preeclamptic women had significantly higher percentage of blood vessels stained for thromboxane synthase as compared to normal pregnant women. D) Preeclamptic women had significantly higher percentage of blood vessels with leukocyte stained for thromboxane synthase as compared to normal pregnant women. Data are presented as means ± SEM. ***$p < 0.001$.

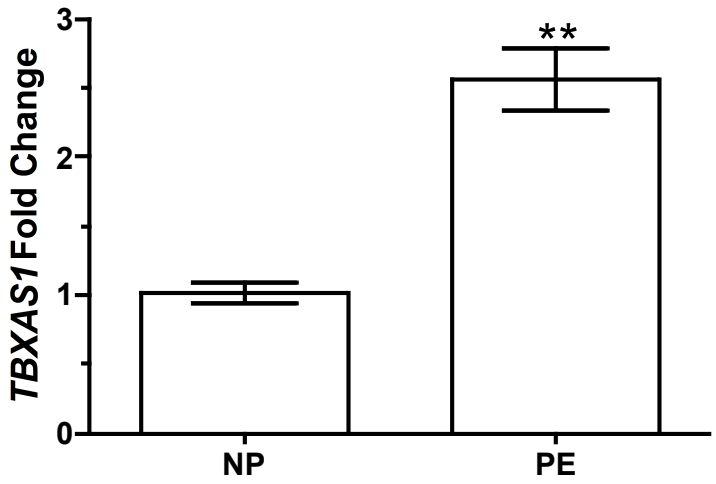

Figure 8: Thromboxane synthase gene expression in omental fat arteries of normal pregnant (NP) and preeclampsia (PE) women. Gene expression of *TBXAS1* was significantly increased in omental arteries from preeclamptic women (n=8) as compared to normal pregnant women (n=5). Data are shown as means ± SEM. **$p < 0.01$.

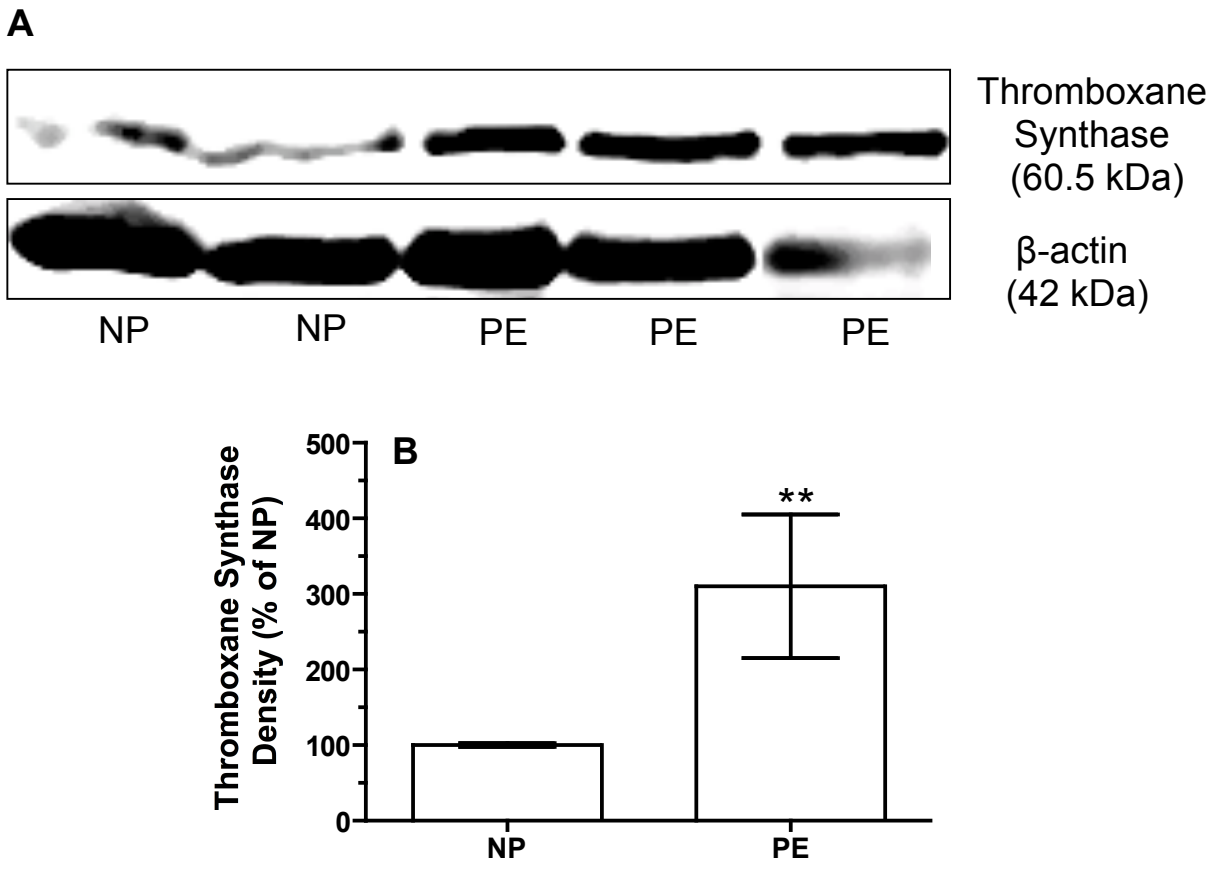

Figure 9: Thromboxane synthase protein expression in omental fat arteries of normal pregnant (NP) and preeclampsia (PE) women. A) Representative Western blot for thromboxane synthase protein expression in omental arteries of normal pregnant and preeclamptic women. B) Density of thromboxane synthase plotted as percentage of average normal pregnant. Thromboxane synthase expression was significantly increased in arteries of preeclamptic women (n=6) as compared to normal pregnant women (n=4). Data are shown as means ± SEM. **$p < 0.01$.

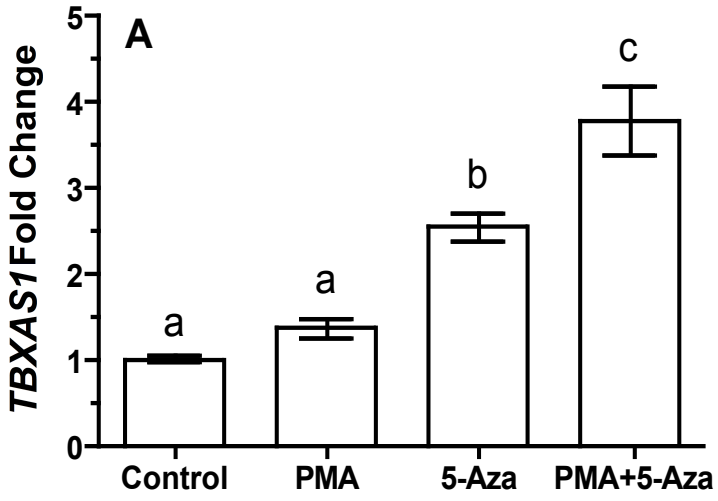

Figure 10: Thromboxane synthase gene expression in HL-60 cells. The expression of *TBXAS1* was significantly increased in 5-Aza treated cells as compared to controls. Activation with PMA after treatment with 5-Aza caused an even greater increase in *TBXAS1* expression as compared to control, PMA alone or 5-Aza alone (n=8). Data are shown as means ± SEM. Groups with different letters are significantly different, $p<0.001$.

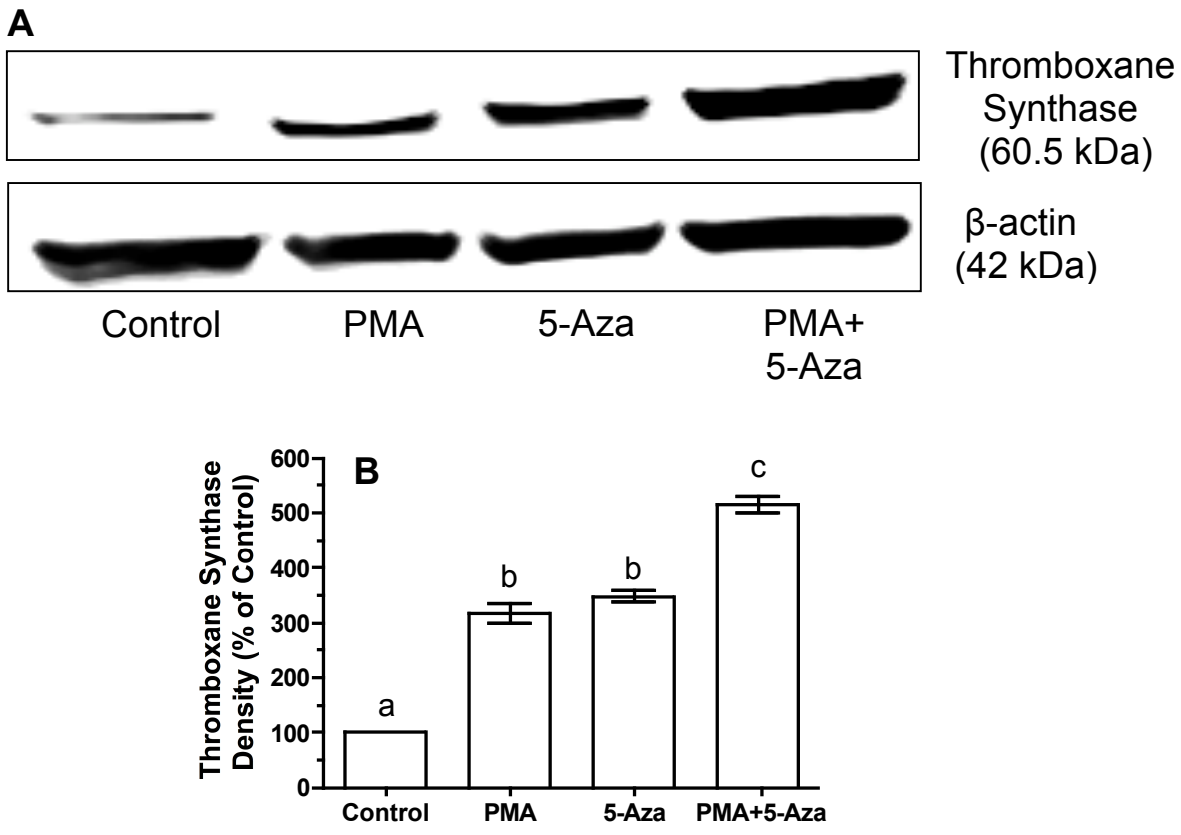

Figure 11: Thromboxane synthase protein expression in HL-60 cells. A) Representative Western blot for thromboxane synthase expression in HL-60 cells. B) Density of thromboxane synthase plotted as percentage of control. Treatment with 5-Aza significantly increased thromboxane synthase expression as compared to control. Activation with PMA after treatment with 5-Aza resulted in significant increase in thromboxane synthase expression as compared to control, PMA alone and 5-Aza alone (n=5). Data are shown as means ± SEM. Groups with different letters are significantly different, $p<0.001$.

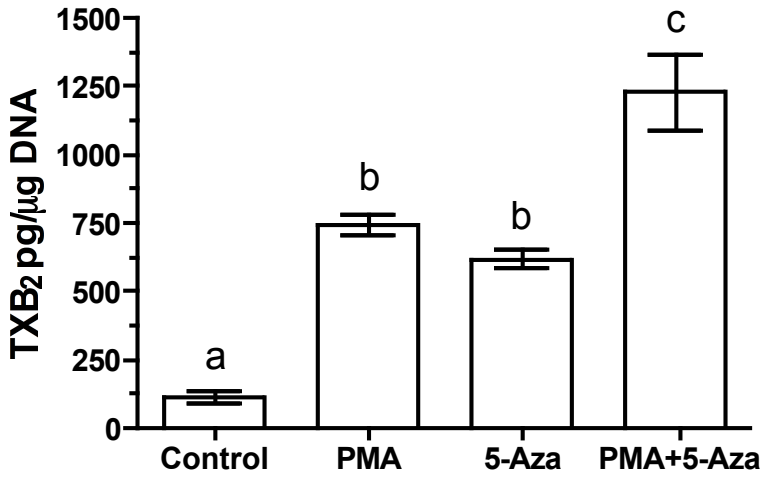

Figure 12: Thromboxane B_2 (TXB_2) secretion into the media by HL-60 cells. TXB_2 secretion was significantly increased in 5-Aza or PMA treated cells as compared to controls. Combined treatment of PMA and 5-Aza caused an even greater increase in TXB_2 secretion as compared to control, PMA alone or 5-Aza alone. Data are shown as means ± SEM, n=6. Groups with different letters are significantly different, $p<0.001$.

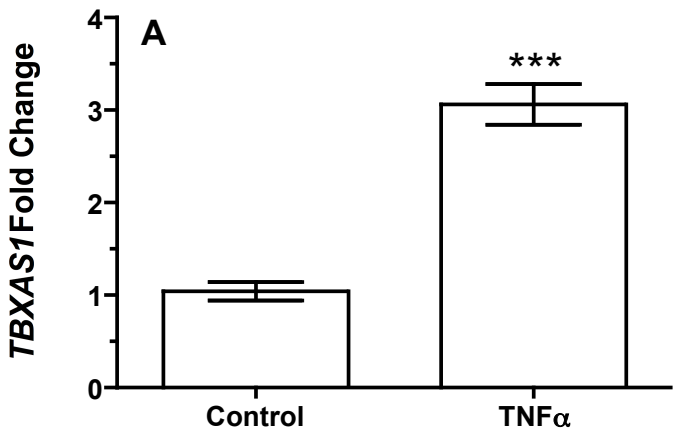

Figure 13: Thromboxane synthase gene expression in cultured human vascular smooth muscle cells treated with TNFα. A) Fold change in the expression for *TBXAS1* gene in cultured VSMCs treated with TNFα for 48 hours. The expression of *TBXAS1* was significantly increased in TNFα treated cells as compared to controls (n=6). Data are shown as means ± SEM. ***$p < 0.001$.

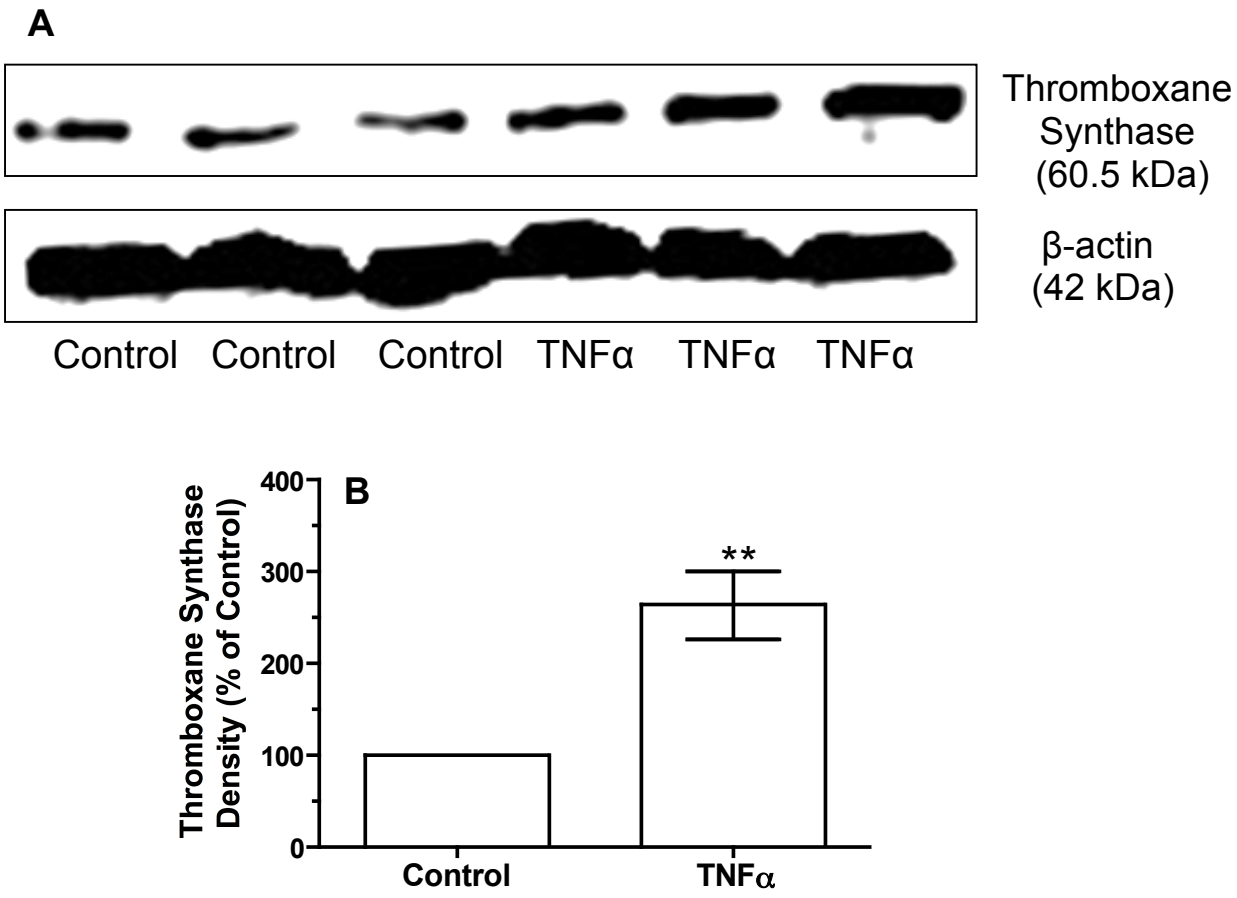

Figure 14: Thromboxane synthase expression in human vascular smooth muscle cells treated with TNFα. A) Representative Western blot for thromboxane synthase protein expression in cultured VSMCs. B) Density of thromboxane synthase plotted as percentage of control (n=6). Treatment with TNFα significantly increased thromboxane synthase protein expression as compared to control. Data are shown as means ± SEM,. **$p<0.01$

CHAPTER 5: PREECLAMPSIA IS ASSOCIATED WITH ALTERATIONS IN DNA METHYLATION OF GENES INVOLVED IN COLLAGEN METABOLISM

A. Abstract

Maternal vascular dysfunction is a hallmark of preeclampsia. A recently described vascular phenotype of preeclampsia involves increased expression of matrix metalloproteinase-1 (MMP-1) in endothelial cells, vascular smooth muscle, and infiltrating neutrophils. In contrast, the expression of tissue inhibitor of matrix metalloproteinase-1 (TIMP-1) and collagen type 1α 1 (COL1A1) is either reduced or not changed in the vessels, suggesting an imbalance in vessel collagen degradation and synthesis in preeclampsia. In the present study, we explored the possible contribution of DNA methylation to the altered expression of genes involved in collagen metabolism. We assayed the differences in DNA methylation in omental arteries from normal pregnant and preeclamptic women, and determined whether reduced DNA methylation increases the expression of the MMP-1 in cultured vascular smooth muscle cells and a neutrophil-like cell line, HL-60. Several *MMP* genes, including *MMP1* and *MMP8*, were significantly less methylated in preeclamptic omental arteries, whereas *TIMP* and *COL* genes were either significantly more methylated or had no significant change in their DNA methylation status as compared to normal pregnancy. Experimentally induced DNA hypomethylation increased MMP-1 expression in cultured vascular smooth muscle cells, and MMP-1 and MMP-8 expression in HL-60 cells. Our findings suggest that epigenetic regulation contributes to the imbalance in genes involved in collagen metabolism in blood vessels of preeclamptic women.

B. Introduction

Preeclampsia is a multisystemic disorder that is diagnosed by new onset of hypertension and proteinuria which occur after twenty weeks of gestation in pregnant women who are otherwise normal[1]. It is also associated with pathological edema due to increased vascular permeability. Preeclampsia and its complications are among the leading causes of obstetrical mortality and morbidity[1]. In the United States, preeclampsia occurs in approximately 6% to 8% of pregnant women, and is estimated to be responsible for 15% of obstetrical deaths[17]. Recently, neutrophil infiltration associated with marked inflammation of maternal systemic blood vessels was reported as a characteristic phenotype in women with preeclampsia[61-63]

We recently reported that MMP-1 expression is increased in systemic blood vessels of preeclamptic women as compared to normal pregnant women[159]. The increased expression of MMP-1 in omental arteries was detected in vascular smooth muscle cells (VSMCs), endothelial cells and infiltrating leukocytes. Plasma levels of MMP-1 were also increased in preeclamptic women. Interestingly, omental arteries collected from preeclamptic women showed no change in the expression of tissue inhibitor of matrix metalloproteinase-1 (TIMP-1), and decreased expression of collagen type 1α 1 (COL1A1), which is the main component of type-1 collagen. Collectively, these observations suggest an imbalance in vascular collagen metabolism that favors degradation in preeclampsia. In addition, MMP-1 was shown to be a regulator of arterial vessel tone, implicating this metalloproteinase in the pathogenesis of systemic hypertension associated with preeclampsia[159]**.**

The expression level of several *MMP* genes, including *MMP1, 2, 3, 7, 9 and 14*, is known to be regulated by DNA methylation[219]. DNA hypomethylation induced by 5-Aza-2-deoxycytidine (5-Aza) treatment resulted in a significant increase in MMP-1 expression in cultured amnion fibroblasts[164]. The increase in MMP-1 expression correlated with decreased DNA methylation at a particular location in the

MMP1 promoter 1538 base pairs upstream from the transcription start site. DNA methylation at the same site was significantly reduced in amnion tissues collected from pregnancies with preterm premature rupture of the fetal membranes[164].

This evidence for epigenetic regulation of *MMP1*, as well as other *MMP genes*, led us to hypothesize that reduced DNA methylation might contribute to the increased expression of MMPs in the systemic vasculature of preeclamptic women leading to the imbalance in genes involved in collagen metabolism[159]. In this study, we examined DNA methylation in the promoter regions of *MMP*, *TIMP* and *COL* genes in omental arteries obtained from normal pregnant and preeclamptic women. We also studied the effect of DNA hypomethylation on a) the expression of MMP-1, TIMP-1, and COL1A1 in primary cultures of human VSMCs, and b) the expression of MMP-1 and the neutrophil collagenase, MMP-8, in a neutrophil-like cell line[220].

C. Materials and methods

1. Study subjects

Omental and subcutaneous fat samples of approximately 2 cm x 2 cm x 0.5 cm in size were obtained at cesarean section from normal pregnant (n=18) and women clinically diagnosed with mild or severe preeclampsia (n=21) at MCV Hospital, Virginia Commonwealth University Medical Center, Richmond, VA. Mild preeclampsia was diagnosed when the blood pressure was more than 140 mm Hg systolic or 90 mm Hg diastolic and 0.3 g of urinary protein per 24 hours after 20 weeks of gestation. Severe preeclampsia was diagnosed when blood pressure was more than 160 mmHg systolic or 110 mm Hg diastolic with 5 g of protein in the urine within 24 hours after 20 weeks of gestation[1]. Omental fat was used because it contains arteries that are representative of systemic blood vessels and that contribute to total peripheral vascular resistance. Women with chorioamnionitis, infections, active sexually transmitted

diseases, lupus or diabetes, and women who were smokers or in labor were excluded because these conditions are associated with inflammatory changes. Patient clinical data are shown in Table 8. This study was approved by the Office of Research Subjects Protection, Virginia Commonwealth University, Richmond, Virginia. All subjects gave informed consent.

2. Sample processing and bisulfite sequencing

Omental arteries from 9 normal pregnant women and 9 preeclamptic women (5 mild, 4 severe) were dissected and cleaned of adhering fat. DNA was extracted from the arteries (~10 mg by weight) using QuickGene DNA tissue kit and QuickGene-Mini80 system (AutoGen, Holliston, MA). DNA was treated with RNase A (Qiagen, Valencia, CA). DNA (1 µg) was bisulfite treated using MethylEasy Exceed kit (Human Genetic Signatures, Randwick, Australia), and DNA sequencing was performed as previously described[164]. Briefly, 100 ng of bisulfite treated DNA was PCR amplified for two rounds using our previously published primers for the -1538 site in the *MMP1* promoter. PCR products were purified with QIAquick PCR Purification kit (Qiagen, Valencia, CA) and 1 µl of each product was cloned into pCR 2.1-TOPO vectors using the TOPO TA cloning kit (Invitrogen, Carlsbad, CA). After bacteria amplification, eight cloned PCR segments for each patient were sequenced in the Nucleic Acids Research Facilities at Virginia Commonwealth University. The -1538 site was selected because we previously demonstrated that its methylation correlates with the expression of MMP-1[164].

3. Illumina Infinium HumanMethylation27 BeadChip assay

Omental arteries from 5 normal pregnant and 7 severe preeclamptic women were processed for DNA extraction. DNA was bisulfite treated and used in the high throughput Illumina Infinium

HumanMethylation27 BeadChip assay (Illumina, San Diego, CA) for global DNA methylation analysis. The BeadChip was run by the Nucleic Acids Research Facilities at VCU using the protocol provided by Illumina. Data analysis was performed using the beadarray package in R programming environment[212]. Methylation values (β values) are expressed as range from 0 to 1 where 0 means not methylated and 1 means fully methylated. Differences in methylation between normal pregnant and preeclamptic women were indicated by Δβ-values.

4. Immunohistochemistry

Omental and subcutaneous fat samples from 6 normal pregnant and 6 preeclamptic women were cut into small pieces, fixed immediately in 10% neutral buffered formalin and embedded in paraffin. Tissues were cut into 8 μm sections which were stained for rabbit antihuman polyclonal antibody specific for MMP-8 (1:100 titer, Proteintech, Chicago, IL). Rabbit primary antibody isotype control (Invitrogen, Camarillo, CA) was used as a negative control. A kit was used for immunohistochemical staining (SuperPicTure Polymer Detection Kit Broad Spectrum (DAB), Invitrogen, Camarillo, CA). To quench endogenous tissue peroxidase activity, slides were incubated in 3% hydrogen peroxide in methanol for 30 min. For antigen retrieval, slides were heat treated in 10 mM citrate buffer for 5 min with a pressure cooker. Tissue slides were counterstained with 1:5 dilution of hematoxylin QS (Vector Laboratories, Burlingame, CA). Vessel staining for MMP-8 was evaluated using an intensity scale ranging from 0 to 4 where 0 was assigned for no staining, and 4 was dark and extensive staining. Scoring was verified by a second investigator and by measuring the optical density of staining (OD) using image analysis software (cellSens Imaging Software, Olympus America, Center Valley, PA) as previously described[61,62]. Optical density of staining for MMP-8 in vessels was normalized to the optical density of the background. Slides were also analyzed for vessels with diffuse staining and leukocyte staining for MMP-8. Images were captured with cellSens Imaging Software.

5. Human vascular smooth muscle cells (VSMCs)

Human VSMCs were cultured from chorionic plate arteries of placentas collected at cesarean section from healthy pregnant women at term deliveries as previously described[165]. Cells were cultured in T-25 flasks using Medium-199 (M-199, Gibco, Invitrogen, Carlsbad, CA) with 10% fetal bovine serum (Gibco, Invitrogen, Carlsbad, CA) and 1% antibiotics and antimycotics (100 U/ml penicillin, 100 µg/ml streptomycin, 25 µg/ml amphotericin B, Gibco, Invitrogen, Carlsbad, CA). Cells were treated with 10 µM of 5-Aza, a hypomethylating agent (Sigma-Aldrich, Saint-Louis, MO) for 48 hours. Treatments were refreshed daily. Cells were 50% confluent at the time of treatment and nearly 100% confluent at the time of harvesting. Conditioned media were collected and centrifuged to remove cell debris. Cells were rinsed in phosphate buffer saline and harvested for RNA or protein extraction.

6. HL-60 cells

HL-60 cells (ATCC, Manassas, VA), a neutrophil-like cell line, were cultured in Iscove's Modified Dulbecco's Medium (IMDM, ATCC, Manassas, VA) supplemented with 10% fetal bovine serum (Gibco, Invitrogen, Carlsbad, CA) and 1% antibiotics and antimycotics (100 U/ml penicillin, 100 µg/ml streptomycin, 25 µg/ml amphotericin B, Gibco, Invitrogen, Carlsbad, CA) as recommended by ATCC. Approximately 500,000 cells per ml were seeded in 5 ml of media in a T-25 flask for treatments. Cell treatments were: 1) 10 µM 5-Aza for 48 hours followed by 10^{-8} M of phorbol 12-myristate 13-acetate (PMA), a protein kinase C activator, (Sigma-Aldrich, Saint-Louis, MO) for 24 hours; 2) 10 µM 5-Aza for 48 hours followed by no treatment for 24 hours; 3) no treatment for 48 hours

followed by 10^{-8} M PMA for 24 hours or 4) no treatment for 72 hours to serve as control. Cells were collected for RNA and protein extraction.

7. Quantitative real time polymerase chain reaction (qRT-PCR)

RNA was extracted using QuickGene RNA cultured cell kit with QuickGene Mini-80 system (AutoGen, Holliston, MA). DNase treatment was performed using Turbo DNAse kit (Ambion, Austin, TX). RNA (1 μg) was reverse transcribed to cDNA using the iScript cDNA Synthesis Kit (Bio-Rad Laboratories, Hercules, CA). qRT-PCR reactions were performed with RT² SYBR® Green qPCR Mastermix (SABiosciences, Frederick, MD) as recommended by the user manual, and 8 ng of cDNA were used per reaction. Glyceraldehyde 3-phosphate dehydrogenase (*GAPDH*) was used as a housekeeping gene. Commercial primers were used for *MMP1* and *MMP8* genes (SABiosciences, Frederick, MD). Primers for *GAPDH*, *TIMP1* and *COL1A1* genes, shown in Table 9, were synthesized by Integrated DNA Technologies (IDT, Coralville, IA). Fold changes were calculated by the ΔΔCt method.

8. Western blotting

Cells were lysed in RIPA buffer containing 150 mM sodium chloride, 1.0% NP-40, 0.5% sodium deoxycholate, 0.1% sodium dodecyl sulphate, 50 mM Tris (pH 8.0) and 1X Halt protease inhibitor (Thermo Scientific, Pittsburgh, PA) using a tip sonicator (Active Motif, Carlsbad, CA). Protein concentrations were measured using BCA assay (Thermo Fisher Scientific, Rockford, IL). Denatured protein lysates (100 μg) were resolved by electrophoresis on 10% tris-glycine sodium dodecyl sulphate polyacrylamide gel and electrotransferred to polyvinylidene fluoride membrane (Immobilon-FL, Millipore, Billerica, MA). Primary antibodies used were goat anti-human MMP-1 (0.2 μg/ml, R&D

Systems, Minneapolis, MN); goat anti-human COL1A1 (1:1,000, Santa Cruz Biotechnology, Santa Cruz, CA); rabbit anti-human MMP-8 (1:250, Proteintech, Chicago, IL); rabbit anti-human β-actin (1:1,000, Sigma-Aldrich, Saint-Louis, MO); and mouse anti-human β-actin (1:1,000, Sigma-Aldrich, Saint-Louis, MO). Secondary antibodies used included Alexa Flour 680 donkey anti-rabbit (1:20,000, Invitrogen, Carlsbad, CA) for the detection of primary antibodies raised in rabbit for β-actin or MMP-8; IRDye800 donkey anti-goat (1:20,000, Rockland, Gilbertsville, PA) for the detection of primary antibodies raised in goat for MMP-1 or COL1A1; and IRDye800 goat anti-mouse (1:20,000, Rockland Immunochemicals, Gilbertsville, PA) for the detection of primary antibody raised in mouse for β-actin. LI-COR Odyssey Infrared Imaging System (Thermo Scientific, Pittsburgh, PA) was used to detect the immunoreactive proteins.

9. Enzyme linked immunosorbent assay (ELISA)

Commercial ELISA kits were used to quantify total MMP-1 (GE Healthcare, Piscataway, NJ) and TIMP-1 (GE Healthcare) in VSMC culture medium. For normalization, the total amount of MMP-1 or TIMP-1 protein in 5 ml (volume of medium used in a T-25 flask) was divided by the total amount of DNA (μg) extracted from the cells of the same flask.

10. Statistical analysis

Mann–Whitney U test was used to analyze the data from bisulfite sequencing. Student's t test was used to make comparisons of parameters between two groups and one-way ANOVA with Newman-Keuls test was used to make comparisons of parameters between more than two groups. Quantitative

results were presented as mean ± SEM. We considered a P value of < 0.05 statistically significant. A statistical software program was used for data analysis (GraphPad Prism version 4.0, San Diego, CA).

D. Results

Illumina BeadChip assay revealed a significant decrease in DNA methylation in the promoter regions of *MMP1* and *MMP8* genes in omental arteries from preeclamptic women as compared to normal pregnant women. However, there were no significant changes in DNA methylation in the promoter regions of *TIMP1* or *COL1A1* genes. Other *MMP*, *TIMP* and *COL* genes that were differentially methylated in preeclamptic arteries are shown in Table 10. All *MMP* genes, except two, were less methylated, whereas *TIMP* and *COL* genes were in general relatively more methylated. Bisulfite DNA sequencing revealed a significant decrease in methylation at the -1538 site in the promoter region of the *MMP1* gene in omental arteries from severe preeclamptic women as compared to normal pregnant women ($p < 0.01$, Figure 15). Methylation at the same site was not significantly different in arteries from women with mild preeclampsia as compared to arteries from normal pregnant women.

Immunohistochemical staining revealed increased expression of MMP-8 in omental and subcutaneous blood vessels of preeclamptic women as compared to normal pregnant women (Figure 16), similar to what we previously showed for MMP-1[159]. MMP-8 was mainly expressed in infiltrating leukocytes, although diffuse staining was also observed in the vessels. Scoring for MMP-8 staining intensity was significantly higher in preeclamptic women as compared to normal pregnant women (2.8 ± 0.1 vs 1.2 ± 0.2, respectively, $p < 0.001$, Figure 17A) as was the density of staining for MMP-8 (121.6 ± 5.2 vs 66.1 ± 7.0, respectively, $p < 0.001$, Figure 17B). Staining intensity scores and optical density of staining were highly correlated ($r = 0.99$). The percentage of vessels with neutrophils stained for MMP-8 was significantly higher in preeclamptic women as compared to normal pregnant women (87.8 ± 1.5% vs

54.0 ± 7.2%, respectively, $p < 0.001$, Figure 17C). The percentage of vessels with diffuse staining for MMP-8 was also significantly higher in preeclamptic women as compared to normal pregnant women (79.8 ± 5.7 vs 38.4 ± 6.1%, respectively, $p < 0.001$, Figure 17D).

To determine whether DNA methylation could be involved in the regulation of *MMP1* gene expression in VSMCs, 5-Aza was used to induce DNA hypomethylation in the cultured cells. Treatment with 5-Aza provoked a significant increase in *MMP1* gene expression as compared to control cells (5.0 ± 0.6-fold, $p < 0.001$, Figure 18A). To confirm that increased *MMP1* gene expression was associated with an increase in protein production, ELISA was used to quantify MMP-1 secretion into the media. Treatment with 5-Aza significantly increased the production of MMP-1 protein (3.4 ± 0.3 vs 1.2 ± 0.3 ng/μg DNA, $p < 0.01$, Figure 18B). In contrast to MMP-1, 5-Aza treatment caused no significant change in gene expression of *TIMP1* or *COL1A1* in cultured VSMCs (Figure19), and did not affect protein levels of TIMP-1 in the media (Figure 20A) or COL1A1 content in cells (Figure 20B).

The effect of reduced DNA methylation on the expression of MMP-1 was also examined in a neutrophil-like cell line, HL-60 cells. The expression of MMP-1 in untreated HL-60 cells was low, but treatment with 5-Aza resulted in a significant increase in *MMP1* gene expression as compared to controls (62.4 ± 6.8-fold, $p < 0.001$). PMA treatment also resulted in significant increase in *MMP1* gene expression (19.6 ± 3.2-fold, $p < 0.001$). Treatment with PMA caused activation of the cells as evidenced by cell adhesion to the culture flask surface. Combined treatment with 5-Aza and PMA resulted in a dramatic increase in *MMP1* gene expression as compared to controls (2622 ± 167-fold $p < 0.001$), PMA alone ($p < 0.001$) or 5-Aza alone ($p < 0.001$) (Figure 21). The gene expression profiles resulting from 5-Aza treatments were shown to correlate with protein expression as indicated by Western blotting (Figure 22A and B). Treatment with 5-Aza significantly increased MMP-1 protein expression (164 ± 6% average density measurement of Western blot as compared to control, $p < 0.001$). PMA alone caused no significant change in MMP-1 protein expression as compared to controls. However, combining 5-Aza

with PMA significantly increased MMP-1 protein expression (261 ± 6% of control, $p < 0.001$), PMA alone ($p < 0.001$) or 5-Aza alone ($p < 0.001$).

The role of DNA methylation in the expression of MMP-8 was also examined in the neutrophil-like cell line. Treatment with 5-Aza caused a significant increase in *MMP8* gene expression as compared to the control (3.2 ± 0.2-fold, $p < 0.001$). In contrast to *MMP1,* PMA treatment down-regulated *MMP8* gene expression, whereas combined treatment of PMA and 5-Aza partially restored *MMP8* gene expression (Figure 23). The changes in gene expression were associated with alterations in protein production as confirmed by Western blotting (Figure 24, B and C).

E. Discussion

In this study we explored the possible contributions of epigenetic regulation to the imbalance in expression of genes involved in collagen metabolism in omental arteries of preeclamptic women[159]. We found that the promoter regions of the *MMP1* and *MMP8* genes had significantly reduced methylation in preeclamptic omental arteries as compared to normal pregnant arteries, but there was no significant difference in the methylation status for *TIMP1* or *COL1A1*. In a global assessment of methylation status for these gene families, we found reduced methylation in several of the *MMP* genes, whereas increased methylation or no significant change was present for *TIMP* and *COL* genes.

In addition to global methylation assessment, we also examined a specific site (-1538) in *MMP1* promoter that we previously showed was hypomethylated in the amnion of pregnancies complicated by preterm premature rupture of membranes[164]. DNA sequencing of that site demonstrated that it was significantly less methylated in omental arteries of sever preeclamptic women, but not mild preeclamptic women, as compared to normal pregnant women. This may suggest a relationship between the severity of the preeclampsia and decreased DNA methylation. These studies demonstrate that in both

preterm premature rupture of membranes and preeclampsia reduced DNA methylation is associated with increased expression of MMP-1 in tissues specific to their pathology.

Similar to the increased expression of MMP-1 we previously reported[159], the expression of MMP-8 was also increased in omental and subcutaneous blood vessels of preeclamptic women as compared to normal pregnant women. MMP-8 was mainly expressed in neutrophils, but diffuse staining for MMP-8 was also present in the vessels, which may represent MMP-8 secreted by the neutrophils.

To study the role of DNA methylation in the regulation of these genes, we experimentally induced DNA hypomethylation in cultured human VSMCs. Hypomethylation resulted in a significant increase in MMP-1 expression, but did not significantly affect TIMP-1 or COL1A1. We also examined the effect of hypomethylation on MMP-1 and MMP-8 expression in a neutrophil-like cell line because neutrophils infiltrate maternal systemic blood vessels in preeclampsia and strongly express these MMPs. We found that DNA hypomethylation significantly increased MMP-1 and MMP-8 expression in HL-60 cells.

Stimulation of HL-60 cells with PMA, a classical inducer of leukocyte activation, resulted in a significant increase in MMP-1 but not MMP-8, suggesting that MMP-1 and MMP-8 are differentially regulated in these cells. This is supported by the fact that when DNA hypomethylation was combined with PMA, there was a dramatic increase in the expression of MMP-1 but not MMP-8. On the other hand, results from 5-Aza treatment suggest that decreased DNA methylation in neutrophils contributes to the increased expression of both MMP-1 and MMP-8 in maternal systemic blood vessels of preeclamptic women by increasing the capacity of infiltrating neutrophils to produce these MMPs. A global decrease in DNA methylation in leukocytes was reported in other diseases involving the cardiovascular system including atherosclerosis[134], ischemic heart disease and stroke[130]. Untreated HL-60 cells showed very low expression of MMP-1, which is similar to un-activated neutrophils. This suggests that MMP-1 expression

in un-activated cells is largely silenced by DNA methylation, and that reduced DNA methylation contributes to increase expression of MMP-1 in infiltrating neutrophils in preeclamptic women.

The increased expression of MMP-1[159] and MMP-8 in maternal blood vessels of preeclamptic women was associated with a decrease or no change in TIMP-1 or COL1A1[159]. This suggests an increase in collagenolytic activity in these vessels, which could contribute to the development of edema and proteinuria by compromising the integrity of the vessels and increasing their permeability to proteins. Increased expression of MMP-1 also contributes to neutrophil infiltration and vasoconstriction in preeclampsia[159]. In regard to neutrophil infiltration, supernatants taken from VSMC cultures treated with MMP-1 stimulated neutrophil migration *in vitro*. This was associated with increased VSMC secretion of interleukin-8 and collagen type I C terminal telopeptide fragment, which are known neutrophil chemoattractants. With regard to vasoconstriction, MMP-1 caused contraction of omental arteries in a dose dependent manner through the activation of protease-activated receptor-1, which is also overexpressed in omental arteries of preeclamptic women[159]. Therefore, increased MMP-1 levels in blood vessels and plasma of preeclamptic women may play an important, but heretofore unrecognized, role in regulating vascular tone.

Our study has several limitations in that our findings are correlative and do not prove a cause and effect relationship between reduced methylation and increased expression of MMP-1 and MMP-8. We also cannot prove that reduced methylation of the *MMP1* or *MMP8* gene promoters *per se* was responsible for increased expression, since methylation changes may have indirectly altered gene expression (e.g., resulting in increased expression of critical transcription factors). In addition, we were not able to determine the cell types where methylation changes were occurring in the omental arteries because of the cellular heterogeneity, which includes endothelial cells, VSMCs and infiltrated neutrophils. However, by experimentally inducing hypomethylation in VSMCs and a neutrophil-like cell line, we were able to document that reduced methylation is strongly associated with increased expression of MMPs in both cell types.

In summary, we have shown that the promoter regions of the *MMP1* and *MMP8* genes have reduced methylation in omental arteries of preeclamptic women as compared to those of normal pregnant women, whereas the promoter regions of *TIMP* and *COL* genes tend to be more methylated or unchanged. By experimentally inducing DNA hypomethylation in cultured human VSMCs and a neutrophil-like cell line, we were able to mimic the imbalance in collagen regulating genes present in systemic blood vessels of preeclamptic women. These findings suggest the possibility that epigenetic mechanisms directly involving the promoters of the target collagen metabolism genes, or possibly genes that regulate their expression (e.g., transcription factors), play an important role in the vascular dysfunction associated with preeclampsia.

Our study may have clinical implications for the treatment or prevention of preeclampsia based on restoring methylation. Folate is an essential component in the folate-methionine cycle that synthesizes methyl donors utilized by methyltransferases to methylate DNA. Therefore, dietary supplementation with folate might restore reduced methylation in MMP genes and protect against development of preeclampsia. Consistent with this notion is a recent large study comprised of almost 3,000 pregnant women, which found supplementation with multivitamins containing folic acid was associated with reduced risk of preeclampsia[206].

Table 8: Clinical Characteristics of Patient Groups.

Variable	Normal Pregnant (n=18)	Preeclamptic (n=21)
Maternal age (y)	26.1 ± 1.3	24.6 ± 1.0
Pre-pregnancy BMI (kg/m^2)	26.2 ± 1.2	30.7 ± 1.6*
Systolic blood pressure (mm Hg)	117.1 ± 2.3	166.8 ± 2.4***
Diastolic blood pressure (mm Hg)	70.18 ± 1.8	93.5 ± 2.6***
Proteinuria (mg/24 h)	ND	286.8 ± 21.6 (n=8)
Dipstick	ND	2.7 ± 0.3 (n=13)
Parity		
Primiparous	3	15
Multiparous	15	6
Gestational age (wk)	39.2 ± 0.2	35.4 ± 0.9***
Infant birth weight (g)	3503 ± 100	2452 ± 248***

Values are presented as mean ± SEM

*$p < 0.05$, *** $p < 0.001$ by t-test.

ND, not detectable.

Table 9: qRT-PCR primers used for gene expression.

Gene	Forward primer	Reverse primer
GAPDH	GATTCCACCCATGGCAAATT	AGATGGTGATGGGATTTCCATT
TIMP1	CTGTGGCTCCCTGGAACA	CCAACAGTGTAGGTCTTGGTGAAG
COL1A1	ACG AAG ACA TCC CAC CAA TCAC	CGTTGTCGCAGACGCAGA

Table 10: List of COL, MMP and TIMP genes that were significantly differentially methylated in preeclamptic omental arteries. NP = normal pregnant, PE = preeclamptic, β = methylation values. Δβ = difference in methylation. Minus values indicate less methylation and positive values more methylation in preeclamptic arteries as compared to normal pregnant arteries.

Symbol	Name	Gene ID	Mean β PE	Mean β NP	Δβ	p-value
COL8A1	collagen, type VIII, alpha 1	1295	0.078	0.054	0.024	0.02
COL9A3	collagen, type IX, alpha 3	1299	0.536	0.480	0.056	0.03
COL19A1	collagen, type XIX, alpha 1	1310	0.202	0.154	0.047	0.02
MMP1	matrix metalloproteinase 1	4312	0.736	0.816	-0.080	0.02
MMP8	matrix metalloproteinase 8	4317	0.807	0.882	-0.075	0.03
MMP12	matrix metalloproteinase 12	4321	0.683	0.740	-0.057	0.01
MMP13	matrix metalloproteinase 13	4322	0.745	0.830	-0.085	0.01
MMP16	matrix metalloproteinase 16	4325	0.025	0.014	0.011	0.02
MMP21	matrix metalloproteinase 21	118856	0.411	0.543	-0.132	0.02
MMP26	matrix metalloproteinase 26	56547	0.762	0.862	-0.100	0.02
MMP27	matrix metalloproteinase 27	64066	0.769	0.726	0.043	0.04
TIMP3	tissue inhibitor of metalloproteinases 3	7078	0.437	0.338	0.098	0.02

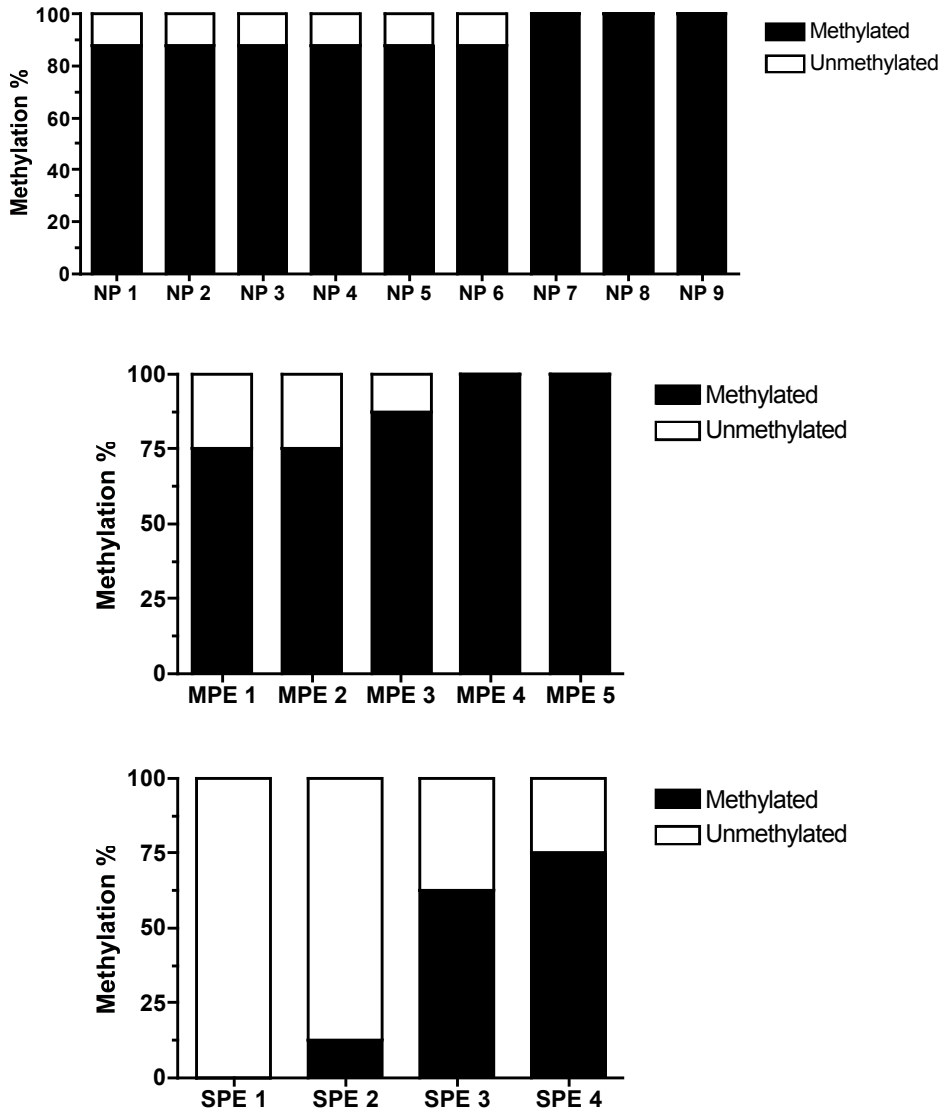

Figure 15: Bisulfite sequencing of the -1538 site in the MMP1 promoter region in omental arteries from normal pregnant (NP), mild preeclamptic (MPE) and severe preeclamptic (SPE) women. Methylation of the -1538 site was significantly reduced in omental arteries from SPE women ($p < 0.01$), but not significantly different in omental arteries form MPE women as compared to NP women.

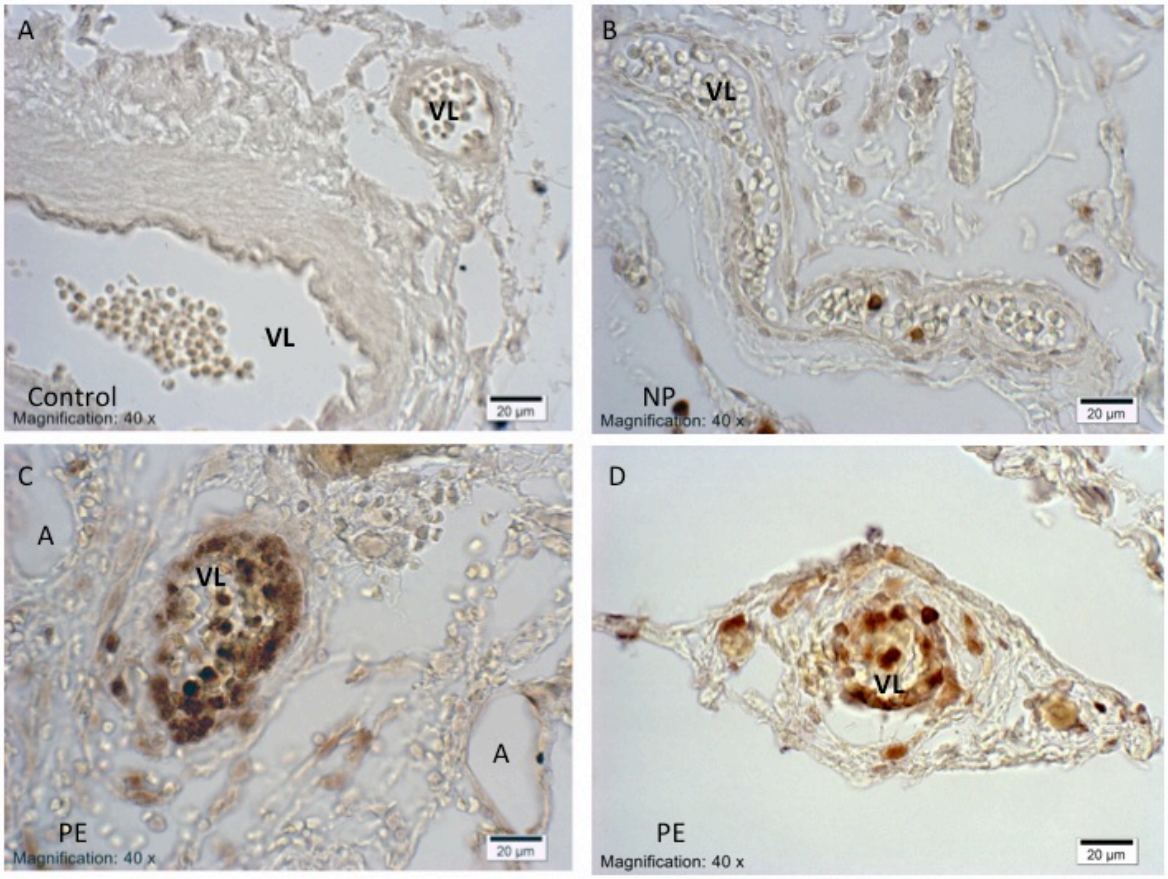

Figure 16: Representative sections of blood vessels in omental fat from normal pregnant and preeclamptic women immunostained for MMP-8. Results for subcutaneous fat were similar. A) There was no brown staining for MMP-8 in negative control sections. B) Blood vessels of normal pregnant women showed little or no staining for MMP-8. C, D) Vessels of preeclamptic women showed significant brown staining for MMP-8. Staining for MMP-8 in preeclamptic blood vessels was observed in neutrophils, which were in the lumen, adherent to the endothelium or infiltrated into the wall of the vessel. Diffused staining for MMP-8 was also present in the vessel wall. A: adipocyte; VL: vessel lumen. Magnification and scale bar are shown on each image.

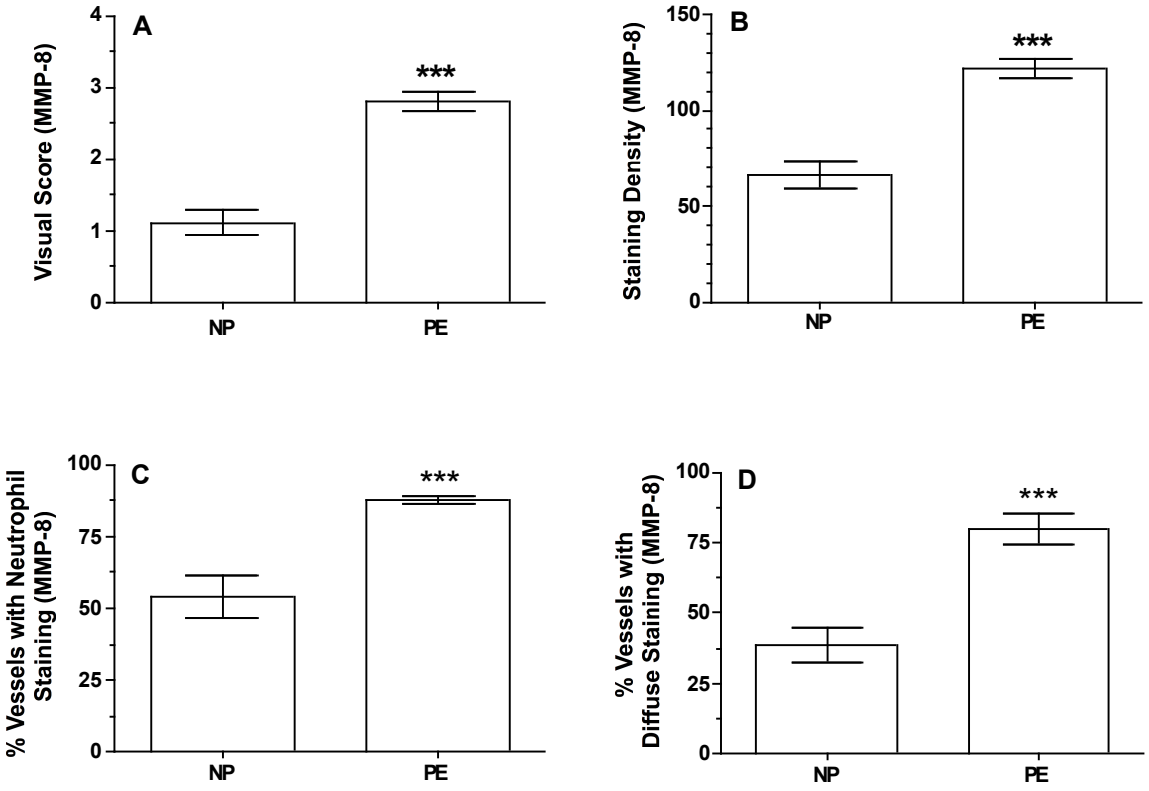

Figure 17: Quantitation of immunohistochemical staining for MMP-8 in omental and subcutaneous blood vessels from normal pregnant (NP) and preeclamptic (PE) women. A) Staining intensity score for MMP-8 was significantly higher in blood vessels of preeclamptic women as compared to normal pregnant women. B) Optical density of staining for MMP-8 was significantly higher in preeclamptic blood vessels. C, D) Preeclamptic women had significantly higher percentage of blood vessels with neutrophils stained for MMP-8 and diffuse staining for MMP-8 as compared to normal pregnant women (n=5). Data are presented as means ± SEM.***$p < 0.001$. These data was done by Juhi Shukla.

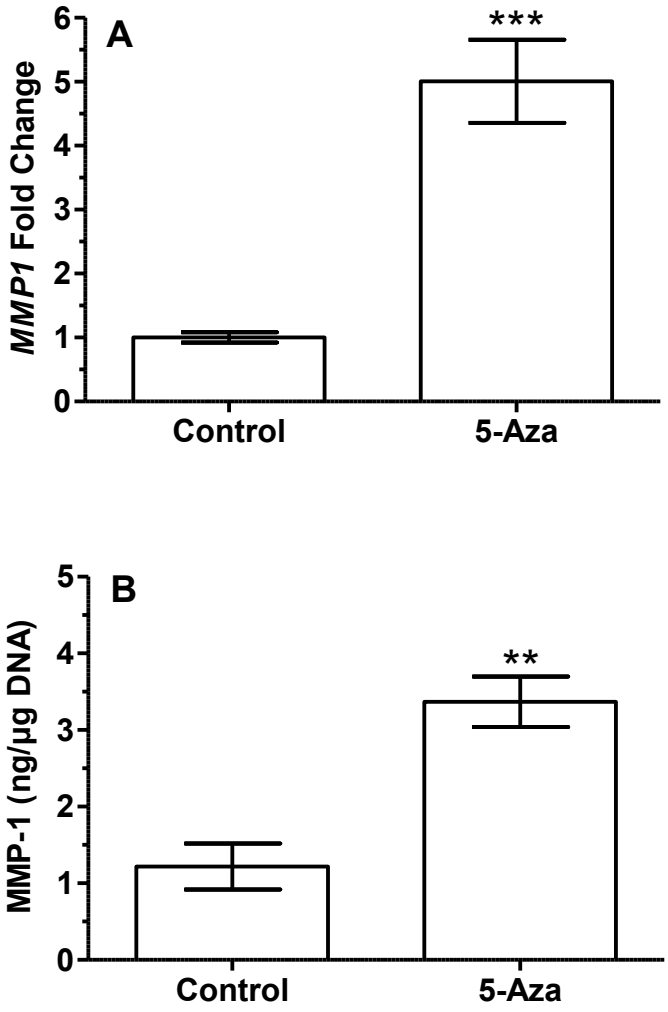

Figure 18: MMP-1 expression in cultured human vascular smooth muscle cells treated with 5-Aza. A) Fold change in gene expression for *MMP1* was significantly increased in treated cells as compared to controls ($p < 0.01$, n=8). B) Levels of MMP-1 protein in media was significantly increased in treated cells as compared to controls ($p < 0.05$, n=4). Data are shown as means ± SEM. **p<0.01, ***p<0.001.

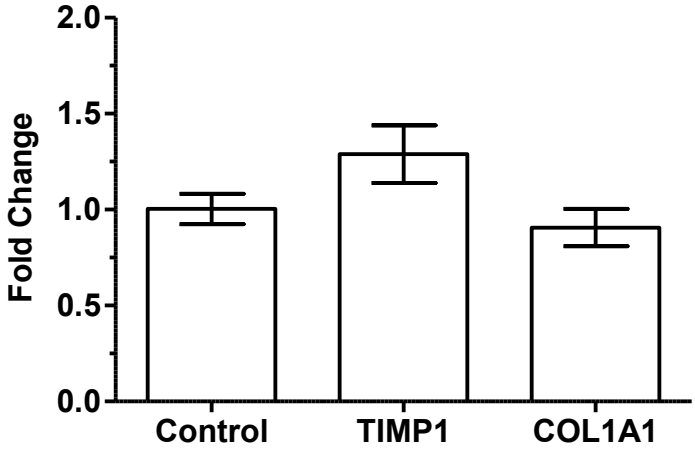

Figure 19: TIMP1 and COL1A1 gene expression in cultured human vascular smooth muscle cells treated with 5-Aza. Fold changes in the expression for *TIMP1* and *COL1A1* were not significantly changed by 5-Aza treatment as compared to control (n=8). Data are shown as means ± SEM.

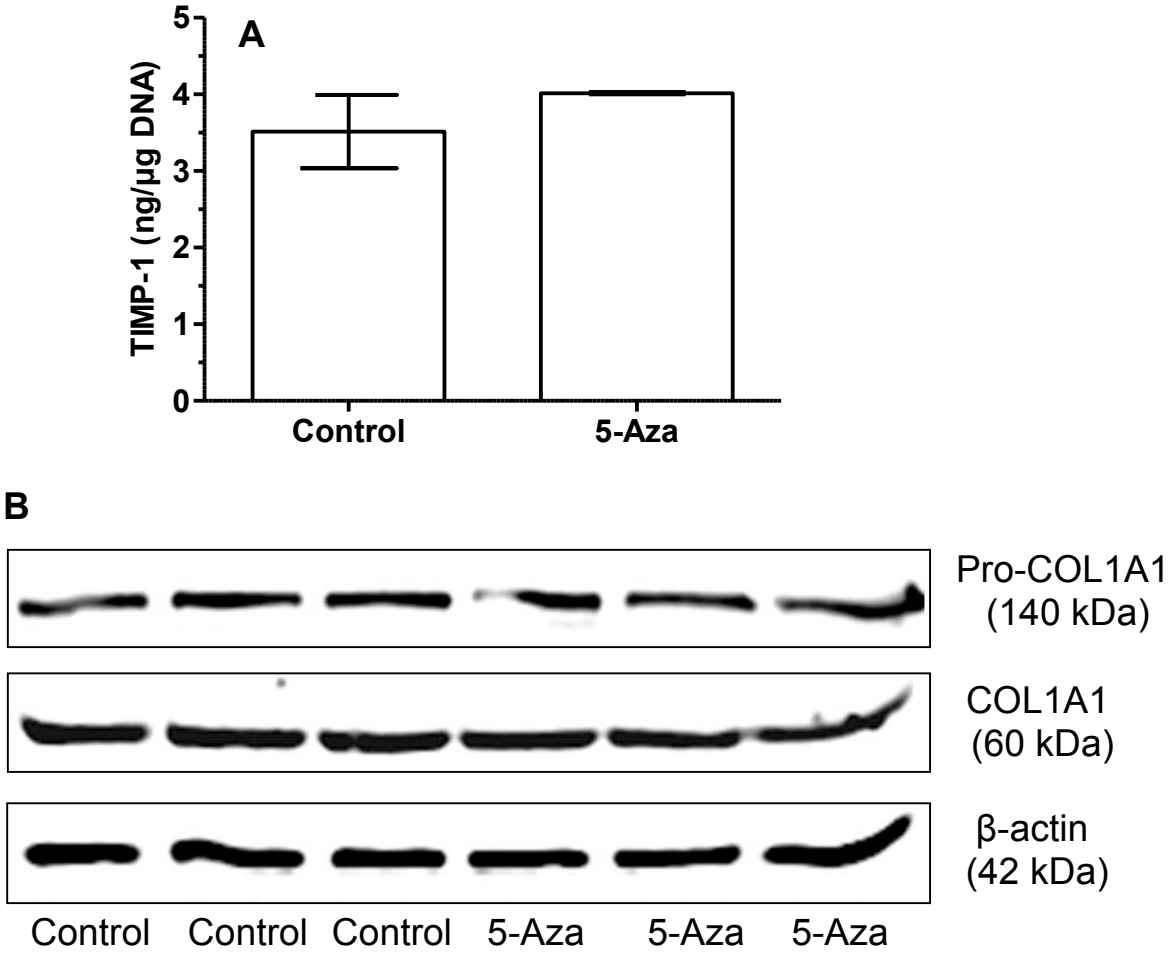

Figure 20: TIMP-1 and COL1A1 protein expression in cultured human vascular smooth muscle cells treated with 5-Aza. A) TIMP-1 protein levels in media was not significantly changed as compared to controls (n=4). B) Western blot for pro-COL1A1 and COL1A1 demonstrated no effect of 5-Aza treatment on the protein expression of COL1A1 (n=3). Data are shown as means ± SEM.

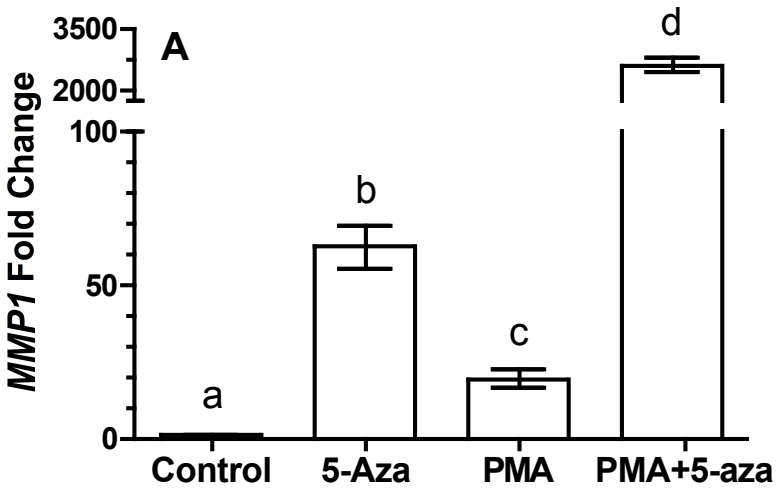

Figure 21: MMP1 gene expression in HL-60 cells. The expression of MMP1 gene was significantly increased in 5-Aza or PMA treated cells as compared to control cells. Treatment with PMA after 5-Aza caused a remarkable increase in *MMP1* gene expression as compared to control, PMA alone or 5-Aza alone (n=8). Data are shown as means ± SEM. Groups with a different letter are significantly different from each other, $p<0.001$.

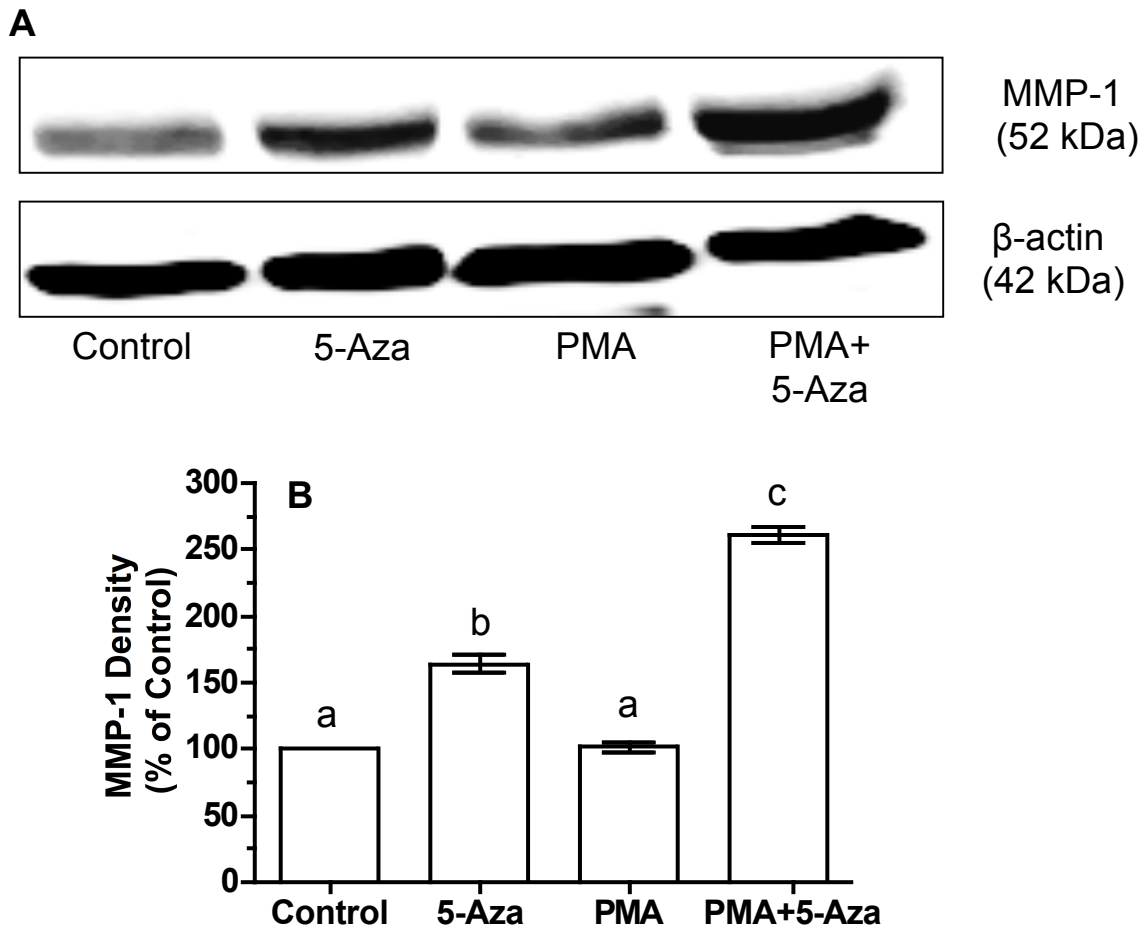

Figure 22: MMP-1 protein expression in HL-60 cells. A) Western blot and B) density measurements of the Western blot showing treatment with 5-Aza significantly increased the expression of MMP-1 protein in HL-60 cells as compared to control. Activation with PMA after treatment with 5-Aza resulted in a greater increase in MMP-1 expression as compared to control, 5-Aza alone or PMA alone (n=4). Data are shown as means ± SEM. Groups with a different letter are significantly different from each other, $p<0.001$.

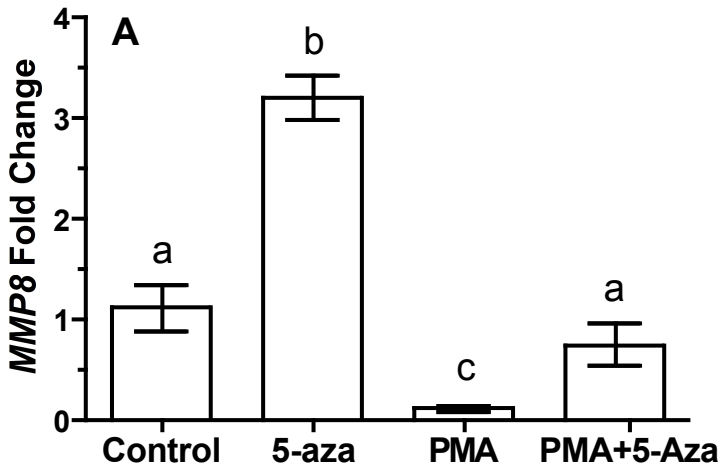

Figure 23: MMP8 gene expression in HL-60 cells. Gene expression of *MMP8* was significantly increased in 5-Aza treated cells as compared to control. PMA down-regulated *MMP8* expression, but 5-Aza partially restored it (n=8). Data are shown as means ± SEM. Groups with a different letter are significantly different from each other at a minimum p-value of < 0.05.

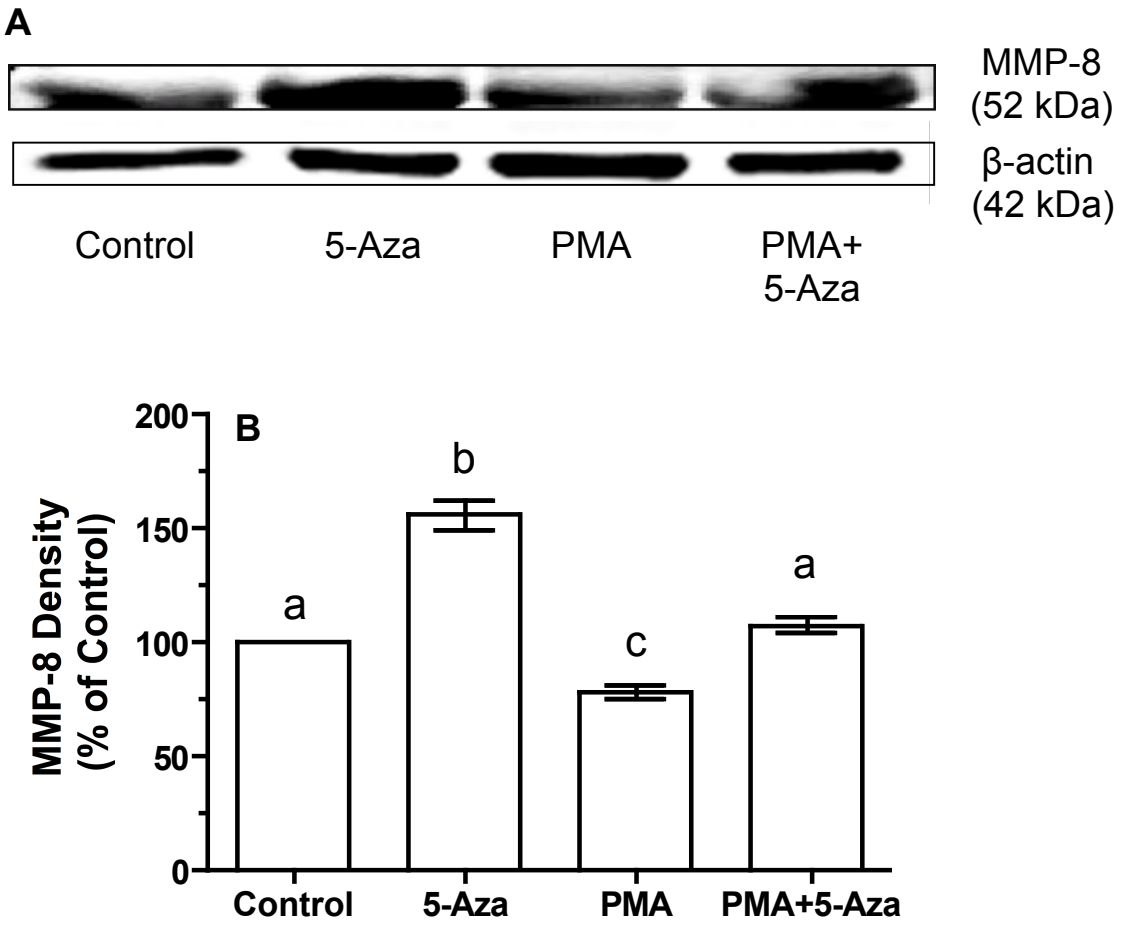

Figure 24: MMP-8 protein expression in HL-60 cells A) Western blot and B) density measurements of the Western blot showing 5-Aza significantly increased the expression of MMP-8. PMA down-regulated MMP-8 expression, but 5-Aza restored it (n=5). Data are shown as means ± SEM. Groups with a different letter are significantly different from each other at a minimum p-value of < 0.05

CHAPTER 6: PRELIMINARY STUDY OF THE EFFECT OF DNA HYPOMETHYLATION, NEUTROPHILS AND NEUTROPHIL PRODUCTS ON THE EXPRESSION OF TRANSCRIPTION FACTORS IN CULTURED VASCULAR SMOOTH MUSCLE CELLS

We showed above in this thesis that decreased DNA methylation increased the expression of MMP-1 in cultures of human VSMCs. Our lab previously showed that activated neutrophils and two of their products, namely TNFα and ROS, also increased the expression of MMP-1 in VSMCs[159]. Some of the effect of these treatments on the expression of MMP-1, as well as other genes, may be due to the upregulation or downregulation of transcription factors that regulate the expression of those genes. In this chapter, a preliminary study was done on the effect of 5-Aza, activated neutrophils, TNFα and ROS on the expression of transcription factors in cultured human VSMCs using human transcription factors PCR arrays (Qiagen, Valencia, CA).

Human VSMCs were cultured in T-25 flasks and treated at 50% confluence with 10 μM of 5-Aza, activated neutrophils (62,500 per T-25 flask), 1 ng/ml of TNFα or a ROS generating solution (0.05 mM of hypoxanthine and 0.003 U/ml xanthine oxidase) for 48 hours as was described in the Materials and Methods section above. Treatments were refreshed every day. Cells were harvested and RNA was extracted. RNA (1 μg) was reversed transcribed and used in the expression microarrays. Microarrays were run and data were analyzed as was recommended by the user manual.

Preliminary results are summarized in Tables 11, 12, 13 and 14. Results are for factors that were either upregulated or downregulated by a factor of 2 or more. No p-values are provided because of the small sample number (3 controls vs 3 experiments for each treatment)

Table 11: List of transcription factors that were upregulated by 5-Aza. None were downregulated.

Upregulated Genes	Fold Change
FOXA2	3.28
GATA3	3.20
NFATC2	2.96
ESR1	2.65
RELB	2.62
IRF1	2.22
PAX6	2.16
HOXA5	2.11
HAND1	2.01

Table 12: List of transcription factors that were upregulated or downregulated by TNFα.

Upregulated Genes	Fold Change
HSF1	16.10
MYC	6.79
HDAC1	4.27
ID1	3.47
HIF1A	2.99
ATF3	2.29
HAND2	2.25
RELB	2.22
NFKB1	2.08
Downregulated Genes	Fold Change
JUN	-2.12
FOS	-2.12
NFAT5	-2.14
MEF2A	-2.37
HAND1	-2.48
PPARG	-2.84
SMAD9	-3.08
EGR1	-3.21
MAX	-3.76
GATA2	-4.21
NFATC3	-5.10
NFATC1	-7.16
GATA1	-7.78
MEF2B	-7.80
NFATC2	-10.83
HNF4A	-11.40
GATA3	-13.03
MYOD1	-17.93
MYF5	-20.88
MEF2C	-30.22
MYB	-30.43

Table 13: List of transcription factors that were upregulated or downregulated by ROS.

Upregulated Genes	Fold Change
CEBPA	4.01
ATF3	3.09
TGIF1	2.32
NFATC2	2.20
CEBPB	2.10
MYB	2.08
STAT6	2.03
HOXA5	2.03
PAX6	2.01
Down-regulated Genes	Fold Change
SMAD9	-2.04
E2F1	-2.06
HNF4A	-2.16

Table 14: List of transcription factors that were downregulated by activated neutrophils. None were upregulated.

Downregulated Genes	Fold Change
ESR1	-2.04
EGR1	-2.12
SMAD9	-2.20
RB1	-2.33
CREB1	-2.49
FOS	-2.58
HNF4A	-4.59
SP3	-30.15
TGIF1	-66.21

CHAPTER 7: GENERAL DISCUSSION

Using a high throughput assay for DNA methylation, 3,736 genes with significantly differentially methylated CpG sites were identified in omental arteries of normal pregnant women and preeclamptic women. Most of these genes were hypomethylated in preeclamptic women as compared to normal pregnant women. Of these genes with significant differences in methylation, 1,685 genes had a FDR of < 10% with many of these genes hypomethylated and related to inflammation in preeclamptic women. A more stringent analysis revealed 65 significantly differentially methylated genes with a FDR of < 5% and difference in methylation ($\Delta\beta$) of > 0.10, all of which were hypomethylated in preeclamptic women.

It is interesting that inflammatory genes were primarily targeted by reduced methylation in preeclampsia. The mechanisms responsible for such selective changes in methylation are not known. It is known that DNA methylation is tissue specific, so tissue specific control mechanisms must be operative.

Pertinent with the systemic vascular inflammation and dysfunction associated with preeclampsia[62], multiple canonical pathways related to inflammation and immune response were associated with the methylation changes in preeclampsia. In addition, multiple gene-to-gene interaction networks, which had inflammatory response, inflammatory disease and cardiovascular disease among their top associated biological functions were identified by the ingenuity pathway analysis (IPA) of genes with significant differences in methylation in preeclamptic women.

Preeclampsia is associated with increased vascular resistance, increased arterial pressure[202], reduced uteroplacental blood flow[203], hypercoagulopathy[204], inflammation[109], oxidative stress[183] and altered carbohydrate and amino acid metabolism[152]. Mapping significantly differentially methylated genes for gene ontology terms identified several molecular functions and biological processes, which were over-represented in preeclampsia and pertinent to its pathophysiology including smooth muscle contraction, thrombosis, inflammation, redox homeostasis, sugar metabolism and amino acid metabolism.

Preeclampsia is also associated with an imbalance of increased thromboxane and decreased prostacyclin, which was first described in placenta[95] and later confirmed for maternal blood[96] and maternal urine[97]. Since thromboxane is a potent vasoconstrictor and platelet activator, whereas prostacyclin is a potent vasodilator and inhibitor of platelet activation[27], this imbalance helps explain hypertension, reduced uteroplacental blood flow and hypercoagulopathy reported in women with preeclampsia. The thromboxane synthase gene (*TBXAS1*), which encodes the enzyme that catalyzes the conversion of prostaglandin H_2 into thromboxane[94], was the most hypomethylated gene in preeclamptic women.

Decreased DNA methylation in the promoter region of the *TBXAS1* gene was associated with a significant increase in its expression in omental fat arteries of preeclamptic women as compared to normal pregnant women. Increased expression of thromboxane synthase was observed in the endothelium, in the VSMCs and in leukocytes, which were flattened and adhered to the endothelium and infiltrated into the wall of the vessel. Increased expression of thromboxane synthase would lead to increased production of thromboxane locally in the vessel, which could explain hypertension and coagulation abnormalities in preeclamptic patients because thromboxane is a potent vasoconstrictor and platelet activator[84].

MMP1 and *MMP8* were genes that also had significantly reduced methylation in omental arteries of preeclamptic women. Similar to thromboxane synthase, their gene and protein expression was significantly increased in preeclamptic omental arteries. The *TBXAS1* gene was the most significantly hypomethylated gene in preeclamptic women with a $\Delta\beta$ of - 0.24 as compared to the $\Delta\beta$ for *MMP1* of – 0.080 and *MMP8* of – 0.075. A more significant difference in methylation, however, does not necessarily mean it is more important. Increases in gene and protein expression were just as marked for MMP-1 and MMP-8 as for thromboxane synthase.

Leukocyte infiltration requires leukocyte activation, which most likely occurs as they circulate through the intervillous space and are exposed to increased lipid peroxides secreted by the placenta[41]. The infiltrating leukocytes are most likely neutrophils because neutrophils normally comprise approximately 60%-70% of all leukocytes[33] , their numbers increase 2.5-fold by 30 weeks of gestation[214] and their numbers are further increased in preeclampsia[215]. In addition, we previously reported that neutrophils, but not lymphocytes or monocytes, infiltrate systemic blood vessels of preeclamptic women[61,62,156,216].

To study the role of DNA methylation in the regulation of thromboxane synthase, we experimentally induced DNA hypomethylation in a neutrophil-like cell line and in cultured human VSMCs. Hypomethylation resulted in increased expression of thromboxane synthase in both cell types, however, the increase was only significant in the neutrophil-like cell line. Increased expression of thromboxane synthase in the neutrophil-like cell line was associated with a parallel increase in the production of TXB_2, the stable metabolite of thromboxane A_2[211]. These data suggest that DNA methylation is important in regulating thromboxane synthase expression in neutrophils but not in VSMCs. In contrast, experimentally induced hypomethylation increased gene and protein expression for MMP-1 and MMP-8 in both VSMCs and the neutrophil cell line. However, treatment of VSMCs with TNFα, a neutrophil product, did significantly increase thromboxane synthase, so increased expression of thromboxane synthase in vascular tissue of preeclamptic women may be due to inflammation caused by neutrophil infiltration. DNA hypomethylation in leukocytes has been reported in other diseases involving the cardiovascular system such as atherosclerosis[134], ischemic heart disease and stroke[26].

Pertinent to our findings of increased expression of thromboxane synthase are previous findings of increased levels of serum arachidonic acid in preeclamptic women[217] and significant activation of NF-κB and increased expression of COX-2 in preeclamptic blood vessels[62]. Similar to thromboxane synthase expression, activation of NF-κB and increased expression of COX-2 were observed in the endothelium, vascular smooth muscle and infiltrating neutrophils[62]. A possible scenario in preeclamptic blood vessels is

that increased COX-2 converts increased arachidonic acid into prostaglandin H_2 and increased thromboxane synthase then converts prostaglandin H_2 into thromboxane.

Preeclampsia is associated with oxidative stress[41] and increased plasma levels of linoleic acid, the fatty acid precursor of arachidonic acid[218]. Neutrophils from normal pregnant women exposed to an oxidizing solution enriched with linoleic acid showed increased production of TNFα and thromboxane[86]. Also, exposure of cultured VSMCs to an oxidizing solution enriched with linoleic acid increased production of thromboxane[85].

Preexisting maternal genetic variation in key genes may also have an impact on DNA methylation. For example, allelic variation in the methylenetetrahydrofolate reductase gene have been associated with preeclampsia[221], and methylenetetrahydrofolate reductase is an important enzyme regulating the synthesis of S-adenosyl methionine that modulates the availability of methyl groups for DNA methylation[209].

The changes in methylation observed may have been preexisting or the result of preeclampsia. If they were preexisting they could have contributed to an increased risk of preeclampsia. The changes could also be the result of the oxidative stress of preeclampsia because oxidative stress and DNA oxidation can result in a loss of DNA methylation. Once the DNA methylation pattern is altered, it is maintained by DNA methyltransferase 1 during future cell divisions, so alterations in DNA methylation occurring as a result of preeclampsia may be maintained and contribute to the increased risk of cardiovascular disease later-in-life experienced by women who have had preeclampsia. Additional alterations in the DNA methylation patterns may also occur after preeclampsia because many factors affect it, such as age, diet, environmental toxins and oxidative stress.

In summary, we found that hypomethylation in the promoter regions of *TBXAS1, MMP1 and MMP8* are correlated with their increased gene and protein expression in systemic blood vessels of preeclamptic women. Increased expression was present in endothelium, VSMCs and infiltrating

neutrophils. We also showed that DNA hypomethylation increases the expression of thromboxane synthase in a neutrophil-like cell line and TNFα, a neutrophil product, increases thromboxane synthase expression in cultured VSMCs. DNA hypomethylation increased MMP-1 expression in both VSMCs and neutrophil-like cells and increased MMP-8 in the neutrophil-like cells. In contrast, experimentally induced hypomethylation did not affect the expression of *COL1A1* or *TIMP1* genes. These data suggest that hypomethylation is responsible for increased expression of thromboxane synthase, MMP-1 and MMP-8 in systemic blood vessels in women with preeclampsia. Increased expression of thromboxane synthase, MMP-1 and MMP-8 in the vasculature of preeclamptic women may help explain hypertension, edema, proteinuria, and coagulation abnormalities.

REFERENCES

1. Cunningham FG, Leveno KJ, Bloom SL, Gilstrap III LC, Hauth JC, Wenstrom KD. *Williams Obstetrics*. 22nd ed. New York: McGraw-Hill; 2005.

2. Pridjian G, Puschett JB. Preeclampsia. Part 1: clinical and pathophysiologic considerations. *Obstet Gynecol Surv.* 2002;57:598-618.

3. Easterling TR. The maternal hemodynamics of preeclampsia. *Clin Obstet Gynecol.* 1992;35:375-386.

4. Gant NF, Daley GL, Chand S, Whalley PJ, MacDonald PC. A study of angiotensin II pressor response throughout primigravid pregnancy. *J Clin Invest.* 1973;52:2682-2689.

5. Khan F, Belch JJ, MacLeod M, Mires G. Changes in endothelial function precede the clinical disease in women in whom preeclampsia develops. *Hypertension.* 2005;46:1123-1128.

6. Hay JE. Liver disease in pregnancy. *Hepatology.* 2008;47:1067-1076.

7. Redman CW, Bonnar J, Beilin L. Early platelet consumption in pre-eclampsia. *Br Med J.* 1978;1:467-469.

8. Kobayashi T, Terao T. Preeclampsia as chronic disseminated intravascular coagulation. Study of two parameters: thrombin-antithrombin III complex and D-dimers. *Gynecol Obstet Invest.* 1987;24:170-178.

9. Norwitz ER, Hsu CD, Repke JT. Acute complications of preeclampsia. *Clin Obstet Gynecol.* 2002;45:308-329.

10. Redman CW, Sargent IL. Latest advances in understanding preeclampsia. *Science.* 2005;308:1592-1594.

11. Smith LG, Jr., Moise KJ, Jr., Dildy GA, 3rd, Carpenter RJ, Jr. Spontaneous rupture of liver during pregnancy: current therapy. *Obstet Gynecol.* 1991;77:171-175.

12. Sibai BM, Mabie BC, Harvey CJ, Gonzalez AR. Pulmonary edema in severe preeclampsia-eclampsia: analysis of thirty-seven consecutive cases. *Am J Obstet Gynecol.* 1987;156:1174-1179.

13. Marti-Carvajal AJ, Comunian-Carrasco G, Pena-Marti GE. Haematological interventions for treating disseminated intravascular coagulation during pregnancy and postpartum. *Cochrane Database Syst Rev.* 2011:CD008577.

14. Vidaeff AC, Carroll MA, Ramin SM. Acute hypertensive emergencies in pregnancy. *Crit Care Med.* 2005;33:S307-312.

15. MacKay AP, Berg CJ, Atrash HK. Pregnancy-related mortality from preeclampsia and eclampsia. *Obstet Gynecol.* 2001;97:533-538.

16. Waterstone M, Bewley S, Wolfe C. Incidence and predictors of severe obstetric morbidity: case-control study. *BMJ.* 2001;322:1089-1093; discussion 1093-1084.

17. Report of the National High Blood Pressure Education Program Working Group on High Blood Pressure in Pregnancy. *Am J Obstet Gynecol.* 2000;183:S1-S22.

18. Khedun SM, Moodley J, Naicker T, Maharaj B. Drug management of hypertensive disorders of pregnancy. *Pharmacol Ther.* 1997;74:221-258.

19. Saftlas AF, Olson DR, Franks AL, Atrash HK, Pokras R. Epidemiology of preeclampsia and eclampsia in the United States, 1979-1986. *Am J Obstet Gynecol.* 1990;163:460-465.

20. Rochat RW, Koonin LM, Atrash HK, Jewett JF. Maternal mortality in the United States: report from the Maternal Mortality Collaborative. *Obstet Gynecol.* 1988;72:91-97.

21. Duley L. Maternal mortality associated with hypertensive disorders of pregnancy in Africa, Asia, Latin America and the Caribbean. *Br J Obstet Gynaecol.* 1992;99:547-553.

22. Knight M. Eclampsia in the United Kingdom 2005. *BJOG.* 2007;114:1072-1078.

23. Geographic variation in the incidence of hypertension in pregnancy. World Health Organization International Collaborative Study of Hypertensive Disorders of Pregnancy. *Am J Obstet Gynecol.* 1988;158:80-83.

24. Norwitz ER, Robinson JN, Repke JT. Prevention of preeclampsia: is it possible? *Clin Obstet Gynecol.* 1999;42:436-454.

25. Askie LM, Duley L, Henderson-Smart DJ, Stewart LA. Antiplatelet agents for prevention of pre-eclampsia: a meta-analysis of individual patient data. *Lancet.* 2007;369:1791-1798.

26. Bujold E, Roberge S, Lacasse Y, Bureau M, Audibert F, Marcoux S, Forest JC, Giguere Y. Prevention of preeclampsia and intrauterine growth restriction with aspirin started in early pregnancy: a meta-analysis. *Obstet Gynecol.* 2010;116:402-414.

27. Walsh SW. Eicosanoids in preeclampsia. *Prostaglandins Leukot Essent Fatty Acids.* 2004;70:223-232.

28. Vadillo-Ortega F, Perichart-Perera O, Espino S, Avila-Vergara MA, Ibarra I, Ahued R, Godines M, Parry S, Macones G, Strauss JF. Effect of supplementation during pregnancy with L-arginine and antioxidant vitamins in medical food on pre-eclampsia in high risk population: randomised controlled trial. *BMJ.* 2011;342:d2901.

29. Redman CW. Current topic: pre-eclampsia and the placenta. *Placenta.* 1991;12:301-308.

30. Shembrey MA, Noble AD. An instructive case of abdominal pregnancy. *Aust N Z J Obstet Gynaecol.* 1995;35:220-221.

31. Brosens IA, Robertson WB, Dixon HG. The role of the spiral arteries in the pathogenesis of preeclampsia. *Obstet Gynecol Annu.* 1972;1:177-191.

32. Edwards SW. *Biochemistry and Physiology of the Neutrophil*. Melbourne: Cambridge University Press; 1994.

33. Witko-Sarsat V, Rieu P, Descamps-Latscha B, Lesavre P, Halbwachs-Mecarelli L. Neutrophils: molecules, functions and pathophysiological aspects. *Lab Invest.* 2000;80:617-653.

34. Greer IA, Haddad NG, Dawes J, Johnstone FD, Calder AA. Neutrophil activation in pregnancy-induced hypertension. *Br J Obstet Gynaecol.* 1989;96:978-982.

35. von Dadelszen P, Wilkins T, Redman CW. Maternal peripheral blood leukocytes in normal and pre-eclamptic pregnancies. *Br J Obstet Gynaecol.* 1999;106:576-581.

36. Prieto JA, Panyutich AV, Heine RP. Neutrophil activation in preeclampsia. Are defensins and lactoferrin elevated in preeclamptic patients? *J Reprod Med.* 1997;42:29-32.

37. Barden A, Graham D, Beilin LJ, Ritchie J, Baker R, Walters BN, Michael CA. Neutrophil CD11B expression and neutrophil activation in pre-eclampsia. *Clin Sci (Lond).* 1997;92:37-44.

38. Sacks GP, Studena K, Sargent K, Redman CW. Normal pregnancy and preeclampsia both produce inflammatory changes in peripheral blood leukocytes akin to those of sepsis. *Am J Obstet Gynecol.* 1998;179:80-86.

39. Greer IA, Dawes J, Johnston TA, Calder AA. Neutrophil activation is confined to the maternal circulation in pregnancy-induced hypertension. *Obstet Gynecol.* 1991;78:28-32.

40. Lampe R, Szucs S, Ormos M, Adany R, Poka R. Effect of normal and preeclamptic plasma on superoxide-anion production of neutrophils from healthy non-pregnant women. *J Reprod Immunol.* 2008;79:63-69.

41. Walsh SW. Maternal-placental interactions of oxidative stress and antioxidants in preeclampsia. *Semin Reprod Endocrinol.* 1998;16:93-104.

42. Aly AS, Khandelwal M, Zhao J, Mehmet AH, Sammel MD, Parry S. Neutrophils are stimulated by syncytiotrophoblast microvillous membranes to generate superoxide radicals in women with preeclampsia. *Am J Obstet Gynecol.* 2004;190:252-258.

43. Johansen M, Redman CW, Wilkins T, Sargent IL. Trophoblast deportation in human pregnancy--its relevance for pre-eclampsia. *Placenta.* 1999;20:531-539.

44. Sattar N, Greer IA, Louden J, Lindsay G, McConnell M, Shepherd J, Packard CJ. Lipoprotein subfraction changes in normal pregnancy: threshold effect of plasma triglyceride on appearance of small, dense low density lipoprotein. *J Clin Endocrinol Metab.* 1997;82:2483-2491.

45. Qiu C, Phung TT, Vadachkoria S, Muy-Rivera M, Sanchez SE, Williams MA. Oxidized low-density lipoprotein (Oxidized LDL) and the risk of preeclampsia. *Physiol Res.* 2006;55:491-500.

46. Lehr HA, Krombach F, Munzing S, Bodlaj R, Glaubitt SI, Seiffge D, Hubner C, von Andrian UH, Messmer K. In vitro effects of oxidized low density lipoprotein on CD11b/CD18 and L-selectin presentation on neutrophils and monocytes with relevance for the in vivo situation. *Am J Pathol.* 1995;146:218-227.

47. Bassingthwaighte JB, Wang CY, Chan IS. Blood-tissue exchange via transport and transformation by capillary endothelial cells. *Circ Res.* 1989;65:997-1020.

48. Feliciano A, do Rosario HS, Goulao I, Borges MG, Silva M, Rego P, Silverio S, Pedro V. Vasoactive endothelial factors. *Rev Port Cardiol.* 1993;12:557-560, 510-551.

49. Wu KK, Thiagarajan P. Role of endothelium in thrombosis and hemostasis. *Annu Rev Med.* 1996;47:315-331.

50. Trepels T, Zeiher AM, Fichtlscherer S. The endothelium and inflammation. *Endothelium.* 2006;13:423-429.

51. Endemann DH, Schiffrin EL. Endothelial dysfunction. *J Am Soc Nephrol.* 2004;15:1983-1992.

52. Roberts JM, Taylor RN, Musci TJ, Rodgers GM, Hubel CA, McLaughlin MK. Preeclampsia: an endothelial cell disorder. *Am J Obstet Gynecol.* 1989;161:1200-1204.

53. Roberts JM, Redman CW. Pre-eclampsia: more than pregnancy-induced hypertension. *Lancet.* 1993;341:1447-1451.

54. Redman CW, Denson KW, Beilin LJ, Bolton FG, Stirrat GM. Factor-VIII consumption in pre-eclampsia. *Lancet.* 1977;2:1249-1252.

55. Taylor RN, de Groot CJ, Cho YK, Lim KH. Circulating factors as markers and mediators of endothelial cell dysfunction in preeclampsia. *Semin Reprod Endocrinol.* 1998;16:17-31.

56. de Groot CJ, Murai JT, Vigne JL, Taylor RN. Eicosanoid secretion by human endothelial cells exposed to normal pregnancy and preeclampsia plasma in vitro. *Prostaglandins Leukot Essent Fatty Acids.* 1998;58:91-97.

57. Remuzzi G, Marchesi D, Zoja C, Muratore D, Mecca G, Misiani R, Rossi E, Barbato M, Capetta P, Donati MB, de Gaetano G. Reduced umbilical and placental vascular prostacyclin in severe pre-eclampsia. *Prostaglandins.* 1980;20:105-110.

58. Fitzgerald DJ, Entman SS, Mulloy K, FitzGerald GA. Decreased prostacyclin biosynthesis preceding the clinical manifestation of pregnancy-induced hypertension. *Circulation.* 1987;75:956-963.

59. Davidge ST, Stranko CP, Roberts JM. Urine but not plasma nitric oxide metabolites are decreased in women with preeclampsia. *Am J Obstet Gynecol.* 1996;174:1008-1013.

60. Karumanchi SA, Maynard SE, Stillman IE, Epstein FH, Sukhatme VP. Preeclampsia: a renal perspective. *Kidney Int.* 2005;67:2101-2113.

61. Leik CE, Walsh SW. Neutrophils infiltrate resistance-sized vessels of subcutaneous fat in women with preeclampsia. *Hypertension.* 2004;44:72-77.

62. Shah TJ, Walsh SW. Activation of NF-kappaB and expression of COX-2 in association with neutrophil infiltration in systemic vascular tissue of women with preeclampsia. *Am J Obstet Gynecol.* 2007;196:48 e1-8.

63. Mishra N, Nugent WH, Mahavadi S, Walsh SW. Mechanisms of enhanced vascular reactivity in preeclampsia. *Hypertension.* 2011;58:867-873.

64. Walsh SW. Lipid peroxidation in pregnancy. *Hypertens Pregnancy.* 1994;13:1–32.

65. Wang YP, Walsh SW, Guo JD, Zhang JY. Maternal levels of prostacyclin, thromboxane, vitamin E, and lipid peroxides throughout normal pregnancy. *Am J Obstet Gynecol.* 1991;165:1690-1694.

66. Bilodeau JF, Hubel CA. Current concepts in the use of antioxidants for the treatment of preeclampsia. *J Obstet Gynaecol Can.* 2003;25:742-750.

67. Babior BM, Kipnes RS, Curnutte JT. Biological defense mechanisms. The production by leukocytes of superoxide, a potential bactericidal agent. *J Clin Invest.* 1973;52:741-744.

68. Tsukimori K, Maeda H, Ishida K, Nagata H, Koyanagi T, Nakano H. The superoxide generation of neutrophils in normal and preeclamptic pregnancies. *Obstet Gynecol.* 1993;81:536-540.

69. Beckman JS, Koppenol WH. Nitric oxide, superoxide, and peroxynitrite: the good, the bad, and ugly. *Am J Physiol.* 1996;271:C1424-1437.

70. Myatt L, Rosenfield RB, Eis AL, Brockman DE, Greer I, Lyall F. Nitrotyrosine residues in placenta. Evidence of peroxynitrite formation and action. *Hypertension.* 1996;28:488-493.

71. Roggensack AM, Zhang Y, Davidge ST. Evidence for peroxynitrite formation in the vasculature of women with preeclampsia. *Hypertension.* 1999;33:83-89.

72. Beckman JS TJ. Reaction rates and diffusion in the toxicity of peroxynitrite. *Biochemistry.* 1994;16:8-10.

73. Pacher P, Beckman JS, Liaudet L. Nitric oxide and peroxynitrite in health and disease. *Physiol Rev.* 2007;87:315-424.

74. Cannon RO, 3rd. Role of nitric oxide in cardiovascular disease: focus on the endothelium. *Clin Chem.* 1998;44:1809-1819.

75. McCarthy AL, Woolfson RG, Raju SK, Poston L. Abnormal endothelial cell function of resistance arteries from women with preeclampsia. *Am J Obstet Gynecol.* 1993;168:1323-1330.

76. Davidge ST. Oxidative stress and altered endothelial cell function in preeclampsia. *Semin Reprod Endocrinol.* 1998;16:65-73.

77. Walsh SW, Wang Y. Secretion of lipid peroxides by the human placenta. *Am J Obstet Gynecol.* 1993;169:1462-1466.

78. Warso MA, Lands WE. Lipid peroxidation in relation to prostacyclin and thromboxane physiology and pathophysiology. *Br Med Bull.* 1983;39:277-280.

79. Wang YP, Walsh SW, Guo JD, Zhang JY. The imbalance between thromboxane and prostacyclin in preeclampsia is associated with an imbalance between lipid peroxides and vitamin E in maternal blood. *Am J Obstet Gynecol.* 1991;165:1695-1700.

80. Redman CW, Sargent IL. Preeclampsia and the systemic inflammatory response. *Semin Nephrol.* 2004;24:565-570.

81. Redman CW, Sargent IL. Pre-eclampsia, the placenta and the maternal systemic inflammatory response--a review. *Placenta.* 2003;24 Suppl A:S21-27.

82. Redman CW, Sacks GP, Sargent IL. Preeclampsia: an excessive maternal inflammatory response to pregnancy. *Am J Obstet Gynecol.* 1999;180:499-506.

83. Barnes PJ, Karin M. Nuclear factor-kappaB: a pivotal transcription factor in chronic inflammatory diseases. *N Engl J Med.* 1997;336:1066-1071.

84. Nakahata N. Thromboxane A2: physiology/pathophysiology, cellular signal transduction and pharmacology. *Pharmacol Ther.* 2008;118:18-35.

85. Leik CE, Walsh SW. Linoleic acid, but not oleic acid, upregulates production of interleukin-8 by human vascular smooth muscle cells via arachidonic acid metabolites under conditions of oxidative stress. *J Soc Gynecol Investig.* 2005;12:593-598.

86. Vaughan JE, Walsh SW. Neutrophils from pregnant women produce thromboxane and tumor necrosis factor-alpha in response to linoleic acid and oxidative stress. *Am J Obstet Gynecol.* 2005;193:830-835.

87. Ramadan FM, Upchurch GR, Jr., Keagy BA, Johnson G, Jr. Endothelial cell thromboxane production and its inhibition by a calcium-channel blocker. *Ann Thorac Surg.* 1990;49:916-919.

88. Heller A, Koch T, Schmeck J, van Ackern K. Lipid mediators in inflammatory disorders. *Drugs.* 1998;55:487-496.

89. Hubel CA. Oxidative stress in the pathogenesis of preeclampsia. *Proc Soc Exp Biol Med.* 1999;222:222-235.

90. Jendryczko A, Drozdz M, Wojcik A. Serum 18:2 (9, 11) linoleic acid in normal pregnancy and pregnancy complicated by pre-eclampsia. *Zentralbl Gynakol.* 1991;113:443-446.

91. Vaughan JE, Walsh SW, Ford GD. Thromboxane mediates neutrophil superoxide production in pregnancy. *Am J Obstet Gynecol.* 2006;195:1415-1420.

92. Ishizuka T, Suzuki K, Kawakami M, Hidaka T, Matsuki Y, Nakamura H. Thromboxane A2 receptor blockade suppresses intercellular adhesion molecule-1 expression by stimulated vascular endothelial cells. *Eur J Pharmacol.* 1996;312:367-377.

93. Woodworth SH, Li X, Lei ZM, Rao CV, Yussman MA, Spinnato JA, 2nd, Yokoyama C, Tanabe T, Ullrich V. Eicosanoid biosynthetic enzymes in placental and decidual tissues from preeclamptic pregnancies: increased expression of thromboxane-A2 synthase gene. *J Clin Endocrinol Metab.* 1994;78:1225-1231.

94. Tanabe T, Ullrich V. Prostacyclin and thromboxane synthases. *J Lipid Mediat Cell Signal.* 1995;12:243-255.

95. Walsh SW. Preeclampsia: an imbalance in placental prostacyclin and thromboxane production. *Am J Obstet Gynecol.* 1985;152:335-340.

96. Chavarria ME, Lara-Gonzalez L, Gonzalez-Gleason A, Garcia-Paleta Y, Vital-Reyes VS, Reyes A. Prostacyclin/thromboxane early changes in pregnancies that are complicated by preeclampsia. *Am J Obstet Gynecol.* 2003;188:986-992.

97. Mills JL, DerSimonian R, Raymond E, Morrow JD, Roberts LJ, 2nd, Clemens JD, Hauth JC, Catalano P, Sibai B, Curet LB, Levine RJ. Prostacyclin and thromboxane changes predating clinical onset of preeclampsia: a multicenter prospective study. *JAMA.* 1999;282:356-362.

98. Rush DS, Kerstein MD, Bellan JA, Knoop SM, Mayeux PR, Hyman AL, Kadowitz PJ, McNamara DB. Prostacyclin, thromboxane A2, and prostaglandin E2 formation in atherosclerotic human carotid artery. *Arteriosclerosis.* 1988;8:73-78.

99. Luo Y. Improvement of prostacyclin-thromboxane A2 balance in patients with acute myocardial infarction by intermittent aspirin. *Zhonghua Xin Xue Guan Bing Za Zhi.* 1993;21:219-221, 253-214.

100. Fu ZZ, Yan T, Chen YJ, Sang JQ. Thromboxane/prostacyclin balance in type II diabetes: gliclazide effects. *Metabolism.* 1992;41:33-35.

101. Gatti L, Tenconi PM, Guarneri D, Bertulessi C, Ossola MW, Bosco P, Gianotti GA. Hemostatic parameters and platelet activation by flow-cytometry in normal pregnancy: a longitudinal study. *Int J Clin Lab Res.* 1994;24:217-219.

102. Halligan A, Bonnar J, Sheppard B, Darling M, Walshe J. Haemostatic, fibrinolytic and endothelial variables in normal pregnancies and pre-eclampsia. *Br J Obstet Gynaecol.* 1994;101:488-492.

103. Haram K, Augensen K, Elsayed S. Serum protein pattern in normal pregnancy with special reference to acute-phase reactants. *Br J Obstet Gynaecol.* 1983;90:139-145.

104. Austgulen R, Lien E, Liabakk NB, Jacobsen G, Arntzen KJ. Increased levels of cytokines and cytokine activity modifiers in normal pregnancy. *Eur J Obstet Gynecol Reprod Biol.* 1994;57:149-155.

105. Melczer Z, Banhidy F, Csomor S, Toth P, Kovacs M, Winkler G, Cseh K. Influence of leptin and the TNF system on insulin resistance in pregnancy and their effect on anthropometric parameters of newborns. *Acta Obstet Gynecol Scand.* 2003;82:432-438.

106. Arntzen KJ, Liabakk NB, Jacobsen G, Espevik T, Austgulen R. Soluble tumor necrosis factor receptor in serum and urine throughout normal pregnancy and at delivery. *Am J Reprod Immunol.* 1995;34:163-169.

107. Morris JM, Gopaul NK, Endresen MJ, Knight M, Linton EA, Dhir S, Anggard EE, Redman CW. Circulating markers of oxidative stress are raised in normal pregnancy and pre-eclampsia. *Br J Obstet Gynaecol.* 1998;105:1195-1199.

108. Martin U, Davies C, Hayavi S, Hartland A, Dunne F. Is normal pregnancy atherogenic? *Clin Sci (Lond).* 1999;96:421-425.

109. Borzychowski AM, Sargent IL, Redman CW. Inflammation and pre-eclampsia. *Semin Fetal Neonatal Med.* 2006;11:309-316.

110. Tost J. DNA methylation: an introduction to the biology and the disease-associated changes of a promising biomarker. *Mol Biotechnol.* 2010;44:71-81.

111. Illingworth RS, Bird AP. CpG islands--'a rough guide'. *FEBS Lett.* 2009;583:1713-1720.

112. Klose RJ, Bird AP. Genomic DNA methylation: the mark and its mediators. *Trends Biochem Sci.* 2006;31:89-97.

113. Sasai N, Defossez PA. Many paths to one goal? The proteins that recognize methylated DNA in eukaryotes. *Int J Dev Biol.* 2009;53:323-334.

114. Ooi SK, Bestor TH. The colorful history of active DNA demethylation. *Cell.* 2008;133:1145-1148.

115. Fraga MF, Ballestar E, Paz MF, Ropero S, Setien F, Ballestar ML, Heine-Suner D, Cigudosa JC, Urioste M, Benitez J, Boix-Chornet M, Sanchez-Aguilera A, Ling C, Carlsson E, Poulsen P, Vaag A, Stephan Z, Spector TD, Wu YZ, Plass C, Esteller M. Epigenetic differences arise during the lifetime of monozygotic twins. *Proc Natl Acad Sci U S A.* 2005;102:10604-10609.

116. Fraga MF, Esteller M. Epigenetics and aging: the targets and the marks. *Trends Genet.* 2007;23:413-418.

117. Ulrey CL, Liu L, Andrews LG, Tollefsbol TO. The impact of metabolism on DNA methylation. *Hum Mol Genet.* 2005;14 Spec No 1:R139-147.

118. Waterland RA, Jirtle RL. Transposable elements: targets for early nutritional effects on epigenetic gene regulation. *Mol Cell Biol.* 2003;23:5293-5300.

119. Feil R. Environmental and nutritional effects on the epigenetic regulation of genes. *Mutat Res.* 2006;600:46-57.

120. Bollati V, Baccarelli A, Hou L, Bonzini M, Fustinoni S, Cavallo D, Byun HM, Jiang J, Marinelli B, Pesatori AC, Bertazzi PA, Yang AS. Changes in DNA methylation patterns in subjects exposed to low-dose benzene. *Cancer Res.* 2007;67:876-880.

121. Anway MD, Cupp AS, Uzumcu M, Skinner MK. Epigenetic transgenerational actions of endocrine disruptors and male fertility. *Science.* 2005;308:1466-1469.

122. Laird PW, Jaenisch R. The role of DNA methylation in cancer genetic and epigenetics. *Annu Rev Genet.* 1996;30:441-464.

123. Maeda O, Ando T, Watanabe O, Ishiguro K, Ohmiya N, Niwa Y, Goto H. DNA hypermethylation in colorectal neoplasms and inflammatory bowel disease: a mini review. *Inflammopharmacology.* 2006;14:204-206.

124. Wang L, Wang F, Guan J, Le J, Wu L, Zou J, Zhao H, Pei L, Zheng X, Zhang T. Relation between hypomethylation of long interspersed nucleotide elements and risk of neural tube defects. *Am J Clin Nutr.* 2010;91:1359-1367.

125. Abdolmaleky HM, Cheng KH, Faraone SV, Wilcox M, Glatt SJ, Gao F, Smith CL, Shafa R, Aeali B, Carnevale J, Pan H, Papageorgis P, Ponte JF, Sivaraman V, Tsuang MT, Thiagalingam S. Hypomethylation of MB-COMT promoter is a major risk factor for schizophrenia and bipolar disorder. *Hum Mol Genet.* 2006;15:3132-3145.

126. Balada E, Ordi-Ros J, Vilardell-Tarres M. DNA methylation and systemic lupus erythematosus. *Ann N Y Acad Sci.* 2007;1108:127-136.

127. Neidhart M, Rethage J, Kuchen S, Kunzler P, Crowl RM, Billingham ME, Gay RE, Gay S. Retrotransposable L1 elements expressed in rheumatoid arthritis synovial tissue: association with genomic DNA hypomethylation and influence on gene expression. *Arthritis Rheum.* 2000;43:2634-2647.

128. Junien C, Nathanielsz P. Report on the IASO Stock Conference 2006: early and lifelong environmental epigenomic programming of metabolic syndrome, obesity and type II diabetes. *Obes Rev.* 2007;8:487-502.

129. Dong C, Yoon W, Goldschmidt-Clermont PJ. DNA methylation and atherosclerosis. *J Nutr.* 2002;132:2406S-2409S.

130. Baccarelli A, Wright R, Bollati V, Litonjua A, Zanobetti A, Tarantini L, Sparrow D, Vokonas P, Schwartz J. Ischemic heart disease and stroke in relation to blood DNA methylation. *Epidemiology.* 2010;21:819-828.

131. Bestor TH. The DNA methyltransferases of mammals. *Hum Mol Genet.* 2000;9:2395-2402.

132. Cantoni GL. The role of S-adenosylhomocysteine in the biological utilization of S-adenosylmethionine. *Prog Clin Biol Res.* 1985;198:47-65.

133. Hoffman DR, Cornatzer WE, Duerre JA. Relationship between tissue levels of S-adenosylmethionine, S-adenylhomocysteine, and transmethylation reactions. *Can J Biochem.* 1979;57:56-65.

134. Castro R, Rivera I, Struys EA, Jansen EE, Ravasco P, Camilo ME, Blom HJ, Jakobs C, Tavares de Almeida I. Increased homocysteine and S-adenosylhomocysteine concentrations and DNA hypomethylation in vascular disease. *Clin Chem.* 2003;49:1292-1296.

135. Patrick TE, Powers RW, Daftary AR, Ness RB, Roberts JM. Homocysteine and folic acid are inversely related in black women with preeclampsia. *Hypertension.* 2004;43:1279-1282.

136. Makedos G, Papanicolaou A, Hitoglou A, Kalogiannidis I, Makedos A, Vrazioti V, Goutzioulis M. Homocysteine, folic acid and B12 serum levels in pregnancy complicated with preeclampsia. *Arch Gynecol Obstet.* 2007;275:121-124.

137. Laivuori H, Kaaja R, Turpeinen U, Viinikka L, Ylikorkala O. Plasma homocysteine levels elevated and inversely related to insulin sensitivity in preeclampsia. *Obstet Gynecol.* 1999;93:489-493.

138. Chen Z, Karaplis AC, Ackerman SL, Pogribny IP, Melnyk S, Lussier-Cacan S, Chen MF, Pai A, John SW, Smith RS, Bottiglieri T, Bagley P, Selhub J, Rudnicki MA, James SJ, Rozen R. Mice deficient in methylenetetrahydrofolate reductase exhibit hyperhomocysteinemia and decreased

methylation capacity, with neuropathology and aortic lipid deposition. *Hum Mol Genet.* 2001;10:433-443.

139. Lund G, Andersson L, Lauria M, Lindholm M, Fraga MF, Villar-Garea A, Ballestar E, Esteller M, Zaina S. DNA methylation polymorphisms precede any histological sign of atherosclerosis in mice lacking apolipoprotein E. *J Biol Chem.* 2004;279:29147-29154.

140. Bogdarina I, Welham S, King PJ, Burns SP, Clark AJ. Epigenetic modification of the renin-angiotensin system in the fetal programming of hypertension. *Circ Res.* 2007;100:520-526.

141. Franco R, Schoneveld O, Georgakilas AG, Panayiotidis MI. Oxidative stress, DNA methylation and carcinogenesis. *Cancer Lett.* 2008;266:6-11.

142. Chen XK, Wen SW, Bottomley J, Smith GN, Leader A, Walker MC. In vitro fertilization is associated with an increased risk for preeclampsia. *Hypertens Pregnancy.* 2009;28:1-12.

143. Kanayama N, Takahashi K, Matsuura T, Sugimura M, Kobayashi T, Moniwa N, Tomita M, Nakayama K. Deficiency in p57Kip2 expression induces preeclampsia-like symptoms in mice. *Mol Hum Reprod.* 2002;8:1129-1135.

144. Yu L, Chen M, Zhao D, Yi P, Lu L, Han J, Zheng X, Zhou Y, Li L. The H19 gene imprinting in normal pregnancy and pre-eclampsia. *Placenta.* 2009;30:443-447.

145. Chelbi ST, Mondon F, Jammes H, Buffat C, Mignot TM, Tost J, Busato F, Gut I, Rebourcet R, Laissue P, Tsatsaris V, Goffinet F, Rigourd V, Carbonne B, Ferre F, Vaiman D. Expressional and epigenetic alterations of placental serine protease inhibitors: SERPINA3 is a potential marker of preeclampsia. *Hypertension.* 2007;49:76-83.

146. Wang Z, Lu S, Liu C, Zhao B, Pei K, Tian L, Ma X. Expressional and epigenetic alterations of placental matrix metalloproteinase 9 in preeclampsia. *Gynecol Endocrinol.* 2009;26:96-102.

147. Yuen RK, Penaherrera MS, von Dadelszen P, McFadden DE, Robinson WP. DNA methylation profiling of human placentas reveals promoter hypomethylation of multiple genes in early-onset preeclampsia. *Eur J Hum Genet.* 2010;18:1006-1012.

148. Uz E, Dolen I, Al AR, Ozcelik T. Extremely skewed X-chromosome inactivation is increased in pre-eclampsia. *Hum Genet.* 2007;121:101-105.

149. Shen RF, Tai HH. Thromboxanes: synthase and receptors. *J Biomed Sci.* 1998;5:153-172.

150. Kim E, Gunther W, Yoshizato K, Meissner H, Zapf S, Nusing RM, Yamamoto H, Van Meir EG, Deppert W, Giese A. Tumor suppressor p53 inhibits transcriptional activation of invasion gene thromboxane synthase mediated by the proto-oncogenic factor ets-1. *Oncogene.* 2003;22:7716-7727.

151. Belletti B, Spisni E, Bartolini G, Orlandi M, Tomasi V. Post-transcriptional regulation of thromboxane A2 synthase in U937 cells. *Biochem Biophys Res Commun.* 1995;209:901-906.

152. Lee KD, Baek SJ, Shen RF. Multiple factors regulating the expression of human thromboxane synthase gene. *Biochem J.* 1996;319 (Pt 3):783-791.

153. Tang EH, Vanhoutte PM. Gene expression changes of prostanoid synthases in endothelial cells and prostanoid receptors in vascular smooth muscle cells caused by aging and hypertension. *Physiol Genomics.* 2008;32:409-418.

154. Ravanti L, Kahari VM. Matrix metalloproteinases in wound repair (review). *Int J Mol Med.* 2000;6:391-407.

155. Lemaitre V, D'Armiento J. Matrix metalloproteinases in development and disease. *Birth Defects Res C Embryo Today.* 2006;78:1-10.

156. Parks WC, Wilson CL, Lopez-Boado YS. Matrix metalloproteinases as modulators of inflammation and innate immunity. *Nat Rev Immunol.* 2004;4:617-629.

157. Watanabe N, Ikeda U. Matrix metalloproteinases and atherosclerosis. *Curr Atheroscler Rep.* 2004;6:112-120.

158. Gialeli C, Theocharis AD, Karamanos NK. Roles of matrix metalloproteinases in cancer progression and their pharmacological targeting. *FEBS J.* 2010;278:16-27.

159. Estrada-Gutierrez G, Cappello RE, Mishra N, Romero R, Strauss JF, 3rd, Walsh SW. Increased expression of matrix metalloproteinase-1 in systemic vessels of preeclamptic women: a critical mediator of vascular dysfunction. *Am J Pathol.* 2011;178:451-460.

160. Fernandez-Patron C, Radomski MW, Davidge ST. Vascular matrix metalloproteinase-2 cleaves big endothelin-1 yielding a novel vasoconstrictor. *Circ Res.* 1999;85:906-911.

161. Zitka O, Kukacka J, Krizkova S, Huska D, Adam V, Masarik M, Prusa R, Kizek R. Matrix metalloproteinases. *Curr Med Chem.* 2010;17:3751-3768.

162. Nagase H, Visse R, Murphy G. Structure and function of matrix metalloproteinases and TIMPs. *Cardiovasc Res.* 2006;69:562-573.

163. Butler GS, Overall CM. Updated biological roles for matrix metalloproteinases and new "intracellular" substrates revealed by degradomics. *Biochemistry.* 2009;48:10830-10845.

164. Wang H, Ogawa M, Wood JR, Bartolomei MS, Sammel MD, Kusanovic JP, Walsh SW, Romero R, Strauss JF, 3rd. Genetic and epigenetic mechanisms combine to control MMP1 expression and its association with preterm premature rupture of membranes. *Hum Mol Genet.* 2008;17:1087-1096.

165. Leik CE, Willey A, Graham MF, Walsh SW. Isolation and culture of arterial smooth muscle cells from human placenta. *Hypertension.* 2004;43:837-840.

166. Storey JD, Tibshirani R. Statistical significance for genomewide studies. *Proc Natl Acad Sci U S A.* 2003;100:9440-9445.

167. Roberts JM, Gammill HS. Preeclampsia: recent insights. *Hypertension.* 2005;46:1243-1249.

168. Pridjian G, Puschett JB. Preeclampsia. Part 2: experimental and genetic considerations. *Obstet Gynecol Surv.* 2002;57:619-640.

169. Williams PJ, Pipkin FB. The genetics of pre-eclampsia and other hypertensive disorders of pregnancy. *Best practice & research. Clinical obstetrics & gynaecology.* 2011;25:405-417.

170. Wilson CB, Makar KW, Shnyreva M, Fitzpatrick DR. DNA methylation and the expanding epigenetics of T cell lineage commitment. *Semin Immunol.* 2005;17:105-119.

171. Zaina S, Lindholm MW, Lund G. Nutrition and aberrant DNA methylation patterns in atherosclerosis: more than just hyperhomocysteinemia? *J Nutr.* 2005;135:5-8.

172. Paulsen M, Ferguson-Smith AC. DNA methylation in genomic imprinting, development, and disease. *J Pathol.* 2001;195:97-110.

173. Agrawal A, Murphy RF, Agrawal DK. DNA methylation in breast and colorectal cancers. *Mod Pathol.* 2007;20:711-721.

174. Connor CM, Akbarian S. DNA methylation changes in schizophrenia and bipolar disorder. *Epigenetics.* 2008;3:55-58.

175. van der Linden IJ, Heil SG, van Egmont Petersen M, van Straaten HW, den Heijer M, Blom HJ. Inhibition of methylation and changes in gene expression in relation to neural tube defects. *Birth Defects Res A Clin Mol Teratol.* 2008;82:676-683.

176. Walsh SW. Obesity: a risk factor for preeclampsia. *Trends in endocrinology and metabolism: TEM.* 2007;18:365-370.

177. Wang JX, Knottnerus AM, Schuit G, Norman RJ, Chan A, Dekker GA. Surgically obtained sperm, and risk of gestational hypertension and pre-eclampsia. *Lancet.* 2002;359:673-674.

178. Chelbi ST, Vaiman D. Genetic and epigenetic factors contribute to the onset of preeclampsia. *Mol Cell Endocrinol.* 2008;282:120-129.

179. Clark SJ, Statham A, Stirzaker C, Molloy PL, Frommer M. DNA methylation: bisulphite modification and analysis. *Nat Protoc.* 2006;1:2353-2364.

180. Grunau C, Clark SJ, Rosenthal A. Bisulfite genomic sequencing: systematic investigation of critical experimental parameters. *Nucleic Acids Res.* 2001;29:E65-65.

181. Xiong Z, Laird PW. COBRA: a sensitive and quantitative DNA methylation assay. *Nucleic Acids Res.* 1997;25:2532-2534.

182. Weisenberger DJ, Berg, D. V. D., Pan, F., Berman, B. P., Laird, P. W. Comprehensive DNA Methylation Analysis on the Illumina Infinium Assay Platform. *Illumina and Inc., San Diego, CA*. 2008.

183. Bibikova M, Lin Z, Zhou L, Chudin E, Garcia EW, Wu B, Doucet D, Thomas NJ, Wang Y, Vollmer E, Goldmann T, Seifart C, Jiang W, Barker DL, Chee MS, Floros J, Fan JB. High-throughput DNA methylation profiling using universal bead arrays. *Genome Res.* 2006;16:383-393.

184. Li B, Carey M, Workman JL. The role of chromatin during transcription. *Cell.* 2007;128:707-719.

185. Archer KJ, Mas VR, Maluf DG, Fisher RA. High-throughput assessment of CpG site methylation for distinguishing between HCV-cirrhosis and HCV-associated hepatocellular carcinoma. *Mol Genet Genomics*. 2010;283:341-349.

186. Bellamy L, Casas JP, Hingorani AD, Williams DJ. Pre-eclampsia and risk of cardiovascular disease and cancer in later life: systematic review and meta-analysis. *BMJ.* 2007;335:974.

187. Mousa AA, Archer KJ, Strauss III JF, Walsh SW. Thromboxane synthase expression is increased and its DNA methylation decreased in systemic vasculature of women with preeclampsia. *Reprod Sci (Supplement).* 2011;18:170A.

188. Cappello R, Estrada-Gutierrez G, Gerk PM, Strauss III JF, Walsh SW. Epigenetic control of collagen regulating genes in vascular smooth muscle. *Reprod Sci.* 2008;15 (Supplement):73A.

189. Lurie S, Rahamim E, Piper I, Golan A, Sadan O. Total and differential leukocyte counts percentiles in normal pregnancy. *Eur J Obstet Gynecol Reprod Biol.* 2008;136:16-19.

190. Barriga C, Rodriguez AB, Ortega E. Increased phagocytic activity of polymorphonuclear leukocytes during pregnancy. *Eur J Obstet Gynecol Reprod Biol.* 1994;57:43-46.

191. Smarason AK, Gunnarsson A, Alfredsson JH, Valdimarsson H. Monocytosis and monocytic infiltration of decidua in early pregnancy. *J Clin Lab Immunol.* 1986;21:1-5.

192. Barden A. Circulating markers of oxidative stress are raised in normal pregnancy and pre-eclampsia. *Br J Obstet Gynaecol.* 1999;106:1232.

193. Plutzky J. The PPAR-RXR transcriptional complex in the vasculature: energy in the balance. *Circ Res.* 2011;108:1002-1016.

194. Lotze MT, Tracey KJ. High-mobility group box 1 protein (HMGB1): nuclear weapon in the immune arsenal. *Nat Rev Immunol.* 2005;5:331-342.

195. Yu M, Wang H, Ding A, Golenbock DT, Latz E, Czura CJ, Fenton MJ, Tracey KJ, Yang H. HMGB1 signals through toll-like receptor (TLR) 4 and TLR2. *Shock.* 2006;26:174-179.

196. Inoue K, Kawahara K, Biswas KK, Ando K, Mitsudo K, Nobuyoshi M, Maruyama I. HMGB1 expression by activated vascular smooth muscle cells in advanced human atherosclerosis plaques. *Cardiovasc Pathol.* 2007;16:136-143.

197. Mihu D, Costin N, Mihu CM, Blaga LD, Pop RB. C-reactive protein, marker for evaluation of systemic inflammatory response in preeclampsia. *Rev Med Chir Soc Med Nat Iasi.* 2008;112:1019-1025.

198. Qiu C, Luthy DA, Zhang C, Walsh SW, Leisenring WM, Williams MA. A prospective study of maternal serum C-reactive protein concentrations and risk of preeclampsia. *Am J Hypertens.* 2004;17:154-160.

199. Fiuza C, Bustin M, Talwar S, Tropea M, Gerstenberger E, Shelhamer JH, Suffredini AF. Inflammation-promoting activity of HMGB1 on human microvascular endothelial cells. *Blood.* 2003;101:2652-2660.

200. Narumiya H, Zhang Y, Fernandez-Patron C, Guilbert LJ, Davidge ST. Matrix metalloproteinase-2 is elevated in the plasma of women with preeclampsia. *Hypertens Pregnancy.* 2001;20:185-194.

201. Poon LC, Nekrasova E, Anastassopoulos P, Livanos P, Nicolaides KH. First-trimester maternal serum matrix metalloproteinase-9 (MMP-9) and adverse pregnancy outcome. *Prenat Diagn.* 2009;29:553-559.

202. Khalil RA, Granger JP. Vascular mechanisms of increased arterial pressure in preeclampsia: lessons from animal models. *Am J Physiol Regul Integr Comp Physiol.* 2002;283:R29-45.

203. Lunell NO, Nylund LE, Lewander R, Sarby B. Uteroplacental blood flow in pre-eclampsia measurements with indium-113m and a computer-linked gamma camera. *Clin Exp Hypertens B.* 1982;1:105-117.

204. Perry KG, Jr., Martin JN, Jr. Abnormal hemostasis and coagulopathy in preeclampsia and eclampsia. *Clin Obstet Gynecol.* 1992;35:338-350.

205. von Versen-Hoeynck FM, Powers RW. Maternal-fetal metabolism in normal pregnancy and preeclampsia. *Front Biosci.* 2007;12:2457-2470.

206. Wen SW, Chen XK, Rodger M, White RR, Yang Q, Smith GN, Sigal RJ, Perkins SL, Walker MC. Folic acid supplementation in early second trimester and the risk of preeclampsia. *Am J Obstet Gynecol.* 2008;198:45 e1-7.

207. Needleman P, Turk J, Jakschik BA, Morrison AR, Lefkowith JB. Arachidonic acid metabolism. *Annu Rev Biochem.* 1986;55:69-102.

208. Weitzman SA, Turk PW, Milkowski DH, Kozlowski K. Free radical adducts induce alterations in DNA cytosine methylation. *Proc Natl Acad Sci U S A.* 1994;91:1261-1264.

209. Hitchler MJ, Domann FE. An epigenetic perspective on the free radical theory of development. *Free Radic Biol Med.* 2007;43:1023-1036.

210. Arora CP, Adeniji A, Hobel CJ. Oxidative stress leading to DNA damage is associated with development of preeclampsia *Reprod Sci.* 2009;16 (Supplement):348-349A.

211. Gerrard JM, Taback S, Singhroy S, Docherty JC, Kostolansky I, McNicol A, Kobrinsky NL, McKenzie JK, Rowe R. In vivo measurement of thromboxane B2 and 6-keto-prostaglandin F1 alpha in humans in response to a standardized vascular injury and the influence of aspirin. *Circulation.* 1989;79:29-38.

212. Dunning MJ, Smith ML, Ritchie ME, Tavare S. beadarray: R classes and methods for Illumina bead-based data. *Bioinformatics.* 2007;23:2183-2184.

213. Mousa AA, Archer KJ, Cappello R, Estrada-Gutierrez G, Isaacs C, Romero R, Strauss III JF, Walsh SW. Epigenetic alterations in omental artery genes in women with preeclampsia. *Reprod Sci (Supplement).* 2011;18:356A.

214. Walsh SW. Plasma from preeclamptic women stimulates transendothelial migration of neutrophils. *Reprod Sci.* 2009;16:320-325.

215. Lurie S, Frenkel E, Tuvbin Y. Comparison of the differential distribution of leukocytes in preeclampsia versus uncomplicated pregnancy. *Gynecol Obstet Invest.* 1998;45:229-231.

216. Cadden KA, Walsh SW. Neutrophils, but not lymphocytes or monocytes, infiltrate maternal systemic vasculature in women with preeclampsia. *Hypertens Pregnancy.* 2008;27:396-405.

217. Ogburn PL, Jr., Williams PP, Johnson SB, Holman RT. Serum arachidonic acid levels in normal and preeclamptic pregnancies. *Am J Obstet Gynecol.* 1984;148:5-9.

218. Lorentzen B, Drevon CA, Endresen MJ, Henriksen T. Fatty acid pattern of esterified and free fatty acids in sera of women with normal and pre-eclamptic pregnancy. *Br J Obstet Gynaecol.* 1995;102:530-537.

219. Sato N, Maehara N, Su GH, Goggins M. Effects of 5-aza-2'-deoxycytidine on matrix metalloproteinase expression and pancreatic cancer cell invasiveness. *J Natl Cancer Inst.* 2003;95:327-330.

220. Gallagher R, Collins S, Trujillo J, McCredie K, Ahearn M, Tsai S, Metzgar R, Aulakh G, Ting R, Ruscetti F, Gallo R. Characterization of the continuous, differentiating myeloid cell line (HL-60) from a patient with acute promyelocytic leukemia. *Blood.* 1979;54:713-733.

221. Hill LD, York TP, Kusanovic JP, Gomez R, Eaves LJ, Romero R, Strauss JF, 3rd. Epistasis between COMT and MTHFR in maternal-fetal dyads increases risk for preeclampsia. *PloS one.* 2011;6:e16681.

VITA

Ahmad A Mousa was born on August the 16th, 1982 in Jordan, Irbid. His family roots are from Palestine. He received his bachelor degree in dental surgery from Jordan University of Science and Technology in 2005. He worked as a teaching assistant at the Department of Anatomy, Jordan University of Science and Technology and as a teaching assistant at the Department of Physiology and Biophysics during his graduate studies at Virginia Commonwealth University.